

DEVELOPMENT OF ENGINEERED MENISCI WITH NATIVE-LIKE ORGANIZATION  
USING HIGH DENSITY COLLAGEN GELS AND MECHANICAL STIMULATION

A Dissertation

Presented to the Faculty of the Graduate School

of Cornell University

In Partial Fulfillment of the Requirements for the Degree of

Doctor of Philosophy

by

Jennifer Lauren Puetzer

August 2014

© 2014 Jennifer Lauren Puetzer

# DEVELOPMENT OF ENGINEERED MENISCI WITH NATIVE-LIKE ORGANIZATION USING HIGH DENSITY COLLAGEN GELS AND MECHANICAL STIMULATION

Jennifer Lauren Puetzer, Ph. D.

Cornell University 2014

Meniscal injuries are one of the most common traumatic injuries in the knee accounting for over 1 million surgeries a year in the United States. Treatment of meniscus lesions is the most frequent procedure carried out by orthopaedic surgeons, and while there have been advances in partial repair strategies, improvements are still needed for whole meniscal replacement. Currently, the only treatment for total meniscal replacement is meniscectomy followed by cadaveric allograft, which is applicable in only a small percentage of patients, demonstrating the potential for a tissue engineered meniscus.

The focus of this dissertation was to investigate the effect of mechanical stimulation, chemical stimulation, and material choice on the development of tissue engineered menisci. The goal was to move toward a viable whole meniscus replacement. The completion of this body of work resulted in the development of an anatomical meniscal construct with native-like organization, equilibrium modulus, and anisotropic tensile properties. First, mechanical and chemical stimulation was found to significantly improve biochemical and mechanical properties of alginate menisci (Chapters 3 and 4). Next, high density type I collagen gels were investigated as a potential new scaffold choice and were found to be superior to alginate menisci (Chapter 5). Finally, mechanical stimulation was used to guide native-like organization in high density collagen menisci. Culturing with biomimetic horn-

anchored boundary conditions produced scaffolds with native-like circumferential and radial fiber organization, and development of anisotropic mechanical properties (Chapter 6). These horn-anchored conditions were then combined with compressive loading to investigate the effect of a bioreactor capable of applying physiological loading patterns (Chapter 7). This compressive-tensile loading regime accelerated the development of collagen menisci and improved all fibrocartilage properties.

This work has been at the forefront of a paradigm shift in the field to capture native organization, which is believed to be fundamental to meniscal load distribution *in vivo*. These are some of the most organized meniscal scaffolds produced to date and demonstrate great promise as meniscal replacements. This work establishes the potential of collagen constructs as meniscal replacements and presents many new research directions while providing the platform necessary to move toward clinical meniscal replacements.

## BIOGRAPHICAL SKETCH

Jenny was born and raised in Raleigh, North Carolina. Growing up with two older brothers, she was constantly involved in sports, triggering her love of orthopaedics.

For her undergraduate, Jenny attended North Carolina State University, where she graduated valedictorian and *summa cum laude* in 2009 with a B.S. in Biomedical Engineering. While at NC State, Jenny spent 3 years in the Cell Mechanics Laboratory, under Dr. Elizabeth Lobo performing experiments on the chondrogenesis of human adipose derived stem cells and publishing 2 papers. In addition to her time in lab, Jenny volunteered as an emergency medicine technician and led a group of students to provide a community in Sierra Leone, Africa with clean water through Engineers without Borders. Jenny received the College of Engineering Senior Scholarly Achievement Award, and was awarded the prestigious National Science Foundation (NSF) Graduate Research Fellowship as an undergrad.

In 2009, Jenny began pursuing her Ph.D. at Cornell University under the direction of Dr. Lawrence Bonassar. She has been extremely productive in graduate school mentoring multiple students and publishing 3 first-author papers, with 4 more in progress. Jenny participated in the NSF GK-12 program in 2012 cementing her interests in teaching. In 2014, Jenny was honored to be placed (1 of 6 worldwide) on the Young Investigator Council for the journal of Tissue Engineering where she will serve one year shaping the direction of the journal.

Following the completion of Jenny's Ph.D. she will take a postdoctoral position in the lab of Dr. Molly Stevens at Imperial College in London. She will be continuing her passion for orthopaedic research, with a concentration in material science. Following her postdoctoral work, she plans to begin a career in academia with a lab centered on orthopaedic tissue engineering and 3<sup>rd</sup> world regenerative medicine solutions.

Dedicated to my amazingly supportive family and friends  
In loving memory and dedication to Robert Mozia

## ACKNOWLEDGMENTS

I would like to first and foremost thank my advisor Dr. Larry Bonassar for his guidance and support during the completion of this degree. It has been a true pleasure working in his lab the last five years. I would also like to thank the members of my committee, Dr. Cindy Reinhart-King and Dr. Lisa Fortier for their insight, advice, and encouragement.

I would like to thank the countless people I have had the honor to work with. A special thank you to Dr. Peter Doerschuk for help with Matlab codes, Dr. Rajesh Bhaskaran for COMSOL aid, and Dr. Hod Lipson and John Cheeseborough for 3D printing countless molds and culture dishes. Thank you to Dr. Suzanne Maher and Dr. Scott Rodeo for opening their doors to me at Hospital for Special Surgery and allowing me to immerse myself in the clinical world. Thank you to Dr. Shivaun Archer, Dr. Christopher Schaffer, Nev Singhota, and Lorraine Buckley for a very memorable and rewarding GK-12 experience.

A special thank you to Judy Thoroughman and Belinda Floyd for making sure all my forms were turned in, I always got paid, and ordering all our supplies. You both have definitely allowed this experience to run as smoothly as possible.

I feel truly honored to have been able to work with so many great lab members through the years. A special thank you to the group of people I lovingly call Team Meniscus, especially Dr. Jeff Ballyns, Mary Clare McCorry, Sunjoo Park, Ritu Raman, and Esther Koo, without whom much of this work would not be complete. I would also like to thank all the members of the Bonassar Lab, both past and present, especially Dr. Robby Bowles, Dr. Natalie Galley, Kirk Samaroo, Nizeet Aguilar, Darwin Griffin, Brandon Borde, Eddie Bonnevie, Katie Hudson and Jorge Mojica Santiago for their constant support, feedback and entertainment. Thank you to graduate students

outside the lab as well for lending supplies, knowledge, and lifelong friendships, especially Jen Richards, Shawn Carey, Katie Melville, Jon Charest, and Mitch Cooper. I would like to especially thank Jen and Amy for proof reading many documents through the years and Jen for always listening to my endless reasoning of experimental hurdles.

I would like to give a specially thank you and dedication to Bobby Mozia who left us too soon. Bobby and I were inseparable the first 2 and half years of graduate school and I cannot imagine what those years would have been like without him. We took all our classes together (include the dreaded self-taught Biochemistry), did most of our group projects together, debugged each other's experiments, and always kept each other company in lab. He was everyone's number one fan and supporter. Bobby was an amazing person that I was privileged to call a friend.

Finally, I would like to thank my family for always supporting me and encouraging me to follow my dreams. I would not be where I am today without such a strong and loving family.

Funding for this work was provided by National Science Foundation Graduate Research Fellowship Program, the Cornell BME NSF GK-12 program: DGE 0841291, and Cornell University.

## TABLE OF CONTENTS

<b>BIOGRAPHICAL SKETCH</b> .....	<b>iii</b>
<b>DEDICATION</b> .....	<b>iv</b>
<b>ACKNOWLEDGMENTS</b> .....	<b>v</b>
<b>LIST OF FIGURES</b> .....	<b>xiii</b>
<b>LIST OF TABLES</b> .....	<b>xv</b>

### CHAPTER 1

<b>Introduction</b> .....	<b>1</b>
An Introduction to the Meniscus.....	1
Meniscal Composition .....	2
Meniscal Structure .....	3
Meniscal Mechanical Properties.....	4
Meniscal Development.....	6
Meniscal Injuries and Repair.....	6
Meniscus Tissue Engineering .....	7
Previous Research .....	8
Research Objectives.....	10
Improvement of Alginate Menisci .....	10
Development of Collagen Menisci .....	12
<i>Specific Aims</i> .....	13
References .....	18

### CHAPTER 2

<b>Mechanical Stimulation of Tissue-Engineered Articular Cartilage (Nature Reviews Rheumatology, in review)</b> .....	<b>26</b>
Abstract .....	26
Key Points .....	26
Introduction.....	27
Mechanical Loading in Native Cartilage.....	28
Mechanisms of Mechanotransduction.....	30
Mechanical Stimulation of Engineered Cartilage.....	30
Modes of Stimulation .....	32
Tissue Deformation .....	32
Compression .....	32
Combined Shear and Loading .....	35
Hydrostatic Pressure.....	35
Media Mixing.....	37

Perfusion.....	40
Surface Shear Flow Bioreactors .....	42
Load, Growth Factors, and Stem Cells .....	43
Synergistic Effect of Growth Factors and Load.....	43
Load-induced Chondrogenesis in Stem Cells.....	43
Conclusions .....	44
References .....	46

### CHAPTER 3

<b>The Effect of Duration of Mechanical Stimulation and Post-Stimulation Culture on the Structure and Properties of Dynamically Compressed Tissue-Engineered Menisci</b> ( <i>Tissue Engineering</i> , 18, 1365, 2012) .....	<b>57</b>
Abstract .....	57
Introduction.....	58
Methods.....	60
Injection Molding .....	60
Dynamic Loading .....	62
Post Culture Construct Analysis .....	63
Statistics .....	64
Results .....	65
Meniscal Construct Shape Fidelity and Composition.....	65
Biochemical Properties .....	68
Equilibrium Modulus.....	71
Discussion .....	72
References .....	78

### CHAPTER 4

<b>The Effect of IGF-I on Anatomically Shaped Tissue-Engineered Menisci</b> ( <i>Tissue Engineering</i> , 19, 1443, 2013) .....	<b>84</b>
Abstract .....	84
Introduction.....	85
Materials and Methods .....	86
Generation of Engineered Alginate Menisci .....	86
Postculture Analysis.....	87
Histological Analysis.....	88
Immunohistochemistry.....	88
Biochemical Analysis .....	89

Mechanical Analysis .....	89
Statistics .....	89
Results .....	91
Histological Analysis .....	91
Immunohistochemical Analysis .....	92
Biochemical Analysis .....	94
Mechanical Analysis.....	95
Discussion .....	96
References .....	100

## CHAPTER 5

### High Density Type I Collagen Gels for Tissue Engineering of Whole Menisci

( <i>Acta Biomaterialia</i> , 9, 7787, 2013) .....	105
Abstract .....	105
Introduction.....	105
Materials and Methods .....	108
Collagen Extraction and Reconstitution.....	108
Cell Isolation and Injection Molding .....	108
Post-culture Analysis.....	109
Gross Appearance and Contraction.....	109
Confocal Image Analysis .....	110
Histological Analysis.....	110
Biochemical Analysis.....	111
Mechanical Analysis .....	111
Statistics .....	112
Results .....	112
Construct Shape Fidelity and Appearance .....	112
Collagen Localization and Organization Analysis .....	113
Biochemical Analysis .....	117
Mechanical Analysis.....	119
Biochemical and Mechanical Correlations.....	120
Discussion .....	121
Conclusions.....	126
Supplementary Data.....	127
References .....	129

## CHAPTER 6

### **Native-like Fiber Development and Mechanical Anisotropy in Tissue Engineered Menisci with Long-term Horn-anchored Culture (Publication in preparation) .... 134**

Abstract .....	134
Introduction.....	135
Materials and Methods .....	136
Construct Fabrication .....	136
Application of Boundary Conditions.....	137
Constructs Analysis.....	138
Gross Appearance and Contraction.....	138
Confocal Image Analysis .....	138
Histological Analysis.....	140
Biochemical Analysis.....	141
Mechanical Analysis .....	141
Statistics .....	142
Results .....	142
Construct Appearance and Shape Fidelity .....	142
Collagen Organization and Analysis.....	143
Biochemical Analysis .....	148
Mechanical Analysis.....	150
Discussion .....	152
References .....	158

## CHAPTER 7

### **Effects of Physiologic Loading Patterns on the Development of Tissue Engineered Menisci (Publication in preparation) ..... 164**

Abstract .....	164
Introduction.....	164
Materials and Methods .....	167
Bioreactor Design and Fabrication .....	167
Finite Element Analysis.....	168
Meniscus Fabrication and Dynamic Loading .....	170
Post Culture Analysis .....	171
Statistics .....	173
Results .....	173
FE Model .....	173

Construct Appearance and Shape Fidelity .....	176
Collagen Organization.....	178
Mechanical Analysis.....	181
Biochemical Analysis .....	183
Local Mechanical and Biochemical Heterogeneity .....	184
Discussion .....	186
References .....	193

## CHAPTER 8

<b>Conclusions .....</b>	<b>200</b>
Future Directions .....	207
<i>In Vitro</i> Development toward Whole Meniscal Replacement .....	207
Use of Culture Techniques for Alternative Applications .....	211
<i>In Vivo</i> Partial Meniscal Replacement .....	213
References .....	215

## CHAPTER 9

<b>Tissue Engineering and Collagen Gels: A Total STEM Experience</b> (Publication in preparation) .....	<b>221</b>
Preface.....	221
Introduction.....	223
Science Content for the Teacher .....	225
Tissue Engineering Content: .....	225
Scaffold Content .....	226
Collagen Content .....	227
Preparation.....	229
Classroom Procedure .....	232
Experiment 1: The Effect of NaOH .....	233
Experiment 2: The Effect of Temperature.....	235
Experiment 3: Recommend a Formula to Develop a Collagen Gel..	237
Assessment.....	240
Safety .....	240
Supplemental Information .....	241
Experiment Worksheet.....	241
Assessment Quiz/Key .....	244

## APPENDICES

<b>APPENDIX A: MATLAB Code for Collagen Bundle Code .....</b>	<b>246</b>
<b>APPENDIX B: Riboflavin Treatment of High Density Collagen gels .....</b>	<b>248</b>
Introduction .....	248
Materials and Methods .....	248
Results .....	249
Discussion .....	251
References .....	253
<b>APPENDIX C: MATLAB Code for Fiber Alignment and Diameter .....</b>	<b>255</b>
Diameter.m .....	255
fourierTransform.m.....	261
radonTransform.m.....	262
Sumangle.m.....	262
allindex.m.....	284
CalculateDiameter.m.....	286
Reference .....	287
<b>APPENDIX D: MATLAB Code for Load Cell Data Analysis .....</b>	<b>288</b>
Pkpk.m.....	288
Peakfinder.m.....	297

## LIST OF FIGURES

### CHAPTER 1

- Figure 1.1: Red/White zone of native meniscus ..... 2  
Figure 1.2: Three-layer collagen fiber organization of meniscus ..... 4

### CHAPTER 2

- Figure 2.1: Modes of deformation in native cartilage ..... 29  
Figure 2.2: Bioreactors of cartilage tissue engineering ..... 31  
Figure 2.3: GAG synthesis according to applied strain and frequency ..... 33

### CHAPTER 3

- Figure 3.1: Experimental setup, bioreactor and loading waveform ..... 62  
Figure 3.2: Photographs, Safranin-O, and picosirius red staining of part I menisci . 65  
Figure 3.3: Photographs, Safranin-O, and picosirius red staining of part II menisci 66  
Figure 3.4: Collagen bundle image analysis ..... 68  
Figure 3.5: GAG content in engineered menisci and media ..... 69  
Figure 3.6: Collagen content in engineered menisci and media ..... 70  
Figure 3.7: Equilibrium Modulus of part I and part II menisci ..... 72

### CHAPTER 4

- Figure 4.1: Photographs of alginate menisci upon removal from culture..... 90  
Figure 4.2: Safranin-O and picosirius red staining ..... 90  
Figure 4.3: Picosirius red staining of construct surface under polarized light ..... 91  
Figure 4.4: Immunohistochemistry for type I and II collagen ..... 93  
Figure 4.5: Immunohistochemistry for lubricin on the surface of 4 week constructs . 93  
Figure 4.6: Biochemical content in menisci and media and equilibrium modulus ..... 95

### CHAPTER 5

- Figure 5.1: Photographs of constructs, percent area and percent mass ..... 113  
Figure 5.2: Brightfield picosirius red staining of engineered and native menisci ... 115  
Figure 5.3: Confocal reflectance and polarized picosirius red staining ..... 116  
Figure 5.4: DNA, GAG and collagen content in constructs and media ..... 117  
Figure 5.5: Equilibrium and tensile modulus of meniscal scaffolds ..... 119  
Figure 5.6: Correlation of biochemical components and mechanical properties .... 121  
Figure 5.S1: Immunohistochemistry staining for type II collagen ..... 128

## **CHAPTER 6**

Figure 6.1: Injection molding process and clamping of menisci .....	137
Figure 6.2: Depiction of fast Fourier transform based image analysis.....	140
Figure 6.3: Photographs of constructs, percent area retention and percent mass ..	143
Figure 6.4: Circumferential and radial confocal reflectance images .....	145
Figure 6.5: Circumferential confocal images throughout the meniscus .....	145
Figure 6.6: Circumferential image analysis for alignment and diameter of fibers ....	146
Figure 6.7: Circumferential and radial polarized picosirius red images .....	148
Figure 6.8: GAG and collagen content per meniscus and in media per day .....	150
Figure 6.9: Equilibrium modulus and circumferential and radial tensile modulus ...	151

## **CHAPTER 7**

Figure 7.1: Custom bioreactor capable of applying physiological loading patterns	167
Figure 7.2: FE model mesh, boundary conditions, and strain maps .....	169
Figure 7.3: FE model spatial strain analysis and validation .....	175
Figure 7.4: Circumferential and radial confocal reflectance analysis .....	177
Figure 7.5: Circumferential and radial polarized picosirius red images .....	179
Figure 7.6: Confocal analysis of spatial organization of loaded cross-section .....	180
Figure 7.7: High magnification confocal images of cellular organization .....	181
Figure 7.8: Equilibrium modulus and circumferential and radial tensile modulus ...	182
Figure 7.9: GAG and collagen content of menisci and media .....	184
Figure 7.10: Correlation of local loading environment and biochemical synthesis ..	186
Figure 7.s1: Photographs of constructs, percent area and percent mass .....	176

## **CHAPTER 9**

Figure 9.1: Supplies needed for inquiry experiments .....	231
Figure 9.2: Experiment 1 representative results .....	234
Figure 9.3: Experiment 2 representative results .....	236
Figure 9.4: Experiment 3 setup .....	239

## **APPENDIX B**

Figure B.1: Photographs of constructs and percent area retention .....	250
Figure B.2: Biochemical content of scaffolds .....	251

## LIST OF TABLES

### **CHAPTER 1**

Table 1.1: Native Tensile Properties.....	5
---	---

### **CHAPTER 2**

Table 2.1: Media mixing studies .....	39
Table 2.2: Perfusion studies .....	42

### **CHAPTER 9**

Table 9.1: Collagen Working Solutions.....	232
--	-----

## CHAPTER 1

### Introduction

#### ***An Introduction to the Meniscus***

Menisci are semi-lunar wedge-shaped fibrocartilage discs located on top of the tibial plateau. There are two in each knee which work together to act as shock absorbers, secondary joint stabilizers, load distributors, and joint lubricators<sup>1-3</sup>. Due to the many roles of menisci, they must be able to withstand compressive forces, shear stresses, and tensile hoop stresses<sup>1</sup>.

During each gait cycle, the meniscus is exposed to a compressive load from the femoral condyle. Due to the wedge shape of the meniscus, this compressive load pushes the meniscus outward, however firm ligament attachments at the horns hold the meniscus in place and the compressive load is primarily translated into a circumferential tensile-hoop stress<sup>3, 4</sup>. Thus, the compressive vertical force is redirected into a lateral tensile force and spread across the tibial plateau. The meniscus is able to withstand this loading due to its unique composition, structure, and mechanical properties.

A disruption in any of these properties due to degeneration or tearing results in pain, swelling, and mechanical instability<sup>2</sup>. Meniscal injury is one of the most common traumatic injuries in the knee second only to osteoarthritis, and accounts for over one million surgeries a year in the United States<sup>2, 5</sup>. Treatment of meniscal lesions is the most frequent procedure carried out by orthopedic surgeons, representing 10-20% of all procedures performed<sup>6, 7</sup>.

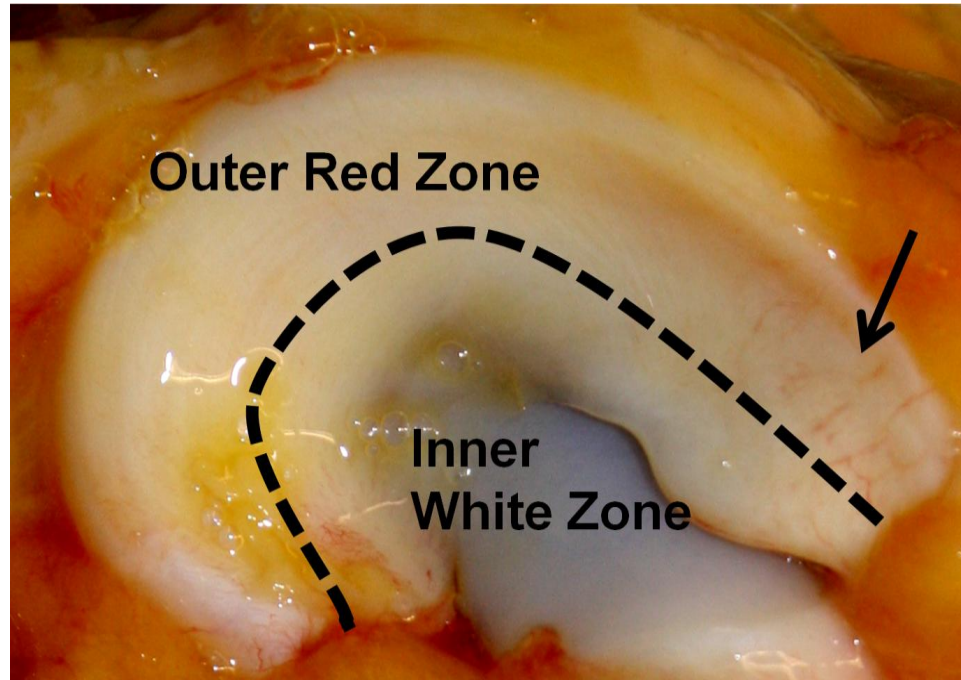


**Figure 1.1:** Native bovine medial meniscus attached to the tibial plateau. Depiction of outer vascularized red zone, and inner avascular white zone. Arrow points to visible blood vessels. The inner white zone is cartilage-like and exposed to compressive loading, while the outer red zone is composed of aligned collagen fibers and exposed to circumferential tensile hoop stresses.

### Meniscal Composition

The meniscus is a fibrocartilaginous structure composed of water (72%), collagen (22% of wet weight), proteoglycans (0.8% of wet weight), cells, and adhesion glycoproteins<sup>2, 5</sup>. Menisci are composed of two main zones divided into the red and white zone (Figure 1.1). The red zone is the peripheral, vascularized region (10-25%), with a more fibrous phenotype<sup>1</sup>. The white zone is the inner more highly loaded region of the meniscus, which is avascular and resembles articular cartilage<sup>1</sup>.

The meniscal matrix is primarily composed of collagen<sup>2, 5</sup>. Type I, II, III, V and VI collagen have all been found within meniscal tissue, accounting for 60-70% of the dry weight, however type I collagen accounting for 90% of the collagen found in the meniscus<sup>2</sup>. Type I collagen, primarily organized into circumferential fibers within the

middle to deep zone (red zone) of the meniscus, provides the tensile strength necessary to resist hoop stresses and shear forces<sup>1, 5</sup>.

The inner, more highly compressed zone (white zone) of the meniscus resembles articular cartilage, however it is not as well organized or extensive. This inner zone is composed predominately of type II collagen and proteoglycans<sup>2, 7</sup>. Proteoglycans, the second major component of the meniscus, are eight-fold less than that found in articular cartilage and are responsible for the hydration, compressive stiffness, and viscoelasticity of the meniscus<sup>2</sup>.

The meniscus is populated by fibrochondrocytes which are capable of making fibrous matrix, while still appearing rounded like a chondrocyte<sup>3, 8</sup>. Four morphologically distinct cells have been identified in the meniscus, however all of these cells are considered to be fibrochondrocytes<sup>9</sup>. Fibrochondrocytes appear fusiform/elongated near the surface of the tissue, rounded and stacked with projections along the outside of fibers in the red zone, and rounded like chondrocytes without projections in the inner white zone<sup>9</sup>.

### Meniscal Structure

The meniscus is uniquely organized into 3 distinct layers of collagen organization to withstand and distribute the complex loads of the knee (Figure 1.2)<sup>10-12</sup>. The outer superficial and lamellar layer consists mainly of thin unorganized collagen fibrils, with a few radial fibers in the lamellar layer<sup>12</sup>. The central layer makes up the majority of the meniscus and is divided into the inner and outer deep zone. The outer zone consists largely of circumferentially aligned collagen bundles in the outer 2/3 of the meniscus. These circumferential fibers are anchored by a small number of perpendicular radial tie fibers that begin at the periphery of the meniscus and travel inward<sup>12-15</sup>. The inner deep zone resembles hyaline cartilage and lacks the strong

circumferential organization. This fibrous outer zone and cartilage like inner zone creates a biphasic, fiber-reinforced, porous-permeable composition which allows the meniscus to optimize its force transmission within the knee<sup>5</sup>.

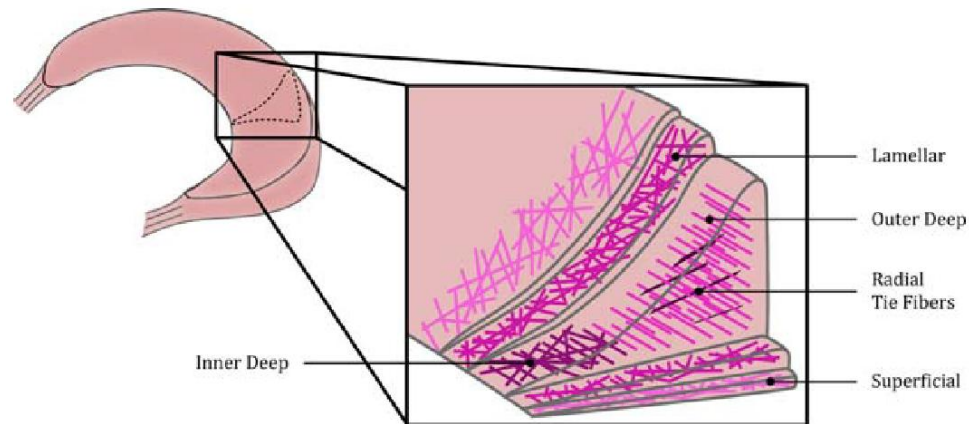


**Figure 1.2** Meniscus three-layer collagen fiber organization. The outer superficial and lamellar layers are thin and consist mostly of unorganized collagen. The inner central deep zone makes up the majority of the meniscus and consists primarily of circumferentially aligned fibers with a few dispersed radial tie fibers. Image reproduced with permission from Hasan et al.<sup>7</sup>

### Meniscal Mechanical Properties

The complex organization of the meniscus results in anisotropic mechanical properties, which is essential to the function of the tissue. The compressive equilibrium modulus has been reported to vary across the meniscus from 110-200 kPa in humans, and vary from 100-450 kPa across species, with the anterior horn often being the stiffest location<sup>2, 16, 17</sup>.

Reported native tensile properties vary greatly due to location, testing method, and age of the animal (Table 1.1). Due to the strong circumferential alignment of fibers, the meniscus has anisotropic tensile properties which are 3-10 times greater circumferentially compared to the radial direction<sup>12, 13, 18, 19</sup>. Actual magnitudes of these directional tensile properties vary widely due to size of sample, location, and

age of animal<sup>10, 19-23</sup>. Early studies tested very thin samples ( $\leq 0.5$  mm) and reported circumferential tensile properties of 100-300 MPa, and radial properties of 30-70 MPa that varied with location in the meniscus<sup>10, 19, 23</sup>. However, more recent studies have examined the effect of thickness and location. They found that a more appropriate thickness of  $\sim 3$ mm, which accounts for the macroscopic properties, results in a circumferential modulus of 50 MPa in humans and bovine<sup>20, 22</sup>. They also reported no change in modulus with location in the meniscus<sup>22</sup>. Additionally, immature menisci have been shown to have further reduced tensile properties (Chapter 6)<sup>21</sup>.

**Table 1.1: Native Tensile Properties**

<b>Study</b>	<b>Thickness x Width (mm)</b>	<b>Species</b>	<b>Age</b>	<b>Circumferential Modulus (MPa)</b>	<b>Radial Modulus (MPa)</b>
Proctor 1989 <sup>16</sup>	0.4 x 1	Bovine	Adult	50-200	3-70
Fithian 1990 <sup>10</sup>	0.4 x 1	Human	Adult	160-300	-
Skaggs 1994 <sup>23</sup>	0.4 x 1	Bovine	Adult	-	10-45
Tissakht 1995 <sup>19</sup>	0.8-2 x 1.75-3	Human	Adult	70-130	4-17
Lechner 2000 <sup>22</sup>	0.5 x 1	Human	Adult	110-140	-
	1.5 x 1			60-105	-
	3.0 x 1			40-70	-
Danso 2014 <sup>20</sup>	0.4 x 3	Bovine	Adult	50	-
Eleswarapu 2011 <sup>21</sup>	$\leq 1 \times \leq 1$	Bovine	Immature	20-25	-
Puetzer (Chapter 6)	1.5-2 x 3	Bovine	Immature	12-14	3-4

### Meniscal Development

Although only a few studies have examined the development of the meniscus, it is apparent meniscal development is dependent on mechanical stimulation<sup>24-27</sup>. During development, menisci start out as dense unorganized cellular structures. At 10 weeks the attachments to the tibial plateau are visible<sup>26</sup>. At 14 weeks spindle-shaped cells begin to align and form collagen bundles which grow in size with time. Later, perpendicular radial fibers begin to appear<sup>24, 25</sup>. Meniscal fibrochondrocytes are thought to have an intrinsic ability to form specific structures<sup>9, 28, 29</sup> and it has been demonstrated that these early stages of development are intrinsically regulated<sup>27</sup>. However, mechanical stimulation is needed in order for collagen fibers to continue to grow and develop. If mechanical stimulation is removed the meniscus fails to mature and ultimately degenerates<sup>24, 27</sup>. The importance of mechanical stimulation in development is further evident throughout adolescence, as the circumferential and radial fibers continue to align and develop with increased joint motion and weight-bearing<sup>24</sup>.

### ***Meniscal Injuries and Repair***

Injuries to menisci are most commonly tears, although menisci can also be injured by separation from the tibial attachments and degeneration of the tissue. There are many different kinds of tears such as bucket-handle, radial, longitudinal, and complex<sup>2</sup>. Tears in the peripheral vascularized region tend to heal naturally, as expected, but do not always return to native mechanical function. However the majority of tears are in the inner avascular region and do not heal<sup>2, 5</sup>. The most common causes of meniscal tears are traumatic injury (often caused by athletic activity) and degenerative processes. Osteoarthritic degenerative changes in the

meniscus have been associated with ~75% of all meniscal tears and are often non-repairable<sup>7</sup>. Failure due to tearing or defects results in pain, swelling, and mechanical instability<sup>2</sup>.

Historically, the first major way to repair meniscal defects was to perform a total meniscectomy. This was when the meniscus was believed to have no role in the knee. It was quickly observed that total meniscectomy resulted in the early onset of osteoarthritis and total knee instability<sup>2</sup>. While there have been improvements in suturing techniques and materials for repair of focal lesions<sup>30-32</sup>, only ~15% of tears are believed to be repairable<sup>33</sup>. Partial meniscectomy is still used today to treat tears in the avascular zone, however it often results in degenerative changes leading to osteoarthritis<sup>2</sup>. The best available treatment for total meniscal damage is meniscectomy and replacement with cadaveric allograft. However this treatment is only available to a small percentage of people because donor tissue is scarce, it is difficult to match the native joint architecture, allografts have been shown to create high friction in the joint resulting in abrasion and damage to surrounding cartilage, and there is risk of disease transmission<sup>1,2,6</sup>.

### ***Meniscal Tissue Engineering***

Due to the negatives of allograft transplantation, the use of tissue engineering (TE) to develop a meniscal construct is very promising. A TE meniscus is believed to need to be geometrically accurate to ensure the appropriate distribution of pressures across the joint, it must be able to withstand anatomical compressive and tensile loading conditions prior to implantation, and should achieve the heterogeneous mechanical and biochemical properties found in native menisci<sup>1, 2, 34</sup>. There have been a lack of attempts to tissue engineer the meniscus in comparison to attempts to tissue engineer other musculoskeletal tissues such as bone and articular cartilage.

Research concentrated for many years on treatment of point defects and extracellular matrix (ECM) production in plugs due to the complicated geometry of the meniscus<sup>28, 35-37</sup>. Recently, several studies have attempted to create whole TE meniscal replacements made from either synthetic or natural materials<sup>1, 2, 29, 38-51</sup>. Natural scaffolds often lack the necessary mechanical properties; while synthetic scaffolds cause an immune response or degradation of surround articular cartilage<sup>1, 2, 6</sup>. Further, most scaffolds lack the anisotropic properties and organization of native tissue which are known to be fundamental to the ability of the meniscus to properly distribute the loads of the knee. None of these efforts have achieved clinical use, as many lack the organization, mechanical properties, or means of attachment necessary to withstand implantation *in vivo*.

### ***Previous Research***

Efforts to tissue engineer a meniscal replacement are a driving force in the Bonassar lab. Previously, we have developed a method of creating anatomically shaped menisci through the use of an image guided injection molding system<sup>42</sup>. Briefly, this method consists of obtaining images from micro computed tomography ( $\mu$ CT) and/or magnetic resonance imaging (MRI). Using computer software, the meniscus shape is abstracted and used as a negative solid to create a mold. Injection molding techniques are then used to create a meniscal construct that mimics the geometry of native tissue<sup>42</sup>. This technique has been used to create seeded alginate meniscal constructs, which maintain their shape fidelity while significantly increasing mechanical and biochemical properties through 8 weeks of static culture<sup>42</sup>. However the construct properties were still inferior to native properties.

Mechanical conditioning is widely used to enhance the *in vitro* formation of various types of TE cartilage, often resulting in increased mechanical and

biochemical properties (see chapter 2 for a review). Several studies have utilized dynamic compression to characterize the mechanical and biochemical properties of meniscal explants<sup>52-62</sup>. Many of these studies<sup>52-55, 60-62</sup>, and several TE studies<sup>36, 41, 63, 64</sup> have established that mechanical conditioning stimulates meniscal fibrochondrocytes to enhance ECM production and mechanical properties of explants and scaffolds.

In an effort to further increase the mechanical and biochemical properties of alginate meniscal constructs, a bioreactor was constructed to apply mechanical stimulation in the form of dynamic compression<sup>41</sup>. The bioreactor was designed using the MRI images previously used to create the meniscal molds. A loading platen and tray were created that conformed to the complex geometry of the meniscal constructs to apply a uniform deformation. The loading tray was also designed to restrict the motion of the engineered constructs when exposed to dynamic loading so to apply correct compressive strain<sup>41</sup>. A poroelastic finite element model simulation was performed using COMSOL Multiphysics to confirm that local strains throughout the meniscal constructs were relatively uniform and that loading was within physiological ranges<sup>41</sup>.

Recently, we reported that dynamic compression of anatomically shaped TE alginate menisci significantly enhanced ECM production and mechanical properties after 2 weeks of loading<sup>41</sup>. However, prolonged loading resulted in decreased mechanical performance and matrix retention due to either increased alginate degradation<sup>64</sup> or an induced catabolic cellular responses<sup>58, 62, 65-67</sup>. Further, these menisci had inferior properties and organization compared to native menisci, particularly in tensile modulus and collagen content, and a large amount of produced matrix was lost to the media during culture, primarily due to the alginate scaffold.

This dissertation sought to improve these alginate menisci and engineer a meniscus more analogous to native tissue

### ***Research Objectives***

The focus of this dissertation was to investigate mechanical stimulation, chemical stimulation, and material choice on the structure, composition and mechanical properties of tissue engineered menisci. The long term goal of this research project was development of an anatomically correct meniscal construct with native-like organization, composition and mechanical properties. The overriding hypotheses were that 1) varied mechanical loading and growth factor treatment would further improve the properties of alginate menisci, 2) seeded TE menisci composed of type I collagen would produce constructs with biochemical and mechanical properties more analogous to native menisci than alginate, and 3) that mechanical stimulation would further increase the properties and organization of these collagen menisci. The completion of this dissertation has resulted in the creation of a bioreactor capable of applying physiological loading patterns and the development of the most organized meniscal constructs to date. These high density collagen menisci not only match native circumferential fiber alignment and diameter, but are the first meniscal constructs to have native-like radial development.

### **Improvement of Alginate Menisci**

The first two studies of this dissertation are concentrated on improving the properties of alginate menisci. As mentioned previously, mechanical stimulation has been well established to improve the properties of engineered cartilage (see chapter 2 for a review), and we have previously found that just 2 weeks of dynamic compression could significantly improve the properties of alginate menisci<sup>41</sup>.

However, prolonged loading resulted in a decrease in properties. This was consistent with a growing trend in the literature that prolonged mechanical stimulation was not optimal for meniscal tissue explants<sup>58, 62</sup> and engineered cartilage<sup>65-67</sup>. It is believed that load induced catabolic responses are important to initiate proteoglycan turnover and development of a functional construct, however sustained expression of these catabolic genes as a result of prolonged loading can lead to tissue degradation<sup>65, 68-70</sup>.

Recently, it has been demonstrated that removal of mechanical stimulation downregulates catabolic activity while anabolic activity continues, resulting in significant improvements in tissue development<sup>69, 70</sup>. These studies show great promise for how the duration and timing of dynamic compression affect the development of engineered articular cartilage. However, such effects have never been studied in engineered fibrocartilage. We hypothesized that the timing and duration of loading (i.e. duty cycle) regulates ECM assembly of TE menisci. The specific goal of the first aim (Chapter 3) was to examine the effects of varying the duration of load and static culture on the structure, composition, and mechanical properties of seeded alginate menisci.

The second aim sought to improve the properties of alginate menisci using chemical stimulation. A limited number of studies have investigated the use of growth factors to improve engineered menisci<sup>43, 71-74</sup>, of which only two have examined the effect of insulin-like growth factor (IGF)-I<sup>71, 73</sup>. IGF-I is known to have a stimulatory effect on musculoskeletal soft tissue regeneration and while it has shown promise in meniscal fibrochondrocytes seeded scaffolds, its effect on large constructs and mechanical properties was unknown. The objective of aim 2 (Chapter 4) was to determine the effect of IGF-I on the development of alginate menisci.

## Development of Collagen Menisci

Despite the improvements gained in Aim 1 and 2, the alginate menisci still had inferior properties to native tissue. Alginate menisci had collagen and glycosaminoglycans (GAGs) content less than native menisci, poor tensile properties, and due to the lack of ligands in alginate<sup>75</sup>, a large amount of produced matrix and cells was being lost to the media during culture<sup>41</sup>.

Collagen was an attractive alternative to alginate. As mentioned previously, type I collagen is the major component of the meniscus and its circumferential fiber organization plays a large role in the transmission of load in the knee<sup>2, 3</sup>. Due to the prevalence and large roll type I collagen plays in the meniscus, it makes sense to start with a scaffold primarily composed of collagen. Collagen is a natural material composed of fibers that allow for increased tensile properties, better retention of cells and matrix material, and a place for cells to attach and remodel the matrix into a more mechanically stable material<sup>37, 76</sup>. The remainder of this thesis will concentrate on the investigation of high density type I collagen gels and their response to mechanical stimulation (Chapters 5-7).

Collagen freeze-dried matrixes are the most successful meniscal scaffold to date, however these matrixes often have high resorption without replacement of organized collagen, weak mechanical properties, contraction, and are not anatomically shaped<sup>30, 37, 77-79</sup>. We sought to overcome these obstacles by making an anatomical meniscal construct using an injection molded collagen gel and *in vitro* culture. Low density collagen gels (1-5 mg/ml) have been investigated for decades in many different TE applications, but have often been avoided in orthopaedic applications due to weak mechanical strength, low shape fidelity, and high contraction<sup>76</sup>. Recently, high density gels (10-20 mg/ml) were shown to be moldable, have stronger mechanical properties and have decreased contraction, while still allowing the cells to proliferate

and rearrange the matrix<sup>76</sup>. The third aim of this dissertation investigated the potential of high density collagen gels as meniscal replacements and compared results to the previous alginate system (Chapter 5).

Finally, all of the previous collagen gel studies have investigated minimal *in vitro* culture techniques to improve the mechanical and biochemical properties of the constructs prior to implantation. Collagen fibrils and cells are known to align when exposed to mechanical boundary conditions and mechanical stimulation<sup>80-85</sup>. However, the effects of mechanical constraints and simulation on fibrochondrocyte seeded collagen gels or high density collagen gels had not been studied. The objectives of aim 4 were to investigate the use of physiologically relevant boundary conditions, develop a bioreactor that applies physiological loading patterns and investigate the effect of mechanical stimulation on the organization and development of high density collagen menisci. In aim 4a (Chapter 6) we investigated the use of biomimetic horn-anchored boundary conditions to drive toward native-like circumferential alignment and anisotropic tensile properties in collagen menisci. In aim 4b (Chapter 7) we developed a bioreactor that better mimics the complex compressive-tensile loading environment of native menisci by combining the horn-anchored boundary conditions from Chapter 6 with compressive dynamic loading. We then investigated the application of this mechanical stimulation to develop engineered menisci with heterogenic properties.

### *Specific Aims*

#### **Specific Aim 1 (Chapter 3)**

Examine the effects of varying load and static culture duration on the biochemical and mechanical properties of alginate menisci

This study was divided into two parts in which dynamic compressive loading was applied by I) varying the duration of dynamic loading over 4 weeks of culture, and II) altering the period of static culture after 2 weeks of loading. Anatomical meniscal constructs were created by injection molding a mixture of 2% w/v alginate and bovine meniscal fibrochondrocytes. Constructs were dynamically compressed three times a week via a custom bioreactor for up to 4 weeks and then placed in static culture. After 4 weeks of culture, increased load duration was found to be beneficial to matrix formation and mechanical properties, with no additional benefit from loading past 2 weeks. Samples loaded for 2 weeks followed by 4 week static culture yielded the most mature matrix with significant improvements in collagen bundle formation, 2.8 fold increase in GAG content, 2 fold increase in collagen content, and 4.3 fold increase in the compressive equilibrium modulus. Overall this study demonstrated the importance of timing and duration of loading and provided a new *in vitro* mechanism for conditioning engineered menisci. By switching to prolonged static culture after 2 weeks of loading, meniscal constructs not only maintained meniscal properties but further significantly improve them.

#### **Specific Aim 2 (Chapter 4)**

Examine the effect insulin-like growth factor (IGF)-I on the development of alginate menisci.

Fibrochondrocyte seeded alginate menisci were created by injection molding and cultured for up to 4 weeks with or without 100 ng/mL IGF-I supplementation. After 4 weeks of culture, IGF-I treatment resulted in a 26 fold increase in GAG content, 10

fold increase in collagen content, and a 3 fold increase in the equilibrium modulus. Interestingly, IGF-I treated menisci developed a distinct surface layer similar to native tissue which stained positive for type I and II collagen and lubricin. Overall, this study demonstrated IGF-I treatment can significantly improve the biochemical and mechanical properties of engineered tissues and aids in the development of a distinct surface zone similar to the native superficial zone. This was the first study to demonstrate the accumulation of endogenous lubricin and the production of a well defined surface zone in engineered menisci, which will most likely be necessary for successful function when implanted into the knee.

### **Specific Aim 3 (Chapter 5)**

Investigate the potential of high density type I collagen gels as meniscal scaffolds and compare to alginate controls.

First a method for injection molding high density collagen gels was developed. Then, bovine meniscal fibrochondrocytes were mixed into collagen, injected into anatomical meniscal molds to create 10 and 20 mg/ml collagen menisci and cultured for up to 4 weeks. By 4 weeks of culture, collagen menisci preserved their shape and DNA content while significantly improving GAG and collagen concentrations above alginate controls. Further, collagen menisci matched alginate equilibrium modulus while developing a 3-6 fold higher tensile modulus by 4 weeks. Generally, 10 and 20 mg/ml collagen menisci performed similarly; however 20 mg/ml collagen menisci did contract less while having higher mechanical properties. Both 10 and 20 mg/ml collagen menisci did significantly contract with time in culture and fibrochondrocytes were able to reorganize the collagen gels into a more fibrous appearance. This

suggested that by harnessing fibrochondrocyte interaction with high density collagen scaffolds, it could be possible to induce native organization.

#### **Specific Aim 4 (Chapter 6 and 7)**

Characterization of the effect of mechanical stimulations on the development of tissue engineered collagen menisci.

##### *Specific Aim 4a (Chapter 6)*

Investigate the effect of long-term biomimetic boundary conditions on the organization and development of high density collagen menisci

In order to apply biomimetic horn-anchored boundary conditions, meniscal molds were redesigned with extensions at each horn. Further, culture trays were designed to have clamps that screwed down over the extensions, securing them in place throughout culture. This culture condition not only mimics the native horn attachment sites but also restricts contraction circumferentially, in turn creating hoop stress to encourage circumferential alignment. Ten and 20 mg/ml collagen menisci seeded with bovine fibrochondrocytes were again created and cultured for up to 8 weeks. Clamped menisci preserved their size and shape and by 8 weeks of culture developed native-like aligned and sized circumferential fibers, native-like radial organizations, increased collagen accumulation and improved mechanical properties compared to unclamped menisci. These are the first meniscal constructs to demonstrate native-like radial development. The clamped menisci organization was further reflected in the development of anisotropic tensile properties that matched anisotropic ratios of native menisci with 2-3 fold higher circumferential moduli compared to radial moduli.

*Specific Aim 4b (Chapter 7)*

Investigate the effect of physiological loading patterns on the organization, composition and mechanical properties of engineered collagen menisci.

A more physiological bioreactor was developed by combining horn-anchored boundary conditions with compressive loading. Compressive load was applied with a loading platen the shape of the femoral condyles. FE analysis confirmed the bioreactor applied physiological load patterns with more compression in the horns and more tensile load in the back of the meniscus. Twenty mg/ml collagen menisci seeded with bovine fibrochondrocytes were injection molded and clamped as in the previous studies and then loaded for up to 4 weeks. Loading was found to accelerated organization and development. After 4 weeks of culture, loaded menisci matched native organization, tensile anisotropy ratios and equilibrium modulus. Loaded menisci improved GAG accumulation 3.5 fold, collagen accumulation 1.5 fold, equilibrium modulus 19 fold, and tensile moduli 6-13 fold, demonstrating native-like compressive-tensile loading can enhance all fibrocartilage properties. Further this study demonstrated that local changes in mechanical environment can drive heterogeneous tissue synthesis and organization. These are some of the most organized meniscal scaffold developed to date and demonstrate great promise as meniscal replacements.

## REFERENCES

1. Buma P., Ramrattan N.N., van Tienen T.G., Veth R.P. Tissue engineering of the meniscus. *Biomaterials*.**25**:1523. 2004.
2. Sweigart M.A., Athanasiou K.A. Toward tissue engineering of the knee meniscus. *Tissue Eng*.**7**:111. 2001.
3. Kawamura S., Lotito K., Rodeo S.A. Biomechanics and healing response of the meniscus. *Oper Techn Sport Med*.**11**:68. 2003.
4. AufderHeide A.C., Athanasiou K.A. Mechanical stimulation toward tissue engineering of the knee meniscus. *Ann Biomed Eng*.**32**:1161. 2004.
5. Khetia E.A., McKeon B.P. Meniscal allografts: biomechanics and techniques. *Sports Med Arthrosc*.**15**:114. 2007.
6. Peters G., Wirth C.J. The current state of meniscal allograft transplantation and replacement. *Knee*.**10**:19. 2003.
7. Hasan J., Fisher J., Ingham E. Current strategies in meniscal regeneration. *J Biomed Mater Res B Appl Biomater*. 2013.
8. Webber R.J., Harris M.G., Hough A.J., Jr. Cell culture of rabbit meniscal fibrochondrocytes: proliferative and synthetic response to growth factors and ascorbate. *J Orthop Res*.**3**:36. 1985.
9. Hellio Le Graverand M.P., Ou Y., Schield-Yee T., Barclay L., Hart D., Natsume T., et al. The cells of the rabbit meniscus: their arrangement, interrelationship, morphological variations and cytoarchitecture. *J Anat*.**198**:525. 2001.
10. Fithian D.C., Kelly M.A., Mow V.C. Material properties and structure-function relationships in the menisci. *Clin Orthop Relat Res*.**19**. 1990.
11. Haut Donahue T.L., Hull M.L., Rashid M.M., Jacobs C.R. How the stiffness of meniscal attachments and meniscal material properties affect tibio-femoral contact pressure computed using a validated finite element model of the human knee joint. *J Biomech*.**36**:19. 2003.

12. Petersen W., Tillmann B. Collagenous fibril texture of the human knee joint menisci. *Anat Embryol.***197**:317. 1998.
13. Rattner J.B., Matyas J.R., Barclay L., Holowaychuk S., Sciore P., Lo I.K., et al. New understanding of the complex structure of knee menisci: implications for injury risk and repair potential for athletes. *Scand J Med Sci Sports.***21**:543. 2011.
14. Aspden R.M., Yarker Y.E., Hukins D.W. Collagen orientations in the meniscus of the knee joint. *J Anat.***140 ( Pt 3)**:371. 1985.
15. Kambic H.E., McDevitt C.A. Spatial organization of types I and II collagen in the canine meniscus. *J Orthop Res.***23**:142. 2005.
16. Proctor C.S., Schmidt M.B., Whipple R.R., Kelly M.A., Mow V.C. Material properties of the normal medial bovine meniscus. *J Orthop Res.***7**:771. 1989.
17. Sweigart M.A., Zhu C.F., Burt D.M., DeHoll P.D., Agrawal C.M., Clanton T.O., et al. Intraspecies and interspecies comparison of the compressive properties of the medial meniscus. *Ann Biomed Eng.***32**:1569. 2004.
18. Makris E.A., Hadidi P., Athanasiou K.A. The knee meniscus: structure-function, pathophysiology, current repair techniques, and prospects for regeneration. *Biomaterials.***32**:7411. 2011.
19. Tissakht M., Ahmed A.M. Tensile stress-strain characteristics of the human meniscal material. *J Biomech.***28**:411. 1995.
20. Danso E.K., Honkanen J.T., Saarakkala S., Korhonen R.K. Comparison of nonlinear mechanical properties of bovine articular cartilage and meniscus. *J Biomech.***47**:200. 2014.
21. Eleswarapu S.V., Responde D.J., Athanasiou K.A. Tensile properties, collagen content, and crosslinks in connective tissues of the immature knee joint. *PLoS One.***6**:e26178. 2011.
22. Lechner K., Hull M.L., Howell S.M. Is the circumferential tensile modulus within a human medial meniscus affected by the test sample location and cross-sectional area? *J Orthop Res.***18**:945. 2000.

23. Skaggs D.L., Warden W.H., Mow V.C. Radial tie fibers influence the tensile properties of the bovine medial meniscus. *J Orthop Res.***12**:176. 1994.
24. Clark C.R., Ogden J.A. Development of the menisci of the human knee joint. Morphological changes and their potential role in childhood meniscal injury. *J Bone Joint Surg Am.***65**:538. 1983.
25. Fukazawa I., Hatta T., Uchio Y., Otani H. Development of the meniscus of the knee joint in human fetuses. *Congenit Anom (Kyoto).***49**:27. 2009.
26. Merida-Velasco J.A., Sanchez-Montesinos I., Espin-Ferra J., Rodriguez-Vazquez J.F., Merida-Velasco J.R., Jimenez-Collado J. Development of the human knee joint. *Anat Rec.***248**:269. 1997.
27. Mikic B., Johnson T.L., Chhabra A.B., Schalet B.J., Wong M., Hunziker E.B. Differential effects of embryonic immobilization on the development of fibrocartilaginous skeletal elements. *J Rehabil Res Dev.***37**:127. 2000.
28. Ibarra C., Jannetta C., Vacanti C.A., Cao Y., Kim T.H., Upton J., et al. Tissue engineered meniscus: a potential new alternative to allogeneic meniscus transplantation. *Transplant Proc.***29**:986. 1997.
29. Puetzer J.L., Bonassar L.J. High density type I collagen gels for tissue engineering of whole menisci. *Acta Biomater.***9**:7787. 2013.
30. Stone K.R., Steadman J.R., Rodkey W.G., Li S.T. Regeneration of meniscal cartilage with use of a collagen scaffold. Analysis of preliminary data. *J Bone Joint Surg Am.***79**:1770. 1997.
31. Farnig E., Sherman O. Meniscal repair devices: a clinical and biomechanical literature review. *Arthroscopy.***20**:273. 2004.
32. McDermott I. Meniscal tears, repairs and replacement: their relevance to osteoarthritis of the knee. *Br J Sports Med.***45**:292. 2011.
33. Tudor F., McDermott I.D., Myers P. Meniscal Repair: a review of current practice. *Orthopaedics and Trauma.* **In press**. 2014.
34. Hoben G.M., Athanasiou K.A. Meniscal repair with fibrocartilage engineering. *Sports Med Arthrosc.***14**:129. 2006.

35. Aufderheide A.C., Athanasiou K.A. Comparison of scaffolds and culture conditions for tissue engineering of the knee meniscus. *Tissue Eng.***11**:1095. 2005.
36. Gunja N.J., Athanasiou K.A. Effects of hydrostatic pressure on leporine meniscus cell-seeded PLLA scaffolds. *J Biomed Mater Res A.***92**:896. 2010.
37. Mueller S.M., Shortkroff S., Schneider T.O., Breinan H.A., Yannas I.V., Spector M. Meniscus cells seeded in type I and type II collagen-GAG matrices in vitro. *Biomaterials.***20**:701. 1999.
38. Balint E., Gatt C.J., Jr., Dunn M.G. Design and mechanical evaluation of a novel fiber-reinforced scaffold for meniscus replacement. *J Biomed Mater Res A.***100**:195. 2012.
39. Zur G., Linder-Ganz E., Elsner J.J., Shani J., Brenner O., Agar G., et al. Chondroprotective effects of a polycarbonate-urethane meniscal implant: histopathological results in a sheep model. *Knee Surg Sports Traumatol Arthrosc.***19**:255. 2011.
40. Aufderheide A.C., Athanasiou K.A. Assessment of a bovine co-culture, scaffold-free method for growing meniscus-shaped constructs. *Tissue Eng.***13**:2195. 2007.
41. Ballyns J.J., Bonassar L.J. Dynamic compressive loading of image-guided tissue engineered meniscal constructs. *J Biomech.***44**:509. 2011.
42. Ballyns J.J., Gleghorn J.P., Niebrzydowski V., Rawlinson J.J., Potter H.G., Maher S.A., et al. Image-guided tissue engineering of anatomically shaped implants via MRI and micro-CT using injection molding. *Tissue Eng Part A.***14**:1195. 2008.
43. Huey D.J., Athanasiou K.A. Maturation growth of self-assembled, functional menisci as a result of TGF-beta1 and enzymatic chondroitinase-ABC stimulation. *Biomaterials.***32**:2052. 2011.
44. Kang S.W., Son S.M., Lee J.S., Lee E.S., Lee K.Y., Park S.G., et al. Regeneration of whole meniscus using meniscal cells and polymer scaffolds in a rabbit total meniscectomy model. *J Biomed Mater Res A.***78**:659. 2006.
45. Mandal B.B., Park S.H., Gil E.S., Kaplan D.L. Multilayered silk scaffolds for meniscus tissue engineering. *Biomaterials.***32**:639. 2011.

46. Stabile K.J., Odom D., Smith T.L., Northam C., Whitlock P.W., Smith B.P., et al. An acellular, allograft-derived meniscus scaffold in an ovine model. *Arthroscopy*.**26**:936. 2010.
47. Gunja N.J., Huey D.J., James R.A., Athanasiou K.A. Effects of agarose mould compliance and surface roughness on self-assembled meniscus-shaped constructs. *J Tissue Eng Regen Med*.**3**:521. 2009.
48. Kon E., Chiari C., Marcacci M., Delcogliano M., Salter D.M., Martin I., et al. Tissue engineering for total meniscal substitution: animal study in sheep model. *Tissue Eng Part A*.**14**:1067. 2008.
49. Stapleton T.W., Ingram J., Fisher J., Ingham E. Investigation of the regenerative capacity of an acellular porcine medial meniscus for tissue engineering applications. *Tissue Eng Part A*.**17**:231. 2011.
50. Tienen T.G., Heijkants R.G., de Groot J.H., Schouten A.J., Pennings A.J., Veth R.P., et al. Meniscal replacement in dogs. Tissue regeneration in two different materials with similar properties. *J Biomed Mater Res B Appl Biomater*.**76**:389. 2006.
51. Higashioka M.M., Chen J.A., Hu J.C., Athanasiou K.A. Building an anisotropic meniscus with zonal variations. *Tissue Eng Part A*.**20**:294. 2014.
52. Aufderheide A.C., Athanasiou K.A. A direct compression stimulator for articular cartilage and meniscal explants. *Ann Biomed Eng*.**34**:1463. 2006.
53. Bursac P., Arnoczky S., York A. Dynamic compressive behavior of human meniscus correlates with its extra-cellular matrix composition. *Biorheology*.**46**:227. 2009.
54. Chia H.N., Hull M.L. Compressive moduli of the human medial meniscus in the axial and radial directions at equilibrium and at a physiological strain rate. *J Orthop Res*.**26**:951. 2008.
55. Fink C., Fermor B., Weinberg J.B., Pisetsky D.S., Misukonis M.A., Guilak F. The effect of dynamic mechanical compression on nitric oxide production in the meniscus. *Osteoarthritis Cartilage*.**9**:481. 2001.
56. Hennerbichler A., Fermor B., Hennerbichler D., Weinberg J.B., Guilak F. Regional differences in prostaglandin E2 and nitric oxide production in the knee meniscus

- in response to dynamic compression. *Biochem Biophys Res Commun.***358**:1047. 2007.
57. Lai J.H., Levenston M.E. Meniscus and cartilage exhibit distinct intra-tissue strain distributions under unconfined compression. *Osteoarthritis Cartilage.***18**:1291. 2010.
58. McHenry J.A., Zielinska B., Donahue T.L. Proteoglycan breakdown of meniscal explants following dynamic compression using a novel bioreactor. *Ann Biomed Eng.***34**:1758. 2006.
59. McNulty A.L., Estes B.T., Wilusz R.E., Weinberg J.B., Guilak F. Dynamic loading enhances integrative meniscal repair in the presence of interleukin-1. *Osteoarthritis Cartilage.***18**:830. 2010.
60. Shin S.J., Fermor B., Weinberg J.B., Pisetsky D.S., Guilak F. Regulation of matrix turnover in meniscal explants: role of mechanical stress, interleukin-1, and nitric oxide. *J Appl Physiol.***95**:308. 2003.
61. Upton M.L., Chen J., Guilak F., Setton L.A. Differential effects of static and dynamic compression on meniscal cell gene expression. *J Orthop Res.***21**:963. 2003.
62. Zielinska B., Killian M., Kadmiel M., Nelsen M., Haut Donahue T.L. Meniscal tissue explants response depends on level of dynamic compressive strain. *Osteoarthritis Cartilage.***17**:754. 2009.
63. Huey D.J., Athanasiou K.A. Tension-compression loading with chemical stimulation results in additive increases to functional properties of anatomic meniscal constructs. *PLoS One.***6**:e27857. 2011.
64. Ballyns J.J., Wright T.M., Bonassar L.J. Effect of media mixing on ECM assembly and mechanical properties of anatomically-shaped tissue engineered meniscus. *Biomaterials.***31**:6756. 2010.
65. Kisiday J.D., Lee J.H., Siparsky P.N., Frisbie D.D., Flannery C.R., Sandy J.D., et al. Catabolic responses of chondrocyte-seeded peptide hydrogel to dynamic compression. *Ann Biomed Eng.***37**:1368. 2009.

66. Kock L.M., Schulz R.M., van Donkelaar C.C., Thummler C.B., Bader A., Ito K. RGD-dependent integrins are mechanotransducers in dynamically compressed tissue-engineered cartilage constructs. *J Biomech.***42**:2177. 2009.
67. Villanueva I., Hauschulz D.S., Mejjic D., Bryant S.J. Static and dynamic compressive strains influence nitric oxide production and chondrocyte bioactivity when encapsulated in PEG hydrogels of different crosslinking densities. *Osteoarthritis Cartilage.***16**:909. 2008.
68. Blain E.J. Mechanical regulation of matrix metalloproteinases. *Front Biosci.***12**:507. 2007.
69. De Croos J.N., Dhaliwal S.S., Grynepas M.D., Pilliar R.M., Kandel R.A. Cyclic compressive mechanical stimulation induces sequential catabolic and anabolic gene changes in chondrocytes resulting in increased extracellular matrix accumulation. *Matrix Biol.***25**:323. 2006.
70. Nicodemus G.D., Bryant S.J. Mechanical loading regimes affect the anabolic and catabolic activities by chondrocytes encapsulated in PEG hydrogels. *Osteoarthritis Cartilage.***18**:126. 2010.
71. Stewart K., Pabbruwe M., Dickinson S., Hollander A.P., Chaudhuri J.B. The effect of growth factor treatment on meniscal chondrocyte proliferation and differentiation on polyglycolic acid scaffolds. *Tissue Engineering.***13**:271. 2007.
72. Ionescu L.C., Lee G.C., Huang K.L., Mauck R.L. Growth factor supplementation improves native and engineered meniscus repair in vitro. *Acta Biomater.* 2012.
73. Pangborn C.A., Athanasiou K.A. Growth factors and fibrochondrocytes in scaffolds. *Journal of Orthopaedic Research.***23**:1184. 2005.
74. Zaleskas J.M., Kinner B., Freyman T.M., Yannas I.V., Gibson L.J., Spector M. Growth factor regulation of smooth muscle actin expression and contraction of human articular chondrocytes and meniscal cells in a collagen-GAG matrix. *Experimental Cell Research.***270**:21. 2001.
75. Awad H.A., Wickham M.Q., Leddy H.A., Gimple J.M., Guilak F. Chondrogenic differentiation of adipose-derived adult stem cells in agarose, alginate, and gelatin scaffolds. *Biomaterials.***25**:3211. 2004.

76. Cross V.L., Zheng Y., Won Choi N., Verbridge S.S., Sutermaster B.A., Bonassar L.J., et al. Dense type I collagen matrices that support cellular remodeling and microfabrication for studies of tumor angiogenesis and vasculogenesis in vitro. *Biomaterials*.**31**:8596. 2010.
77. Martinek V., Ueblacker P., Braun K., Nitschke S., Mannhardt R., Specht K., et al. Second generation of meniscus transplantation: in-vivo study with tissue engineered meniscus replacement. *Arch Orthop Trauma Surg*.**126**:228. 2006.
78. Stone K.R., Rodkey W.G., Webber R., McKinney L., Steadman J.R. Meniscal regeneration with copolymeric collagen scaffolds. In vitro and in vivo studies evaluated clinically, histologically, and biochemically. *Am J Sports Med*.**20**:104. 1992.
79. Walsh C.J., Goodman D., Caplan A.I., Goldberg V.M. Meniscus regeneration in a rabbit partial meniscectomy model. *Tissue Eng*.**5**:327. 1999.
80. Ferdous Z., Lazaro L.D., Iozzo R.V., Hook M., Grande-Allen K.J. Influence of cyclic strain and decorin deficiency on 3D cellularized collagen matrices. *Biomaterials*.**29**:2740. 2008.
81. Girton T.S., Barocas V.H., Tranquillo R.T. Confined compression of a tissue-equivalent: collagen fibril and cell alignment in response to anisotropic strain. *J Biomech Eng*.**124**:568. 2002.
82. Tower T.T., Neidert M.R., Tranquillo R.T. Fiber alignment imaging during mechanical testing of soft tissues. *Ann Biomed Eng*.**30**:1221. 2002.
83. Vader D., Kabla A., Weitz D., Mahadevan L. Strain-induced alignment in collagen gels. *PLoS One*.**4**:e5902. 2009.
84. Costa K.D., Lee E.J., Holmes J.W. Creating alignment and anisotropy in engineered heart tissue: role of boundary conditions in a model three-dimensional culture system. *Tissue Eng*.**9**:567. 2003.
85. Thomopoulos S., Fomovsky G.M., Holmes J.W. The development of structural and mechanical anisotropy in fibroblast populated collagen gels. *J Biomech Eng*.**127**:742. 2005.

## CHAPTER 2

### **Mechanical Stimulation of Tissue-Engineered Articular Cartilage<sup>\*</sup>**

#### ***Abstract***

Cell-based strategies for repair and regeneration of articular cartilage have been in clinical use for two decades. Increasingly, these strategies have used scaffolds or matrices both to help localize chondrocytes in defects and to provide some level of ability to sustain loads immediately upon implantation. As such, strategies to enhance the composition and mechanical performance of cell-seeded cartilage scaffolds have become of interest. Based on data from mechanical stimulation of native articular cartilage tissue, a variety of strategies have been employed to enhance the formation of engineered cartilage *in vitro*. Such approaches include direct loading of constructs via compression or hydrostatic pressure and development of bioreactors that optimize transport of nutrients in or around constructs. This manuscript reviews the fundamental basis for cartilage stimulation and compares the different types of stimulation that have been used to enhance matrix production in engineered cartilage. Optimal approaches for dynamic compressive stimulation of cartilage appear to occur at strain amplitudes of 10% and at frequencies at or above 1 Hz, which enhance cartilage matrix production by 50-100%.

#### ***Key Points***

- Strategies for stimulating articular cartilage fall into two categories: application of loads via compression or hydrostatic pressure; and enhanced nutrient transport by media mixing or perfusion

---

<sup>\*</sup> This chapter was recently submitted for publication: Puetzer, JL, Hudson, KD, Bonassar, LJ. Mechanical Stimulation of Tissue-Engineered Articular Cartilage. Nature Reviews Rheumatology, In review.

- Protocols for mechanical stimulation of engineered tissues are based on protocols established for stimulation of native cartilage tissue
- Optimal stimulation for dynamic compression occurs at 10% strain amplitude and at frequencies greater than or equal to 1 Hz
- The majority of studies on sample perfusion are designed to induce flows inside tissues at velocities ranging from 10-20  $\mu\text{m/s}$ , similar to those induced during loading of cartilage during walking
- Successful strategies for mechanical stimulation enhance matrix production in engineered cartilage by 50-100%

### ***Introduction***

Traumatic injury and associated damage to cartilage are known to predispose joints to osteoarthritis<sup>1</sup>. Focal cartilage lesions raise the chances of developing arthritis up to 5-fold<sup>2</sup> and decrease quality of life both in long term and short term outcomes<sup>3</sup>. As such, there is great interest in developing methods to treat focal cartilage lesions. Cell-based methods of chondrocyte transplantation have been used to treat focal cartilage lesions for almost two decades<sup>4</sup>. While the results of these approaches show promise over conventional treatments<sup>5</sup>, there remains great interest in enhancing the performance of such transplants.

Because cell engraftment and localization are critical for success of these approaches, the use of biomaterials for chondrocyte delivery remains an active area of investigation. A variety of materials have been used as scaffolds for chondrocyte growth, including implantable and injectable biomaterials<sup>6</sup>. The use of such materials for chondrocyte delivery is attractive for a number of reasons, including ease of surgical delivery and graft fixation, as well as the potential for such scaffolds to provide signals to chondrocytes that enhance cartilage growth.

Seeding of chondrocytes onto scaffolds also facilitates *in vitro* culture to allow for the partial elaboration of an extracellular matrix (ECM) prior to implantation. Because cartilage is load-bearing, the ability of constructs to bear load and the biological response of transplanted cells to loading are both important for their long term success. In this way, the use of scaffolds for cell delivery is additionally attractive in that the scaffold can bear load immediately after graft placement as well as act as a structure to transmit such loads to chondrocytes carried within. Further, mechanical loading can also be used to pre-condition seeded constructs and accelerate the production of successful grafts.

### ***Mechanical Loading in Native Cartilage***

Articular cartilage provides a low friction surface that facilitates joint motion, and distributes and dissipates loads. During everyday activities, cartilage must withstand large and repetitive loads up to 20 MPa<sup>7</sup> and shears of up to 15 degrees<sup>8</sup>. Dynamic tissue-level strains of up to 13%<sup>8-10</sup> have been measured *in vivo*, though microscale strains may be as large as 50%<sup>11</sup>. Though both over- and under-loading have been shown to lead to injury and or degradation, normal mechanical loading is important for maintaining correct form and function *in vivo*<sup>12,13</sup>.

Native cartilage has two distinct deformation conditions that may act alone or in concert: (1) compression, both static and dynamic, and (2) shear (Figure 2.1). These loading modes cause a variety of coupled stimuli to the chondrocytes embedded in cartilage. While both compression and shear cause changes in cell shape and pore size, compression also causes increases in hydrostatic pressure, fixed charge density, streaming potentials, and fluid flow. Though these physical phenomena can be understood using biphasic or poroelastic models<sup>14,15</sup>, the individual influences of

these stimuli on ECM synthesis or degradation are difficult to parse *in vivo*. This has led to numerous *ex vivo* loading studies of cartilage.

Static compression causes a dose-dependent decrease in collagen and proteoglycan synthesis, while cyclic/oscillatory compression increases synthesis in both a frequency and amplitude dependent manner<sup>16,17</sup>. At higher frequencies proteoglycan synthesis is region-dependent, due to differences in pressures and flow that occur in the tissue<sup>18,19</sup>. Additionally, during dynamic compression, streaming potentials are created that are related to load amplitude, frequency, and ionic strength<sup>20-22</sup>. Applying an electric field to cartilage or chondrocytes increases ECM synthesis<sup>23</sup> and causes release of  $\text{Ca}^{2+}$  ions into the extracellular space through voltage-gated channels<sup>24</sup>, one of the many mechanotransduction mediators triggered by loading.

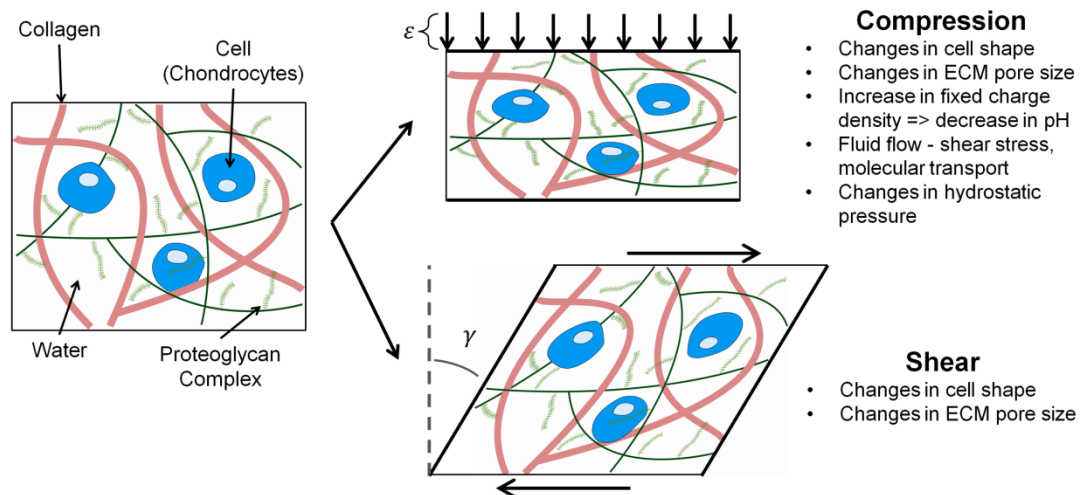


**Figure 2.1** Modes of deformation in native cartilage: compression and/or shear and the resulting changes to the ECM and chondrocytes.

### ***Mechanisms of Mechanotransduction***

Dynamic compression triggers a variety of mechanotransduction pathways including activation of ion channels, integrins and other surface receptors, and convective transport of macromolecules. Streaming potentials causes a release of calcium ions through voltage-gated ion channels, which increase aggrecan mRNA expression<sup>25</sup>. Direct changes in cell shape triggers stretch-activated ion channels which are also mediated by calcium ions<sup>26</sup>.

Chondrocytes in articular cartilage actively interact with the ECM through integrins such as the  $\alpha5\beta1$ , which mediate proteoglycan synthesis through cell spreading and TGF- $\beta3$  dependent pathways<sup>27-29</sup>. Other surface receptor proteins activated by growth factors also influence ECM synthesis<sup>30</sup>. Because of limited vascularization, diffusive transport of nutrients and waste products is essential to tissue homeostasis. While static loading hinders diffusion, modeling of cartilage mechanics has shown that dynamic compression helps move solutes through the matrix through forced convection<sup>31,32</sup>. Though there is a consensus that dynamic loading increases larger solute transport, it is unclear if there is an increase in small solute transport<sup>32-34</sup>.

The underlying basis for the mechanical stimulation of tissue-engineered cartilage grafts is derived from decades of study of the metabolic response of native articular cartilage to mechanical loading. These mechanisms inform the design of bioreactors that mimic the mechanical stimulation pathways to enhance the quantity and quality of matrix produced.

### ***Mechanical Stimulation of TE Cartilage***

Mechanical stimulation has been widely used to precondition engineered cartilage scaffolds to improve their biochemical and mechanical properties prior to implantation. Multiple bioreactor systems have been produced to reproduce an

aspect of the native mechanical environment, including: direct scaffold deformation, hydrostatic pressure vessels, mixing bioreactors, and perfusion systems<sup>8</sup> (Figure 2.2). Scaffold deformation systems traditionally apply static or dynamic uniaxial compression or shear, resulting in cell and matrix deformation. Recently, biaxial systems have been developed that apply compression and shear in unison<sup>35–41</sup>. Hydrostatic pressure vessels pressurize samples without direct contact or deformation. This pressure is typically applied by compressing a gas phase that transmits load to the cells, or more commonly by applying compression to the fluid phase<sup>42</sup>. Mixing bioreactors have evolved to include turbulent mixing, rotating wall, and wavy-walled bioreactors which enhance diffusion and convection within samples, while minimizing boundary layers. Finally, perfusion systems use fluid-induced shear throughout the constructs or across the surface to enhance convection transport and development of engineered cartilage.

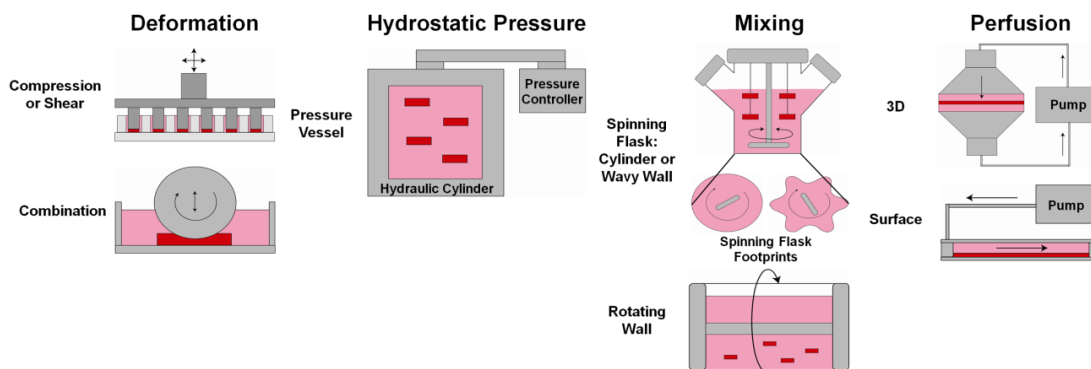


**Figure 2.2:** Bioreactor designs grouped into the 4 major stimulation types; deformation, hydrostatic pressure, mixing, and perfusion.

The majority of these bioreactors are operated at normoxic conditions (21% oxygen); however cartilage exists primarily in a hypoxic 7.5-1% oxygen environment. In development it has been shown reduced oxygen promotes development of cartilage attributes, stimulates proliferation, decreases cellular size, and increased biosynthesis<sup>43</sup>. Further, a few studies have investigated the effects of a hypoxic environment with hydrostatic pressure<sup>43</sup> or compression<sup>44</sup> and found it to have a stimulative effect resulting in improved proteoglycan accumulation, collagen II mRNA expression, and suppressed collagen I expression. Controlling tissue exposure to oxygen offers a mode of stimulation that is complementary to mechanical stimuli, and there appears to be great promise in incorporating such capability into future versions of bioreactors.

### ***Modes of stimulation***

#### Tissue Deformation

##### *Compression*

Uniaxial static and dynamic compression is by far the most studied form of stimulation in cartilage engineering<sup>19,38,44-57</sup>. Similar to *in vivo* loading, Dynamic loading has been found to be more beneficial than static compression, with static compression down-regulating proteoglycan biosynthesis in a time- and dose-dependent manner<sup>45,51</sup>. Thus the majority of studies have examined the effect of dynamic compression over a range of strains and frequencies.

Dynamic compression has been applied at peak strains from 1-40% and 0.01-3 Hz frequency, with the most studied loading regime being 10% strain at 1 Hz (Figure 2.3). In general, it has been found compressive strains of 1-10% and frequencies of 0.01-1 Hz results in increased glycosaminoglycan (GAG) synthesis and improved compressive properties, with the greatest fold increase in GAG production at 10%

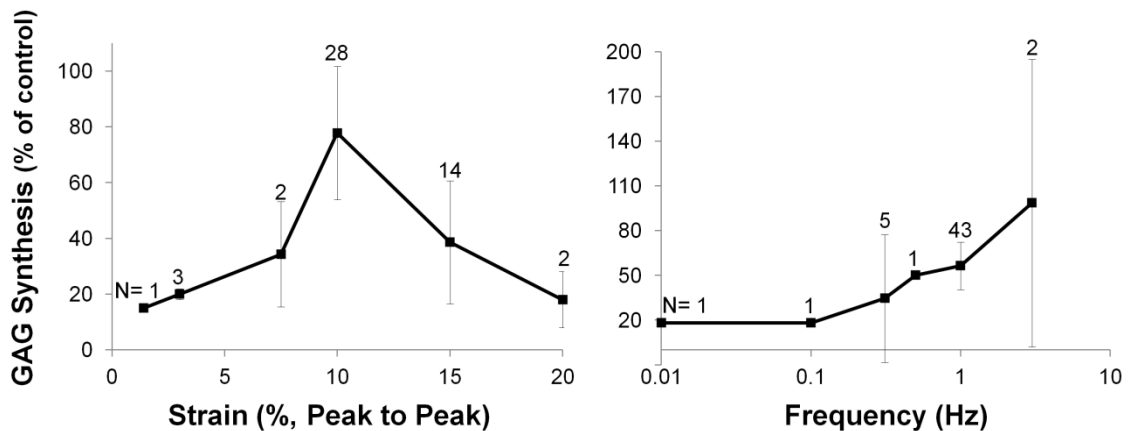


**Figure 2.3** GAG synthesis according to strain and frequency in tissue engineered cartilage constructs exposed to dynamic compression. Data collected from 23 studies<sup>19,36,38,40,45,47-49,53-58</sup> and reported N represents number of data points collected at each strain or frequency. Data reported as mean  $\pm$  SE. The most popular loading regime, which has yielded the greatest GAG synthesis, is 10% strain at 1 Hz.

and 1 Hz loading. Collagen production is often either not stimulated or stimulated less than GAG production<sup>38,53,55</sup>. The response of engineered cartilage to dynamic compression has been found to be dependent on amplitude, frequency, timing, scaffold, and spatial location.

In general it has been reported to be more beneficial to load early and intermittently than continuously<sup>38,47,53,54</sup>. Continuous loading over prolonged periods often results in increased catabolic activity (metabolic breakdown) and correspondingly a decreased in collagen and proteoglycan accumulation<sup>52</sup>. It is believed catabolic activity induced by mechanical loading is necessary to initiate proteoglycan turnover, remodeling, and further development of scaffolds, however sustained catabolic activity will result in tissue degradation<sup>49,54,58</sup>. It has been demonstrated that once mechanical stimulation is removed catabolic activity is downregulated while anabolic activity (metabolic synthesis) continues, explaining why intermittent loading often results in increased accumulation of GAG and collagen<sup>49,54</sup>.

Additionally, it has been demonstrated that early loading, rather than delayed loading, is more beneficial to cartilage development<sup>38,48,54</sup>; however these responses are very reliant on the scaffold properties.

Scaffolds in cartilage engineering range from encapsulating hydrogels to fibrous materials. These scaffolds have a wide range of moduli and permeabilities spanning multiple orders of magnitudes, but all are exposed to similar loading regimes. This results in drastically different environments for the cells<sup>45,57</sup>. Although chondrocytes are often rounded and unattached *in vivo*, it has been suggested that compression has the greatest effect when cells are anchored in scaffolds, demonstrating the importance of cellular interaction/binding within matrices<sup>45,59</sup>. Further it has been demonstrated in non-adherent hydrogel scaffolds the full effect of loading is not until chondrocytes develop a pericellular matrix<sup>36,60,61</sup>. However, delaying loading until the development of a well-established matrix often results in unresponsive chondrocytes<sup>38,48,54</sup>, thus the timing of loading is extremely important to the development of engineered cartilage.

A common thread among all scaffolds used in cartilage TE is that scaffolds exhibit a classic poro-elastic behavior under unconfined compression, with a pressurized low fluid flow core and high radial fluid velocities along the edge<sup>19,45,57</sup>. Several studies have examined the distribution of accumulated ECM and found enhanced biosynthesis co-localized with increased interstitial fluid flow along the edge of scaffolds, demonstrating the importance of fluid flow in cartilage development<sup>19,45,62</sup>. These findings have helped to encourage the development of mixing, perfusion and surface flow bioreactors to further develop engineered cartilage.

### *Combined Shear and Loading*

Shear bioreactors are often designed similar to tribometers and apply a static compression with a cyclic 1-6% peak shear strain at 0.1-1 Hz<sup>56,63,64</sup>. It has been found shear loading at 4% strain over 4 weeks resulted in samples containing more proteoglycans and collagen compared to 10% compressed samples<sup>56</sup>. Generally, shear loaded constructs demonstrated improved collagen and GAG concentrations.

Recently, numerous studies have developed and examined the effect of bioreactors capable of applying dynamic shear and compressive load<sup>35-41</sup>. It is not well established yet whether dynamic biaxial compression and shear loading result in an increase<sup>36</sup> or decrease<sup>35</sup> in GAG synthesis and mechanical properties in comparison to uniaxial loading. However, it is clear this biaxial loading leads to increased collagen synthesis<sup>41</sup> and development of the superficial zone. Biaxial sliding and compression produced a lower coefficient of friction, localized lubricin (a glycoprotein believed to aid in lubrication), and significantly improved hyaluronan synthases<sup>38-40</sup>. This is of particular interest since a well-developed surface zone capable of lubrication will most likely be a key component of a successful tissue engineered scaffold *in vivo*.

### Hydrostatic Pressure

When cartilage is loaded compressively *in vivo* 95% of the load is borne by hydrostatic pressure (HP) developed from the pressurization of interstitial fluid<sup>8,42,65</sup>. Cells exposed to HP experience a uniform normal stress, without any measurable tissue strain. Prolonged HP in the physiological range of 7-10 MPa promotes matrix synthesis and increases mechanical properties in engineered cartilage, while applying HP above physiologic ranges (>15MPa) results in decreased ECM production and a heat shock response<sup>42,65-72</sup>. Hydrostatic pressure often results in

increased GAG synthesis; however higher magnitudes of load (>7MPa) and longer culture periods are needed to stimulate collagen formation<sup>69,73,74</sup>. Frequency, duration, onset, and magnitude of load are all factors that can be varied.

Unlike deformational loading, hydrostatic loading can be beneficial statically and intermittently. Several studies have reported static hydrostatic pressure in the range of 2-10MPa to improve biochemical and mechanical properties of chondrocyte-seeded constructs over cyclically loaded constructs<sup>67-69</sup>. However, it has also been reported cyclic loading is better than static<sup>65,66</sup>. It is believed cyclic loading is better than static due to increased interstitial fluid flow and or induced cytoskeleton changes. Interestingly, despite these contradictory findings with chondrocyte seeded scaffolds, the majority of studies that examine the effect of hydrostatic pressure on stem cell seed scaffold have only applied cyclic loading<sup>65,74-77</sup>. These studies have found cyclic hydrostatic pressure induces chondrogenesis in a dose- and time-dependent manner. Further, it is has been reported applying cyclic HP to osteoarthritic<sup>42,70</sup> and dedifferentiated<sup>42,72</sup> chondrocyte constructs can result in redifferentiation and increased GAG and collagen synthesis.

There is a lack of studies examining the timing of hydrostatic pressure, effect of duty cycle, anabolic/catabolic response and how development of a pericellular matrix/scaffold may affect results. Recently, Elder et al.<sup>71</sup> examined static hydrostatic pressure for 5 days, spread over 8 weeks, to determine the effect of temporal application and immediate verse long term effects of loading. They found delaying load to day 10 immediately increased aggregate modulus, GAG and collagen concentrations, and with prolonged static culture after load young's modulus increased in scaffold-free constructs<sup>71</sup>. This study demonstrates the importance of evaluating timing and duty cycle applications of loading.

## Media Mixing

The dynamic flow of media mixing bioreactors enhances ECM deposition and uniformity of tissue by increasing mass and convection transport within constructs (Table 2.1)<sup>78-85</sup>. Through the years media mixing bioreactors have evolved to allow more precise control of media flow and development of scaffolds. The first generation of media mixing bioreactors were modified spinner flasks with constructs freely floating in media or fixed on an impeller. The use of such devices enabled uniform seeding of scaffolds; however localized regions of high shear/turbulent flow on the surface of constructs was noted to drive the formation of a type I collagen fibrous capsule<sup>78,79,82</sup>.

Rotating wall vessels or concentric cylinder bioreactors were developed to decrease the turbulent flow and thus prevent the development of a capsule. These bioreactors operate with a low-shear dynamic laminar flow that results in high mass/nutrient transfer rates and yields constructs with improved GAG composition and mechanical properties<sup>44,79,85-88</sup>. The constructs in this system are suspended in laminar flow and thus not only experiencing flow but also centrifugal, drag and gravity forces<sup>79</sup>. Additionally as constructs develop the rotation rate is often increase to maintain suspension of the constructs. This gradual increase could possibly supply additional loads necessary to stimulate cells further as matrix develops.

The wavy-walled bioreactor was designed to allow for fine control of the scaffold's hydrodynamic environment<sup>83,84,89</sup>. This bioreactor is very similar to the turbulent spinner flask; however the flask has wavy walls which allow for tuning of focused hydrodynamic forces and development of high-axial yet reduced shear mixing. This hydrodynamic environment allows for initial turbulent flows for uniform cell seeding but reduced shear flow with prolonged loading. This results in improved GAG and collagen composition over spinner flask, and a significant reduction in the

outer fibrous capsule. Further this treatment has been combined with growth factors to eliminate the fibrous capsule, and improve tissue homogeneity<sup>89</sup>.

**Table 2.1: Mixing Media Studies**

Study	Source	Scaffold	Bioreactor	RPMS	Results
Vunjak-Novakovic 1996 <sup>78</sup>	Bovine	PGA	Spinning	50	Improved composition, formation of outer capsule
Gooch 2001 <sup>82</sup>	Bovine	PGA	Spinning	80-160	Examined 9 mixing intensities, presence of mixing increased GAG and collagen, no effect from intensity
Saini 2003 <sup>85</sup>	Bovine	PLLA	Concentric Circle	19, 38, 76	Homogeneous tissue, with higher RPMS resulting in fibrous capsule and suppression of ECM
Vunjak-Novakovic 1999 <sup>79</sup>	Bovine	PGA	Rotating wall and Spinning	15-30, 50	Rotating vessel had most homogeneous cartilage-like matrix, and improved GAG and mechanical properties
Freed 1998 <sup>87</sup>	Bovine	PGA	Rotating wall	15 – 30	Homogeneous scaffolds with increased GAG and type II collagen
Li 2008 <sup>88</sup>	Bovine	PLLA	Rotating wall	15 – 30	Homogeneous scaffolds with increased GAG, collagen, and mechanical properties
Villanueva 2009 <sup>86</sup>	Steer	PEG	Rotating wall	22	Decreased nitric oxide and GAG production
Bueno 2005 <sup>83</sup>	Bovine	PGA	Wavy wall and Spinning	50	Wavy wall had increased DNA, ECM, and decreased fibrous capsule over spinner flask.
Bueno 2009 <sup>84</sup>	Bovine	PGA	Wavy wall	50, 80	Rate of collagen and GAG deposition inversely regulated by shear and fluid velocity distribution
Yang 2013 <sup>89</sup>	Bovine	PGA	Wavy wall	50	Transient application of growth factors with mixing improved biochemical and mechanical properties and eliminated fibrous capsule

All cells were chondrocytes. PGA: polyglycolic acid, PLLA: Poly L Lactic Acid, PEG: Polyethylene glycol, RPMS: rotations per minute, GAG: glycosaminoglycans, ECM: extracellular matrix

## Perfusion

Flow bioreactors, mixing and perfusion, increase the transport of nutrients to and away from cells. Perfusion bioreactors provide a means of controlling the flow rate through the scaffold and help maintain a more optimal pH<sup>90,91</sup>. Fluid flow at 0.01-0.2 ml/min directly through the scaffold enhances mass transfer providing constant supply of nutrients to cells, aids in proliferation, and results in uniform cell and GAG deposition (Table 2.2)<sup>90-97</sup>. It is believed ECM synthesis is increased due to convection transport and shear stress applied by fluid flow to chondrocytes. Traditionally, perfusion is applied unidirectionally, and cells orient in the direction of fluid flow. As scaffolds develop this alignment and the overall permeability decreases. However, recently it was found periodically reversing the flow results in more homogeneously developed tissue and an increase in GAG and collagen accumulation<sup>97</sup>. These scaffolds matched GAG concentration of native tissue but still require further development of collagen.

Perfusion modulates cell content and GAG synthesis in a time- and dose-dependent manner. Early perfusion at flow rates greater than 0.2 ml/min decreased cell concentration and ECM production, however delaying load and gradually increasing flow with time in culture has been found to significantly improve DNA, GAG, and collagen concentrations<sup>92,96</sup>. Low flow rates (<0.001 ml/min) have been reported to be ineffective, but needed for the maintenance of alginate scaffolds<sup>98</sup>.

The type of scaffold used plays a large role in the effect fluid flow has on the construct's development. Chondrocytes may be more responsive when attached to fibrous scaffolds than in non-adherent hydrogels. It has been demonstrated cells are more responsive to strain when attached to RGD ligands in modified alginate than when just encapsulated in non-adherent alginate<sup>99</sup>. The scaffold dictates the flow rate that should be used due to the different shear stresses applied to cells<sup>96,98,100</sup>. The

majority of perfusion studies have been performed with fibrous scaffolds and there is a need for further studies on the effect of magnitude, timing and duration of perfusion in hydrogel scaffolds.

Perfusion bioreactors have evolved for the treatment of large scale constructs. Santoro et al.<sup>95</sup> has developed a perfusion system capable of developing 50mm diameter scaffolds for joint resurfacing<sup>95</sup>. Perfusion of these scaffolds results in a homogeneous distribution of ECM and no necrotic center. Additionally, a hollow fiber bioreactor, adopted from commercial antibody production, has been used to stimulate much thicker (60mm) samples<sup>101</sup>. This bioreactor consists of 6 porous polypropylene hollow fibers within a glass tube. Fluid is flown through the pores resulting in spatial variation of ECM deposition with more ECM concentrated at the inflow and near the hollow fibers. This gradient of distribution is beneficial to developing new techniques for evaluation of proteoglycan content *in vivo*<sup>101-103</sup>.

**Table 2.2: Perfusion Studies**

<b>Study</b>	<b>Source</b>	<b>Scaffold</b>	<b>Fluid Velocity</b> ( $\mu\text{m/s}$ )	<b>Flow Rate</b> (ml/min)	<b>Results</b>
Dunkelman 1995 <sup>93</sup>	Leporine	PGA	11	0.05	Increased DNA, GAG and Collagen II
Pazzano 2000 <sup>90</sup>	Bovine	PGA/PLLA	0.3-10	0.1-2	Increased DNA, GAG and Collagen
Davisson 2002 <sup>104</sup>	Ovine	PGA	11 or 170	0.05 or 0.8	Increased DNA and GAG with increased flow rate
Mahmoudifar 2005 <sup>97</sup>	Human fetal	PGA	19	0.2	Uni-and bidirectional flow increased composition, further improvements in GAG and collagen with bidirectional
Shahin 2012 <sup>37</sup>	Human	PGA (with/without alginate)	7, 19, or 7->19	0.075-0.2	Pre-culture for 5 days improved results, gradually increasing flow rate had best composition
Bujia 1995 <sup>94</sup>	Human	poly-L-lactid fleece with agarose	-	0.0167	Synthesis of GAG and Collagen II
Mizuno 2001 <sup>100</sup>	Bovine	Collagen sponge	140	0.33	Decreased GAG and Collagen compared to static controls
Wendt 2006 <sup>91</sup>	Human	PolyActive© foam disc	100	0.3	Homogenous distribution of cells and matrix
Santoro 2010 <sup>95</sup>	Human	Hyaff-II non-woven mesh	100	12	Homogeneous large scaffolds with improved mechanical properties
Forsey 2012 <sup>98</sup>	Human	alginate-chitosan	-	0.0007	No significant advantage over static

All cells were chondrocytes. PGA: polyglycolic acid, PLLA: Poly L Lactic Acid, GAG: glycosaminoglycans

#### *Surface Shear Flow bioreactors*

Recently surface flow bioreactors have gained popularity as a means to develop native anisotropic organization and a well-organized surface zone<sup>105-108</sup>. These

studies have demonstrated that flow-induced shear stresses, similar to deformation induced shear, results in spatial heterogeneity of ECM and organization, with increased type II collagen, improved tensile properties, and expression of lubricin in the superficial region. Further this system has demonstrated how varying the flow rate can affect the penetration depth of fluid and develop gradients of interstitial fluid flow<sup>107</sup>. In the future the organization benefits of this system could be combined with other loading regimes to produce well organized and developed scaffolds.

### ***Load, Growth Factors, and Stem Cells***

#### **Synergistic effect of growth factors and load**

Combining growth factor treatment and mechanical stimulation generally results in a synergistic improvement in biochemical and mechanical properties, suggesting chondrocytes respond to biochemical and biomechanical stimuli via separate pathways. However results vary depending on the growth factors applied and timing of load<sup>38,46,69,89,109</sup>. Early growth factor treatment can be used to improve pericellular matrix development, which in-turn increases the effect of early load and shortens the culture time needed for improved development<sup>38</sup>. Further, growth factor treatment with load has been shown to improve tissue homogeneity and overall development of constructs<sup>46,89</sup>.

#### **Load-induced Chondrogenesis in Stem Cells**

An appropriate cell source that is readily available is necessary in order for engineered cartilage to serve as a replacement *in vivo*. Chondrocytes are in limited supply and known to dedifferentiate when expanded, thus mesenchymal stem cells (MSCs) are a promising alternative. However the use of MSCs requires a reliable means of inducing chondrogenesis. This has typically been achieved with growth

factor stimulation; however an increasing number of studies are demonstrating chondrogenesis can be achieved with mechanical stimulation alone and further improved with growth factor stimulation. MSC seeded constructs have been reported to undergo chondrogenesis and develop cartilaginous matrix when exposed to dynamic compression<sup>62</sup>, combined shear/compressive load<sup>59</sup>, rotating wall mixing<sup>110</sup>, perfusion<sup>111</sup>, and cyclic hydrostatic pressure<sup>65,74-76</sup>.

### **Conclusions**

A wide body of evidence has been accumulated demonstrating that application of appropriate physical stimuli enhances the quality of tissue-engineered cartilage. The strategies for such stimulation fall broadly into two categories: direct mechanical stimulation through applied deformation or hydrostatic pressure; and enhancement of nutrient transport through mixing of media or perfusion of samples. For each type of stimulus, ranges of 1-2 orders of magnitude have been explored for respective operating conditions (e.g. loading amplitudes, flow and mixing rates). Although there are no definitive findings of optimal stimulation protocols, dynamic compression of 10% amplitude at frequencies above 1 Hz have been explored most thoroughly and typically enhance the rate of cartilage matrix formation by more than 50%. Similarly, physiologic levels of hydrostatic pressure of ~10MPa also enhance matrix production, although there is insufficient data to identify optimal stimulation ranges. Perfusion studies demonstrate consistent benefits to matrix synthesis, with most studies focusing on bioreactors that induce local fluid flows in the range of 10-20  $\mu\text{m/s}$ . Controlling nutrient delivery by media mixing also enhances matrix synthesis, although differences in mixing rates and reactor geometries make it difficult to infer which local mechanical conditions in or near cartilage constructs are most responsible for this stimulation.

Despite the collective evidence from many studies that physical stimulation enhances cartilage formation *in vitro*, there is little to no data on how such stimulation enhances the formation of articular cartilage *in vivo*. A major motivation for physical stimulation *in vitro* is the generation of cartilage constructs that are mechanically robust enough to be implanted in the challenging environment of the joint. However, there is no consensus on thresholds for material properties that constructs must have before they are effectively implantable. Further, it may be desirable to implant constructs that are not fully mature, either biochemically or mechanically, implant maturation *in vivo* may enhance integration with surrounding tissue. Collectively, this leads to the clear conclusion that more data is needed on whether *in vitro* mechanical stimulation leads to better outcomes *in vivo*.

While articular cartilage has been studied most thoroughly, tissue engineering and regenerative medicine approaches are receiving more attention for other kinds of cartilage as well, including meniscus and intervertebral disc. As load bearing is important for these tissues as well, the approaches outlined above for mechanical stimulation of articular cartilage may be applied to these tissues as well. Indeed, such studies have already begun<sup>112-114</sup>, but there is much progress to be made in these areas as well.

## REFERENCES

1. Lohmander, L. S., Englund, P. M., Dahl, L. L. & Roos, E. M. The Long-term Consequence of Anterior Cruciate Ligament and Meniscus Injuries. *Am. J. Sports Med.* **35**, 1756–1769 (2007).
2. Stufkens, S. a, Knupp, M., Horisberger, M., Lampert, C. & Hintermann, B. Cartilage Lesions and the Development of Osteoarthritis After Internal Fixation of Ankle Fractures. *J. Bone Jt. Surg.* **92**, 279–286 (2010).
3. Røtterud, J. H., Sivertsen, E. a, Forssblad, M., Engebretsen, L. & Arøen, A. Effect of meniscal and focal cartilage lesions on patient-reported outcome after anterior cruciate ligament reconstruction: a nationwide cohort study from Norway and Sweden of 8476 patients with 2-year follow-up. *Am. J. Sports Med.* **41**, 535–543 (2013).
4. Brittberg, M. *et al.* Treatment of Deep Cartilage Defects in the Knee with Autologous Chondrocyte Transplantation. *N. Engl. J. Med.* 889–895 (1994).
5. Iwasa, J., Engebretsen, L., Shima, Y. & Ochi, M. Clinical application of scaffolds fro cartilage tissue engineering. *Knee surgery, Sport. Traumatol. Arthrosc.* **17**, 561–577 (2009).
6. Johnstone, B. *et al.* Tissue Engineering for Articular Cartilage Repair - The State of the Art. *Eur. Cell. Mater.* **25**, 248–267 (2013).
7. Hodge, W. A. *et al.* Contact pressures in the human hip joint measured in vivo. *Proc. Natl. Acad. Sci.* **83**, 2879–2883 (1986).
8. Schulz, R. M. & Bader, A. Cartilage tissue engineering and bioreactor systems for the cultivation and stimulation of chondrocytes. *Eur. Biophys. J.* **36**, 539–568 (2007).
9. Grodzinsky, A. J., Levenston, M. E., Jin, M. & Frank, E. H. Cartilage Tissue Remodeling in Response to Mechanical Forces. *Annu. Rev. Biomed. Eng.* **2**, 691–713 (2000).
10. Chan, D. D., Neu, C. P. & Hull, M. L. In situ deformation of cartilage in cyclically loaded tibiofemoral joints by displacement-encoded MRI. *Osteoarthr. Cartil.* **17**, 1461–8 (2009).

11. Chan, D. D. & Neu, C. P. Transient and Microscale Deformations and Strains Measured under Exogenous Loading by Noninvasive Magnetic Resonance. *PLoS One* **7**, e33463 (2012).
12. Cohen, N. P., Foster, R. J. & Mow, V. C. Composition and Dynamics of Articular Cartilage: Structure, Function, and Maintaining Healthy State. *J. Orthop. Res. Sport. Phys. Ther.* **28**, 203–215 (1998).
13. Eckstein, F., Hudelmaier, M. & Putz, R. The effects of exercise on human articular cartilage. *J. Anat.* **208**, 491–512 (2006).
14. Argoubi, M. & Shirazi-Adl, A. Poroelastic Creep Response Analysis of a Lumbar Motion Segment in Compression. *J. Biomech.* **29**, 1331–1339 (1996).
15. Mow, V. C., Kuei, S. C., Lai, W. M. & Armstrong, C. G. Biphasic Creep and Stress Relaxation of Articular Cartilage in Compression: Theory and Experiments. *J. Biomech. Eng.* **102**, 73–84 (1980).
16. Sah, R. L. *et al.* Biosynthetic Response of Cartilage Explants to Dynamic Compression. *J. Orthop. Res.* **7**, 619–636 (1989).
17. Kim, Y.-J., Sah, R. L., Grodzinsky, A. J., Plaas, A. H. & Sandy, J. D. Mechanical Regulation of Cartilage Biosynthetic Behavior: Physical Stimuli. *Archives Biochem. Biophys.* **311**, 1–12 (1994).
18. Kim, Y.-J., Bonassar, L. J., Grodzinsky, A. J. & Bonassar, J. The Role of Cartilage Streaming Potential, Fluid Flow and Pressure in the Stimulation of Chondrocyte Biosynthesis During Dynamic Compression. *J. Biomech.* **28**, 1055–1066 (1995).
19. Buschmann, M. D. *et al.* Stimulation of Aggrecan Synthesis in Cartilage Explants by Cyclic Loading is Localized to Regions of High Interstitial Fluid Flow. *Arch. Biochem. Biophys.* **366**, 1–7 (1999).
20. Frank, H. & Grodzinsky, A. J. Cartilage Electromechanics - II. Continuum Model of Cartilage Electrokinetics and Correlation with Experiments. *J. Biomech.* **20**, 629–639 (1987).
21. Frank, E. H. & Grodzinsky, A. Cartilage Electromechanics - I. Electrokinetic Transduction and the Effects of Electrolyte pH and Ionic Strength. *J. Biomech.* **20**, 615–627 (1987).

22. Garon, M., Légaré, A., Guardo, R., Savard, P. & Buschmann, M. D. Streaming potentials maps are spatially resolved indicators of amplitude, frequency and ionic strength dependant responses of articular cartilage to load. *J. Biomech.* **35**, 207–16 (2002).
23. Brighton, C. T., Wang, W. & Clark, C. C. Up-regulation of matrix in bovine articular cartilage explants by electric fields. *Biochem. Biophys. Res. Commun.* **342**, 556–561 (2006).
24. Xu, J., Wang, W., Clark, C. C. & Brighton, C. T. Signal transduction in electrically stimulated articular chondrocytes involves translocation of extracellular calcium through voltage-gated channels. *Osteoarthr. Cartil.* **17**, 397–405 (2009).
25. Alford, A. I., Yellowley, C. E., Jacobs, C. R. & Donahue, H. J. Increases in Cytosolic Calcium, but not Fluid Flow, Affect Aggrecan mRNA Levels in Articular Chondrocytes. *J. Cell. Biochem.* **90**, 938–944 (2003).
26. Wright, M., Jobanputra, P., Bavington, C., Salter, D. M. & Nuki, G. Effects of Intermittent Pressure-induced strain on the electrophysiology of cultured human chondrocytes: evidence for the presence of stretch-activated membrane ion channels. *Clin. Sci.* **90**, 61–71 (1996).
27. Chowdhury, T. T., Salter, D. M., Bader, D. L. & Lee, D. A. Integrin-mediated mechanotransduction processes in TGFbeta-stimulated monolayer-expanded chondrocytes. *Biochem. Biophys. Res. Commun.* **318**, 873–881 (2004).
28. Spiteri, C., Raizman, I., Pilliar, R. M. & Kandel, R. a. Matrix accumulation by articular chondrocytes during mechanical stimulation is influenced by integrin-mediated cell spreading. *J. Biomed. Mater. Res. Part A* **94**, 122–129 (2010).
29. Chai, D. H., Arner, E. C., Griggs, D. W. & Grodzinsky, a J. Alpha-v and beta-1 integrins regulate dynamic compression-induced proteoglycan synthesis in 3D gel culture by distinct complementary pathways. *Osteoarthr. Cartil.* **18**, 249–256 (2010).
30. Bonassar, L. J. *et al.* The effect of dynamic compression on the response of articular cartilage to insulin-like growth factor-I. *J. Orthop. Res.* **19**, 11–17 (2001).
31. Zhang, L. & Szeri, A. Z. Transport of neutral solute in articular cartilage: effects of loading and particle size. *Proc. R. Soc. A* **461**, 2021–2042 (2005).

32. Evans, R. C. & Quinn, T. M. Solute convection in dynamically compressed cartilage. *J. Biomech.* **39**, 1048–1055 (2006).
33. O'Hara, B. P., Urban, J. P. G. & Maroudas, A. Influence of cyclic loading on nutrition of articular cartilage. *Ann. Rheum. Dis.* **49**, 536–539 (1990).
34. Garcia, A. M., Frank, E. H., Grimshaw, P. E. & Grodzinsky, A. J. Contributions of Fluid Convection and Electrical Migration to Transport in Cartilage: Relevance to Loading. *Arch. Biochem. Biophys. Biophys.* **333**, 317–325 (1996).
35. Waldman, S. D., Couto, D. C., Grynblas, M. D., Pilliar, R. M. & Kandel, R. a. Multi-axial mechanical stimulation of tissue engineered cartilage: review. *Eur. Cells Mater.* **13**, 66–73; discussion 73–4 (2007).
36. Pinguan-Murphy, B. & Nawal, I. Upregulation of matrix synthesis in chondrocyte-seeded agarose following sustained bi-axial cyclic loading. *Clinics* **67**, 939–944 (2012).
37. Shahin, K. & Doran, P. M. Tissue Engineering of Cartilage Using a Mechanobioreactor Exerting Simultaneous Mechanical Shear and Compression to Simulate the Rolling Action of Articular Joints. *Biotechnol. Bioeng.* **109**, 1060–1073 (2012).
38. Bian, L. *et al.* Dynamic Mechanical Loading Enhances Functional Properties of Tissue-Engineered Cartilage Using Mature Canine Chondrocytes. *Tissue Eng. Part A* **16**, 17–20 (2010).
39. Grad, S. *et al.* Surface Motion Upregulates Superficial Zone Protein and Hyaluronan Production in Chondrocyte-Seeded Three-Dimensional Scaffolds. *Tissue Eng.* **11**, 249–256 (2005).
40. Grad, S. *et al.* Sliding motion modulates stiffness and friction coefficient at the surface of tissue engineered cartilage. *Osteoarthr. Cartil.* **20**, 288–295 (2012).
41. Wimmer, M. A. *et al.* Tribology Approach to the Engineering and Study of Articular Cartilage. *Tissue Eng.* **10**, 1436–1445 (2004).
42. Elder, B. D. & Athanasiou, K. a. Hydrostatic Pressure in Articular Cartilage Tissue Engineering: From Chondrocytes to Tissue Regeneration. *Tissue Eng. Part B* **15**, 43–53 (2009).

43. Hansen, U. *et al.* Combination of reduced oxygen tension and intermittent hydrostatic pressure: a useful tool in articular cartilage tissue engineering. *J. Biomech.* **34**, 941–949 (2001).
44. Wernike, E., Li, Z., Alini, M. & Grad, S. Effect of reduced oxygen tension and long-term mechanical stimulation on chondrocyte-polymer constructs. *Cell Tissue Res.* **331**, 473–483 (2008).
45. Buschmann, M. D., Gluzband, Y. a, Grodzinsky, a J. & Hunziker, E. B. Mechanical compression modulates matrix biosynthesis in chondrocyte/agarose culture. *J. Cell Sci.* **108**, 1497–1508 (1995).
46. Mauck, R. L., Nicoll, S. B., Seyhan, S. L., Ateshian, G. a & Hung, C. T. Synergistic action of growth factors and dynamic loading for articular cartilage tissue engineering. *Tissue Eng.* **9**, 597–611 (2003).
47. Waldman, S. D., Spiteri, C. G., Gryn timer, M. D., Pilliar, R. M. & Kandel, R. A. Long-Term Intermittent Compressive Stimulation Improves the Composition and Mechanical Properties of Tissue-Engineered Cartilage. *Tissue Eng.* **10**, 1323–1331 (2004).
48. Waldman, S. D., Couto, D. C., Gryn timer, M. D., Pilliar, R. M. & Kandel, R. A. A single application of cyclic loading can accelerate matrix deposition and enhance the properties of tissue-engineered cartilage. *Osteoarthr. Cartil.* **14**, 323–330 (2006).
49. De Croos, J. N. a, Dhaliwal, S. S., Gryn timer, M. D., Pilliar, R. M. & Kandel, R. a. Cyclic compressive mechanical stimulation induces sequential catabolic and anabolic gene changes in chondrocytes resulting in increased extracellular matrix accumulation. *Matrix Biol.* **25**, 323–331 (2006).
50. Lee, D. A. & Bader, D. L. Compressive Strains at Physiological Frequencies Influence the Metabolism of Chondrocytes Seeded in Agarose. *J. Orthop. Res.* **15**, 181–188 (1997).
51. Lee, C. R., Grodzinsky, A. J. & Spector, M. Biosynthetic response of passaged chondrocytes in a type II collagen scaffold to mechanical compression. *J. Biomed. Mater. Res. Part A* **64**, 560–569 (2003).
52. Hunter, C., Mouw, J. K. & Levenston, M. E. Dynamic compression of chondrocyte-seeded fibrin gels: effects on matrix accumulation and mechanical stiffness. *Osteoarthr. Cartil.* **12**, 117–130 (2004).

53. Kisiday, J. D., Jin, M., DiMicco, M. a, Kurz, B. & Grodzinsky, A. J. Effects of dynamic compressive loading on chondrocyte biosynthesis in self-assembling peptide scaffolds. *J. Biomech.* **37**, 595–604 (2004).
54. Nicodemus, G. D. & Bryant, S. J. Mechanical loading regimes affect the anabolic and catabolic activities by chondrocytes encapsulated in PEG hydrogels. *Osteoarthr. Cartil.* **18**, 126–137 (2010).
55. Tran, S. C., Cooley, A. J. & Elder, S. H. Effect of a Mechanical Stimulation Bioreactor on Tissue Engineered, Scaffold-Free Cartilage. *Biotechnol. Bioeng.* **108**, 1421–1429 (2011).
56. Waldman, S. D. *et al.* Effect of Biomechanical Conditioning on Cartilaginous Tissue Formation in Vitro. *J. bone Jt. Surg.* **85-A**, 101–105 (2003).
57. Babalola, O. M. & Bonassar, L. J. Parametric Finite Element Analysis of Physical Stimuli Resulting From Mechanical Stimulation of Tissue Engineered Cartilage. *J. Biomech. Eng.* **131**, 061014–1 – 061014–7 (2009).
58. Kisiday, J. D., Frisbie, D. D., McIlwraith, C. W. & Grodzinsky, A. J. Dynamic Compression Stimulates Proteoglycan Synthesis by Mesenchymal Stem Cells in the Absence of Chondrogenic Cytokines. *Tissue Eng. Part A* **15**, 2817–2824 (2009).
59. Schatti, O. *et al.* A Combination of Shear and Dynamic Compression Leads to Mechanically Induced Chondrogenesis of Human Mesenchymal Stem Cells. *Eur. Cell. Mater.* **22**, 214–225 (2011).
60. Giannoni, P., Siegrist, M., Hunziker, E. B. & Wong, M. The mechanosensitivity of cartilage oligomeric matrix protein (COMP). *Biorheology* **40**, 101–109 (2003).
61. Nicodemus, G. D. & Bryant, S. J. The role of hydrogel structure and dynamic loading on chondrocyte gene expression and matrix formation. *J. Biomech.* **41**, 1528–1536 (2008).
62. Mauck, R. L., Byers, B. a, Yuan, X. & Tuan, R. S. Regulation of cartilaginous ECM gene transcription by chondrocytes and MSCs in 3D culture in response to dynamic loading. *Biomech. Model. Mechanobiol.* **6**, 113–25 (2007).

63. Waldman, S. D., Spiteri, C. G., Gryn timer, M. D., Pilliar, R. M. & Kandel, R. A. Long-term intermittent shear deformation improves the quality of cartilaginous tissue formed in vitro. *J. Orthop. Res.* **21**, 590–596 (2003).
64. Jin, M., Frank, E. H., Quinn, T. M., Hunziker, E. B. & Grodzinsky, a J. Tissue Shear Deformation Stimulation Proteoglycan and Protein Biosynthesis in Bovine Cartilage Explants. *Arch. Biochem. Biophys.* **395**, 41–48 (2001).
65. Correia, C. *et al.* Dynamic Culturing of Cartilage Tissue: The Significance of Hydrostatic Pressure. *Tissue Eng. Part A* **18**, 1979–1991 (2012).
66. Sharma, G., Saxena, R. K. & Mishra, P. Differential effects of cyclic and static pressure on biochemical and morphological properties of chondrocytes from articular cartilage. *Clin. Biomech.* **22**, 248–255 (2007).
67. Toyoda, T. *et al.* Hydrostatic Pressure Modulates Proteoglycan Metabolism in Chondrocytes Seeded in Agarose. *Arthritis Rheum.* **48**, 2865–2872 (2003).
68. Mizuno, S., Tateishi, T., Ushida, T. & Glowacki, J. Hydrostatic fluid pressure enhances matrix synthesis and accumulation by bovine chondrocytes in three-dimensional culture. *J. Cell. Physiol.* **193**, 319–327 (2002).
69. Elder, B. D. & Athanasiou, K. a. Synergistic and Additive Effects of Hydrostatic Pressure and Growth Factors on Tissue Formation. *PLoS One* **3**, e2341 (2008).
70. Gavénis, K. *et al.* Effects of cyclic hydrostatic pressure on the metabolism of human osteoarthritic chondrocytes cultivated in a collagen gel. *Artif. Organs* **31**, 91–8 (2007).
71. Elder, B. D. & Athanasiou, K. a. Effects of Temporal Hydrostatic Pressure on Tissue-Engineered Bovine Articular Cartilage Constructs. *Tissue Eng. Part A* **15**, 1151–1158 (2009).
72. Heyland, J. *et al.* Redifferentiation of chondrocytes and cartilage formation under intermittent hydrostatic pressure. *Biotechnol. Lett.* **28**, 1641–1648 (2006).
73. Carver, S. E. & Heath, C. a. Increasing Extracellular Matrix Production in Regenerating Cartilage with Intermittent Physiological Pressure. *Biotechnol. Bioeng.* **62**, 166–174 (1999).

74. Miyanishi, K. *et al.* Dose- and Time-Dependent Effects of Cyclic Hydrostatic Pressure on Transforming Growth Factor- b 3-Induced Chondrogenesis. *Tissue Eng.* **12**, 2253–2262 (2006).
75. Puetzer, J., Williams, J., Gillies, A., Bernacki, S. H. & Lobo, E. G. The Effects of Cyclic Hydrostatic Pressure on Chondrogenesis and Viability of Human Adipose- and Bone Marrow-Derived Mesenchymal Stem Cells in Three-Dimensional Agarose Constructs. *Tissue Eng. Part A* **19**, 299–306 (2013).
76. Ogawa, R., Mizuno, S., Murphy, G. F. & Orgill, D. P. The effect of hydrostatic pressure on three-dimensional chondroinduction of human adipose-derived stem cells. *Tissue Eng. Part A* **15**, 2937–2945 (2009).
77. Finger, A. R., Sargent, C. Y., Dulaney, K. O., Bernacki, S. H. & Lobo, E. G. Differential Effects on Messenger Ribonucleic Acid Expression by Bone Marrow-Derived Human Mesenchymal Stem Cells Seeded in Agarose Constructs Due to Ramped and Steady Applications of Cyclic Hydrostatic Pressure. *Tissue Eng.* **13**, 1151–1158 (2007).
78. Vunjak-Novakovic, G., Freed, L. E., Biron, R. J. & Langer, R. Effects of mixing on the composition and morphology of tissue-engineered cartilage. *Bioeng. Food, Nat. Prod.* **42**, 850–860 (1996).
79. Vunjak-Novakovic, G. *et al.* Bioreactor cultivation conditions modulate the composition and mechanical properties of tissue-engineered cartilage. *J. Orthop. Res.* **17**, 130–138 (1999).
80. Freed, L. E., Langer, R., Martin, I., Pellis, N. R. & Vunjak-Novakovic, G. Tissue engineering of cartilage in space. *Proc. Natl. Acad. Sci.* **94**, 13885–13890 (1997).
81. Kuettner, K. E. *et al.* Synthesis of Cartilage Matrix by Mammalian Chondrocytes In Vitro II. Maintenance of Collagen and Proteoglycan Phenotype. *J. Cell Biol.* **93**, 751–757 (1982).
82. Gooch, K. J. *et al.* Effects of Mixing Intensity on Tissue-Engineered Cartilage. *Biotechnol. Bioeng.* **72**, 402–407 (2001).
83. Bueno, E. M., Bilgen, B. & Barabino, G. A. Wavy-Walled Bioreactor Supports Increased Cell Proliferation and Matrix Deposition in Engineered Cartilage Constructs. *Tissue Eng.* **11**, 1699–1709 (2005).

84. Bueno, E. M., Bilgen, B. & Barabino, G. A. Hydrodynamic Parameters Modulate Biochemical, Histological and Mechanical Properties of Engineered Cartilage. *Tissue Eng. Part A* **15**, 773–785 (2009).
85. Saini, S. & Wick, T. M. Concentric cylinder bioreactor for production of tissue engineered cartilage: effect of seeding density and hydrodynamic loading on construct development. *Biotechnol. Prog.* **19**, 510–521 (2003).
86. Villanueva, I., Klement, B. J., Deutsch, D. Von & Bryant, S. J. Cross-Linking Density Alters Early Metabolic Activities in Chondrocytes Encapsulated in Poly (Ethylene Glycol) Hydrogels and Cultured in the Rotating Wall Vessel. *Biotechnol. Bioeng.* **102**, 1242–1250 (2009).
87. Freed, L. E. *et al.* Chondrogenesis in a Cell-Polymer-Bioreactor System. *Exp. Cell Res.* **240**, 58–65 (1998).
88. Li, W.-J., Jiang, Y. J. & Tuan, R. S. Cell-nanofiber-based Cartilage Tissue Engineering using Improved Cell Seeding, Growth Factor, and Bioreactor Technologies. *Tissue Eng. Part A* **14**, 639–648 (2008).
89. Yang, Y.-H. & Barabino, G. A. Differential Morphology and Homogeneity of Tissue-Engineered Cartilage in Hydrodynamic Cultivation with Transient Exposure to Insulin-Like Growth Factor-1 and Transforming Growth Factor-B1. *Tissue Eng. Part A* **19**, 2349–2360 (2013).
90. Pazzano, D. *et al.* Comparison of chondrogenesis in static and perfused bioreactor culture. *Biotechnol. Prog.* **16**, 893–896 (2000).
91. Wendt, D., Stroebel, S., Jakob, M., John, G. T. & Martin, I. Uniform tissues engineered by seeding and culturing cells in 3D scaffolds under perfusion at defined oxygen tensions. *Biorheology* **43**, 481–488 (2006).
92. Davisson, T., Kunig, S., Chen, A., Sah, R. & Ratcliffe, A. Static and dynamic compression modulate matrix metabolism in tissue engineered cartilage. *J. Orthop. Res.* **20**, 842–848 (2002).
93. Dunkelman, N. S. *et al.* Cartilage Production by Rabbit Articular Chondrocytes on Polyglycolic Acid Scaffolds in a Closed Bioreactor System. *Biotechnol. Bioeng.* **46**, 299–305 (1995).

94. Bujia, J. *et al.* Engineering of Cartilage Tissue Using Bioresorbable Polymer Fleeces and Perfusion Culture. *Acta Otolaryngol* **115**, 307–310 (1995).
95. Santoro, R. *et al.* Bioreactor based engineering of large-scale human cartilage grafts for joint resurfacing. *Biomaterials* **31**, 8946–8952 (2010).
96. Shahin, K. & Doran, P. M. Strategies for Enhancing the Accumulation and Retention of Extracellular Matrix in Tissue-Engineered Cartilage Cultured in Bioreactors. *PLoS One* **6**, e23119 (2011).
97. Mahmoudifar, N. & Doran, P. M. Tissue engineering of human cartilage in bioreactors using single and composite cell-seeded scaffolds. *Biotechnol. Bioeng.* **91**, 338–355 (2005).
98. Forsey, R. W., Tare, R., Oreffo, R. O. C. & Chaudhuri, J. B. Perfusion bioreactor studies of chondrocyte growth in alginate-chitosan capsules. *Biotechnol. Appl. Biochem.* **59**, 142–152 (2012).
99. Degala, S., Zipfel, W. R. & Bonassar, L. J. Chondrocyte calcium signaling in response to fluid flow is regulated by matrix adhesion in 3-D alginate scaffolds. *Arch. Biochem. Biophys.* **505**, 112–117 (2011).
100. Mizuno, S., Allemann, F. & Glowacki, J. Effects of medium perfusion on matrix production by bovine chondrocytes in three-dimensional collagen sponges. *J. Biomed. Mater. Res.* **56**, 368–375 (2001).
101. Potter, K. *et al.* Cartilage formation in a hollow fiber bioreactor studied by proton magnetic resonance microscopy. *Matrix Biol.* **17**, 513–523 (1998).
102. Chen, C.-T. *et al.* Matrix Fixed-Charge Density as Determined by Magnetic Resonance Microscopy of Bioreactor-Derived Hyaline Cartilage Correlates With Biochemical and Biomechanical Properties. *Arthritis Rheum.* **48**, 1047–1056 (2003).
103. Kim, M., Bi, X., Horton, W. E., Spencer, R. G. & Camacho, N. P. Fourier transform infrared imaging spectroscopic analysis of tissue engineered cartilage: histologic and biochemical correlations. *J. Biomed. Opt.* **10**, 031105 (2005).
104. Davisson, T., Sah, R. & Ratcliffe, A. Perfusion Increases Cell Content and Matrix Synthesis in Chondrocyte Three-Dimensional Cultures. *Tissue Eng.* **8**, 807–816 (2002).

105. Gemmiti, C. V & Guldberg, R. E. Fluid Flow Increases Type II Collagen Deposition and Tensile Mechanical Properties in Bioreactor-Grown Tissue-Engineered Cartilage. *Tissue Eng.* **12**, 469–479 (2006).
106. Gemmiti, C. V & Guldberg, R. E. Shear Stress Magnitude and Duration Modulates Matrix Composition and Tensile Mechanical Properties in Engineered Cartilaginous Tissue. *Biotechnol. Bioeng.* **104**, 809–820 (2009).
107. Chen, T., Buckley, M., Cohen, I., Bonassar, L. & Awad, H. a. Insights into interstitial flow, shear stress, and mass transport effects on ECM heterogeneity in bioreactor-cultivated engineered cartilage hydrogels. *Biomech. Model. Mechanobiol.* **11**, 689–702 (2012).
108. Chen, T., Hilton, M. J., Brown, E. B., Zuscik, M. J. & Awad, H. a. Engineering Superficial Zone Features in Tissue Engineered Cartilage. *Biotechnol. Bioeng.* **110**, 1476–1486 (2013).
109. Lima, E. G. *et al.* The beneficial effect of delayed compressive loading on tissue-engineered cartilage constructs cultured with TGF-beta3. *Osteoarthr. Cartil.* **15**, 1025–1033 (2007).
110. Sakai, S. *et al.* Rotating three-dimensional dynamic culture of adult human bone marrow-derived cells for tissue engineering of hyaline cartilage. *J. Orthop. Res.* **27**, 517–521 (2009).
111. Tigli, R. S., Cannizaro, C., Gumusderelioglu, M. & Kaplan, D. Chondrogenesis in perfusion bioreactors using porous silk scaffolds and hESC-derived MSCs. *J. Biomed. Mater. Res. A* **96**, 21–28 (2010).
112. Ballyns, J. J. & Bonassar, L. J. Dynamic compressive loading of image-guided tissue engineered meniscal constructs. *J. Biomech.* **44**, 509–516 (2011).
113. Ballyns, J. J., Wright, T. M. & Bonassar, L. J. Effect of media mixing on ECM assembly and mechanical properties of anatomically-shaped tissue engineered meniscus. *Biomaterials* **31**, 6756–6763 (2010).
114. See, E. Y.-S., Toh, S. L. & Goh, J. C.-H. Effects of Radial Compression on a Novel Simulated Intervertebral Disc-Like Assembly Using Bone Marrow-Derived Mesenchymal Stem Cell Cell-Sheets for Annulus Fibrosus Regeneration. *Spine (Phila. Pa. 1976)*. **36**, 1744–1751 (2011).

## CHAPTER 3

### **The Effect of the Duration of Mechanical Stimulation and Post-Stimulation Culture on the Structure and Properties of Dynamically Compressed Tissue-Engineered Menisci<sup>\*</sup>**

#### ***Abstract***

This study investigated the hypothesis that timing and duration of dynamic compression is integral to regulating extracellular matrix (ECM) assembly of tissue engineered (TE) menisci. The goal of this study was to examine the effects of varying load and static culture duration on structure, composition and mechanical properties of TE menisci. We accomplished this by varying the duration of dynamic loading over 4 weeks of culture, and by examining increasing periods of static culture after 2 weeks of dynamic loading. Bovine meniscal fibrochondrocytes were seeded into 2% w/v alginate, crosslinked with CaSO<sub>4</sub>, injected into anatomical  $\mu$ CT based molds, and post-crosslinked with CaCl<sub>2</sub>. Meniscal constructs were dynamically compressed three times a week via a custom bioreactor for a total of 2 hours, with an hour of rest between loading cycles, for 1, 2 or 4 weeks. They were then placed in static culture. After 4 weeks of culture, increased load duration was found to be beneficial to matrix formation and mechanical properties, with superior mechanical and biochemical properties in samples loaded for 2 or 4 weeks. Further, the mechanical properties of these constructs were similar, suggesting that the additional two weeks of loading may not be necessary. Samples loaded for 2 weeks followed by a 4 week static culture period yielded the most mature matrix with significant improvements in collagen bundle formation, 2.8 fold increase in glycosaminoglycan(GAG) content, 2

---

<sup>\*</sup> This chapter is published: Puetzer JL, Ballyns JJ, Bonassar LJ. The Effect of the Duration of Mechanical Stimulation and Post-Stimulation Culture on the Structure and Properties of Dynamically Compressed Tissue-Engineered Menisci. *Tissue Eng Part A* 2012;18:1365-75.

fold increase in collagen content, and 4.3 fold increase in the compressive equilibrium modulus. Overall this study demonstrated the importance of timing and duration of loading. By switching to prolonged static culture after 2 weeks of loading we decreased the amount of ECM lost to the media, while significantly increasing biochemical and mechanical properties of TE menisci.

### ***Introduction***

Meniscal injury is one of the most common traumatic injuries in the knee, second only to osteoarthritis, and accounts for over 1 million surgeries a year in the United States<sup>1,2</sup>. Treatment of meniscus lesions is the most frequent procedure carried out by orthopaedic surgeons<sup>3</sup>, and while there have been improvements in suturing techniques and materials for repair of focal lesions<sup>4-6</sup>, improvements are still needed for treatment of whole meniscal replacement. Currently the only option for whole meniscal replacement is meniscectomy followed by cadaveric allografts transplant. However donor tissue is scarce, it is difficult to match the native joint architecture, and there is risk of disease transmission<sup>1,3</sup>.

Due to the challenges associated with allograft transplantation, the use of tissue engineering to develop a meniscal construct is of much interest. A tissue engineered (TE) meniscus should be geometrically accurate in order to ensure the appropriate distribution of pressures across the joint, it must be able to withstand anatomical compressive and tensile loading conditions prior to implantation, and needs to achieve the heterogeneous mechanical and biochemical properties found in native menisci<sup>2,7,8</sup>. For many years research has concentrated on treatment of focal defects and extracellular matrix production in plugs. Recently, several studies have attempted to create a whole TE meniscal replacement, whether anatomical or not, made from either synthetic or natural materials<sup>9-21</sup>. None of these efforts have

achieved clinical use, as many lack the mechanical properties necessary to withstand implantation *in vivo*. Thus, mechanical conditioning may be necessary for engineered constructs prior to implantation.

Mechanical conditioning is widely used to enhance the *in vitro* formation of various types of TE cartilage, often resulting in increased mechanical and biochemical properties. Several studies have utilized dynamic compression to characterize the mechanical and biochemical properties of meniscal explants<sup>22-32</sup>. Many of these studies<sup>22-25, 30-32</sup>, and a few TE studies<sup>12, 14, 33</sup> established that mechanical conditioning enhances extracellular matrix (ECM) production and mechanical properties of scaffolds seeded with meniscal fibrochondrocytes.

Recently, we reported that dynamic compression of anatomically shaped TE alginate menisci significantly enhanced ECM production and mechanical properties after 2 weeks of loading<sup>14</sup>. However, prolonged loading subsequently decreased mechanical performance and matrix retention due to either increased alginate degradation<sup>12</sup>, or by induced catabolic cellular responses<sup>28, 32, 34-36</sup>.

This data is consistent with several other recent observations that prolonged mechanical stimulation is not optimal for engineered tissues. Several studies of meniscal tissue explants<sup>28, 32</sup> and articular chondrocytes seeded in PEG<sup>36</sup>, agarose<sup>35</sup>, and peptide hydrogels<sup>34</sup> have demonstrated that moderate dynamic strains of 5-20% over extended periods of time (12-48 hours) results in inhibited cell proliferation and proteoglycan synthesis, increased breakdown of proteoglycans, and increased expression of matrix metalloproteinases (MMP-1, -3, -9, and -13) and aggrecanases. Collectively these studies demonstrate that prolonged dynamic compression induces a cellular catabolic response and may not be optimal for engineered tissues. While the catabolic response may be important to initiate proteoglycan turnover and stimulate matrix remodeling, sustained expression of the catabolic genes can lead to

tissue degradation<sup>34</sup>. This may explain the decrease in mechanical and biochemical properties with prolonged loading of TE alginate menisci<sup>14</sup>.

Nicodemus et al.<sup>37</sup> recently demonstrated that intermittent dynamic compression at 5-20% strain over one week significantly increases expression of MMP-1, -3, and -13 and collagen II in articular chondrocytes encapsulated in PEG hydrogels. However, MMP levels dropped significantly once dynamic compression was removed. Furthermore, at 7 days post-loading, MMP expression levels were lower than before loading was applied, while collagen and GAG levels continued to increase<sup>37</sup>. This study is an excellent example of how the duration and timing of dynamic compression affect the catabolic and anabolic responses of TE articular cartilage; however, such effects have never been documented in scaffolds with meniscal fibrochondrocytes. We hypothesize that the timing and duration of loading (i.e. duty cycle) regulates ECM assembly of TE menisci. The specific goal of this study was to examine the effects of varying the duration of loading and post-loading static culture duration on the structure, composition, and mechanical properties of seeded anatomical alginate menisci. We accomplished this by I) varying the duration of dynamic loading over 4 weeks of culture, and II) altering the period of static culture after 2 weeks of dynamic loading.

## **Methods**

### **Injection Molding**

Meniscal constructs were generated as previously described<sup>11, 38, 39</sup>. Briefly, bovine menisci were isolated from freshly slaughtered 1-3 day old calves and diced into 1 mm<sup>3</sup> cubes. The tissue was digested overnight in 0.3% collagenase, 100 µg/mL penicillin, and 100 µg/mL streptomycin in Dulbecco's modified Eagle's medium (DMEM). The bovine meniscal fibrochondrocytes were seeded into sterile 2% w/v

low viscosity high G-content alginate at  $50 \times 10^6$  cells/ml. The alginate-cell suspension was combined with 0.02 g/mL  $\text{CaSO}_4$  at a 2:1 ratio and injected into ABS plastic molds of ovine menisci, designed as previously described from micro computed tomography ( $\mu\text{CT}$ ) scans<sup>12, 38</sup>. Molds were then allowed to further crosslink for 40 minutes in 60 mM  $\text{CaCl}_2$  before removal of the construct.

A total of 44 constructs were created and incubated in DMEM with 10% fetal bovine serum, 100 U/mL penicillin, 100  $\mu\text{g}/\text{mL}$  streptomycin, 0.1 mM non-essential amino acids, 50  $\mu\text{g}/\text{mL}$  ascorbate, and 0.4 mM L-proline. Media was changed three times a week after loading. The experiment was divided into two parts where first the duration of intermittent dynamic loading was varied over 4 weeks of culture to investigate the effect of duration of loading, and second the total culture duration after 2 weeks of dynamic loading was varied to investigate the effect of prolonged static culture. In part I of the experiment, five treatment groups were examined, including a 0.28 week loaded control and 4 groups loaded for 0, 1, 2 or 4 weeks and then free swell static cultured for 4, 3, 2, or 0 weeks, respectively, for a total culture period of 4 weeks (Figure 3.1A). These 4 treatment groups are referred to as 0wL/4wS, 1wL/3wS, 2wL/2wS, and 4wL/0wS where #wL denotes the number of weeks the samples were loaded and #wS denotes the additional number of weeks the samples were static cultured after loading was complete, e.g. 2wL/2wS means samples were loaded for 2 weeks followed by 2 weeks of static culture. In part II, samples were loaded for 2 weeks followed by static culture for 0, 2, or 4 weeks and compared to samples that were static cultured for 2, 4, or 6 weeks (Figure 3.1B). Control 0.28 week static and loaded samples were also included.

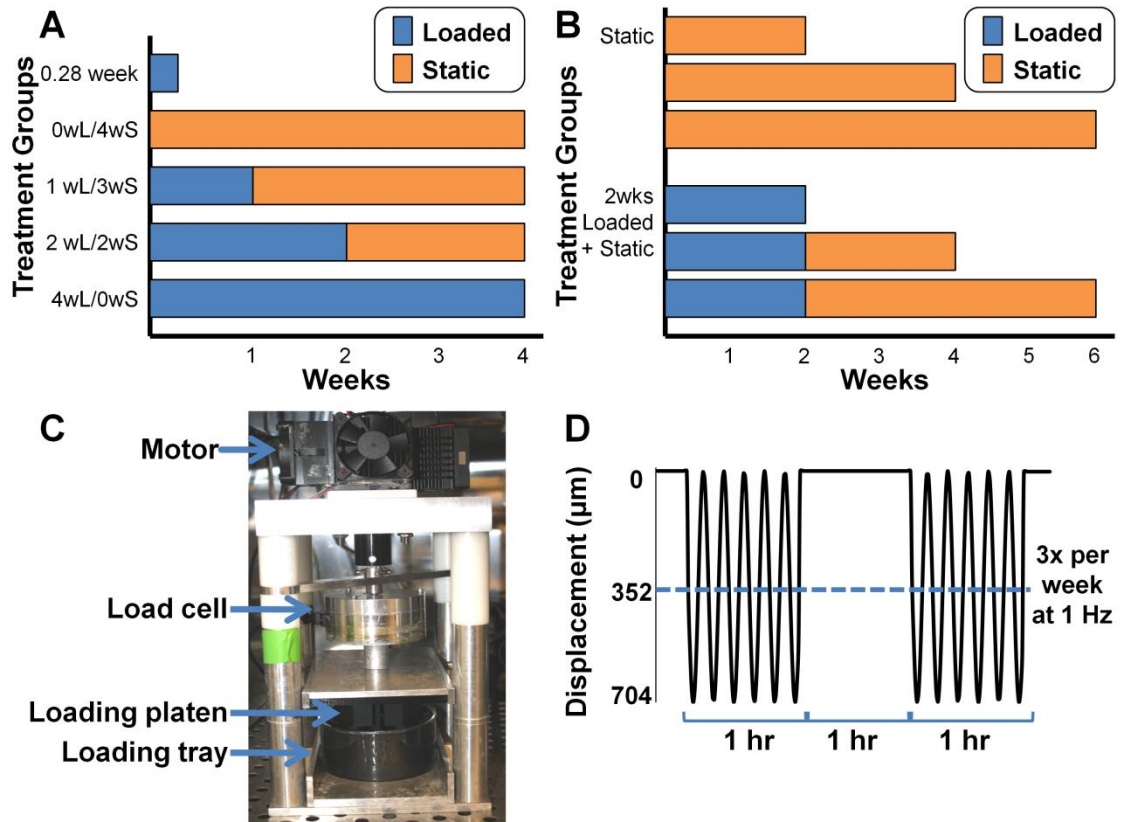


**Figure 3.1:** Depiction of experimental setup for part I (A) and part II (B). Custom designed bioreactor with loading platen and tray designed to match construct geometry so it can apply uniform dynamic compression (C) and waveform depicting loading regime of bioreactor (D).

### Dynamic Loading

Dynamic compression was applied with a custom in-house designed bioreactor outfitted with a loading platen and tray designed to match construct geometry and apply uniform deformation as previously described (Figure 3.1C)<sup>14</sup>. Briefly, the loading platen and tray were designed based on the same  $\mu\text{CT}$  scans used to design the menisci molds, thus allowing the loading platen to match surface geometry of the meniscus and the loading tray to have an impression that restricts motion of the construct under loading<sup>14</sup>.

Loaded meniscal constructs were exposed to dynamic compression for an hour twice every other day with an hour of rest in between loading cycles. The constructs

were exposed to a compressive sinusoidal displacement at 1 Hz with a 352  $\mu\text{m}$  offset and 352  $\mu\text{m}$  amplitude, resulting in a maximal displacement of 704  $\mu\text{m}$  as previously described<sup>14</sup>(Figure 3.1D). This loading condition was chosen due to work that identified it as the ideal loading frequency and most physiologically relevant loading regime to mimic the native meniscal environment<sup>32, 34, 40</sup>. Linear poroelastic finite element analysis confirmed this loading regime applies a compressive strain of 15% to the majority of the concave surface of the meniscus<sup>14</sup>, which is within the range of strain values used in other dynamic compressive studies<sup>32, 34, 36</sup>.

#### Post Culture Construct Analysis

Upon removal from culture, meniscal constructs were photographed and visually inspected for changes in opacity and shape fidelity. Constructs were then processed for histology, biochemistry, and mechanical analysis as previously described<sup>11, 12, 38</sup>. Briefly, cross-sections of constructs were cut and fixed in 10% buffered formalin with 1 mM  $\text{CaCl}_2$  to prevent gel solubilization. Fixed sections were then sectioned and stained with Safranin-O and Picrosirius red to observe glycosaminoglycan (GAG) and collagen localization, respectfully. Twenty representative images of each treatment group stained with Picrosirius red were taken at 400x brightfield for image analysis of collagen bundle formation. Images were analyzed with a custom MATLAB program, which isolated collagen bundles based on color, size and shape, and provided a collagen bundle count and area for each image. Data was collected and analyzed to determine the percentage of fibers per sample (measurement of the fraction of selected area occupied by fibers in each sample), the average number of collagen bundles per  $\text{mm}^2$ , and the average size of collagen bundles.

The remainder of each meniscal construct had 4mm diameter by 2 mm thick plugs cut from the face, center, and bottom of samples. Excess surrounding tissue

from each spatial location was used for biochemical analysis, while plugs were used for mechanical analysis. A total of 6 plugs and 6 biochemical samples were obtained from each meniscal construct.

Biochemical samples were weighed to obtain the wet weight (WW), frozen, lyophilized, and weighed again to obtain the dry weight (DW). The samples were then digested in 1.25 mg/mL papain solution overnight at 60°C and analyzed for DNA, GAG, and collagen content via a Hoechst dye assay<sup>41</sup>, a modified DMMB dye assay at pH 1.5<sup>42</sup>, and a hydroxyproline assay<sup>43</sup>, respectively. Media samples, obtained when media was changed three times a week, were analyzed biochemically for DNA, GAG, and collagen content using the same assays. Retention percentages for biochemical properties were calculated as the fraction of total accumulation within the scaffolds to the sum of accumulation within the scaffold plus accumulated lost to the media.

Plugs were tested in confined compression to determine equilibrium modulus (EnduraTech; Electroforce (ELF) 3200 System, Minnetonka, MN) as previously described<sup>39, 44</sup>. Briefly, stress relaxation tests were performed by imposing 10x50 µm steps on the plug with the resultant loads fit to a poroelastic model using a custom MATLAB program to calculate the equilibrium modulus.

### Statistics

All data were analyzed by 2-way ANOVA using Tukey's t-test for post-hoc analysis and  $p < 0.05$  as a threshold of statistical significance. All statistical analysis was performed using Sigmastat version 3.0 and all data expressed as mean $\pm$ SD.

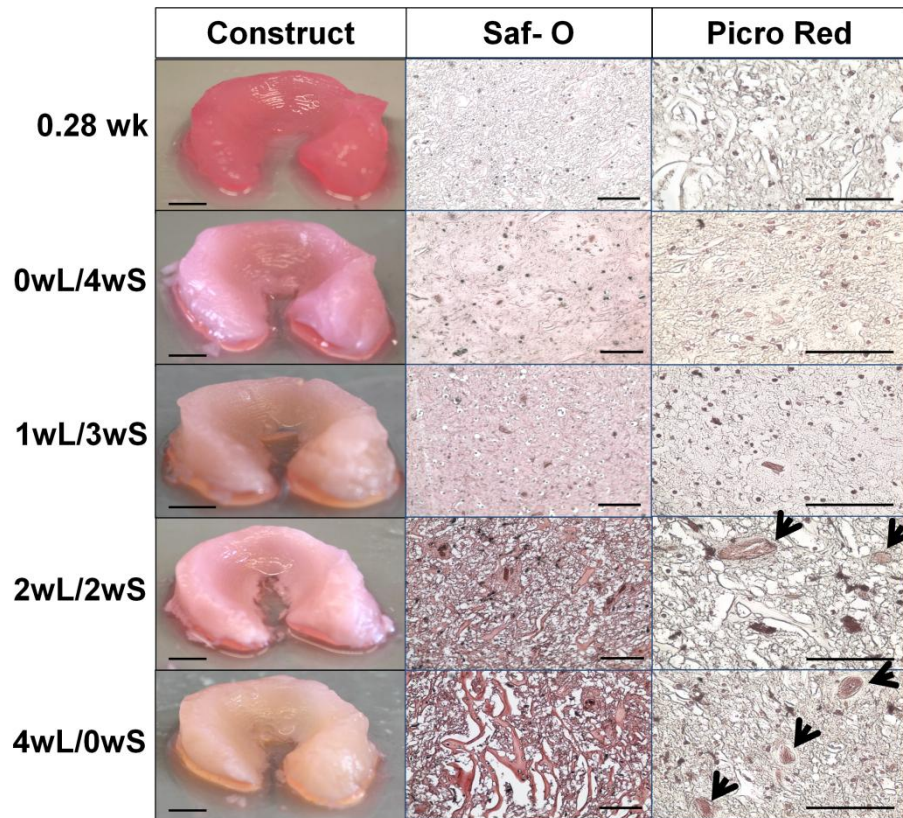


**Figure 3.2:** Photographs of Part I engineered constructs after removal from culture (Column 1), tissue sections stained with Safranin-O at 200x (Column 2) and Picrosirius red at 400x under brightfield (Column 3). Scale bars for constructs = 5 mm and for stained sections = 100  $\mu$ m, arrows point to collagen bundles

## Results

### Meniscal construct shape fidelity and composition

Gross inspection of engineered constructs demonstrated that shape fidelity was maintained in all treatment groups for the entire length of culture (Figure 3.2 and 3.3). Also, there was a noticeable increase in opacity with loading and time in culture, which suggests an increase in matrix accumulation (Figure 3.2).

Overall, histology for both parts of the experiment demonstrated an increase in tissue development with time in culture, with increased development in loaded samples. In part I, Safranin-O and Picrosirius red staining demonstrated increased

GAG localization and collagen bundles in the 2wL/2wS and 4wL/0wS treatment groups, respectively, with a noticeable change to a more heterogeneous morphology in the 2wL/2wS and 4wL/0wS groups, similar to that of native menisci (Figure 3.2 column 2 and 3). In part II, Safranin-O staining exhibited increased GAG localization in static and loaded samples with time in culture, along with a more heterogeneous composition in loaded samples (Figure 3.3 columns 2 and 5). Picrosirius red staining demonstrated increased collagen content with time in culture for static and loaded samples, with more prominent localization in the 2 week loaded samples. Collagen bundle formation was evident starting at week 2 and increased through week 6 in loaded samples, while only a few collagen bundles formed in static samples by week 6 (Figure 3.3 columns 3 and 6).

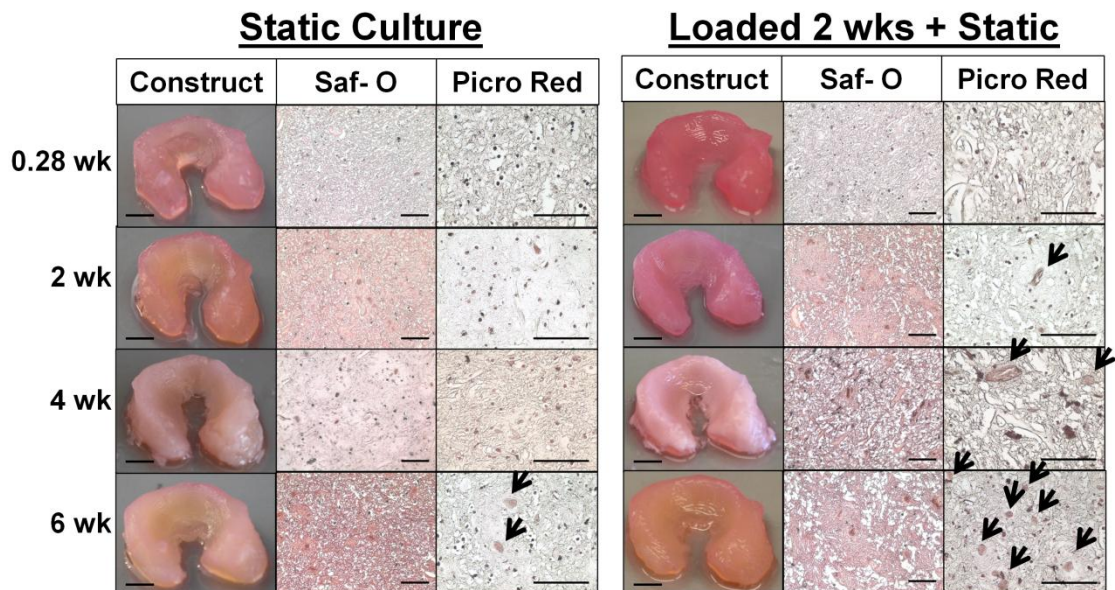


**Figure 3.3:** Photographs of Part II engineered constructs after removal from culture (Column 1 and 4), tissue sections stained with Safranin-O at 200x (Column 2 and 5) and Picrosirius red at 400x under brightfield (Column 3 and 6). Scale bars for constructs =5 mm, and for stained sections = 100  $\mu$ m, arrows point to collagen bundles.

Image analysis of Picrosirius red staining demonstrated that the percentage of fiber content, number of bundles per  $\text{mm}^2$ , and average size of collagen bundles significantly increased with 2 weeks of loading (Figure 3.4). Collagen bundles were present after just 1 day of loading as evident in the 0.28 wk samples. In part I, the 2wL/2wS and 4wL/0wS samples had a greater than 2.5 fold increase in fiber content ( $P<0.001$ ), 3 fold increase in number of collagen bundles ( $P<0.001$ ), and 2 fold increase in average size of individual collagen bundles ( $P<0.05$ ) over all other samples (Figure 3.4A-C). In part II, percent fiber content and number of collagen bundles increased 13 and 9.5 fold, respectively, after just two weeks of loading ( $P<0.02$ ). Loaded samples continued to significantly increase with prolonged static culture, with six week samples significantly greater than all other time points for loaded and static samples and 3 fold higher than 6 week static samples ( $P<0.001$ ) (Figure 3.4D&E). Average individual bundle area significantly increased with loading, and appeared to plateau for both static and loaded samples by week six (Figure 3.4F). Notably, fiber sizes observed at early times in culture were quite large,  $\sim 200 \mu\text{m}^2$  in area or  $\sim 16 \mu\text{m}$  in diameter. This size may represent some critical nucleation size for fibers in this system, or may be a technical limitation of this technique due to the inability to accurately distinguish between extracellular and intracellular fibers.

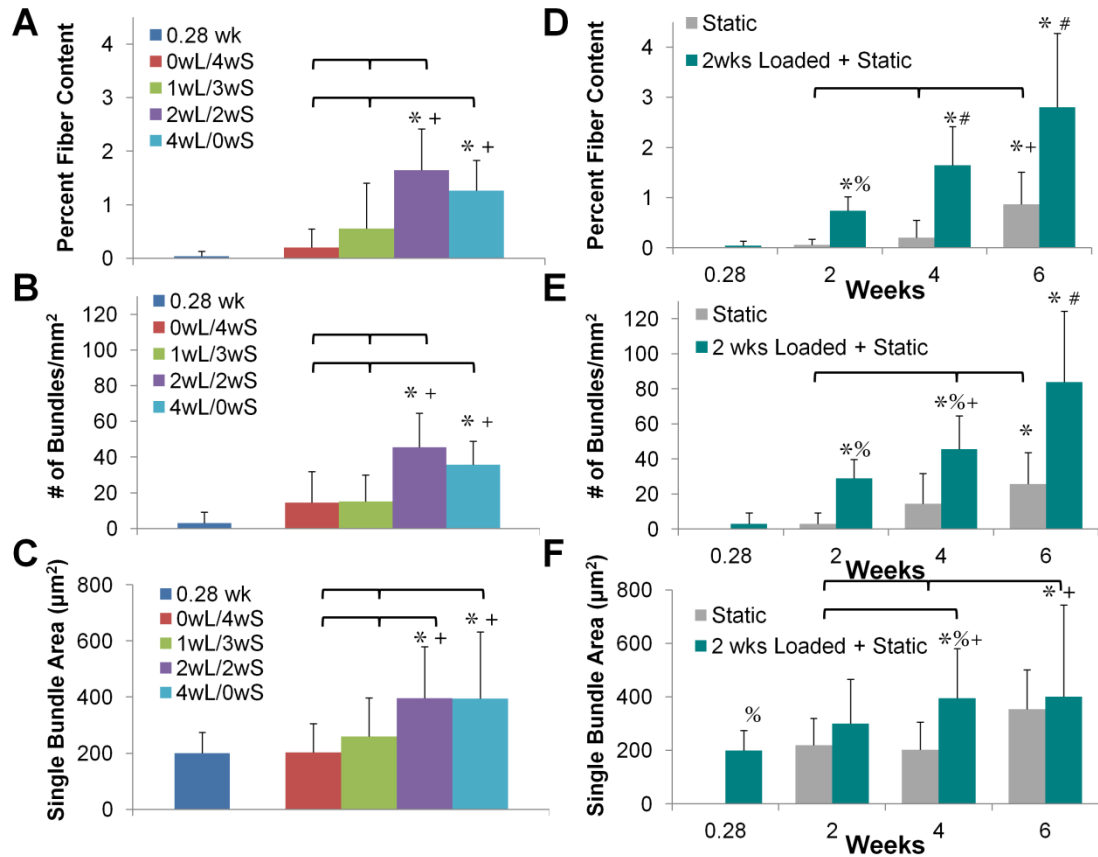


**Figure 3.4:** Collagen bundle content determined by image analysis of 20 representative images of each treatment group stained with Picrosirius red. Percent fiber content of constructs, number of collagen bundles per mm<sup>2</sup>, and average area of individual collagen bundles for part I (A-C) and II (D-F) respectively. \* =difference from 0.28 week cultures, + = difference from bracketed groups, % = difference from respective group at time point, and # = difference from all other treatment groups at all other time points. Data presented as mean±SD and P<0.05.

### Biochemical Properties

Biochemical analysis demonstrated an increase in GAG content with time in culture, with no effect or a decrease in GAG content for loaded constructs. In part I, where duration of loading was varied over 4 weeks of culture, GAG content increased with time for all groups, with the 4wL/0wS and 0wL/4wS treatment groups having significantly higher GAG concentration than the 1wL/3wS and 2wL/2wS groups (P<0.02) (Figure 3.5A). In part II, where the period of static culture duration was

varied after 2 weeks of dynamic loading, GAG content for static culture constructs significantly increased at 2 weeks by 2 fold, and plateaued for the remainder of culture. In contrast, constructs loaded 2 weeks then static cultured had significantly lower GAG content than the static samples until week 6 when the GAG concentration increased 2.8 fold and became significantly greater than static constructs ( $P < 0.001$ ) and all other time points for loaded samples ( $P < 0.02$ ) (Figure 3.5C).

All treatment groups had an initial large loss of GAG to the media, which decreased to a significantly lower level throughout the remainder of culture ( $P < 0.001$ ) (Figure 3.5B and D). Treatment had no apparent effect on release of GAG to the media. In part I, GAG retention remained relatively similar for 0wL/4wS, 1wL/3wS, and 4wL/0wS with retentions of 39%, 30%, and 36% respectively, while 2wL/2wS had 20% retention. In part II, static samples began with a high 38% retention at 2 weeks which decreased by week 6 to 15%. Samples loaded 2 weeks and then static cultured maintained 20% retention of GAG throughout culture.

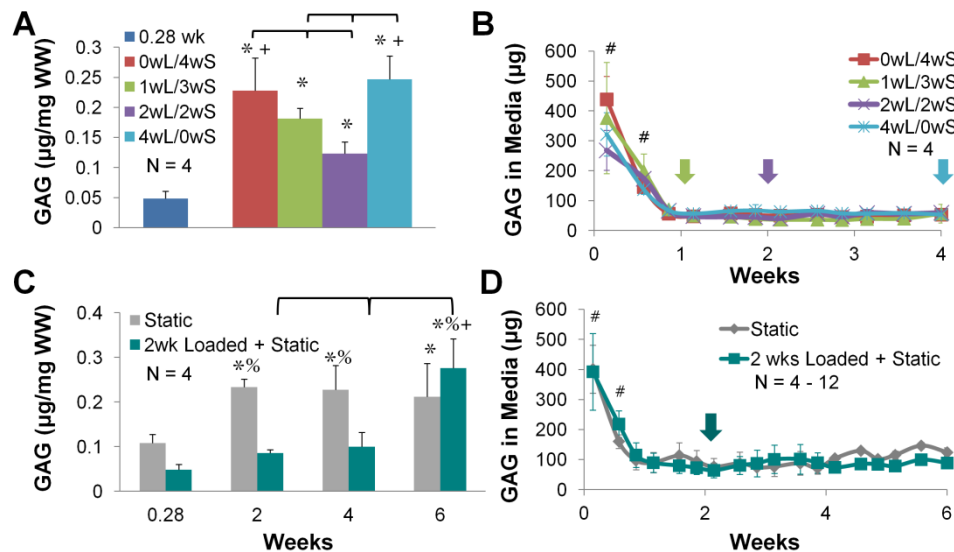


**Figure 3.5:** GAG content found in meniscal constructs (A&C) and release to the culture media per day (B&D) for different culture conditions in Part I (A&B) and Part II (C&D). \* = difference from 0.28 week cultures, + = difference from bracketed groups, % = difference from respective group at time point, and # = difference of all culture conditions at that day from all other days. Data presented as mean $\pm$ SD and  $P < 0.05$ . Arrows indicate when respective loading was removed.

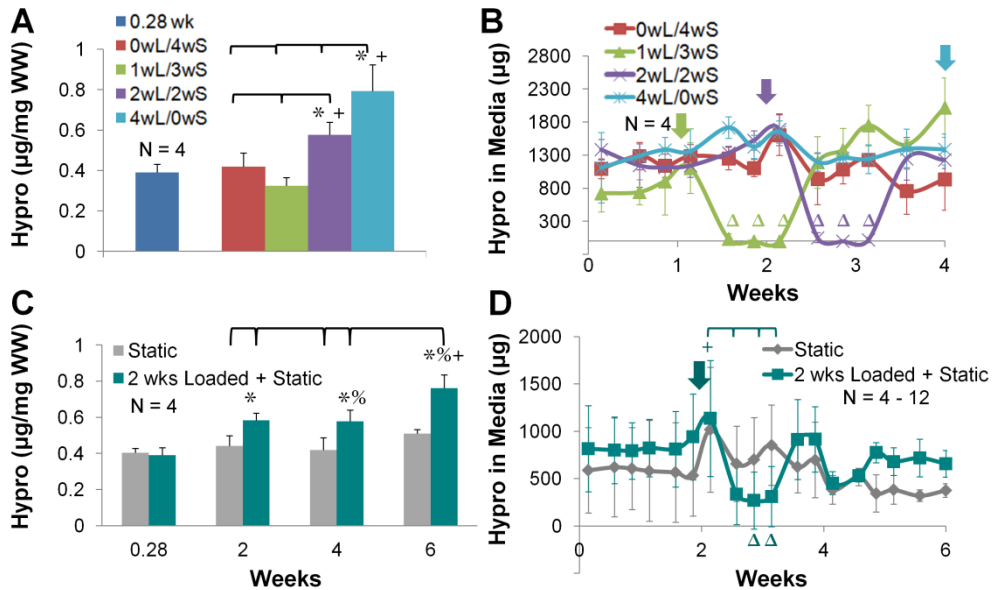


**Figure 3. 6:** Collagen content found in meniscal constructs (A&C) and release to the culture media per day (B&D) for different culture conditions in Part I (A&B) and Part II (C&D). \* = difference from 0.28 week cultures, % = difference from respective group at time point, + = difference from bracketed groups, and Δ=difference between respective culture conditions at that day. Data presented as mean±SD and P<0.05. Arrows indicate when loading was removed.

Prolonged loading significantly increased collagen content. In part I, collagen content was significantly higher in 2wL/2wS and 4wL/0wS groups in comparison to all other treatment groups (P<0.001), while the 4wL/0wS group had a significantly higher concentration of collagen than the 2wL/2wS group (Figure 3.6A). In part II, samples loaded for 2 weeks had significantly higher collagen content at 2, 4 and 6 weeks than respective static and 0.28 week construct. By week 6, 2 week loaded samples had a 2 fold increase in collagen content and was significantly higher than all other time points (P<0.002) (Figure 3.6C).

Collagen released to the media was abolished in part I and significantly reduced in part II for the week following removal of load, after which collagen loss returned to previous levels for the duration of culture (Figure 3.6B and D). In part I, collagen

retention increased with prolonged loading with 2wL/2wS and 4wL/0wS having 8% retention, and 0wL/4wS and 1wL/3wS having 5% retention. In part II, collagen retention decreased with time in culture with static and loaded samples having retentions of 46% and 27% at 2 weeks and 11% and 10% at 6 weeks.

Despite increased ECM content, DNA content demonstrated a significant drop after 2 days for all treatment groups in both part I and II ( $P < 0.001$  data not shown). Similarly, DNA released to the media demonstrated a large amount of DNA in the media over the first few days, which decreased and leveled off with time to a very low level (below 20  $\mu\text{g}/\text{day}$ ) in the media for all treatment groups (data not shown).

There was no consistent difference seen spatially for DNA, GAG, and collagen content in all treatment groups (data not shown).

### Equilibrium modulus

The equilibrium modulus significantly increased with prolonged loading. In part I, the equilibrium modulus was significantly higher for 2wL/2wS and 4wL/0wS groups with a 4.3 and 3.4 fold increase over 0.28 week controls respectively ( $P < 0.012$ ) (Figure 3.7A). In part II, the equilibrium modulus for samples loaded 2 weeks and then static cultured significantly increased 2.0-2.8 fold over the static and 0.28 week controls by 2 weeks of culture and further significantly increased by 4 weeks of culture for a final 4.3 fold increase over 0.28 week controls (Figure 3.7B). Loaded samples were significantly greater than static samples at 2, 4 and 6 weeks ( $P < 0.05$ ).

There were no consistent significant spatial differences in equilibrium modulus; however the bottom of the construct did trend toward being higher than the face and center of the constructs in samples loaded for two weeks and then static cultured ( $P < 0.1$  data not shown).

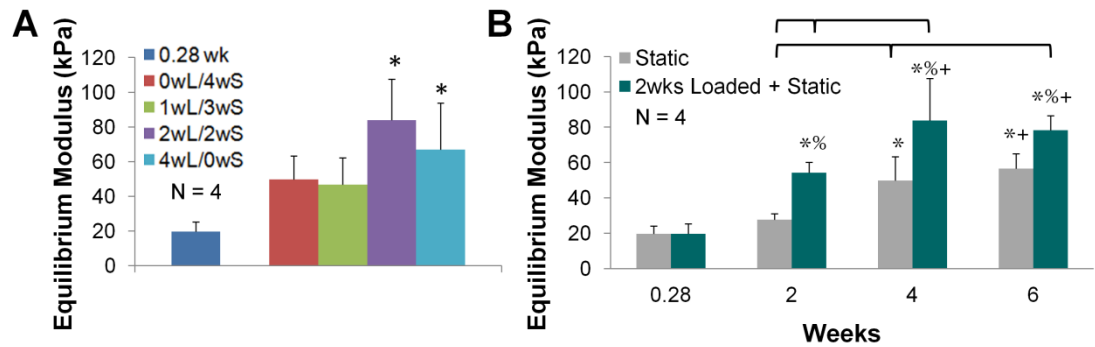


**Figure 3.7:** Compressive equilibrium modulus from part I (A) and part II (B) of the experiment. \* = difference from 0.28 week cultures, % = difference from respective group at time point, + = difference from bracket groups. Data presented as mean $\pm$ SD and  $P < 0.05$ .

### Discussion

This study investigated the hypothesis that altering the duration of loading and total culture time is key to regulation of ECM assembly. This was achieved in two parts: I) the duration of dynamic loading was varied over 4 weeks of culture, and II) the period of static culture after 2 weeks of dynamic loading was varied. In part I we demonstrated that the effect of dynamic stimulation on TE menisci was dependent on load duration. In general, increased load duration was beneficial to matrix formation, collagen accumulation and mechanical properties, with 2wL/2wS and 4wL/0wS superior to static and 1wL/3wS. Loading decreased or had no effect on GAG accumulation. Further, the mechanical properties of 2wL/2wS and 4wL/0wS were similar suggesting that the additional two weeks of loading may not be necessary. In part II we demonstrated that static culture after 2 weeks of loading improves ECM properties, with further significant increases in GAG, collagen content, formation of collagen bundles and equilibrium modulus by 6 weeks of culture. Overall this study demonstrated that we were able to maintain and improve biochemical and mechanical properties with static culture after 2 weeks of loading.

In this study, meniscal fibrochondrocytes seeded in alginate responded to dynamic compression by differentially regulating collagen and GAG accumulation, which is contrary to how TE articular cartilage typically responds. We demonstrated that meniscal fibrochondrocytes seeded in alginate respond immediately to load by increasing collagen concentrations after 2 weeks of loading, while decreasing or not affecting GAG concentrations. GAG concentrations only increased with time in culture and/or accumulation of collagen content. Further, removal of loading demonstrated a significant change in release of collagen to the media but had no effect on the release of GAG. In contrast, TE cartilage exposed to dynamic compression has been repeatedly shown to have increased GAG and collagen accumulation, often with a greater accumulation of GAG than collagen<sup>45-49</sup>. This response of TE menisci and articular cartilage to dynamic compression is further supported by a study which has observed a differential response of loaded explants of articular cartilage and meniscus tissue<sup>22</sup>, and by another study which has observed articular chondrocytes and meniscal fibrochondrocytes to synthesize and accumulate aggrecan differently<sup>50</sup>. Further, meniscal fibrochondrocytes may differentially regulate collagen and GAG based on the composition of the native tissue. GAG concentration in fibrocartilage are eight-fold less than that found in articular cartilage<sup>1</sup>, thus demonstrating the importance of collagen in fibrocartilage.

However, the lower concentration of GAG seen in this study could be due to other factors besides cellular response to loading. Multiple studies have demonstrated mechanical stimulation of cell seed scaffolds to result in loss of GAG to the media and/or no effect on GAG accumulation<sup>14, 37, 51, 52</sup>. We have seen this previously with significant increases in release of GAG to the media with prolonged loading<sup>14</sup> and in this study with a 18% and 38% retention in 2 week loaded and static samples respectively. It is believed that a collagen matrix must be present in order to maintain

GAG within the scaffold, otherwise GAG could be easily washed out of the sample by mechanical loading<sup>51, 52</sup>. This could also explain why at 6 weeks in our 2 week loaded and then static cultured samples we see significantly increased GAG accumulation coinciding with significantly increased collagen accumulation.

Additionally, in this study we observed significant increases in collagen content and collagen bundle formation coincided with significant increases in the compressive modulus. This suggests that collagen has a more direct relationship to the compressive equilibrium modulus in TE fibrocartilage, contrary to the relationship between GAG and the compressive modulus often seen in TE articular cartilage<sup>49, 51, 53</sup>. This relationship between collagen and the compressive modulus could be due to increased organization attributed to collagen fiber accumulation and not necessarily the properties of collagen<sup>51, 53</sup>. Once GAG accumulation increases, its contribution to the compressive equilibrium modulus may increase.

Previously, we reported that dynamic compression of anatomically shaped TE alginate menisci significantly enhanced ECM production and mechanical properties after only 2 weeks of loading<sup>14</sup>. However, we also reported that prolonged loading subsequently decreased mechanical performance and matrix retention. We believe that this decrease in properties could be caused by either a degradation of alginate<sup>12</sup> or a cellular catabolic response induced by prolonged loading resulting in increased expression of MMPs and aggrecanases, and increased loss of ECM to the media<sup>28, 32, 34-36</sup>. In this experiment, loading for two weeks and then switching to prolonged static culture eliminated the decrease in mechanical and biochemical properties we previously saw with prolonged loading and resulted in significantly increased mechanical and biochemical properties. Further, we saw no change in release of DNA, GAG, or collagen content in the media, which we previously demonstrated to significantly increase with prolonged loading<sup>14</sup>. By eliminating loading after 2 weeks

we are able to decrease the amount of ECM lost to the media, while still inducing significant increase in ECM accumulation and mechanical properties. Removing load could be slowing alginate degradation or it may be down regulating catabolic activities often induced by mechanical loading.

It has been increasingly suggested that catabolic activity induced by mechanical loading is necessary to initiate proteoglycan turnover and remodeling for a biomechanically functional tissue<sup>34, 37, 54, 55</sup>. Further, it has been demonstrated that catabolic activity is downregulated while anabolic activity continues when mechanical stimulation is removed<sup>37, 55</sup>. Recently, De Croos et al.<sup>55</sup> demonstrated that a single application of dynamic compression for 30 minutes to chondrocytes in calcium polyphosphate substrates results in upregulation of MMPs within 2 hours post application, release of proteoglycans and collagen by 6 hours post application and finally a rebuilding phase of collagen and proteoglycan accumulation within 24 hours. Further, Nicodemus et al.<sup>37</sup> demonstrated that intermittent dynamic compression over one week significantly increased expression of MMPs and collagen type II in chondrocytes encapsulated in PEG hydrogels and once dynamic compression was removed MMP levels significantly dropped. Seven days after loading, MMPs were expressed at levels below that expressed before loading was applied, while collagen and GAG accumulation increased. Several other studies have suggested that mechanical stimulation's upregulation of MMPs and aggrecanases which results in degradation and release of GAGs is a necessary rebuilding process for turnover of ECM and continued development of tissue<sup>34, 54</sup>. This pattern of upregulation of an anabolic and catabolic response with mechanical stimulation, followed by downregulation of the catabolic response once loading is removed could suggest why our constructs continue to increase in mechanical and biochemical properties after loading is removed at 2 weeks. It could also suggest why during loading we see a

decrease in GAG accumulation and after loading is removed we observe a significant increase in GAG accumulation. However, further evaluation of MMP and aggrecanase expression during culture would be required to verify.

We observed a significant temporary reduction in collagen released to the media for the week following removal of load. To our knowledge this is the first study to observe such a delayed effect of loading, likely due to previous studies focusing on shorter culture times after loading<sup>34, 37, 55</sup>. Further analysis will be required to determine whether the lack of loss of collagen after loading is due to a temporary downregulation in collagen synthesis (which seems unlikely, given the continued accumulation of collagen in the samples) or a downregulation in MMP expression or activity, as has been reported for mechanical stimulation of articular chondrocytes<sup>37</sup>.

There are some limitations to this study that should be considered. Although we describe how combinations of loading and culture can enhance the assembly of ECM by meniscal fibrochondrocytes, the mechanisms behind these phenomena are not clear and will require significant future study. Further, as these studies were conducted on healthy neonatal bovine fibrochondrocytes, it is unclear how the results here would translate to adult human fibrochondrocytes, particularly if obtained with a patient with joint disease. As such, understanding the catabolic components of matrix assembly in greater detail will be a focus of future study.

Overall, in this study we demonstrated that altered loading protocols significantly affect the mechanical properties and matrix production of TE menisci, providing an *in vitro* mechanism for conditioning TE menisci replacements. We demonstrated we are able to maintain and improve mechanical and biochemical properties past 2 weeks of loading however these properties (3% collagen fiber concentration, 7.3-9.4 µg/mg DW GAG, 144-158 µg/mg DW collagen, and 84-108 kPa equilibrium modulus) are still not equivalent to native values (19.1% collagen fiber concentration<sup>56</sup>, 20-30

$\mu\text{g}/\text{mg}$  DW GAG<sup>10, 38</sup>, 600-700  $\mu\text{g}/\text{mg}$  DW collagen<sup>10, 38</sup>, and 150-220 kPa equilibrium modulus<sup>1</sup>). Further investigations need to be performed to further improve the properties of our anatomically correct TE menisci. Prolonged culture past 6 weeks, treatment with growth factors, or use of a material which encourages cell attachment and better retention of ECM products could all serve to further improve the mechanical and biochemical properties of these menisci scaffolds.

## REFERENCES

1. Sweigart M.A., Athanasiou K.A. Toward tissue engineering of the knee meniscus. *Tissue Eng.***7**:111. 2001.
2. Khetia E.A., McKeon B.P. Meniscal allografts: biomechanics and techniques. *Sports Med Arthrosc.***15**:114. 2007.
3. Peters G., Wirth C.J. The current state of meniscal allograft transplantation and replacement. *Knee.***10**:19. 2003.
4. Stone K.R., Steadman J.R., Rodkey W.G., Li S.T. Regeneration of meniscal cartilage with use of a collagen scaffold. Analysis of preliminary data. *J Bone Joint Surg Am.***79**:1770. 1997.
5. Farnig E., Sherman O. Meniscal repair devices: a clinical and biomechanical literature review. *Arthroscopy.***20**:273. 2004.
6. McDermott I. Meniscal tears, repairs and replacement: their relevance to osteoarthritis of the knee. *Br J Sports Med.***45**:292. 2011.
7. Buma P., Ramrattan N.N., van Tienen T.G., Veth R.P. Tissue engineering of the meniscus. *Biomaterials.***25**:1523. 2004.
8. Hoben G.M., Athanasiou K.A. Meniscal repair with fibrocartilage engineering. *Sports Med Arthrosc.***14**:129. 2006.
9. Kang S.W., Son S.M., Lee J.S., Lee E.S., Lee K.Y., Park S.G., et al. Regeneration of whole meniscus using meniscal cells and polymer scaffolds in a rabbit total meniscectomy model. *J Biomed Mater Res A.***78**:659. 2006.
10. Aufderheide A.C., Athanasiou K.A. Assessment of a bovine co-culture, scaffold-free method for growing meniscus-shaped constructs. *Tissue Eng.***13**:2195. 2007.
11. Ballyns J.J., Cohen D.L., Malone E., Maher S.A., Potter H.G., Wright T., et al. An optical method for evaluation of geometric fidelity for anatomically shaped tissue-engineered constructs. *Tissue Eng Part C Methods.***16**:693. 2010.

12. Ballyns J.J., Wright T.M., Bonassar L.J. Effect of media mixing on ECM assembly and mechanical properties of anatomically-shaped tissue engineered meniscus. *Biomaterials*.**31**:6756. 2010.
13. Stabile K.J., Odom D., Smith T.L., Northam C., Whitlock P.W., Smith B.P., et al. An acellular, allograft-derived meniscus scaffold in an ovine model. *Arthroscopy*.**26**:936. 2010.
14. Ballyns J.J., Bonassar L.J. Dynamic compressive loading of image-guided tissue engineered meniscal constructs. *J Biomech*.**44**:509. 2011.
15. Huey D.J., Athanasiou K.A. Maturation growth of self-assembled, functional menisci as a result of TGF-beta1 and enzymatic chondroitinase-ABC stimulation. *Biomaterials*.**32**:2052. 2011.
16. Mandal B.B., Park S.H., Gil E.S., Kaplan D.L. Multilayered silk scaffolds for meniscus tissue engineering. *Biomaterials*.**32**:639. 2011.
17. Tienen T.G., Heijkants R.G., de Groot J.H., Schouten A.J., Pennings A.J., Veth R.P., et al. Meniscal replacement in dogs. Tissue regeneration in two different materials with similar properties. *J Biomed Mater Res B Appl Biomater*.**76**:389. 2006.
18. Kon E., Chiari C., Marcacci M., Delcogliano M., Salter D.M., Martin I., et al. Tissue engineering for total meniscal substitution: animal study in sheep model. *Tissue Eng Part A*.**14**:1067. 2008.
19. Gunja N.J., Huey D.J., James R.A., Athanasiou K.A. Effects of agarose mould compliance and surface roughness on self-assembled meniscus-shaped constructs. *J Tissue Eng Regen Med*.**3**:521. 2009.
20. Stapleton T.W., Ingram J., Fisher J., Ingham E. Investigation of the regenerative capacity of an acellular porcine medial meniscus for tissue engineering applications. *Tissue Eng Part A*.**17**:231. 2011.
21. Zur G., Linder-Ganz E., Elsner J.J., Shani J., Brenner O., Agar G., et al. Chondroprotective effects of a polycarbonate-urethane meniscal implant: histopathological results in a sheep model. *Knee Surg Sports Traumatol Arthrosc*.**19**:255. 2011.

22. Aufderheide A.C., Athanasiou K.A. A direct compression stimulator for articular cartilage and meniscal explants. *Ann Biomed Eng.***34**:1463. 2006.
23. Bursac P., Arnoczky S., York A. Dynamic compressive behavior of human meniscus correlates with its extra-cellular matrix composition. *Biorheology.***46**:227. 2009.
24. Chia H.N., Hull M.L. Compressive moduli of the human medial meniscus in the axial and radial directions at equilibrium and at a physiological strain rate. *J Orthop Res.***26**:951. 2008.
25. Fink C., Fermor B., Weinberg J.B., Pisetsky D.S., Misukonis M.A., Guilak F. The effect of dynamic mechanical compression on nitric oxide production in the meniscus. *Osteoarthritis Cartilage.***9**:481. 2001.
26. Hennerbichler A., Fermor B., Hennerbichler D., Weinberg J.B., Guilak F. Regional differences in prostaglandin E2 and nitric oxide production in the knee meniscus in response to dynamic compression. *Biochem Biophys Res Commun.***358**:1047. 2007.
27. Lai J.H., Levenston M.E. Meniscus and cartilage exhibit distinct intra-tissue strain distributions under unconfined compression. *Osteoarthritis Cartilage.***18**:1291. 2010.
28. McHenry J.A., Zielinska B., Donahue T.L. Proteoglycan breakdown of meniscal explants following dynamic compression using a novel bioreactor. *Ann Biomed Eng.***34**:1758. 2006.
29. McNulty A.L., Estes B.T., Wilusz R.E., Weinberg J.B., Guilak F. Dynamic loading enhances integrative meniscal repair in the presence of interleukin-1. *Osteoarthritis Cartilage.***18**:830. 2010.
30. Shin S.J., Fermor B., Weinberg J.B., Pisetsky D.S., Guilak F. Regulation of matrix turnover in meniscal explants: role of mechanical stress, interleukin-1, and nitric oxide. *J Appl Physiol.***95**:308. 2003.
31. Upton M.L., Chen J., Guilak F., Setton L.A. Differential effects of static and dynamic compression on meniscal cell gene expression. *J Orthop Res.***21**:963. 2003.

32. Zielinska B., Killian M., Kadmiel M., Nelsen M., Haut Donahue T.L. Meniscal tissue explants response depends on level of dynamic compressive strain. *Osteoarthritis Cartilage*.**17**:754. 2009.
33. Gunja N.J., Athanasiou K.A. Effects of hydrostatic pressure on leporine meniscus cell-seeded PLLA scaffolds. *J Biomed Mater Res A*.**92**:896. 2010.
34. Kisiday J.D., Lee J.H., Siparsky P.N., Frisbie D.D., Flannery C.R., Sandy J.D., et al. Catabolic responses of chondrocyte-seeded peptide hydrogel to dynamic compression. *Ann Biomed Eng*.**37**:1368. 2009.
35. Kock L.M., Schulz R.M., van Donkelaar C.C., Thummler C.B., Bader A., Ito K. RGD-dependent integrins are mechanotransducers in dynamically compressed tissue-engineered cartilage constructs. *J Biomech*.**42**:2177. 2009.
36. Villanueva I., Hauschulz D.S., Mejc D., Bryant S.J. Static and dynamic compressive strains influence nitric oxide production and chondrocyte bioactivity when encapsulated in PEG hydrogels of different crosslinking densities. *Osteoarthritis Cartilage*.**16**:909. 2008.
37. Nicodemus G.D., Bryant S.J. Mechanical loading regimes affect the anabolic and catabolic activities by chondrocytes encapsulated in PEG hydrogels. *Osteoarthritis Cartilage*.**18**:126. 2010.
38. Ballyns J.J., Gleghorn J.P., Niebrzydowski V., Rawlinson J.J., Potter H.G., Maher S.A., et al. Image-guided tissue engineering of anatomically shaped implants via MRI and micro-CT using injection molding. *Tissue Eng Part A*.**14**:1195. 2008.
39. Chang S.C., Rowley J.A., Tobias G., Genes N.G., Roy A.K., Mooney D.J., et al. Injection molding of chondrocyte/alginate constructs in the shape of facial implants. *J Biomed Mater Res*.**55**:503. 2001.
40. Mastrokalos D.S., Papagelopoulos P.J., Mavrogenis A.F., Hantes M.E., Paessler H.H. Changes of the posterior meniscal horn height during loading: an in vivo magnetic resonance imaging study. *Orthopedics*.**31**:68. 2008.
41. Kim Y.J., Sah R.L., Doong J.Y., Grodzinsky A.J. Fluorometric assay of DNA in cartilage explants using Hoechst 33258. *Anal Biochem*.**174**:168. 1988.

42. Enobakhare B.O., Bader D.L., Lee D.A. Quantification of sulfated glycosaminoglycans in chondrocyte/alginate cultures, by use of 1,9-dimethylmethylene blue. *Anal Biochem.***243**:189. 1996.
43. Neuman R.E., Logan M.A. The determination of hydroxyproline. *J Biol Chem.***184**:299. 1950.
44. Gleghorn J.P., Jones A.R., Flannery C.R., Bonassar L.J. Boundary mode frictional properties of engineered cartilaginous tissues. *Eur Cell Mater.***14**:20. 2007.
45. Mauck R.L., Soltz M.A., Wang C.C., Wong D.D., Chao P.H., Valhmu W.B., et al. Functional tissue engineering of articular cartilage through dynamic loading of chondrocyte-seeded agarose gels. *J Biomech Eng.***122**:252. 2000.
46. Ragan P.M., Chin V.I., Hung H.H., Masuda K., Thonar E.J., Arner E.C., et al. Chondrocyte extracellular matrix synthesis and turnover are influenced by static compression in a new alginate disk culture system. *Arch Biochem Biophys.***383**:256. 2000.
47. Chowdhury T.T., Bader D.L., Shelton J.C., Lee D.A. Temporal regulation of chondrocyte metabolism in agarose constructs subjected to dynamic compression. *Arch Biochem Biophys.***417**:105. 2003.
48. Mauck R.L., Wang C.C., Oswald E.S., Ateshian G.A., Hung C.T. The role of cell seeding density and nutrient supply for articular cartilage tissue engineering with deformational loading. *Osteoarthritis Cartilage.***11**:879. 2003.
49. Grad S., Eglin D., Alini M., Stoddart M.J. Physical Stimulation of Chondrogenic Cells In Vitro: A Review. *Clin Orthop Relat Res.* 2011.
50. Wilson C.G., Nishimuta J.F., Levenston M.E. Chondrocytes and meniscal fibrochondrocytes differentially process aggrecan during de novo extracellular matrix assembly. *Tissue Eng Part A.***15**:1513. 2009.
51. Aufderheide A.C., Athanasiou K.A. Comparison of scaffolds and culture conditions for tissue engineering of the knee meniscus. *Tissue Eng.***11**:1095. 2005.

52. Baker B.M., Shah R.P., Huang A.H., Mauck R.L. Dynamic tensile loading improves the functional properties of mesenchymal stem cell-laden nanofiber-based fibrocartilage. *Tissue Eng Part A*.**17**:1445. 2011.
53. Waldman S.D., Spiteri C.G., Gryn timer M.D., Pilliar R.M., Kandel R.A. Long-term intermittent shear deformation improves the quality of cartilaginous tissue formed in vitro. *J Orthop Res*.**21**:590. 2003.
54. Blain E.J. Mechanical regulation of matrix metalloproteinases. *Front Biosci*.**12**:507. 2007.
55. De Croos J.N., Dhaliwal S.S., Gryn timer M.D., Pilliar R.M., Kandel R.A. Cyclic compressive mechanical stimulation induces sequential catabolic and anabolic gene changes in chondrocytes resulting in increased extracellular matrix accumulation. *Matrix Biol*.**25**:323. 2006.
56. Tissakht M., Ahmed A.M. Tensile stress-strain characteristics of the human meniscal material. *J Biomech*.**28**:411. 1995.

## CHAPTER 4

### The Effect of IGF-I on Anatomically-shaped Tissue Engineered Menisci<sup>\*</sup>

#### **Abstract**

This study investigates the effect of insulin-like growth factor (IGF) –I on the development of anatomically shaped alginate menisci seeded with meniscal fibrochondrocytes. To accomplish this, bovine meniscal fibrochondrocytes were seeded into 2% w/v alginate, crosslinked with CaSO<sub>4</sub>, and injected into anatomical molds derived from  $\mu$ CT scans. The meniscal constructs were then cultured for up to 4 weeks with or without 100 ng/mL IGF-I supplemented in the media. Histological, immunohistological, biochemical and mechanical analyses were performed to characterize tissue development, accumulation and localization of ECM, and mechanical properties. After 4 weeks of culture, IGF-I treatment significantly improved mechanical and biochemical properties while maintaining DNA content, with a 26 fold increase in GAG content and 10 fold increase in collagen content compared to 0 week controls, and a 3 fold increase in the equilibrium modulus at 2 weeks compared to controls. IGF-I treated menisci had approximately 60% of the GAG content of native tissue and the compressive equilibrium modulus matched native properties by 2 weeks of culture. Further, IGF-I treated menisci developed a distinct surface layer similar to native tissue with elongated cells and collagen fibers aligned parallel to the surface, the presence of type I and II collagen, and accumulation of lubricin. This study demonstrates that IGF-I treatment can greatly increase the mechanical and biochemical properties of engineered tissues and aid in the

---

<sup>\*</sup> This chapter is published: Puetzer J.L., Brown B.N., Ballyns J.J., Bonassar L.J. The effect of IGF-I on anatomically shaped tissue-engineered menisci. *Tissue Eng Part A*.19:1443. 2013

development of a distinct surface zone similar to the superficial zone of native menisci.

### ***Introduction***

The meniscus is a semi-lunar, wedge-shaped fibrocartilaginous structure that inserts into the top of the tibial plateau and acts as a load transmitter, shock absorber, joint lubricator, and joint stabilizer in the knee<sup>1</sup>. Meniscal injuries are among the most frequent orthopedic injuries in the knee and are characterized by slow healing due to the avascular nature of the tissue<sup>2, 3</sup>. There are over 1 million meniscal surgeries performed in the United States per year<sup>4</sup>. While there have been improvements in surgical techniques and materials for repair of focal lesions<sup>5-7</sup>, improvements are still needed for severe injuries to the meniscus that cannot be treated focally. Currently, the only treatment for whole meniscus replacement is cadaveric allograft; however donor tissue is scarce, there is a risk of disease transmission, immune rejection may occur, and it is difficult to match complex patient specific joint architecture. Further, certain materials and allografts used for meniscal replacements can create high friction in the joint leading to abrasion of surrounding cartilage<sup>2, 3, 8, 9</sup>.

Tissue engineering (TE) could supply an alternative to allograft replacement. Recently, several studies have attempted to create whole TE meniscal replacements that range in size, shape, and materials<sup>10-21</sup>. These efforts are promising but tissue composition and mechanical properties differ greatly from native tissue and thus no such replacement is in clinical use. In an effort to further improve these whole meniscal constructs, several studies have investigated mechanical<sup>12, 14, 17, 22</sup> and chemical stimulation<sup>20</sup> of engineered constructs.

Several studies have documented the effects of different growth factors on proliferation and biochemical synthesis of meniscal fibrochondrocytes in monolayer

culture<sup>23-30</sup>. However few studies have investigated the effect of growth factors on tissue development in 3D scaffolds<sup>20, 25, 31-33</sup> and even fewer have investigated the effects of insulin-like growth factor (IGF)-I on the development of 3D scaffolds<sup>25, 32</sup>.

IGF-I is known as a major mediator in wound healing and connective tissue metabolism<sup>34</sup>. It is known to have a stimulatory effect on musculoskeletal soft tissue regeneration; however very few studies have investigated IGF-I as a potential treatment in meniscal regeneration. Previous studies have demonstrated the stimulatory effect of IGF-I on meniscal fibrochondrocytes in cell growth and extracellular matrix synthesis in monolayer<sup>24, 25, 27, 30</sup>. Two separate groups have investigated the effect of IGF-I on meniscal fibrochondrocytes in 3D polyglycolic acid (PGA) scaffolds and found significant increases in type I collagen and DNA synthesis<sup>25, 32</sup>. These two studies demonstrate great promise for IGF-I treatment in whole meniscal constructs; however, the effect of IGF-I on large constructs, its effect at concentrations greater than 50 ng/mL, and its effect on the development of mechanical properties are unknown. The objective of this study was to determine the effect of IGF-I on the development of biochemical and mechanical properties in anatomically shaped alginate menisci. We hypothesize that tissue development will significantly improve in IGF-I treated menisci with time in culture.

## **Methods**

### Generation of Engineered Alginate Menisci

A total of 65 meniscal constructs were generated as previously described<sup>13, 17, 35</sup>. Briefly, menisci from freshly slaughtered 1-3 day old calves were diced into 1 mm<sup>3</sup> cubes and digested overnight in 0.3% collagenase, 100 µg/mL penicillin, and 100 µg/mL streptomycin in Dulbecco's modified Eagle's medium (DMEM). The bovine meniscal fibrochondrocytes were then seeded into sterile 2% w/v low viscosity high

G-content alginate (FMC BioPolymer, Drammen, Norway) at  $50 \times 10^6$  cells/mL and crosslinked with 0.02 g/mL  $\text{CaSO}_4$  at a 2:1 ratio. Immediately, this alginate-cell suspension was injected into ABS plastic molds, designed as previously described from micro computed tomography ( $\mu\text{CT}$ ) scans of ovine menisci,<sup>13</sup> and allowed to further crosslink for 20 minutes in 60 mM  $\text{CaCl}_2$ . Alginate meniscal constructs were then removed from molds and cultured for up to 4 weeks in DMEM with 10% fetal bovine serum, 100 U/mL penicillin, 100  $\mu\text{g}/\text{mL}$  streptomycin, 0.1 mM non-essential amino acids, 50  $\mu\text{g}/\text{mL}$  ascorbate, and 0.4 mM L-proline.

Meniscal constructs were either treated (n=22) or not treated (n=43) with IGF-I. Treated constructs were supplemented with 100 ng/mL IGF-I in the media throughout culture and in the  $\text{CaSO}_4$  during generation of the constructs. Meniscal constructs from treated and untreated cultures were collected at week 0, 2 and 4 for analysis.

### Post-Culture Analysis

Upon the completion of culture, meniscal constructs were photographed and assessed visually for changes in opacity and shape fidelity. The constructs were then processed for histology, immunohistochemistry, biochemical, and mechanical analysis as previously described<sup>13, 17, 22</sup>. Briefly, cross-sections of the samples were cut and fixed for histological and immunohistochemical analysis. Discs (4 mm diameter by approximately 2 mm thick) were cut from the face, center, and bottom of samples for mechanical analysis while excess surrounding tissue was used for biochemical analysis. A total of 6 discs and 6 biochemical samples, two from each location, were obtained from each meniscal construct.

### *Histological analysis*

Cross-sections of meniscal constructs were fixed in 10% buffered formalin with 1 mM CaCl<sub>2</sub>, embedded into paraffin blocks and sectioned. The sections were then dehydrated through a series of progressively stronger ethanol baths, cleared with xylene and stained with Safranin-O and picosirius red to observe GAG and collagen localization, respectively. Picosirius red stained sections were further visualized using polarized light to observe collagen fiber organization.

### *Immunohistochemistry*

Immunohistochemistry was performed on cross-sections for type I and II collagen and lubricin using a modified Vectastain ABC kit protocol (Vector Laboratories, Burlingame, CA). Briefly, following deparaffinization and hydration, the sections were incubated for 20 minutes in a citrate antigen retrieval buffer (10mM Citric Acid, pH 6.0) at 95-100°C and allowed to cool to room temperature. The slides were then washed in TRIS buffered saline/Tween20 solution (pH 7.4) for 5 minutes, hyaluronidase for 30 minutes, incubated at 37°C in pepsin for 20 minutes, and finally washed with 3% H<sub>2</sub>O<sub>2</sub> for 30 minutes. Between each of these steps the slides were washed twice with PBS. The slides were then incubated at room temperature for 1 hour in a normal horse serum blocking buffer (Vectastain ABC Elite Kit, Vector Laboratories). The slides were transferred to a humidity chamber and incubated at 4°C overnight in anti-type I collagen antibody (1:250 dilution; Abcam), anti-type II collagen antibody (1:250 dilution; Abcam), anti-lubricin antibody (1:250, Abcam), or left in the blocking buffer as a negative control. The slides were then washed with PBS and incubated at room temperature in a biotinylated secondary antibody (1:100, Vectastain ABC Elite Kit) for 30 minutes. After further washing with PBS, the slides were incubated in ABC Reagent (Vectastain ABC Elite Kit) for 30 minutes at 37°C.

Finally slides were stained with ImmPACT DAB (Vector Laboratories, Burlingame, CA) for up to 15 minutes and counterstained with hematoxylin.

### *Biochemical Analysis*

Biochemical samples were weighed to obtain the wet weight (WW), frozen, lyophilized, and weighed again to obtain the dry weight (DW). The samples were digested overnight in 1.25 mg/mL papain solution at 60°C and analyzed for DNA, GAG, and collagen content via a Hoechst dye assay<sup>36</sup>, a modified DMMB dye assay at pH 1.5<sup>37</sup>, and a hydroxyproline assay<sup>38</sup>, respectively. Biochemical content is reported normalized to construct wet weight. Additionally, before each media change, media samples were obtained and analyzed biochemically for DNA, GAG, and collagen content using the same assays to examine loss to the culture media. Biochemical content in the media was summed together for each week and is reported as total DNA, GAG, or collagen content in media for each individual week.

### *Mechanical Analysis*

Discs from meniscal constructs were tested in confined compression to determine equilibrium modulus as previously described<sup>35, 39</sup>. Briefly, stress relaxation tests were performed by imposing 5% increment steps up to 50% strain using an EnduraTech loading frame (EnduraTech; Electroforce (ELF) 3200 System, Minnetonka, MN). The resultant loads were fit to a poroelastic model using a custom MATLAB program to calculate the equilibrium modulus.

### Statistics

All data were analyzed by 2-way ANOVA with time and IGF-I treatment as independent variables using Tukey's t-test for post-hoc pairwise comparisons and

$p < 0.05$  denoting statistical significance. All statistical analysis was performed using Sigmastat version 3.5 and all data expressed as mean  $\pm$  SD.

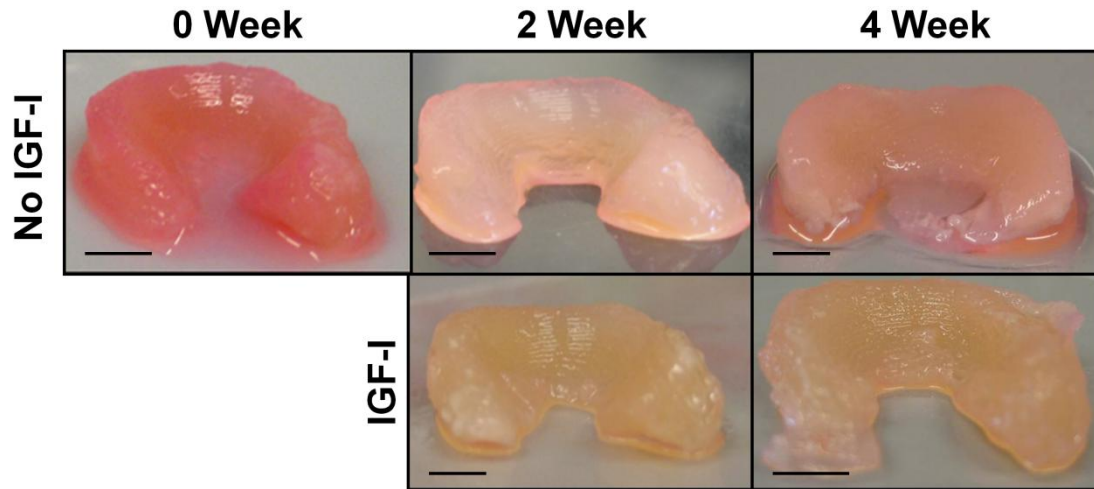


**Figure 4.1:** Photographs of alginate menisci after removal from culture (Bar = 5mm)

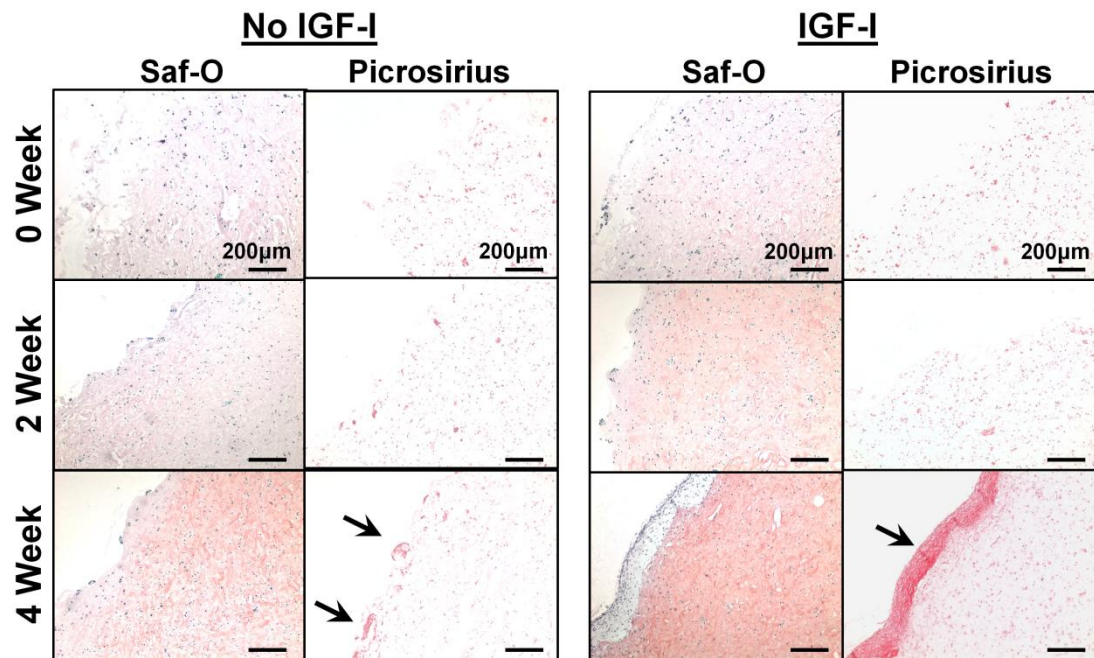


**Figure 4.2:** Tissue sections stained with Safranin-O and picosirius red at 100x under brightfield to determine localization of glycosaminoglycans and collagen, respectively. Arrows point to picosirius red positive staining.

## Results

Gross inspection of meniscal constructs demonstrated that constructs in both groups maintained their shape through 4 weeks of culture with little to no noticeable change in construct opacity between IGF-I treated and untreated samples (Figure 4.1).

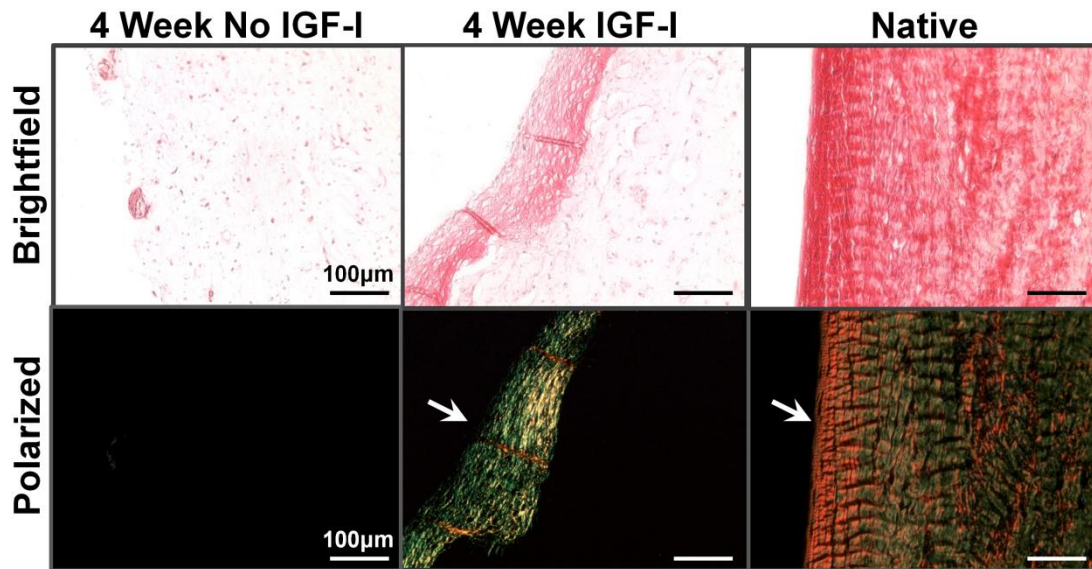


**Figure 4.3:** Surface of 4 week IGF-I untreated and treated alginate menisci and native samples stained with picosirius red under brightfield and polarized light at 200x demonstrating positive staining and organization of collagen fibers, respectively. Arrows point to organized collagen fibers aligned parallel along the surface.

### Histological Analysis

Safranin-O staining demonstrated an increase in GAG localization with time in culture for both IGF-I treated and untreated groups, with a noticeably increased GAG accumulation in IGF-I treated 2 and 4 week constructs (Figure 4.2). Both Safranin-O and picosirius red staining revealed the development of a surface layer in samples cultured in IGF-I for 4 weeks. This surface layer was not stained by Safranin-O suggesting no GAG localization. Overall, picosirius red staining was limited until 4 weeks of culture, at which point untreated constructs had small localized areas of

collagen accumulation and IGF-I treated constructs had strong accumulation of collagen in the surface layer (Figure 4.2). When visualized under polarized light, no collagen was visible in untreated 4 week samples, suggesting the small localized areas of collagen accumulation were not organized into collagen fibers. However, the surface layer of the 4 week IGF-I treated constructs was seen under polarized light and was observed to have a similar organization of collagen to that of the native meniscal surface with fibers aligned parallel to the surface (Figure 4.3).

#### Immunohistochemical Analysis

Immunohistochemical analysis demonstrated slight increases in type I and type II collagen accumulation, concentrated in areas surrounding the cells, in 4 week untreated samples and 2 week treated samples. Constructs cultured in IGF-I for 4 weeks demonstrated a significant increase in collagen accumulation, with strong type I collagen accumulation throughout the construct and surface layer, and type II collagen primarily located in the surface layer (Figure 4.4).

Since 4 week IGF-I treated constructs developed a distinct surface layer similar to that of native tissue, further immunohistochemistry analysis for lubricin, was conducted because it is localized to the surface of native menisci and is believed to aid in lubrication. Lubricin localized at the surface of 4 week IGF-I treated constructs, similar to that seen in native menisci, and elongated cells aligned parallel to the surface are seen throughout the surface layer (Figure 4.5).

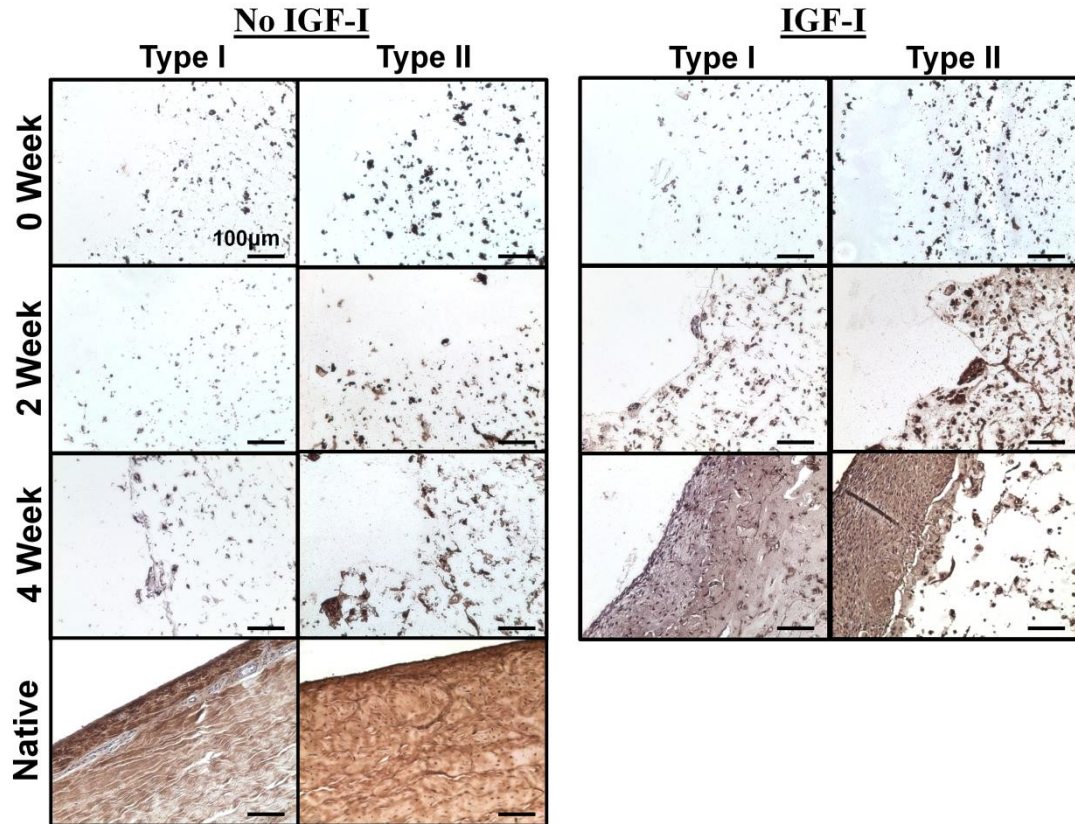


**Figure 4.4:** Immunohistochemistry staining for type I and II collagen at 200x in engineered and native meniscal tissues.

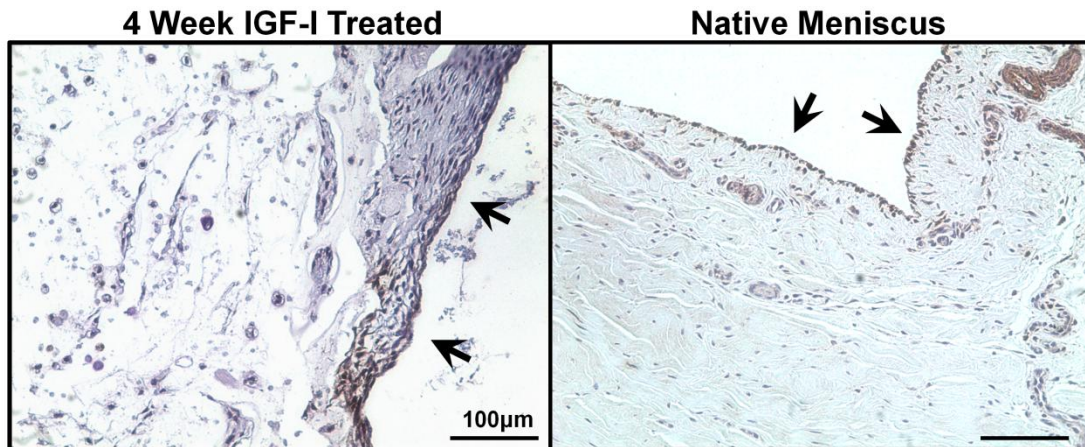


**Figure 4. 5:** Immunohistochemistry staining for lubricin on the surface of 4 week IGF-I treated alginate and native menisci at 200x. Arrows point to surface of construct where lubricin stained positive.

### Biochemical Analysis

Both treated and untreated meniscal constructs were found to maintain their DNA content throughout 4 weeks of culture. DNA lost to the media per week decreased after 2 weeks of culture and then remained constant through 4 weeks with IGF-I treated constructs having significantly more DNA in the media than untreated samples (Figure 4.6).

IGF-I treatment significantly increased ECM content in both the meniscal constructs and the media with time in culture. After 2 and 4 weeks of culture, IGF-I treated constructs had significantly increased GAG accumulation to more than 15 and 26 fold over 0 week constructs at 2 and 4 weeks respectively. IGF-I treated constructs also had 6 and 3 times higher GAG content compared to 2 and 4 weeks untreated constructs respectively. After 2 weeks of culture, IGF-I treated constructs lost significantly more GAG to the media per week than untreated constructs, resulting in an overall significantly greater production of GAG in IGF-I treated construct than untreated controls (Figure 4.6). IGF-I treatment significantly enhanced collagen accumulation at 2 and 4 weeks, with 5 and 10 fold increases over 0 week controls. IGF-I treated constructs also had a 3 and 5 fold increase over 2 and 4 weeks untreated constructs respectively. Treated and untreated constructs had very similar collagen loss profiles to the media until 2 weeks. After 2 weeks of culture IGF-I treated constructs lost significantly more collagen to the media than untreated controls, suggesting greater total production of collagen in IGF-I treated menisci than untreated controls (Figure 4.6).

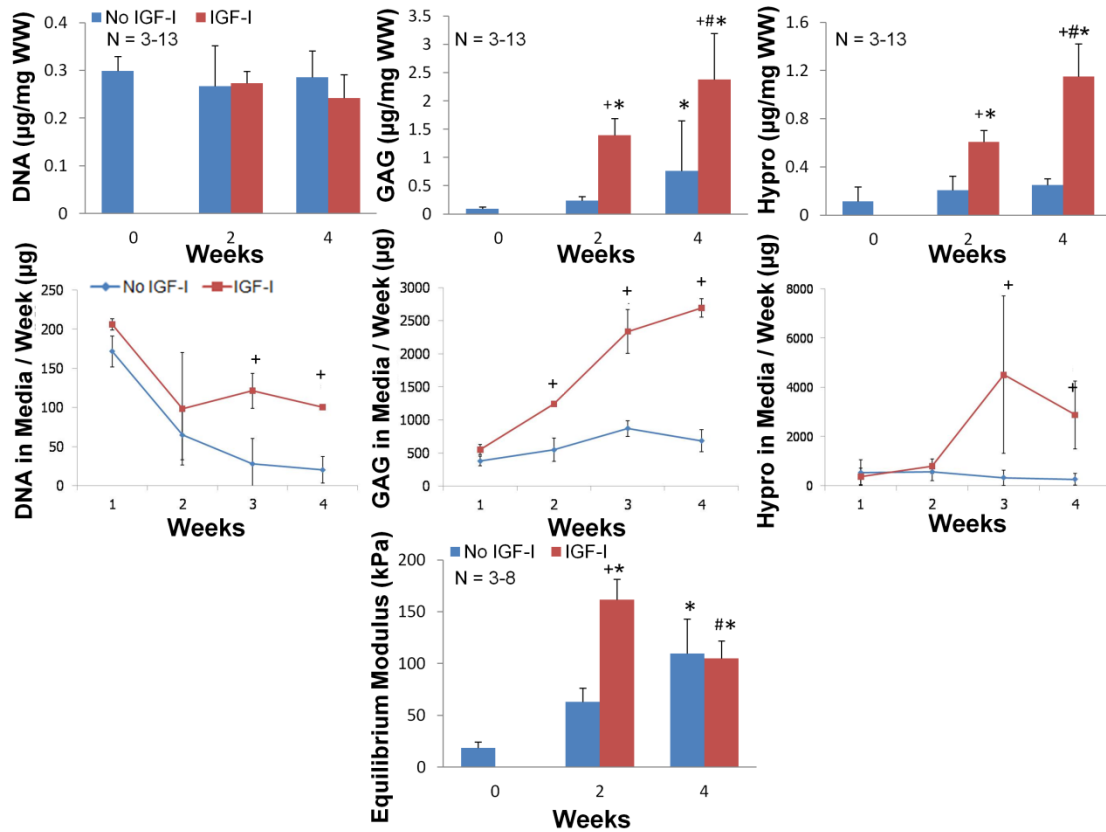


**Figure 4.6:** DNA, GAG and Collagen content of alginate meniscal constructs (1<sup>st</sup> row) and total released to the media per week (2<sup>nd</sup> row). Equilibrium modulus of alginate meniscal constructs with time in culture (3<sup>rd</sup> row). \* = difference from 0 week, + = difference from respective group at time point, and # = difference from all other treatments at all other time points. Data presented as mean±SD and p<0.05.

### Mechanical Analysis

The equilibrium modulus significantly increased with IGF-I treatment. At 2 weeks of culture, IGF-I treated constructs had a significantly increased equilibrium modulus over that of 0 week and untreated constructs, with a 3 fold increase over the untreated control, reaching approximately 80-100% that of human menisci (native tissue = 110-200 kPa<sup>40</sup>). At 4 weeks, treated and untreated constructs had similar equilibrium moduli, which significantly increased from 0 week but decreased from week 2 treated constructs (Figure 4.6).

## ***Discussion***

In this study we found that IGF-I treatment enhanced ECM production and mechanical properties of anatomically shaped tissue engineered alginate menisci as compared to untreated controls. IGF-I treated menisci had significantly more GAG and collagen accumulation in the constructs and in the media from 2 weeks on, demonstrating IGF-I greatly increased overall production of biochemical components. Further, IGF-I treated menisci accumulated 60 % of the GAG and 3% of the collagen found in native menisci by 4 weeks of culture<sup>41</sup> and developed an equilibrium compressive modulus that matched native tissue after 2 weeks of culture<sup>40</sup>. The equilibrium modulus did however decrease after 2 weeks of culture to ~60-90% that of native tissue. There were no bursts in release of biochemical components to the media nor a decrease in matrix composition between 2 and 4 weeks for IGF-I treated constructs, suggesting that this decrease in mechanical properties may be due to degradation of alginate, previously observed in experiments involving culture of anatomically shaped menisci in bioreactor culture<sup>22</sup>.

GAG retention in the IGF-I treated alginate menisci was significantly greater than collagen retention throughout culture. This could be due to the high concentration of IGF-I (100 ng/mL) used in this study. Previous studies have found meniscal explants and fibrochondrocytes in monolayer to produce more GAG than collagen when treated with IGF-I at  $\geq 100$  ng/mL<sup>27, 42</sup>. Additional studies have reported meniscal fibrochondrocytes in monolayer and 3D culture treated with IGF-I at  $\leq 50$  ng/mL resulted in only increased collagen incorporation and accumulation, and had no effect on GAG production<sup>24, 25, 30, 32</sup>.

Further, the accumulation of GAG and collagen in this study could be attributed to a proliferative response. IGF-I has been reported to have a proliferative response at concentrations  $\geq 50$  ng/mL in fibrochondrocytes in monolayer<sup>25, 27</sup> and at 5-10 ng/mL

in 3D scaffolds<sup>25, 32</sup>. Additionally it has been reported that temporomandibular joint fibrochondrocytes typically have a proliferative response to higher concentrations of growth factors (100 ng/mL), while lower concentrations (10 ng/mL) favor biosynthesis<sup>43</sup>. In this study we observed no change in DNA concentrations throughout culture for both IGF-I treated and control constructs; however IGF- I treated constructs did have a significant increase in DNA in the media from approximately 2 weeks on and the development of a very cell laden surface zone by 4 weeks. Thus, the 100 ng/mL IGF-I treatment used in this study could have had a proliferative effect at the surface of the alginate menisci, but it is unknown whether the increase in DNA in the media is from cells leaving the scaffold or dividing in the media. Additionally, the cell laden surface zone stained negatively for GAGs and very strongly for collagen, suggesting a more fibrochondrogenic response in the surface zone. Typically, proliferative responses to growth factors results in increases in accumulation of both GAG and collagen.

The surface zone of the IGF-I treated alginate menisci appears similar to the superficial zone of native menisci. The surface zone of the IGF-I treated menisci at 4 weeks displays organized collagen fibers and elongated cells aligned parallel to the surface very similar to that seen in the superficial zone of native tissue. This organization and alignment of collagen fibers and cells is especially striking since it was developed by IGF-I chemical stimulation, in the absence of any mechanical stimulation. This distinct surface zone also contained type I and II collagen. Type I collagen was located throughout the constructs similar to native tissue, while type II collagen was located primarily in the surface zone. In this system, the action of IGF-I on fibrochondrocytes appears to be highly supportive of fibrochondrogenesis, as indicated by stimulation of the production of both proteoglycans and type I collagen. Notably, at 4 weeks, IGF-I stimulation resulted in uniform deposition of proteoglycan

and type I collagen throughout the scaffold, similar to what would be expected in native meniscus<sup>3</sup>.

Additionally, lubricin, a glycoprotein often localized to the surface of native menisci and believed to aid in lubrication<sup>39, 44</sup>, was shown to accumulate at the outermost edge of the surface zone. Lubricin is known to decrease the boundary friction of cartilaginous tissues and thus is believed to be key to joint lubrication and decreased wear of surrounding cartilage<sup>44</sup>. A tissue engineered meniscus will most likely need a well organized superficial zone and the ability to localize or produce lubricin at its surface in order to be functional when implanted in the knee. Previous studies have shown the ability of tissue engineered meniscal constructs to localize exogenously added lubricin<sup>39</sup>, but the current study is the first to demonstrate the accumulation of endogenously synthesized lubricin in a well defined surface zone.

The mechanism driving the development of the collagen- and lubricin-rich surface zone is not entirely clear. Previous work<sup>45</sup> suggests that IGF-I does not drive lubricin expression in articular chondrocytes, but there is no comparable data for meniscal fibrochondrocytes. Notably, meniscal fibrochondrocytes appear more effective at localizing lubricin in alginate cultures than articular chondrocytes<sup>39</sup>, suggesting that they may be more sensitive to stimulation of lubricin synthesis than articular chondrocytes. Degradation of the alginate scaffold at the surface may facilitate the development of this surface layer, although significant degradation of alginate does not generally occur on this time frame<sup>22</sup> and is not apparent from the appearance of the construct surface (Figure 4.1). However, the accumulation of a highly cellular region on the surface in the absence of encapsulating alginate could drive a significantly different cellular response to high concentrations of IGF-I that results in collagen and lubricin accumulation.

IGF-I treated alginate menisci show great promise as a replacement tissue of the meniscus with a well defined superficial zone, approximately 60% GAGs of native tissue, and an equilibrium modulus that matches native menisci by 4 weeks of culture. However further investigations are needed to improve the collagen content (3% of native tissue) and tensile properties of these engineered menisci. Prolonged culture beyond 4 weeks or decreasing the concentration of IGF-I later in culture could help to further improve collagen content. Additionally, combination of mechanical stimulation and growth factor treatment could serve to be beneficial. We have demonstrated previously that dynamic compression of alginate menisci promotes a fibrochondrogenic response with collagen accumulation and bundle formation over GAG accumulation<sup>17</sup>. Further it has been suggested that meniscal fibrochondrocytes respond to biochemical and biomechanical stimuli via separate cellular pathways, with dynamic load and growth factor treatment leading to a synergic improvement of mechanical and biochemical properties<sup>14, 42</sup>. Thus, combining the response of dynamic compression and IGF-I treatment could serve to further improve the mechanical and biochemical properties of these meniscal scaffolds.

## REFERENCES

1. Kawamura S., Lotito K., Rodeo S.A. Biomechanics and healing response of the meniscus. *Oper Techn Sport Med*.**11**:68. 2003.
2. Peters G., Wirth C.J. The current state of meniscal allograft transplantation and replacement. *Knee*.**10**:19. 2003.
3. Sweigart M.A., Athanasiou K.A. Toward tissue engineering of the knee meniscus. *Tissue Eng*.**7**:111. 2001.
4. Khetia E.A., McKeon B.P. Meniscal allografts: biomechanics and techniques. *Sports Med Arthrosc*.**15**:114. 2007.
5. Stone K.R., Steadman J.R., Rodkey W.G., Li S.T. Regeneration of meniscal cartilage with use of a collagen scaffold. Analysis of preliminary data. *J Bone Joint Surg Am*.**79**:1770. 1997.
6. Farnig E., Sherman O. Meniscal repair devices: a clinical and biomechanical literature review. *Arthroscopy*.**20**:273. 2004.
7. McDermott I. Meniscal tears, repairs and replacement: their relevance to osteoarthritis of the knee. *Br J Sports Med*.**45**:292. 2011.
8. Buma P., Ramrattan N.N., van Tienen T.G., Veth R.P. Tissue engineering of the meniscus. *Biomaterials*.**25**:1523. 2004.
9. Gleghorn J.P., Doty S.B., Warren R.F., Wright T.M., Maher S.A., Bonassar L.J. Analysis of Frictional Behavior and Changes in Morphology Resulting from Cartilage Articulation with Porous Polyurethane Foams (October, pg 1292, 2010). *Journal of Orthopaedic Research*.**28**:1677. 2010.
10. Aufderheide A.C., Athanasiou K.A. Assessment of a bovine co-culture, scaffold-free method for growing meniscus-shaped constructs. *Tissue Eng*.**13**:2195. 2007.
11. Balint E., Gatt C.J., Jr., Dunn M.G. Design and mechanical evaluation of a novel fiber-reinforced scaffold for meniscus replacement. *J Biomed Mater Res A*.**100**:195. 2012.

12. Ballyns J.J., Bonassar L.J. Dynamic compressive loading of image-guided tissue engineered meniscal constructs. *J Biomech.***44**:509. 2011.
13. Ballyns J.J., Gleghorn J.P., Niebrzydowski V., Rawlinson J.J., Potter H.G., Maher S.A., et al. Image-guided tissue engineering of anatomically shaped implants via MRI and micro-CT using injection molding. *Tissue Eng Part A.***14**:1195. 2008.
14. Huey D.J., Athanasiou K.A. Tension-compression loading with chemical stimulation results in additive increases to functional properties of anatomic meniscal constructs. *PLoS One.***6**:e27857. 2011.
15. Kang S.W., Son S.M., Lee J.S., Lee E.S., Lee K.Y., Park S.G., et al. Regeneration of whole meniscus using meniscal cells and polymer scaffolds in a rabbit total meniscectomy model. *J Biomed Mater Res A.***78**:659. 2006.
16. Kon E., Chiari C., Marcacci M., Delcogliano M., Salter D.M., Martin I., et al. Tissue engineering for total meniscal substitution: animal study in sheep model. *Tissue Eng Part A.***14**:1067. 2008.
17. Puetzer J.L., Ballyns J.J., Bonassar L.J. The Effect of the Duration of Mechanical Stimulation and Post-Stimulation Culture on the Structure and Properties of Dynamically Compressed Tissue-Engineered Menisci. *Tissue Eng Part A.***18**:1365. 2012.
18. Tienen T.G., Heijkants R.G., de Groot J.H., Schouten A.J., Pennings A.J., Veth R.P., et al. Meniscal replacement in dogs. Tissue regeneration in two different materials with similar properties. *J Biomed Mater Res B Appl Biomater.***76**:389. 2006.
19. Zur G., Linder-Ganz E., Elsner J.J., Shani J., Brenner O., Agar G., et al. Chondroprotective effects of a polycarbonate-urethane meniscal implant: histopathological results in a sheep model. *Knee Surg Sports Traumatol Arthrosc.***19**:255. 2011.
20. Huey D.J., Athanasiou K.A. Maturation growth of self-assembled, functional menisci as a result of TGF-beta1 and enzymatic chondroitinase-ABC stimulation. *Biomaterials.***32**:2052. 2011.
21. Mandal B.B., Park S.H., Gil E.S., Kaplan D.L. Multilayered silk scaffolds for meniscus tissue engineering. *Biomaterials.***32**:639. 2011.

22. Ballyns J.J., Wright T.M., Bonassar L.J. Effect of media mixing on ECM assembly and mechanical properties of anatomically-shaped tissue engineered meniscus. *Biomaterials*.**31**:6756. 2010.
23. Kasemkijwattana C., Menetrey J., Goto H., Niyibizi C., Fu F.H., Huard J. The use of growth factors, gene therapy and tissue engineering to improve meniscal healing. *Mat Sci Eng C-Bio S*.**13**:19. 2000.
24. Pangborn C.A., Athanasiou K.A. Effects of growth factors on meniscal fibrochondrocytes. *Tissue Engineering*.**11**:1141. 2005.
25. Stewart K., Pabbruwe M., Dickinson S., Hollander A.P., Chaudhuri J.B. The effect of growth factor treatment on meniscal chondrocyte proliferation and differentiation on polyglycolic acid scaffolds. *Tissue Engineering*.**13**:271. 2007.
26. Collier S., Ghosh P. Effects of transforming growth factor beta on proteoglycan synthesis by cell and explant cultures derived from the knee joint meniscus. *Osteoarthritis Cartilage*.**3**:127. 1995.
27. Tumia N.S., Johnstone A.J. Regional regenerative potential of meniscal cartilage exposed to recombinant insulin-like growth factor-I in vitro. *J Bone Joint Surg Br*.**86**:1077. 2004.
28. Tumia N.S., Johnstone A.J. Promoting the proliferative and synthetic activity of knee meniscal fibrochondrocytes using basic fibroblast growth factor in vitro. *Am J Sports Med*.**32**:915. 2004.
29. Bhargava M.M., Attia E.T., Murrell G.A.C., Dolan M.M., Warren R.F., Hannafin J.A. The effect of cytokines on the proliferation and migration of bovine meniscal cells. *Am J Sport Med*.**27**:636. 1999.
30. Esparza R., Gortazar A.R., Forriol F. Cell study of the three areas of the meniscus: Effect of growth factors in an experimental model in sheep. *J Orthop Res*. 2012.
31. Ionescu L.C., Lee G.C., Huang K.L., Mauck R.L. Growth factor supplementation improves native and engineered meniscus repair in vitro. *Acta Biomater*. 2012.
32. Pangborn C.A., Athanasiou K.A. Growth factors and fibrochondrocytes in scaffolds. *Journal of Orthopaedic Research*.**23**:1184. 2005.

33. Zaleskas J.M., Kinner B., Freyman T.M., Yannas I.V., Gibson L.J., Spector M. Growth factor regulation of smooth muscle actin expression and contraction of human articular chondrocytes and meniscal cells in a collagen-GAG matrix. *Experimental Cell Research*.**270**:21. 2001.
34. Skottner A., Arrheniusnyberg V., Kanje M., Fryklund L. Anabolic and Tissue-Repair Functions of Recombinant Insulin-Like Growth Factor-I. *Acta Paediatr Scand*.**63**. 1990.
35. Chang S.C., Rowley J.A., Tobias G., Genes N.G., Roy A.K., Mooney D.J., et al. Injection molding of chondrocyte/alginate constructs in the shape of facial implants. *J Biomed Mater Res*.**55**:503. 2001.
36. Kim Y.J., Sah R.L., Doong J.Y., Grodzinsky A.J. Fluorometric assay of DNA in cartilage explants using Hoechst 33258. *Anal Biochem*.**174**:168. 1988.
37. Enobakhare B.O., Bader D.L., Lee D.A. Quantification of sulfated glycosaminoglycans in chondrocyte/alginate cultures, by use of 1,9-dimethylmethylene blue. *Anal Biochem*.**243**:189. 1996.
38. Neuman R.E., Logan M.A. The determination of hydroxyproline. *J Biol Chem*.**184**:299. 1950.
39. Gleghorn J.P., Jones A.R., Flannery C.R., Bonassar L.J. Boundary mode frictional properties of engineered cartilaginous tissues. *Eur Cell Mater*.**14**:20. 2007.
40. Sweigart M.A., Zhu C.F., Burt D.M., DeHoll P.D., Agrawal C.M., Clanton T.O., et al. Intraspecies and interspecies comparison of the compressive properties of the medial meniscus. *Ann Biomed Eng*.**32**:1569. 2004.
41. Herwig J., Egnér E., Buddecke E. Chemical changes of human knee joint menisci in various stages of degeneration. *Ann Rheum Dis*.**43**:635. 1984.
42. Imler S.M., Doshi A.N., Levenston M.E. Combined effects of growth factors and static mechanical compression on meniscus explant biosynthesis. *Osteoarthritis Cartilage*.**12**:736. 2004.
43. Detamore M.S., Athanasiou K.A. Effects of growth factors on temporomandibular joint disc cells. *Archives of Oral Biology*.**49**:577. 2004.

44. Schumacher B.L., Schmidt T.A., Voegtline M.S., Chen A.C., Sah R.L. Proteoglycan 4 (PRG4) synthesis and immunolocalization in bovine meniscus. *J Orthop Res.***23**:562. 2005.
45. Schmidt T.A., Gastelum N.S., Han E.H., Nugent-Derfus G.E., Schumacher B.L., Sah R.L. Differential regulation of proteoglycan 4 metabolism in cartilage by IL-1alpha, IGF-I, and TGF-beta1. *Osteoarthritis Cartilage.***16**:90. 2008.

## CHAPTER 5

### **High Density Type I Collagen Gels for Tissue Engineering of Whole Menisci<sup>\*</sup>**

#### ***Abstract***

This study investigates the potential of high density type I collagen gels as an injectable scaffold for tissue engineering of whole menisci, and compares these results to previous strategies using alginate as an injectable scaffold. Bovine meniscal fibrochondrocytes were mixed into collagen and injected into  $\mu$ CT based molds to create 10 and 20 mg/mL menisci that were cultured for up to 4 weeks and compared to cultured alginate menisci. Contraction, histological, confocal microscopy, biochemical and mechanical analysis were performed to determine tissue development. By 4 weeks of culture, collagen menisci preserve their shape and significantly improve their biochemical and mechanical properties. Both 10 and 20 mg/mL menisci maintained DNA content while significantly improving glycosaminoglycan and collagen content, at values significantly higher than alginate controls. Collagen menisci matched alginate control equilibrium modulus, and developed a 3-6 fold higher tensile modulus than alginate by 4 weeks. Further fibrochondrocytes were able to reorganize the collagen gels into a more fibrous appearance similar to native menisci.

#### ***Introduction***

Injuries to the meniscus are most commonly tears, with the majority occurring in the avascular region, and are characterized by slow healing<sup>1, 2</sup>. Meniscal injuries are among the most common orthopedic injuries in the knee and result in over 1 million

---

<sup>\*</sup> This chapter is published: Puetzer J.L., Bonassar L.J. High density type I collagen gels for tissue engineering of whole menisci. *Acta Biomater.*9:7787. 2013

surgeries a year in the United States<sup>1-3</sup>. While there have been improvements in suturing techniques and materials for partial repair<sup>4-6</sup>, improvements are still needed for treating injuries too severe for repair of focal lesions. Currently, the only treatment for meniscus replacement is cadaveric allograft; however donor tissue is scarce, it is difficult to match native joint architecture, preservation is difficult, and it carries a risk of disease transmission<sup>3,7</sup>.

Recently, there has been considerable effort to generate appropriately shaped tissue engineered (TE) whole menisci to serve as an alternative to allograft replacement made from either synthetic or natural materials<sup>8-19</sup>. Natural scaffolds often lack the necessary mechanical properties, while synthetic scaffolds often cause an immune response or degradation of surround articular cartilage<sup>2, 3, 7</sup>. None of these efforts have achieved clinical use, as many lack the correct shape, appropriate structure, and native mechanical properties to withstand implantation *in vivo*.

Previously we have developed an injection molding technique to create anatomical meniscal constructs composed of fibrochondrocytes-seeded alginate<sup>11</sup>. We have reported these alginate menisci generate matrix and maintain shape fidelity with and without mechanical stimulation<sup>10, 11, 15, 20</sup>. However these menisci still have levels of collagen and glycosaminoglycans (GAGs) less than native menisci, poor tensile properties, and due to the lack of natural cell- and matrix- binding ligands in alginate<sup>21</sup>, a large amount of produced matrix and cells is lost to the media during culture<sup>10, 11, 15, 20</sup>.

Collagen is an attractive alternative to alginate. Type I collagen is the major component of menisci and its circumferential fiber organization prevents radial extrusion while providing resistance to hoop stresses, thus playing a large role in the transmission of forces<sup>2, 22</sup>. Due to the prevalence and large role type I collagen plays in the meniscus, a scaffold primarily composed of type I collagen is a very appealing

option. Collagen is a natural material composed of fibers that allow for increased tensile properties, better retention of cells and matrix, and a place for cells to attach and remodel the matrix into a more mechanically stable material<sup>23, 24</sup>. Additionally, it is believed a collagen matrix must be established in order to accumulate GAGs, which contribute to the compressive property of menisci<sup>25</sup>.

Freeze-dried collagen matrices have been investigated in TE meniscal constructs and are the most successful scaffold to date; however these matrixes often have high resorption without replacement of organized collagen, weak mechanical properties, contraction, and are not anatomically shaped<sup>4, 24, 26-28</sup>. Due to the fabrication methods used to make these scaffolds, cells must be seeded onto the surface and allowed to migrate into the scaffold instead of being seeded throughout<sup>24, 26</sup>. This process of populating the scaffold is challenging since it is often difficult and time consuming for cells to penetrate the scaffolds. We propose to overcome these obstacles by making an anatomical meniscal construct using an injection molded collagen gel seeded with meniscal fibrochondrocytes.

Collagen gels have been repeatedly shown to allow multiple cell types to organize the fiber alignment and thus improve the mechanical properties of the gel and overall organization<sup>23, 29, 30</sup>. Low density collagen gels (1-3 mg/mL) have been investigated for decades in many different TE applications, but have often been avoided in orthopedic applications due to weak mechanical strength, low shape fidelity, and high contraction<sup>23</sup>. Cell seeded collagen gels have been well established to contract due to cell traction forces; however this contract has been shown to decrease with increasing concentrations of collagen<sup>23, 31, 32</sup>. Recently, high density gels (10-20 mg/mL) have been shown to be moldable and able to carry cells without high viability issues<sup>23</sup>. Further, these high density gels have stronger mechanical properties and decreased contraction, while still allowing the cells to proliferate and rearrange their

matrix<sup>23</sup>. To date, very few studies have characterized seeded high density collagen gels, and no one has investigated meniscal fibrochondrocytes seeded high density collagen gels in anatomical or simple geometry scaffolds.

The objective of this study was to investigate the potential of high density collagen gels as meniscal replacements once seeded, molded and cultured and to compare the results to our previously published alginate menisci over 4 weeks of culture. Further, we investigated the effect of collagen concentration. We hypothesize that high density type I collagen gels will produce a construct with biochemical and mechanical properties more analogous to native menisci than alginate.

## ***Materials and Methods***

### **Collagen Extraction and Reconstitution**

Collagen was extracted and reconstituted as previously described<sup>23, 29, 30</sup>. Briefly, tendons were excised from 7-8 year old mixed gender Sprague rat tails and suspended in 0.1% acetic acid at 150 mL/gram of tendon for at least 48 hours at 4°C. The collagen solution was then centrifuged for 90 minutes at 4500 RPM at 4°C. The clear supernatant was collected and lyophilized, while the pellet was discarded. Finally the collagen was weighed and reconstituted in 0.1% acetic acid at 20 and 30 mg/mL concentrations.

### **Cell Isolation and Injection Molding**

Bovine meniscal fibrochondrocytes were isolated as previously described<sup>11, 15, 33</sup>. Briefly, menisci were dissected from freshly slaughtered 1-3 day old bovine knees. The tissue was diced and digested overnight in 0.3% collagenase, 100 µg/mL penicillin, and 100 µg/mL streptomycin in Dulbecco's modified Eagle's medium (DMEM). The next day the cells were filtered, washed, and counted. The cells were

then suspended into media to have a final concentration in constructs of  $25 \times 10^6$  cells/mL. The stock collagen solution was returned to pH 7.0 and maintained at 300mOsm by mixing it with the appropriate volumes of 1N NaOH, 10xPBS, and 1xPBS as previously described<sup>23, 29</sup>. This collagen solution was immediately mixed with the cell/media solution and injected into  $\mu$ CT based ovine meniscal molds<sup>11</sup> using a syringe stop-cock system to obtain 10 and 20 mg/mL meniscal constructs. The molds were allowed to gel for 50 minutes at 37°C. After 50 minutes the meniscal constructs were removed from the molds and cultured in media composed of DMEM, 10% FBS, 100  $\mu$ g/mL penicillin, 100  $\mu$ g/mL streptomycin, 0.1 mM non-essential amino acids, 50  $\mu$ g/mL ascorbate, and 0.4 mM L-proline.

A total of 24 menisci per collagen concentration were cultured in 20 mLs of media each, changed every 2-3 days. Media samples were collected before each media change for biochemical analysis and photographs were taken throughout culture to track contraction. Ten and 20 mg/mL collagen menisci were cultured for up to 4 weeks and compared to previously reported static cultured alginate menisci<sup>15</sup>. Briefly, alginate menisci were created by suspending cells at  $50 \times 10^6$  cells/mL in sterile 2% w/v alginate and mixing with 0.02 g/mL CaSO<sub>4</sub> at a 2:1 ratio before being injected into ovine meniscal molds. The molds were then allowed to further crosslink for 40 minutes in 60mM CaCl<sub>2</sub> before being removed from the molds. At 0, 2, and 4 weeks, 8 samples from each group were removed from culture for analysis of contraction, organization, biochemical composition, and mechanical properties.

### Post-culture Analysis

#### *Gross Appearance and Contraction*

Upon removal from culture, all meniscal constructs were examined grossly, weighed, photographed and then cut into sections for analysis by confocal imaging,

histology, biochemical assays, and mechanical testing. Photographs taken throughout the culture duration were analyzed using ImageJ software (NIH, Bethesda, MD) to calculate changes in area of the collagen constructs.

#### *Confocal Image Analysis*

Cross-sections of the collagen menisci were fixed in 10% buffered formalin, stored in 70% ethanol, and imaged with confocal reflectance to visualize collagen fiber and cell organization based on previously described methods<sup>29, 34, 35</sup>. Imaging was performed with a Zeiss 710 confocal microscope on a Zeiss Axio Observer Z1 inverted stand using a LCI Plan-Apochromat 25x/0.8 water immersion objective operated by ZEN Software (Carl Zeiss MicroImaging, Jena, Germany). Confocal reflectance imaging was performed in conjunction with fluorescence imaging to visualize collagen organization and cells, respectively, by splitting a 488nm laser. Confocal reflectance microscopy was performed by collecting the backscattered light from collagen fibers captured through a 30- $\mu$ m pinhole and pixel dwell time of 1.58  $\mu$ s at 475-510nm. Fluorescence was captured at 500-580nm produced by the auto-fluorescence of the cells believed to be primarily due to flavin proteins. In images, green color represents collagen content, while the red color is the cells.

#### *Histological Analysis*

Cross-sections of the collagen menisci were fixed, dehydrated and placed into paraffin blocks. The blocks were sectioned and stained with picosirius red. Images were taken in brightfield and polarized light at 40x and 200x to observe collagen localization and collagen fiber organization. Imaging was performed with a Nikon Eclipse TE2000-S microscope (Nikon Instruments, Melville, NY) outfitted with a SPOT RT camera (Diagnostic Instruments, Sterling Heights, MI).

### *Biochemical Analysis*

Biochemical analysis was performed as previously described<sup>11, 15</sup>. Briefly, samples were collected from the center (central region), bottom (inferior surface) and face (superficial and lateral surface) of the constructs as previously described<sup>10, 15, 20</sup> and depicted<sup>20</sup> (totaling 6 samples per meniscus). The samples were then weighed wet (WW), frozen, lyophilized, and weighed again to obtain dry weight (DW). The samples were then digested with 1.25 mg/mL papain solution overnight at 60°C and analyzed for DNA, GAG and collagen content via the Hoechst DNA assay<sup>36</sup>, a modified DMMB assay<sup>37</sup>, and a hydroxyproline assay<sup>38</sup>, respectively. The same assays were used to analyze media samples taken every 2-3 days throughout culture to track DNA, GAG, and collagen content released to the media. Biochemical properties are reported normalized to WW of the samples, total production, and % retention. Total production of the biochemical component was calculated as the summed amount of accumulation in the scaffold and media throughout culture, while the % retention was calculated as the fraction of the biochemical component accumulated in the scaffold compared to the total production. Total accumulation within the scaffolds was determined by multiplying the weight of the entire construct upon removal from culture by the concentration of the biochemical component normalized to weight wet, thus accounting for the contraction of the collagen gels.

### *Mechanical Analysis*

The compressive and tensile moduli were determined as previously described<sup>20, 33, 39</sup>. Briefly, 4mm x 1mm plugs were cut from the center (central region in both the circumferential and radial direction), bottom (inferior surface) and face (superficial and lateral surface) of the meniscal constructs in order to examine spatial and directional

differences in compressive modulus and dog bones were cut circumferentially for tensile testing. All mechanical testing took place on an EnduraTech (Electroforce(ELF) 3200 System, Minnetonka, MN). The equilibrium modulus was determined via a confined compression stress relaxation test performed by imposing 10x50 $\mu$ m steps on the plugs with the resultant loads fit to a poroelastic model using a custom MATLAB program<sup>33, 39</sup>. The tensile modulus was determined by testing to failure at a strain rate of 0.75%/s assuming quasi-static loading and ensuring failure at the central region. The modulus was then calculated as the slope of the linear region of the stress-strain curve<sup>20</sup>.

### Statistics

All biochemical and mechanical data were analyzed by 2 or 3 way ANOVA using Tukey's t-test for post-hoc analysis and  $p < 0.05$  as a threshold of statistical significance. All data expressed as mean $\pm$ SD. Correlation data were fit with a plane and  $R^2$  values were determined significant using r-tables with  $\alpha < 0.05$  considered significant.

## **Results**

### Construct Shape Fidelity and Appearance

Gross inspection of collagen meniscal constructs demonstrated that overall shape was maintained throughout culture, however menisci did contract uniformly with time (Figure 5.1A). Further, 20 mg/mL menisci appeared to contract less than 10 mg/mL and this was confirmed by image analysis, which showed that 10 mg/mL collagen constructs were significantly smaller than 20 mg/mL constructs from 2 weeks on (Figure 5.1B). Alginate scaffolds were not analyzed for change in area since it is well established alginate scaffolds do not change in size with time in culture and we have

previously reported alginate meniscal constructs maintain their volume and mass over 6 weeks of static culture<sup>10</sup>. Percent change in mass of constructs throughout culture matched area change and volume calculations, with alginate menisci maintaining their mass while both 10 and 20 mg/ml collagen menisci had significant decreases in mass with time in culture (Figure 5.1C). Further by 4 weeks, 10 and 20 mg/ml constructs had ~50-60% decreases in percent area and mass. This demonstrates that the percent area calculates are similar to volume and that contraction is uniform in area to volume measurements as well.

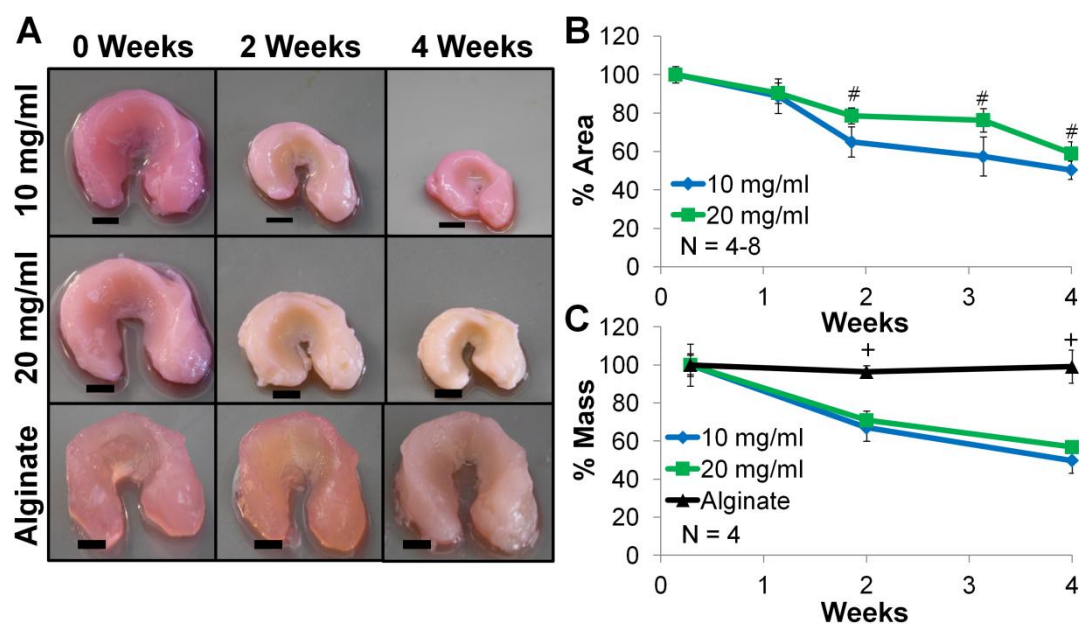


**Figure 5.1:** Photographs of constructs (A), percent area (B) of collagen menisci with time and percent mass of constructs throughout culture (C). Bar=5mm. Significance between # 10 and 20 mg/mL, + alginate and both collagen concentrations ( $p < 0.05$ )

### Collagen Localization and Organization Analysis

Brightfield low magnification images of picrosirius red stained samples reveal both 10 and 20 mg/ml collagen samples stain more robustly and have a more uniform distribution of collagen than alginate samples after 4 weeks of culture (Figure 5.2). Higher magnification images demonstrate alginate constructs have only focal

accumulation of collagen by 4 weeks, while collagen constructs begin to have organized collagen fibers. Due to the apparent organization in collagen constructs, further analysis was performed with confocal reflectance and polarized light.

Confocal reflectance imaging demonstrated 10 and 20 mg/mL collagen menisci began as homogeneous, unorganized collagen/cell mixtures at 0 weeks that changed by 4 weeks to contain large regions of organized collagen with cells localized to non-collagenous regions, similar to native tissue (Figure 5.3). The regions of organized collagen are distinguished by the presence of distinct fibers at 4 weeks of culture with 10 mg/ml collagen constructs forming 5-12  $\mu\text{m}$  diameter single fibers and 20 mg/ml collagen constructs forming 15-50  $\mu\text{m}$  diameter fiber bundles. Further, there was no noticeable depletion of cells anywhere within the scaffolds as depicted by the visible auto-fluorescing cells.

In picrosirius red images, radial cross-sections of native menisci were characterized by smaller randomly oriented collagen fibers that branch off of larger and larger circumferential fibers. Picrosirius red staining demonstrated a similar organization with both concentrations of collagen menisci forming well defined randomly oriented collagen fibers by 4 weeks (Figure 5.3). Twenty mg/mL menisci had additional formation of much thicker collagen fibers. Both concentrations of collagen menisci formed an outer coating of fibers parallel to the surface by 4 weeks.

The collagen menisci are primarily composed of type I collagen since they are created using extracted and reconstituted type I collagen from rat tail tendons. However, meniscal fibrochondrocytes can produce both type I and II collagen, thus immunohistochemistry for type II collagen was performed. Type II collagen was present in detectable levels after 20 days of culture in 20 mg/ml collagen constructs (see supplemental data and Figure 5.S1).

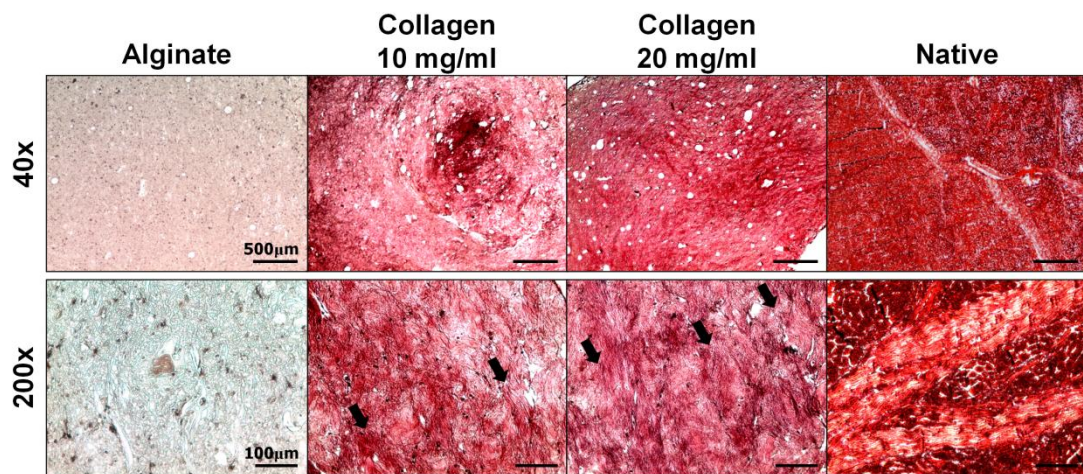


**Figure 5.2:** Brightfield picrosirius red stained images of 4 week static cultured alginate menisci, collagen menisci, and native tissue at 40x (Bar = 500µm) and 200x (Bar = 100µm). Ten and 20 mg/ml collagen menisci demonstrate more robust staining, localization and organization of collagen than alginate. Arrows point to areas of organized collagen fibers in engineered scaffolds.

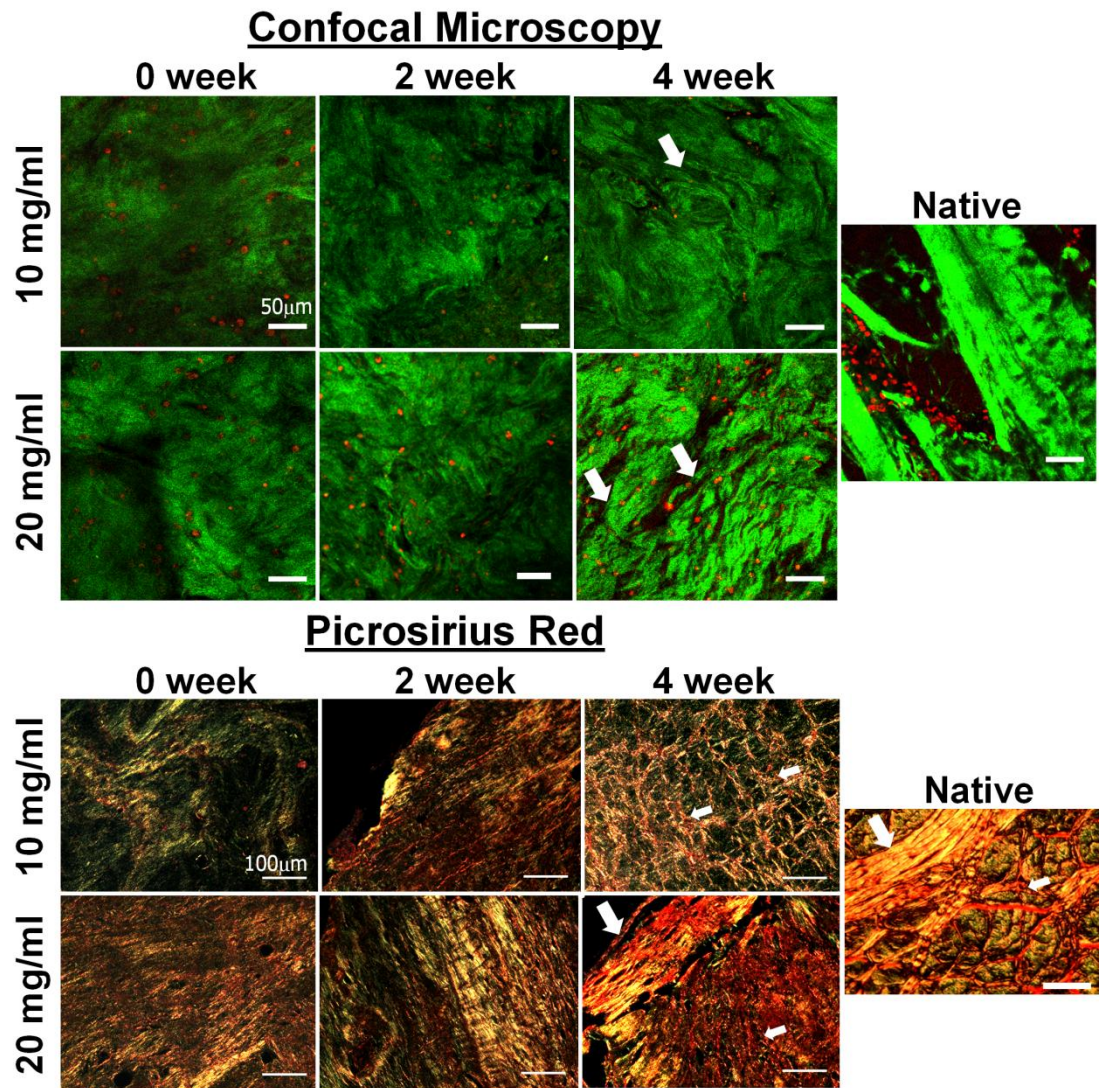


**Figure 5.3:** Confocal reflectance (Green=collagen, red=cells, bar = 50µm) and picrosirius red stained collagen menisci samples visualized with polarized light (Bar = 100µm) to observe collagen and cell organization that increased with time in culture and collagen concentration to have large regions organized similar to native tissue. Arrows point to areas of organization, with large arrows point to large collagen fiber bundles and smaller arrows pointing to radial unorganized single collagen fibers.

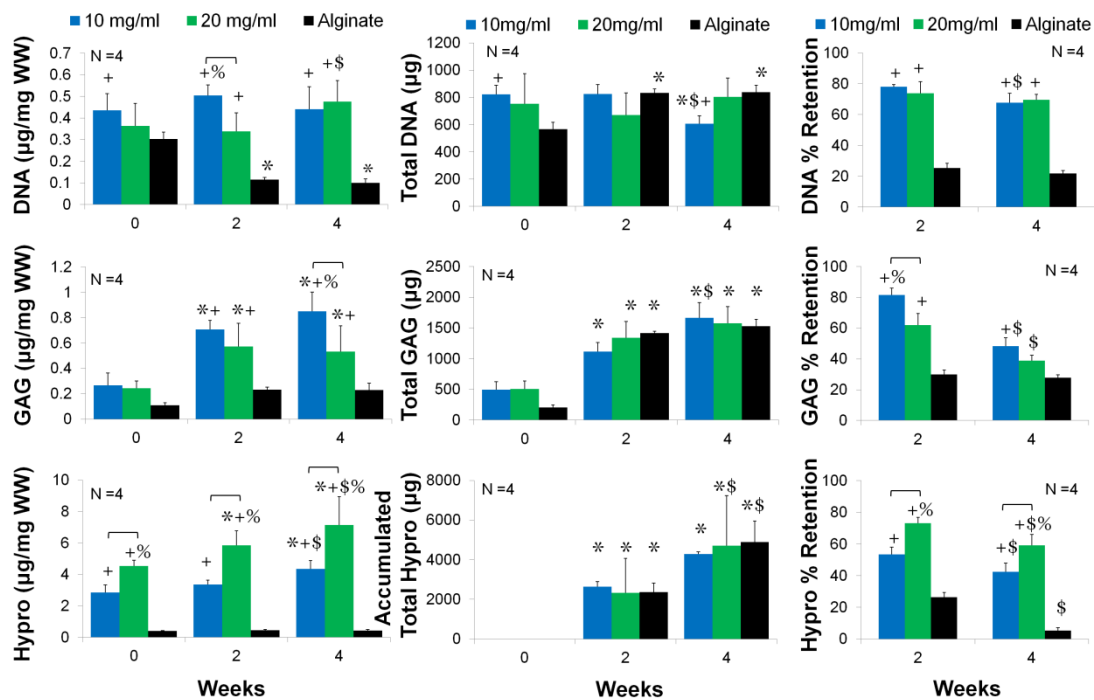


**Figure 5.4:** DNA, GAG, and collagen content in scaffolds normalized to wet weight (1<sup>st</sup> column), cumulative total production found in scaffolds and media throughout culture (2<sup>nd</sup> column), and % retention in scaffolds (3<sup>rd</sup> column). Significant difference from \*0 week, + alginate, \$ week 2, % bracket group. (p<0.05)

### Biochemical Analysis

Biochemical analysis demonstrated that menisci constructed from 10 and 20 mg/mL collagen had significantly more DNA, GAG and collagen at 2 and 4 weeks than alginate menisci. Regardless of scaffold, meniscal fibrochondrocytes produced the same amount of ECM throughout culture with significant improvements in total GAG and collagen production with time in culture. However, both concentrations of collagen menisci retained significantly more DNA, GAG, and hydroxyproline than alginate menisci (Figure 5.4).

Both groups of collagen menisci maintained or improved DNA content while alginate menisci, seeded at double the concentration, lost DNA content with time in culture (p<0.001). Throughout the entire culture period alginate menisci lost

significantly more DNA to the media than collagen menisci (data not shown;  $p < 0.001$ ). Collagen menisci retained ~70-80% of DNA content throughout culture and alginate menisci retained only 20%. This increased retention in collagen menisci was not due to increased production of DNA, as total DNA (i.e. the sum of DNA in samples and media) did not change dramatically, throughout culture for any scaffold groups (Figure 5.4 row 1). Further, there were no significant spatial differences in DNA concentration for any of the scaffolds with time in culture (power of 78%, data not shown), suggesting there were no areas of necrosis within any of the scaffolds.

Collagen menisci had a 3-fold increase in GAG accumulation by 2 weeks ( $p < 0.001$ ), which was maintained through 4 weeks, while alginate menisci demonstrated no significant increases in GAG content throughout culture. Total production of GAG significantly increased at 2 weeks of culture for all scaffolds and was maintained through 4 weeks, and there were no differences in total GAG production between scaffolds. Throughout the 4 weeks, alginate menisci lost significantly more GAG to the media than both concentrations of collagen menisci (data not shown;  $p < 0.001$ ). Alginate menisci retained ~30% of GAG content throughout culture and both groups of collagen menisci retained ~60-80% and ~40-50% at 2 and 4 weeks, respectively (Figure 5.4 row 2).

As expected, both groups of collagen menisci had significantly more collagen content than alginate menisci ( $p < 0.001$ ), and 20 mg/mL menisci had significantly more collagen content than 10 mg/mL menisci throughout culture ( $p < 0.001$ ). Additionally, both collagen menisci had significant increases in collagen density with time in culture ( $p < 0.001$ ), while alginate had no change in content (Figure 5.4 row 3). Because of the significant amount of hydroxyproline in collagen-based samples, total hydroxyproline accumulation was assessed by subtracting the amount of hydroxyproline at 0 weeks from that at subsequent time points (Figure 5.4 row 3,

middle panel). Using this method it was clear that regardless of scaffold type, meniscal fibrochondrocytes produced the same amount of total collagen throughout culture, and significantly improved this production with time in culture. Collagen and alginate menisci lost a similar amount of collagen to the media throughout culture until 4 weeks when alginate menisci lost significantly more than collagen menisci (data not shown;  $p < 0.03$ ). This resulted in 20 mg/mL menisci retained significantly more collagen throughout culture than other scaffolds with ~75% and 60% retention at 2 and 4 weeks respectively. Ten mg/mL menisci retained ~55% and 40% collagen at 2 and 4 weeks, while alginate menisci retained ~20% and 5% at 2 and 4 weeks (Figure 5.4 row 3).

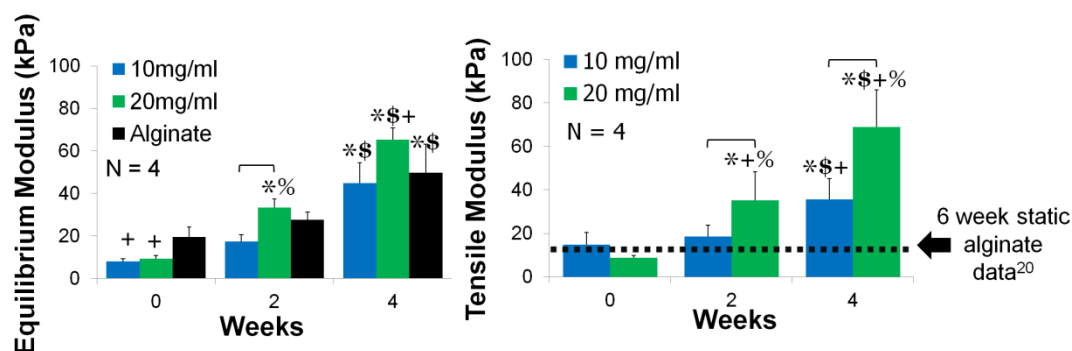


**Figure 5.5:** Equilibrium and tensile modulus of meniscal scaffolds throughout culture. Significant difference from \*0 week, + alginate, \$ week 2, % bracket group ( $p < 0.05$ ).

### Mechanical Analysis

Mechanical analysis demonstrated that the equilibrium modulus and tensile modulus of 10 and 20 mg/mL menisci increased significantly with time in culture (Figure 5.5). Both 10 and 20 mg/mL menisci had a significantly lower equilibrium modulus than alginate at 0 weeks that increased to be similar to alginate at 2 weeks. By 4 weeks both groups of collagen and alginate menisci had significantly increased equilibrium moduli ( $p < 0.001$ ), with 20 mg/mL having a significantly higher equilibrium modulus than the other constructs ( $p < 0.01$ ). There were no spatial or directional

differences in compressive properties for any of the constructs throughout culture (data not shown). At 0 weeks, collagen menisci were able to match the tensile modulus of an alginate meniscus static cultured for 6 weeks. With time in culture, collagen menisci significantly improved the tensile modulus so that by 4 weeks 10 and 20 mg/mL menisci had 3 and 6 fold increases in tensile modulus over 6 week cultured alginate menisci, respectively ( $p < 0.001$ ).

### Biochemical and Mechanical Correlations

In order to examine the underlying connection between construct properties and composition three dimensional multiple correlation analyses were performed with equilibrium and tensile moduli as the dependent variables (z-axis) and GAG and hydroxyproline content as the independent variable (x- and y-axes) (Figure 5.6). Both concentrations of collagen menisci were plotted together on a graph and a plane was fit to the data. A significant positive correlation ( $p < 0.001$ ) was found between GAG and collagen content for both the equilibrium and tensile moduli of collagen menisci. For both mechanical properties, increased collagen content correlated well with increased mechanical moduli. Further, both moduli increased at a similar ratio to collagen content as evident by a slope of 7.9 kPa/( $\mu\text{g}/\text{mg}$ ) and 9.2 kPa/(  $\mu\text{g}/\text{mg}$ ) for collagen content in equilibrium and tensile moduli, respectively. Increased GAG content had little effect on the tensile modulus, but had a much more prominent role in the equilibrium modulus. This relationship is easily visualized in the equations for the planes, where the slope for GAG content in the tensile plane is 13.8 kPa/( $\mu\text{g}/\text{mg}$ ), while the slope in the equilibrium modulus plane is 29.5 kPa/( $\mu\text{g}/\text{mg}$ ). Collectively, these correlations indicate that GAG content has a much higher contribution to mechanical properties at lower collagen contents. For example at 3  $\mu\text{g}/\text{ml}$  collagen, increasing GAG content from 0.3 to 1.2  $\mu\text{g}/\text{mg}$  increases equilibrium modulus by

275%, while this same change in GAG content increases equilibrium modulus by only 45% when the collagen content is 9 ug/mg (Figure 5.6).

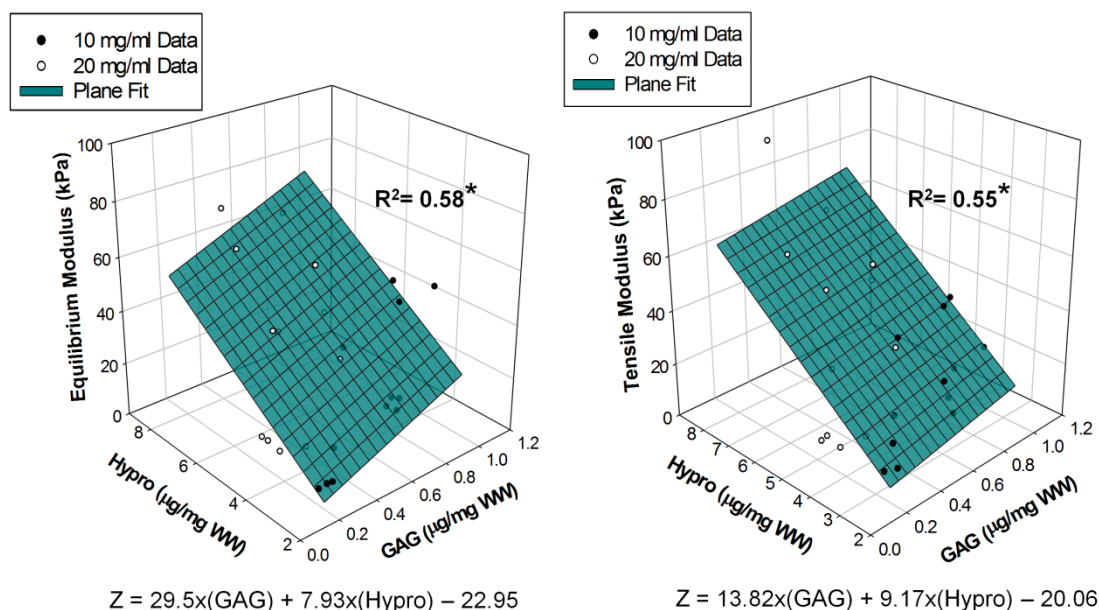


**Figure 5.6:** Correlations of biochemical components to mechanical properties.  
 \*Significant correlation as determined by comparing to critical numbers of R based on the numbers of samples tested ( $p < 0.001$ ).

### Discussion

This study demonstrated that TE menisci composed of high density type I collagen gels preserve their shape and significantly improve their biochemical and mechanical properties with time in culture. Both 10 and 20 mg/mL menisci maintained DNA content while significantly improving content of ECM components. Collagen menisci matched alginate equilibrium modulus, while having a 3-6 fold higher tensile modulus after 4 weeks of culture. Further, 20 mg/mL menisci contracted less while having better organization, ECM and mechanical properties than the 10 mg/mL menisci.

Confocal reflectance and picrosirius red staining revealed meniscal fibrochondrocytes are able to reorganize the collagen scaffolds into a more fibrous appearance similar to native menisci with time in culture. This is in support of a previous study that found meniscal fibrochondrocytes were capable of organizing their surrounding matrix with time *in vivo* and suggested these cells have an intrinsic ability to form specific tissue structures of meniscal tissue<sup>40</sup>. It has been well established in the literature that collagen gels do not change in size or structure without the presence of cells<sup>23, 31</sup>, therefore we believe the cells are responsible for this reorganization in the collagen menisci. Additionally, collagen menisci formed an outer coating of collagen fibers parallel to the surface similar to the superficial zone of native menisci. A well developed superficial zone will most likely be needed for a meniscal replacement in order for the engineered tissue to function properly within the knee.

As discussed in the introduction, contraction is an inherent property of cell seeded collagen gels, which decreases with increasing concentrations of collagen<sup>23, 31, 32</sup>. In this study, the collagen menisci contracted significantly with time in culture, and with that time and contraction, they developed significantly improved ECM and mechanical properties. This data suggests that contraction plays a large role in the increased GAG and collagen concentrations when normalized to wet weight. However, contraction is not the only reason for the increase in properties. Total overall production of GAG and collagen in the scaffold and media significantly improved with time in culture, and collagen menisci retained significantly more GAG and collagen than alginate menisci throughout culture, thus demonstrating contraction was not the sole reason for improved biochemical properties.

Further, we believe the improved biochemical properties is primarily due to the collagen scaffolds retaining more matrix components and thus enhancing the ability

for matrix to be formed, rather than the scaffold influencing the production rate of cells. This theory is in contrast to previous studies that have investigated meniscal fibrochondrocytes seeded on fibers compared to those encapsulated in gels<sup>40, 41</sup>. Aufderheide et al.<sup>41</sup> previously compared meniscal fibrochondrocyte seeded fibrous poly(glycolic acid) (PGA) scaffolds to agarose hydrogels and found significant improvements in biochemical composition of PGA scaffolds over agarose scaffolds. Thus they concluded meniscal fibrochondrocytes produce more ECM when attached to fibers than when encapsulated in gels; however this study did not investigate the amount of ECM released to the media and therefore did not calculate total production amounts<sup>41</sup>. In the current study, when the amount of GAG and collagen in the media and scaffold were added together, there were no differences in the total production of these biochemical components between the collagen and alginate scaffolds. This demonstrates that fibrochondrocytes produce the same amount of ECM whether cultured on fibers or encapsulated in gels, and that a primary advantage of collagen based gels is their ability to retain more produced ECM.

In this study bovine meniscal fibrochondrocytes were used, however for this scaffold to be used clinically it will most likely have to incorporate human cells. There are a variety of cell sources for meniscal repair and regeneration currently being investigated as discussed in the review by Makris et al.<sup>42</sup>. A number of groups are investigating the expansion of autologous meniscal fibrochondrocytes (MFCs), the use of allogeneic MFCs, and the differentiation of human embryonic stem cells (hESCs) and adult mesenchymal stem cells(hMSCs)<sup>42</sup>. Our high density collagen scaffolds could be used for any of these cell sources. The advantage of allogenic MFCs would be they have the right synthetic potential, while autologous hESCs and hMSCs have a better immune profile.

Many previous meniscus TE studies have reported loss of GAG to culture media with mechanical loading and have suggested an established collagen matrix is necessary in order to maintain GAG accumulation within the scaffold<sup>15, 25, 41</sup>. Data from the current study further supports this theory based on the observation of significant improvements in GAG accumulation in both concentrations of collagen menisci, and no improvement in alginate menisci with time in culture.

Both concentrations of collagen menisci not only had significant improvements in biochemical properties but also in compressive and tensile mechanical properties. GAGs are thought to be responsible for the compressive properties of cartilaginous tissues due to their high osmotic pressure, while collagen is thought to provide tensile properties. In this study we performed correlation studies to determine the contribution of biochemical components to the mechanical properties of the collagen menisci. A significant positive correlation was found between GAG and collagen content for both the equilibrium and tensile moduli of collagen menisci. We found that the amount of collagen present was positively correlated to both the compressive and tensile modulus. In keeping with the hypothesized mechanical role of GAGs, GAG had a much more prominent role in the equilibrium modulus than the tensile modulus. Further, GAGs appeared to play more of a role in the mechanical properties at lower concentrations of collagen. This suggests that collagen content plays a significant role in the mechanical properties of TE menisci and that only when there is less collagen present does GAG play a slight role. Similarly, in a previous study on TE menisci<sup>15</sup>, we have found that collagen content had a more direct relationship to the compressive modulus than GAG. This could be due to the increased organization attributed to collagen fiber accumulation and not necessarily the properties of collagen<sup>41, 43</sup>.

There have been many studies to investigate freeze-dried collagen matrices in meniscus tissue engineering. To date they have been some of the most successful scaffolds in meniscal research; however these matrixes often have high resorption, weak mechanical properties, contraction, are not anatomically shaped, and are difficult to seed cells throughout the scaffold<sup>4, 24, 26-28</sup>. Additionally there have been many recent studies to investigate the use of fibrous meniscal scaffolds<sup>9, 16, 19, 44</sup>. The high density collagen gels developed in this study build on the successes of past freeze-dried collagen matrices and overcome many of the obstacles associated with collagen matrixes and other fibrous scaffolds. Injection molding allows cells to be easily seeded throughout anatomically correct scaffolds. Further, with time collagen menisci have improved biochemical and mechanical properties, in the absence of any mechanical or chemical conditioning. Injection molded constructs often have inferior mechanical properties to fibrous scaffolds. However, it is believed with time and conditioning, such as mechanical and chemical stimulation, injection molded constructs can significantly improve their mechanical properties, while fibrous scaffolds often lose mechanical properties with time as cells resorb fiber without replacement of organized collagen. We have previously reported matching native compressive properties in chemically stimulated alginate constructs<sup>45</sup> and we believe tensile properties will increase with mechanical and/or chemical stimulation.

This is the first study to our knowledge to investigate the use of high density collagen gels for injection molding of living engineered tissues. Both 10 and 20 mg/mL concentrations were able to be successfully seeded with cells and injection molded to form meniscal scaffolds. The higher concentration of 20 mg/mL menisci contracted less, had larger collagen fiber formation by 4 weeks, and had better ECM and mechanical properties than the 10 mg/mL menisci. A higher density of collagen did result in less overall contraction as we hypothesized; however 20 mg/mL menisci

did still contract to ~60% their original size. It has been reported a deviation of more than 10% in meniscal size matching can result in detrimental loading across the joint<sup>46</sup>, thus it is important we control contraction. The contraction of the collagen menisci was uniform and consistent, which suggests that we could accommodate for the contraction by simply over-sizing our molds. The contraction of the collagen gels is beneficial, resulting in increased collagen density, construct biochemical and mechanical properties, and improved collagen organization. It is difficult to create collagen meniscal constructs above 20 mg/ml since the collagen becomes too dense to injection mold. However, 20 mg/ml collagen concentrations are still only ~15% the concentration of collagen in native menisci. As the collagen contracts it allows the concentration to increase, reaching a concentration of collagen ~30% that of native menisci by 4 weeks of static culture. Further, the contraction allows for the organization of collagen fibers. Contraction in collagen gels occurs as cells create traction forces within the gel, often resulting in the formation of well defined collagen fibrils<sup>29, 31, 32</sup>. By 4 weeks of culture, we found 10 and 20 mg/ml collagen gels to have increased organization with 10 mg/ml menisci developing 5-12  $\mu$ m diameter single fibers, and 20 mg/ml menisci developed 15-50  $\mu$ m diameter fiber bundles. We could attempt to control this contraction by using glycated collagen<sup>47</sup> or riboflavin crosslinking which we have previously demonstrated to limit contraction in our TE intervertebral discs<sup>48</sup>. However, limiting contraction long term could decrease or impede collagen reorganization and thus may not be the optimal choice for ensuring the constructs are appropriately sized.

### **Conclusions**

This study demonstrates the use of high density type I collagen gels to create whole meniscal constructs with mechanical and biochemical properties similar to

native menisci. GAG and collagen concentrations increased to ~20% and ~15-30% that of native tissue, respectively, while the equilibrium modulus was ~50-70% that of native menisci. Although the tensile modulus improved 6 fold in collagen menisci over alginate controls, this is still 1-2 orders of magnitude lower than native menisci and does not mirror the anisotropic properties of native tissue. Thus, although the use of constructs seeded with bovine meniscal fibrochondrocytes demonstrate great promise as meniscal replacements future work should focus on the use of human cells and improving tissue organization and tensile properties to achieve the functional anisotropic organization and properties of native tissue.

### ***Supplemental Data***

#### **Immunohistochemistry Methods**

Immunohistochemistry was performed for type II collagen using a modified Vectastain ABC kit protocol (Vector Laboratories, Burlingame, CA)<sup>45</sup>. Twenty mg/ml type I collagen constructs were cultured for 10 or 20 days, fixed in 10% buffered formalin, embedded in paraffin blocks, and sectioned. Following deparaffinization and hydration, samples were stained as previously described<sup>45</sup>. Briefly, slides were incubated for an hour in anti-type II collagen antibody (1:200 dilution; Abcam) or left in the blocking buffer as a negative control. Sections were washed with PBS and incubated in a biotinylated secondary antibody (1:200, Vectastain ABC Elite Kit) for 30 minutes. Finally, slides were incubated in ABC Reagent (Vectastain ABC Elite Kit) for 30 minutes and stained with ImmPact DAB (Vector Laboratories, Burlingame, CA) for up to 10 minutes.

### Immunohistochemistry Results

Type II collagen immunohistochemistry of the 20 mg/ml collagen samples demonstrated no apparent positive staining at 10 days, and only slight staining throughout the constructs at 20 days in comparison to the strong positive staining in the native tissue (Figure 5.S1). This data demonstrates there is minimal type II collagen accumulation in high density collagen menisci with time in culture, and suggests these collagen constructs remain primarily composed of type I collagen throughout culture.

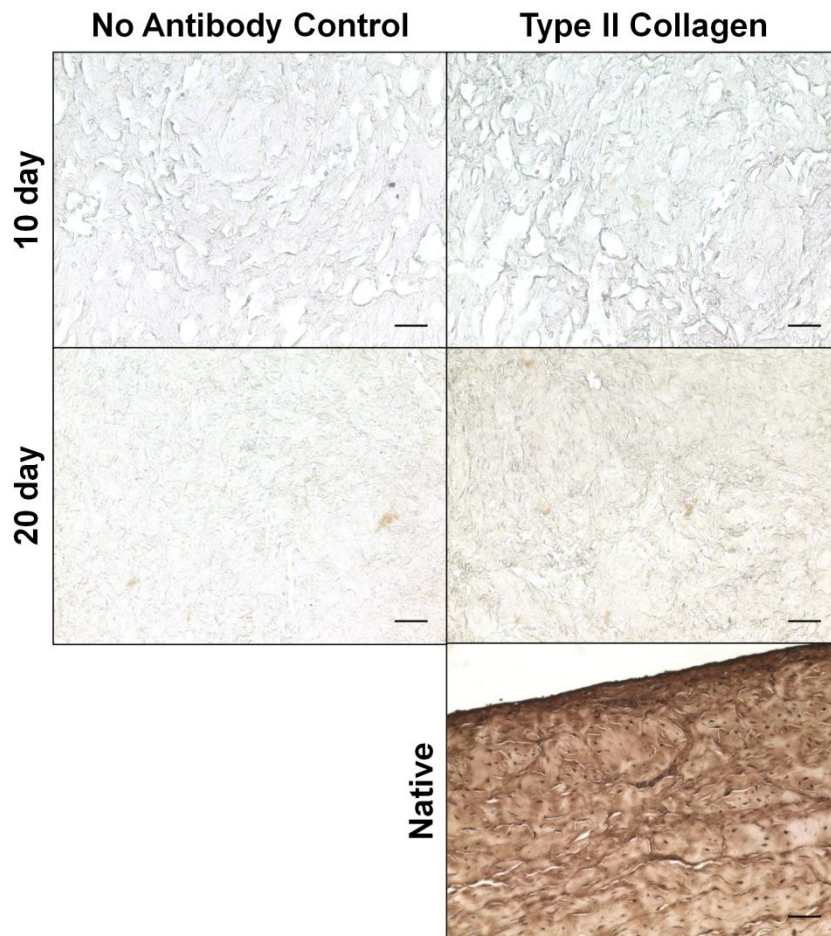


**Figure 5.S1:** Immunohistochemistry staining for type II collagen at 200x in 20 mg/ml type I collagen constructs at 10 and 20 days and native meniscal tissue. Scale bar = 50 $\mu$ m

## REFERENCES

1. Khetia E.A., McKeon B.P. Meniscal allografts: biomechanics and techniques. *Sports Med Arthrosc.***15**:114. 2007.
2. Sweigart M.A., Athanasiou K.A. Toward tissue engineering of the knee meniscus. *Tissue Eng.***7**:111. 2001.
3. Peters G., Wirth C.J. The current state of meniscal allograft transplantation and replacement. *Knee.***10**:19. 2003.
4. Stone K.R., Steadman J.R., Rodkey W.G., Li S.T. Regeneration of meniscal cartilage with use of a collagen scaffold. Analysis of preliminary data. *J Bone Joint Surg Am.***79**:1770. 1997.
5. Farnig E., Sherman O. Meniscal repair devices: a clinical and biomechanical literature review. *Arthroscopy.***20**:273. 2004.
6. McDermott I. Meniscal tears, repairs and replacement: their relevance to osteoarthritis of the knee. *Br J Sports Med.***45**:292. 2011.
7. Buma P., Ramrattan N.N., van Tienen T.G., Veth R.P. Tissue engineering of the meniscus. *Biomaterials.***25**:1523. 2004.
8. Aufderheide A.C., Athanasiou K.A. Assessment of a bovine co-culture, scaffold-free method for growing meniscus-shaped constructs. *Tissue Eng.***13**:2195. 2007.
9. Balint E., Gatt C.J., Jr., Dunn M.G. Design and mechanical evaluation of a novel fiber-reinforced scaffold for meniscus replacement. *J Biomed Mater Res A.***100**:195. 2012.
10. Ballyns J.J., Bonassar L.J. Dynamic compressive loading of image-guided tissue engineered meniscal constructs. *J Biomech.***44**:509. 2011.
11. Ballyns J.J., Gleghorn J.P., Niebrzydowski V., Rawlinson J.J., Potter H.G., Maher S.A., et al. Image-guided tissue engineering of anatomically shaped implants via MRI and micro-CT using injection molding. *Tissue Eng Part A.***14**:1195. 2008.

12. Huey D.J., Athanasiou K.A. Tension-compression loading with chemical stimulation results in additive increases to functional properties of anatomic meniscal constructs. *PLoS One*.**6**:e27857. 2011.
13. Kang S.W., Son S.M., Lee J.S., Lee E.S., Lee K.Y., Park S.G., et al. Regeneration of whole meniscus using meniscal cells and polymer scaffolds in a rabbit total meniscectomy model. *J Biomed Mater Res A*.**78**:659. 2006.
14. Kon E., Chiari C., Marcacci M., Delcogliano M., Salter D.M., Martin I., et al. Tissue engineering for total meniscal substitution: animal study in sheep model. *Tissue Eng Part A*.**14**:1067. 2008.
15. Puetzer J.L., Ballyns J.J., Bonassar L.J. The Effect of the Duration of Mechanical Stimulation and Post-Stimulation Culture on the Structure and Properties of Dynamically Compressed Tissue-Engineered Menisci. *Tissue Eng Part A*.**18**:1365. 2012.
16. Tienen T.G., Heijkants R.G., de Groot J.H., Schouten A.J., Pennings A.J., Veth R.P., et al. Meniscal replacement in dogs. Tissue regeneration in two different materials with similar properties. *J Biomed Mater Res B Appl Biomater*.**76**:389. 2006.
17. Zur G., Linder-Ganz E., Elsner J.J., Shani J., Brenner O., Agar G., et al. Chondroprotective effects of a polycarbonate-urethane meniscal implant: histopathological results in a sheep model. *Knee Surg Sports Traumatol Arthrosc*.**19**:255. 2011.
18. Huey D.J., Athanasiou K.A. Maturation growth of self-assembled, functional menisci as a result of TGF-beta1 and enzymatic chondroitinase-ABC stimulation. *Biomaterials*.**32**:2052. 2011.
19. Mandal B.B., Park S.H., Gil E.S., Kaplan D.L. Multilayered silk scaffolds for meniscus tissue engineering. *Biomaterials*.**32**:639. 2011.
20. Ballyns J.J., Wright T.M., Bonassar L.J. Effect of media mixing on ECM assembly and mechanical properties of anatomically-shaped tissue engineered meniscus. *Biomaterials*.**31**:6756. 2010.
21. Awad H.A., Wickham M.Q., Leddy H.A., Gimble J.M., Guilak F. Chondrogenic differentiation of adipose-derived adult stem cells in agarose, alginate, and gelatin scaffolds. *Biomaterials*.**25**:3211. 2004.

22. Kawamura S., Lotito K., Rodeo S.A. Biomechanics and healing response of the meniscus. *Oper Techn Sport Med.***11**:68. 2003.
23. Cross V.L., Zheng Y., Won Choi N., Verbridge S.S., Sutermaster B.A., Bonassar L.J., et al. Dense type I collagen matrices that support cellular remodeling and microfabrication for studies of tumor angiogenesis and vasculogenesis in vitro. *Biomaterials.***31**:8596. 2010.
24. Mueller S.M., Shortkroff S., Schneider T.O., Breinan H.A., Yannas I.V., Spector M. Meniscus cells seeded in type I and type II collagen-GAG matrices in vitro. *Biomaterials.***20**:701. 1999.
25. Baker B.M., Shah R.P., Huang A.H., Mauck R.L. Dynamic tensile loading improves the functional properties of mesenchymal stem cell-laden nanofiber-based fibrocartilage. *Tissue Eng Part A.***17**:1445. 2011.
26. Martinek V., Ueblacker P., Braun K., Nitschke S., Mannhardt R., Specht K., et al. Second generation of meniscus transplantation: in-vivo study with tissue engineered meniscus replacement. *Arch Orthop Trauma Surg.***126**:228. 2006.
27. Stone K.R., Rodkey W.G., Webber R., McKinney L., Steadman J.R. Meniscal regeneration with copolymeric collagen scaffolds. In vitro and in vivo studies evaluated clinically, histologically, and biochemically. *Am J Sports Med.***20**:104. 1992.
28. Walsh C.J., Goodman D., Caplan A.I., Goldberg V.M. Meniscus regeneration in a rabbit partial meniscectomy model. *Tissue Eng.***5**:327. 1999.
29. Bowles R.D., Williams R.M., Zipfel W.R., Bonassar L.J. Self-assembly of aligned tissue-engineered annulus fibrosus and intervertebral disc composite via collagen gel contraction. *Tissue Eng Part A.***16**:1339. 2010.
30. Elsdale T., Bard J. Collagen substrata for studies on cell behavior. *J Cell Biol.***54**:626. 1972.
31. Bell E., Ivarsson B., Merrill C. Production of a tissue-like structure by contraction of collagen lattices by human fibroblasts of different proliferative potential in vitro. *Proc Natl Acad Sci U S A.***76**:1274. 1979.
32. Vernon R.B., Sage E.H. Contraction of fibrillar type I collagen by endothelial cells: A study in vitro. *Journal of Cellular Biochemistry.***60**:185. 1996.

33. Chang S.C., Rowley J.A., Tobias G., Genes N.G., Roy A.K., Mooney D.J., et al. Injection molding of chondrocyte/alginate constructs in the shape of facial implants. *J Biomed Mater Res*.**55**:503. 2001.
34. Carey S.P., Kraning-Rush C.M., Williams R.M., Reinhart-King C.A. Biophysical control of invasive tumor cell behavior by extracellular matrix microarchitecture. *Biomaterials*.**33**:4157. 2012.
35. Mason B.N., Starchenko A., Williams R.M., Bonassar L.J., Reinhart-King C.A. Tuning three-dimensional collagen matrix stiffness independently of collagen concentration modulates endothelial cell behavior. *Acta Biomater*. 2012.
36. Kim Y.J., Sah R.L., Doong J.Y., Grodzinsky A.J. Fluorometric assay of DNA in cartilage explants using Hoechst 33258. *Anal Biochem*.**174**:168. 1988.
37. Enobakhare B.O., Bader D.L., Lee D.A. Quantification of sulfated glycosaminoglycans in chondrocyte/alginate cultures, by use of 1,9-dimethylmethylene blue. *Anal Biochem*.**243**:189. 1996.
38. Neuman R.E., Logan M.A. The determination of hydroxyproline. *J Biol Chem*.**184**:299. 1950.
39. Gleghorn J.P., Jones A.R., Flannery C.R., Bonassar L.J. Boundary mode frictional properties of engineered cartilaginous tissues. *Eur Cell Mater*.**14**:20. 2007.
40. Ibarra C., Jannetta C., Vacanti C.A., Cao Y., Kim T.H., Upton J., et al. Tissue engineered meniscus: a potential new alternative to allogeneic meniscus transplantation. *Transplant Proc*.**29**:986. 1997.
41. Aufderheide A.C., Athanasiou K.A. Comparison of scaffolds and culture conditions for tissue engineering of the knee meniscus. *Tissue Eng*.**11**:1095. 2005.
42. Makris E.A., Hadidi P., Athanasiou K.A. The knee meniscus: structure-function, pathophysiology, current repair techniques, and prospects for regeneration. *Biomaterials*.**32**:7411. 2011.
43. Waldman S.D., Spiteri C.G., Grynpas M.D., Pilliar R.M., Kandel R.A. Long-term intermittent shear deformation improves the quality of cartilaginous tissue formed in vitro. *J Orthop Res*.**21**:590. 2003.

44. Fisher M.B., Henning E.A., Soegaard N., Esterhai J.L., Mauck R.L. Organized nanofibrous scaffolds that mimic the macroscopic and microscopic architecture of the knee meniscus. *Acta Biomater.***9**:4496. 2013.
45. Puetzer J.L., Brown B., Ballyns J.J., Bonassar L.J. The Effect of IGF-I on Anatomically-shaped Tissue Engineered Menisci. *Tissue Eng Part A*. 2013.
46. Dienst M., Greis P.E., Ellis B.J., Bachus K.N., Burks R.T. Effect of lateral meniscal allograft sizing on contact mechanics of the lateral tibial plateau: an experimental study in human cadaveric knee joints. *Am J Sports Med.***35**:34. 2007.
47. Roy R., Boskey A.L., Bonassar L.J. Non-enzymatic glycation of chondrocyte-seeded collagen gels for cartilage tissue engineering. *J Orthop Res.***26**:1434. 2008.
48. Mozia R.I., Bowels R., Saroka J., Gebhard H., Hartl R., Bonassar L.J. Riboflavin crosslinking of composite tissue engineered intervertebral discs. presented at the" 2011 Annual Meeting of the Orthopedic Research Society, Long Beach, California, Year.

## CHAPTER 6

### **Native-like Fiber Development and Mechanical Anisotropy in Tissue Engineered Menisci with Long-term Horn-anchored Culture<sup>\*</sup>**

#### ***Abstract***

This study investigated the effect of long-term biomimetic horn-anchored boundary conditions on the organization and development of high density collagen menisci. Bovine meniscal fibrochondrocytes were mixed with collagen and injected into meniscal molds designed to have 12 mm extensions at each horn. After a day of static culture, 10 and 20 mg/ml collagen menisci were either clamped or unclamped and cultured for up to 8 weeks. Clamped menisci were placed in culture trays with steel bars that screwed down over the extensions, securing them in place throughout culture. This culture condition mimics the native horn attachment sites and restricts contraction circumferentially to encourage circumferential alignment. Clamped menisci preserved their size and shape, and by 8 weeks developed native-like aligned and sized circumferential fibers, native-like radial organizations, increased collagen accumulation and improved mechanical properties compared to unclamped menisci. The clamped menisci organization was further reflected in the development of anisotropic tensile properties that matched ratios of native menisci with 2-3 fold higher circumferential moduli compared to radial moduli. Ten and 20 mg/ml clamped menisci had similar levels of organization, with 20 mg/ml menisci producing larger diameter fibers and significantly better mechanical properties.

---

<sup>\*</sup> This chapter is in preparation for publication: Puetzer JL, Koo, E, Bonassar LJ. Native-like Fiber Development and Mechanical Anisotropy in Tissue Engineered Meniscus with Long-term Horn-anchored Culture. In preparation

## ***Introduction***

Menisci are semi-lunar wedge shaped discs located on top of the tibial plateau that distribute and absorb loads in the knee. Menisci are primarily anchored by ligament-like extensions at the horns<sup>1</sup>. These extensions prevent extrusion of the meniscus, while allowing movement to conform to the condyles during each gait cycle. The extensions play a major role in menisci's ability to withstand and distribute loads<sup>1,2</sup>.

Meniscal organization is also fundamental to menisci being able to withstand and distribute the complex loads of the knee<sup>1, 3</sup>. Native menisci consist largely of circumferentially aligned collagen bundles anchored by a small number of perpendicular radial tie fibers<sup>4-7</sup>. This organization results in anisotropic properties, with the circumferential tensile modulus 3-10 times larger than the radial modulus<sup>8,9</sup>.

Any tear that disrupts this organization or the attachment sites of the meniscus results in pain, swelling, mechanical instability and degradation of surrounding cartilage<sup>10</sup>. Due to the avascular nature of the meniscus, tears are characterized by slow to no healing, resulting in over 1 million surgeries a year in the US<sup>8, 10-12</sup>. While there have been improvements in treatments for small tears<sup>13</sup>, advancements are still needed for treatment of large tears that lead to whole meniscal replacement. Currently, the only treatment for total meniscal replacement is meniscectomy followed by cadaveric allograft which is applicable in a small percentage of patients. Allograft donor tissue is scarce, it is difficult to match the native joint architecture, and there is risk of disease transmission<sup>10</sup>.

Although there has been great effort to generate whole tissue engineered menisci to serve as an alternative to allografts<sup>14-22</sup>, none have achieved clinical use. These attempts often lack the native collagen fiber organization and anisotropic properties essential for the replacement to withstand and distribute the loads of the knee

accurately. Recently, we have developed high density type I collagen menisci that have significant improvements in biochemical and mechanical properties with time in culture, but lack the native organization<sup>19</sup>.

It has been well established that contraction of collagen gels under a variety of mechanical boundary conditions can be used to guide the formation of aligned collagen fibers<sup>23-27</sup>. It is believed cellular traction forces align collagen fibers along the free edge, or line of greatest tension<sup>25, 26</sup>. Further, it has been demonstrated these aligned collagen gels develop anisotropic mechanical properties<sup>27-29</sup>. However, all of this work has been done with low density collagen gels (1-6 mg/ml) and very thin, simple geometries. To date, mechanical boundary conditions have not been investigated in high density collagen gels (10-20 mg/ml) or used with large complex geometries such as the meniscus.

The objective of this study was to investigate the effect of long-term boundary conditions on the organization and development of tissue engineered meniscal constructs at multiple high density collagen concentrations. We hypothesize that high density type I collagen menisci, cultured with native horn-anchored boundary conditions, will result in alignment of collagen fibers and development of anisotropic tensile properties

## ***Materials and Methods***

### **Construct Fabrication**

A total of 68 meniscal constructs were fabricated as previously described<sup>19</sup>. Briefly, type I collagen was extracted from 7-8 year old mixed gender Sprague-Dawley rat tails (Pel-Freez Biologicals, Rogers, AZ) and reconstituted at 20 and 30 mg/ml concentrations using previously established techniques<sup>19, 24, 30</sup>. Bovine fibrochondrocytes were isolated from the meniscus of freshly slaughtered 1-3 day old

calves with 0.3% collagenase digestion and suspended in media. The stock collagen solution was then mixed with appropriate volumes of 1N NaOH, 10x phosphate-buffered saline (PBS), and 1x PBS to return the collagen to a neutral 7.0 pH and 300mOsm osmolarity and begin the gelling process<sup>24, 30</sup>. This collagen solution was immediately mixed with the cell/medium solution using a syringe stop-cock system and injected into ovine meniscus micro-computed tomography (micro-CT)-based molds<sup>15</sup> to obtain 10 and 20 mg/ml meniscal constructs at  $25 \times 10^6$  cells/ml. The molds were allowed to gel for 1 hour at 37°C (Figure 6.1). After 1 hour, the meniscal constructs were removed from the molds and cultured in media composed of DMEM, 10% FBS, 100 µg/mL penicillin, 100 µg/mL streptomycin, 0.1 mM non-essential amino acids, 50 µg/mL ascorbate, and 0.4 mM L-proline, changed every 2-3 days.

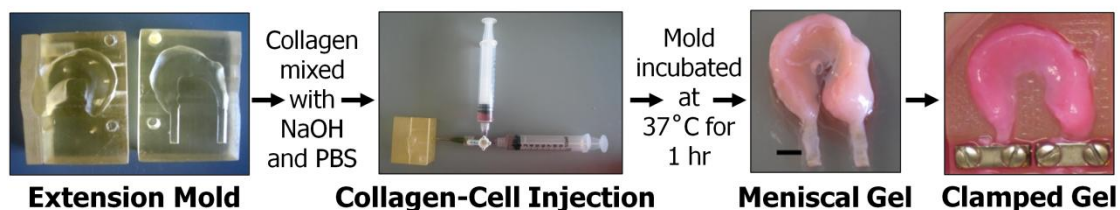


**Figure 6.1:** Injection molding process and clamping of meniscal constructs. Ovine based meniscal molds had 12 mm long extension added to the horns, high density collagen meniscal constructs were created using injection molding techniques and constructs were clamped at the extensions throughout culture.

#### Application of Boundary Conditions

In order to apply biomimetic horn-anchored boundary conditions, meniscal molds<sup>15</sup> were redesigned with a 12 x 2.5 x 2 mm (LxWxH) extension at each horn. Further, previously described ABS loading trays<sup>31, 32</sup> were redesigned to have a trough at the base of the meniscus that extensions lay in and stainless steel clamps infused with bronze (Shapeways, NY) screw down over the extensions to secure the extensions throughout culture (Figure 6.1). This boundary condition of anchoring the

meniscus at the horns was chosen to mimic the native tibial attachment sites *in vivo* and to restricted contraction of collagen gels circumferentially. By restricting contraction circumferentially we hope to induce a residual hoop stress to encourage circumferential alignment. After a day of static culture, 10 and 20 mg/ml collagen menisci were either clamped or unclamped and cultured for up to 8 weeks.

### Construct Analysis

At 0, 2, 4, and 8 weeks 4-6 samples from each group were removed from culture. Upon removal from culture all meniscal constructs were examined grossly, weighed, photographed, and sectioned for analysis of organization, biochemical composition, and mechanical properties, with attention to radial vs. circumferential directions.

### *Gross Appearance and Contraction*

Serial photographs taken throughout the culture duration were analyzed using ImageJ software (NIH, Bethesda, MD) to calculate changes in area of the collagen constructs with time in culture. Additionally, the total weight of the constructs at the completion of culture was compared to determine change in mass with time in culture.

### *Confocal Image Analysis*

Cross-sections from throughout the meniscal scaffolds were fixed in 10% buffered formalin, stored in 70% ethanol, and imaged with confocal reflectance and fluorescence in both the circumferential and radial direction to visualize collagen fiber and cell organization using previously described methods<sup>19, 24, 33, 34</sup>. Briefly, confocal reflectance imaging was performed in conjunction with fluorescence imaging by splitting a 488 nm laser on a Zeiss 710 confocal microscope with a Zeiss Axio Observer Z1 inverted stand using a 40x /1.2 C-Apochromat water immersion

objective. Confocal reflectance microscopy was performed at 475-510 nm with a 30  $\mu\text{m}$  pinhole and pixel dwell time of 1.58  $\mu\text{s}$ , while auto-fluorescent cells were captured at 500-580 nm, believed to be primarily due to flavin-containing proteins. In the images, green represents the collagen content, while auto-fluorescent cells are red.

Four to six circumferential confocal images from 4-6 cross-sections throughout the meniscus (total of 16-36 images per treatment group) were analyzed with a custom MATLAB code to determine the degree of alignment and mean fiber diameter. Degree of alignment is reported using a previously established alignment index measure<sup>24, 35, 36</sup>. The code is based on a series of 2D fast Fourier transforms (FFT)(Figure 6.2). An initial FFT is performed to determine the maximum angle of alignment within the image by summing the intensity of the FFT along lines at 5° increments from 0 – 180° around the image. This was further confirmed to be the maximum angle of alignment with a radon transform. The alignment index (AI), a measure of the degree of alignment, is then determined using the following equation and summing the intensity  $\pm 20^\circ$  from the maximum alignment angle as previously described<sup>24</sup>. AI values range from 1(unaligned) to 4.5(completely aligned).

$$AI = \frac{\int_{\theta_m - 20^\circ}^{\theta_m + 20^\circ} I \partial\theta}{\left(\frac{40^\circ}{180^\circ}\right) * \int_0^{180^\circ} I \partial\theta}$$

To determine the diameter of fibers, the original image is rotated so the maximum angle of alignment is at 90° to ensure the majority of fibers are vertical in the image (Figure 6.2). The image is cropped and resized to avoid border effects and another FFT is performed. The FFT is now rotated with major alignment along the x-axis, providing information on the frequency of sinusoidal patterns along the x axis (Figure 6.2). This is translated to diameter of fibers with the smallest fibers having the largest frequency and being the farthest from the center of the FTT. To determine the

average fiber size a histogram of intensity along the x-axis (cycle count) was created and averaged (Figure 6.2). The span along the histogram corresponding to the average intensity is then converted to pixels and further microns using the size of the image. The code was validated using control sinusoidal phantom images and by relating results to ImageJ calculated fiber diameters.

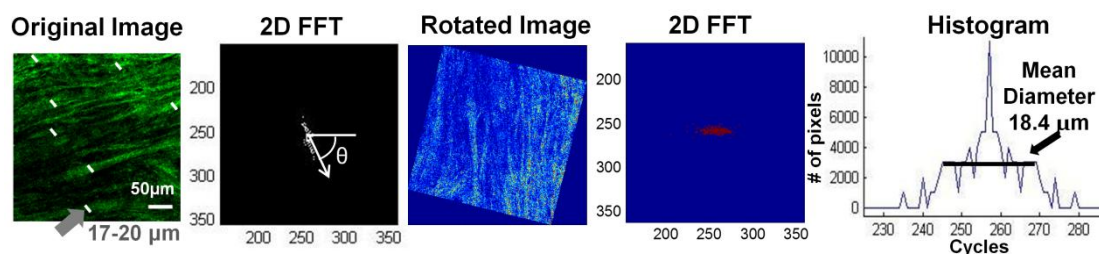


**Figure 6.2:** Fast Fourier transform based image analysis. An initial FFT is used to determine major alignment angle and alignment index. Image is rotated to major alignment angle and 2<sup>nd</sup> FFT is converted to a histogram which is averaged to find mean diameter. Mean diameter determined by code matches ImageJ calculated diameters represented by white bars on original image.

### *Histological Analysis*

In order to investigate a larger length-scale of organization, radial and circumferential cross-sections of the collagen menisci were fixed, dehydrated and embedded into paraffin blocks. The blocks were sectioned and stained with picosirious red and visualized under polarized light at 200x to observe collagen fiber organization. Images were obtained with a SPOT RT camera (Diagnostic Instruments, Sterling Heights, MI) attached to a Nikon Eclipse TE2000-S microscope (Nikon Instruments, Melville, NY).

### *Biochemical Analysis*

Tissue and media samples obtained throughout culture were analyzed biochemically for DNA, glycosaminoglycan (GAG), and collagen content as previously described<sup>15, 32</sup>. Briefly, a total of 4 samples from the extensions and throughout each meniscus were weighed wet (WW), frozen, lyophilized, and weighed again dry (DW). The samples were then digested overnight in a 1.25 mg/ml papain solution and analyzed for DNA, GAG and collagen content via the Hoechst DNA assay<sup>37</sup>, a modified 1,9-dimethylmethylene blue (DMMB) assay at pH 1.5<sup>38</sup>, and a hydroxyproline assay<sup>39</sup>, respectively. Biochemical properties are reported as the total accumulated within each meniscus so to account for any contraction of the gels. This was determined by multiplying the weight of the entire meniscus upon removal from culture by the concentration of the biochemical component normalized to WW. Media samples taken every 2-3 days were analyzed with the same assays to track the release of DNA, GAG and collagen to the media.

### *Mechanical Analysis*

The equilibrium and tensile moduli were determined as previously described<sup>19, 40, 41</sup>. Briefly, 2-4 4x1 mm plugs from each meniscal constructs were obtained to determine the equilibrium modulus while radial and circumferential dogbone punches were taken to determine the directional tensile properties. All mechanical testing was performed on an Enduratec ElectroForce 3200 System (Bose, Eden Prairie, MN) using a 250g and 1000g load cell. The equilibrium modulus was determined in confined compression via a stress relaxation test performed by imposing 10x50  $\mu\text{m}$  steps. The resulting load was then fit to a poroelastic model using a custom MATLAB program<sup>41</sup>. The tensile modulus was determined by testing at a strain rate of 0.75%/s to failure and calculated as the slope of the linear region of the stress-strain curve<sup>40</sup>.

Quasi-static loading was assumed and it was ensured failure was not near the edges. Circumferential and radial dogbone punches from neonatal bovine menisci were tested using the same tensile procedure for native baseline comparison.

### *Statistics*

All data are expressed as mean  $\pm$ SD and were analyzed by 3- and 2-way-ANOVA using Tukey's t-test for post hoc analysis. Significance was determined with  $p < 0.05$ .

### **Results**

#### Construct Appearance and Shape fidelity

Gross inspection of constructs demonstrated that both 10 and 20 mg/ml clamped menisci maintained their size and shape throughout culture while unclamped menisci had significant contraction (Figure 6.3A). This was further confirmed by percent area and mass calculations. Unclamped 10 and 20 mg/ml collagen menisci contracted to ~20% and 40% of their original area and mass by 8 weeks of culture, respectively, while clamped menisci maintained their percent area at 100% throughout the 8 week. Ten mg/ml clamped menisci did have a significant decrease in percent mass to ~80% their original size, however 20 mg/ml clamped menisci maintained their mass throughout culture with no significant changes (Figure 6.3B).

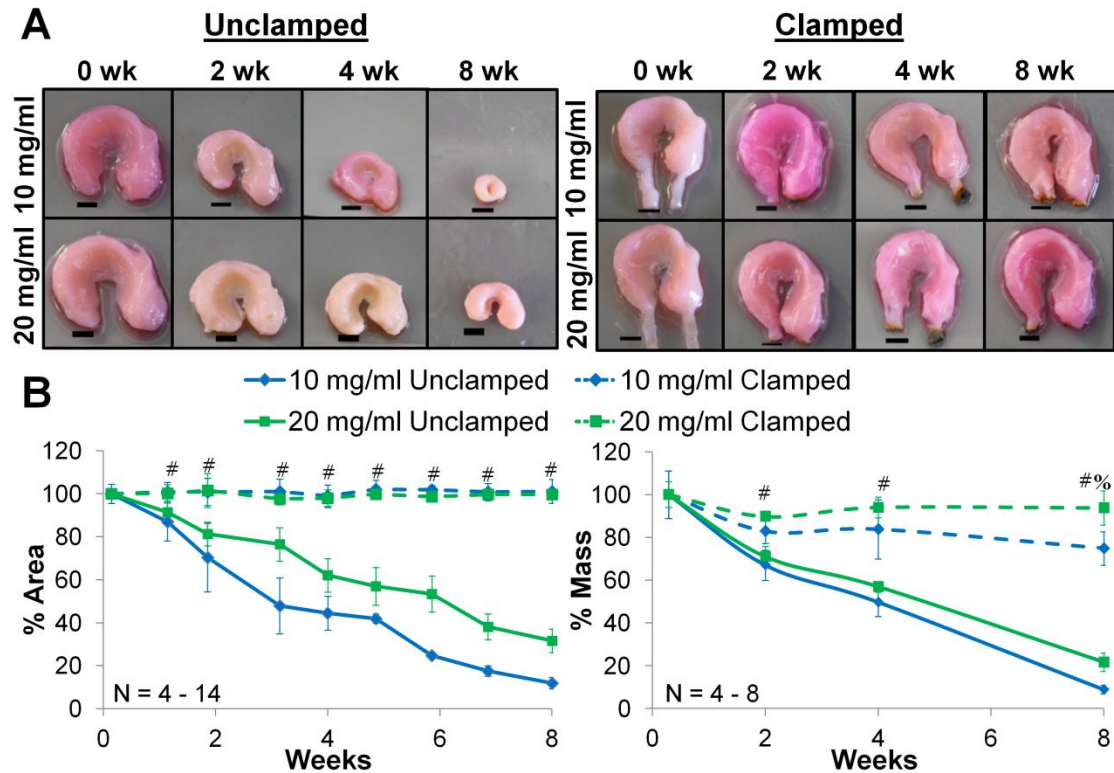


**Figure 6.3:** A) Photographs of constructs, B) percent area and percent mass of constructs throughout culture. Clamped menisci maintain size and shape throughout culture. Bar=5mm. Significance between # clamped and unclamped, % 10 and 20 mg/ml clamped menisci ( $p < 0.05$ )

### Collagen Organization Analysis

Confocal reflectance microscopy, image analysis, and picrosirius red staining demonstrated clamped menisci developed native-like sized and aligned circumferential fibers and location-dependent radial morphologies very similar to native tissue by 8 weeks of culture (Figure 6.4-6.7). Further this organization was present over a range of length scales.

In the circumferential direction, native tissue is characterized by strongly aligned collagen fibers throughout the middle to deep zone. Confocal reflectance analysis in the circumferential direction demonstrated that at 0 weeks both the 10 and 20 mg/ml collagen gels start out as unorganized homogeneous mixtures of collagen and cells

(Figure 6.4). With time in culture, unclamped menisci had some improvement in collagen organization, but nothing resembling circumferential alignment. Clamped menisci (both 10 and 20 mg/ml) began to develop areas of aligned fibers at 2 weeks (data not shown), by 4 weeks the fibers were strongly aligned circumferentially throughout the entire scaffold (Figure 6.5), and by 8 weeks these fibers appeared to grow in size to match that of native fibers (Figure 6.4).

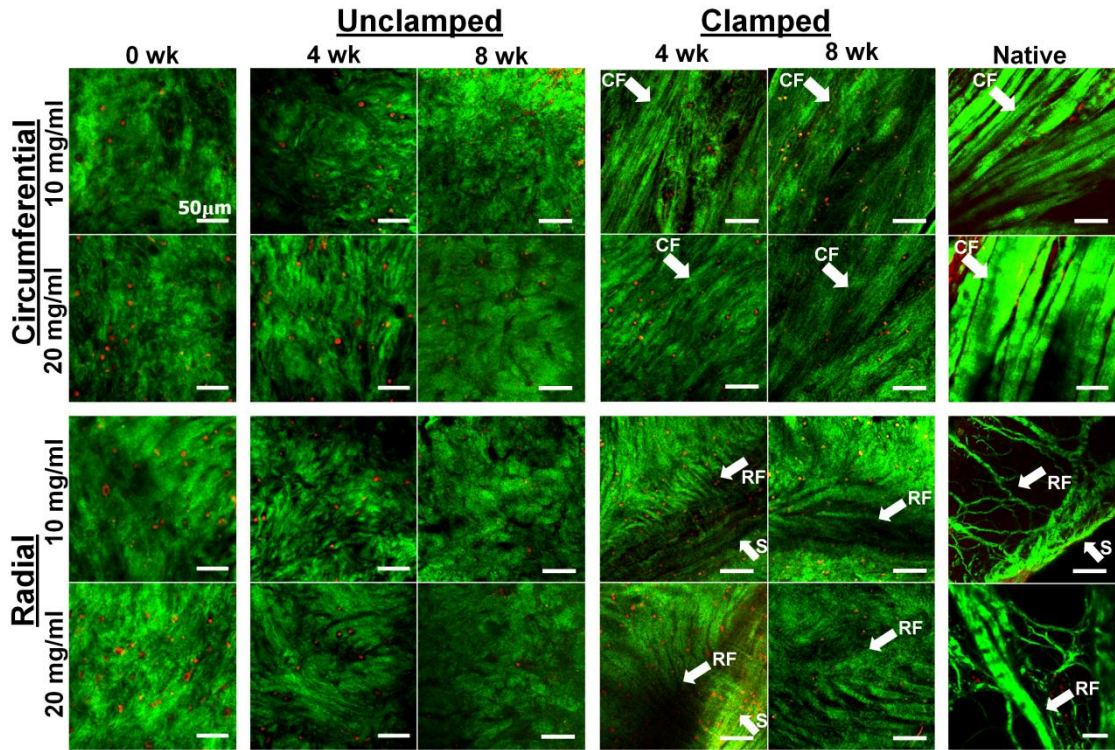


**Figure 6.4:** Circumferential and radial confocal reflectance images of engineered and native menisci. Clamped menisci develop circumferentially aligned fibers by 4 weeks and radial morphologies very similar to native tissue. Collagen = green, cells = red. Arrows point to areas of developing circumferential fibers (CF), radial fibers (RF), and the surface (S).

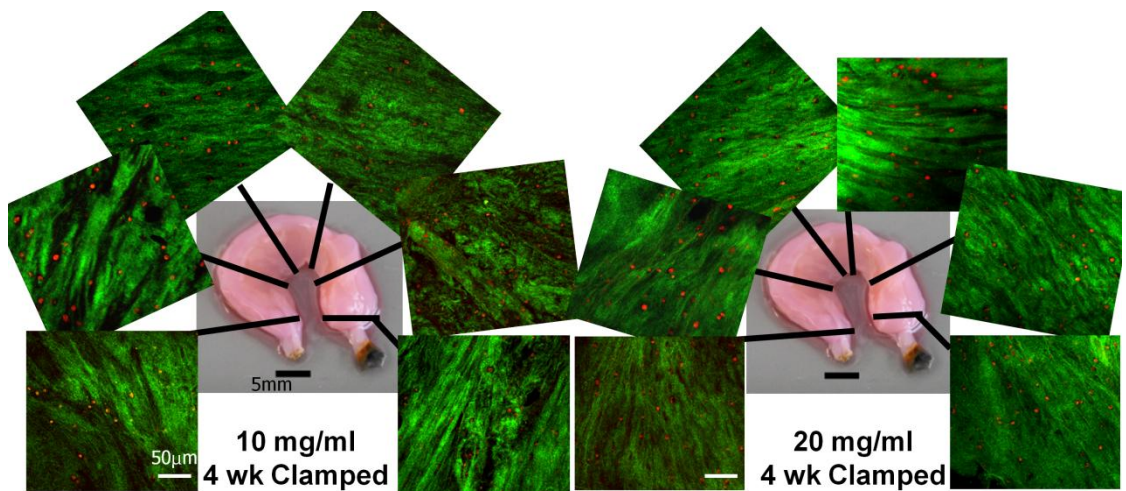


**Figure 6.5:** Circumferential confocal reflectance images from cross-sections throughout the menisci demonstrate circumferential alignment all the way around the meniscus at 4 weeks for both 10 and 20 mg/ml menisci. This was maintained through 8 weeks. Collagen = green, cells = red

Image analysis performed on circumferential confocal reflectance images from throughout the meniscus demonstrated clamped menisci had improved alignment and size of fibers with time in culture. Both concentrations of clamped menisci had significant improvements in alignment with time in culture over that of unclamped menisci ( $p < 0.001$ ) (Figure 6.6). At 4 weeks, clamped menisci matched the alignment index of native menisci and maintained this alignment through 8 weeks. Clamped menisci collagen fiber diameter improved  $\sim 3.5$  fold to match native diameters at 250x magnification by 8 weeks of culture, while unclamped menisci maintained 10  $\mu\text{m}$  diameter fibers throughout culture. Further, from 2 weeks on 20 mg/ml clamped menisci maintained significantly larger diameters than 10 mg/ml clamped menisci ( $p < 0.001$ ).

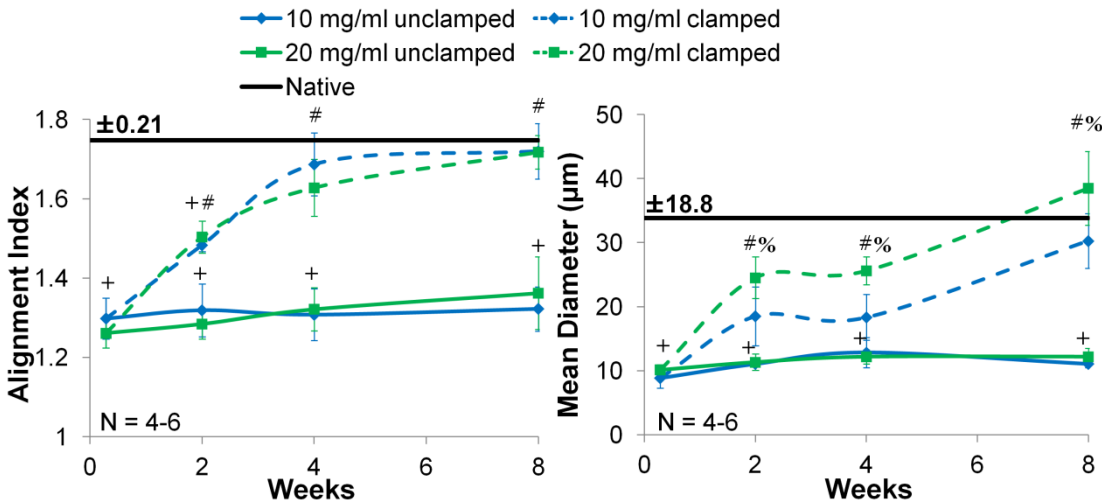


**Figure 6.6:** Circumferential image analysis for alignment index (1 unorganized, 4.5 organized) and mean fiber diameter in engineered vs native menisci. Clamped menisci match native alignment by 4 weeks and diameter by 8 weeks. Significance between # clamped and unclamped, + engineered to native, % 10 vs 20 mg/ml clamped menisci ( $p < 0.05$ )

In the radial direction, native tissue morphologies vary depending on the location within the tissue. The outer portion of the meniscus is characterized by radial tie fibers that extend perpendicular from the surface, while in the central portion of the meniscus there are much larger collagen fibers with branches of smaller randomly oriented fibers (Figure 6.4). Confocal reflectance analysis in the radial direction demonstrated again at 0 weeks, both 10 and 20 mg/ml collagen gels are unorganized mixtures of collagen and cells. With time in culture, unclamped menisci had some improvement in organization but nothing similar to native morphologies and nothing strikingly different from the circumferential direction. Clamped menisci (both 10 and 20 mg/ml) start to develop perpendicular radial fibers off the surface at 4 weeks very similar to the native radial tie fibers (Figure 6.4), and maintain this morphology through 8 weeks (data not shown). Further, at 8 weeks clamped menisci developed larger collagen fibers in the central portion of the menisci with smaller fibers branching off, similar to the radial morphology found in the central portion of native menisci (Figure 6.4).

Picrosirius red staining revealed that clamped menisci maintained native-like circumferential and radial morphologies at double the length scale of confocal analysis (Figure 6.7). Again, unclamped menisci demonstrated little improvement in organization with time in culture aside from compaction of the collagen, and no differences between circumferential and radial directions. Clamped menisci (both 10 and 20 mg/ml) developed circumferentially aligned fibers by 4 weeks, that appear to grow in size by 8 weeks similar to native menisci. In the radial direction, clamped menisci develop larger fibers with smaller randomly oriented fiber branches in the center of the construct similar to native fiber organization by 4 weeks. By 8 weeks, large radial fibers running perpendicularly across the scaffold were visible in both 10 and 20 mg/ml clamped menisci.

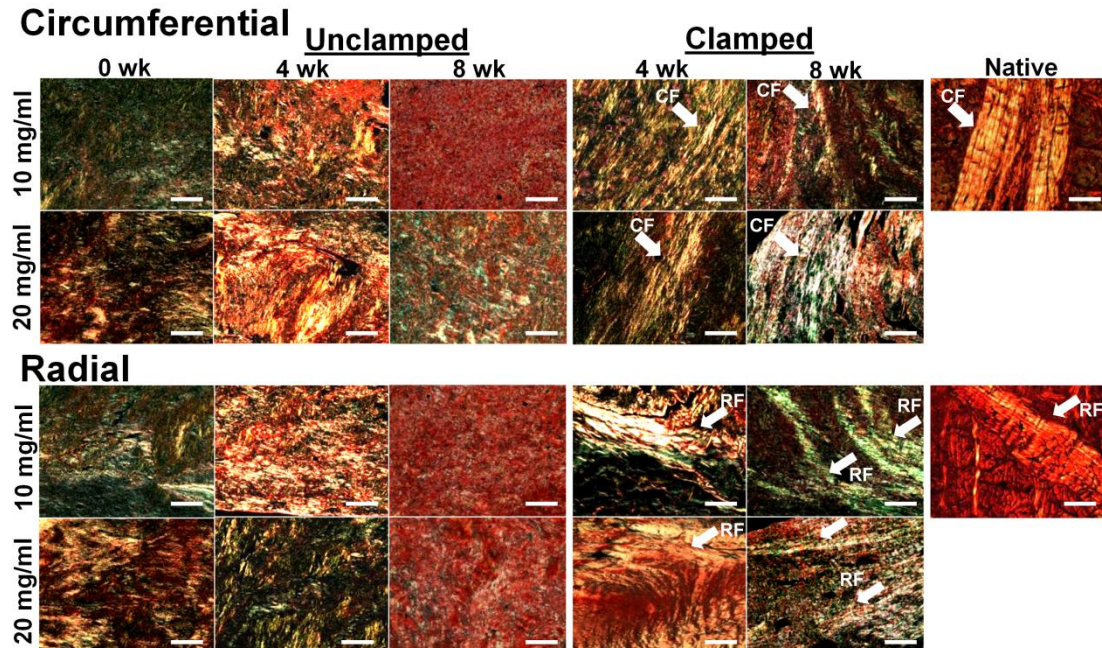


**Figure 6.7:** Circumferential and radial picosirius red samples imaged with polarized light. Clamped menisci develop native-like circumferentially aligned fibers and radial morphologies by 4 weeks, which further develop by 8 weeks. Arrows point to areas of developing circumferential fibers (CF), radial fibers (RF).

### Biochemical Analysis

Biochemical analysis demonstrated clamping had little effect on biochemical synthesis with both 10 and 20 mg/ml clamped menisci maintaining consistent GAG and collagen properties throughout culture (Figure 6.8). Clamped menisci did have a significant decrease in DNA content compared to unclamped menisci by 2 weeks, but then maintained that level of DNA throughout the remainder of culture (data not shown).

Both concentrations of clamped menisci maintained consistent GAG content throughout culture, while unclamped menisci had significant improvements in GAG beginning at 2 weeks (Figure 6.8). This increased accumulation of GAG in unclamped menisci could be due to a decrease in pore sizes resulting from the significant contraction of these scaffolds. Interestingly, when GAG content was normalized to DNA content both clamped and unclamped menisci had a similar

significant ~1.5 fold increase in GAG/DNA concentration by 8 weeks ( $p < 0.001$ ) (data not shown). This demonstrates, whether clamped or unclamped, the cells are stimulated to create the same amount of GAGs. Additionally, both clamped and unclamped menisci released the same amount of GAG to the media throughout culture (Figure 6.8). Interestingly, between the 2<sup>nd</sup> and 4<sup>th</sup> week all menisci had a similar increase in GAG release that was significantly higher from all other points throughout the 8 weeks of culture ( $p < 0.001$ ). After 4 weeks, all menisci decreased the release of GAG to levels below that recorded in the first two weeks (Figure 6.8).

As expected, both clamped and unclamped 20 mg/ml menisci had significantly higher collagen concentration than 10 mg/ml menisci. Unclamped menisci maintained relatively consistent collagen content throughout culture, with a slight decrease by 8 weeks. Both concentrations of clamped menisci however demonstrated a slight decrease in collagen concentration at 2 weeks and then a progressive increase in collagen with time. By 8 weeks, both 10 and 20 mg/ml clamped menisci had significantly more collagen content than their unclamped counterparts ( $p < 0.05$ ) (Figure 6.8). Again, there were no distinct differences in release of collagen/day to the media between clamped and unclamped menisci (Figure 6.8); however clamped menisci did accumulate less collagen overall in the media from 2-3 weeks on compared to unclamped menisci ( $p < 0.001$ ) (Data not shown).

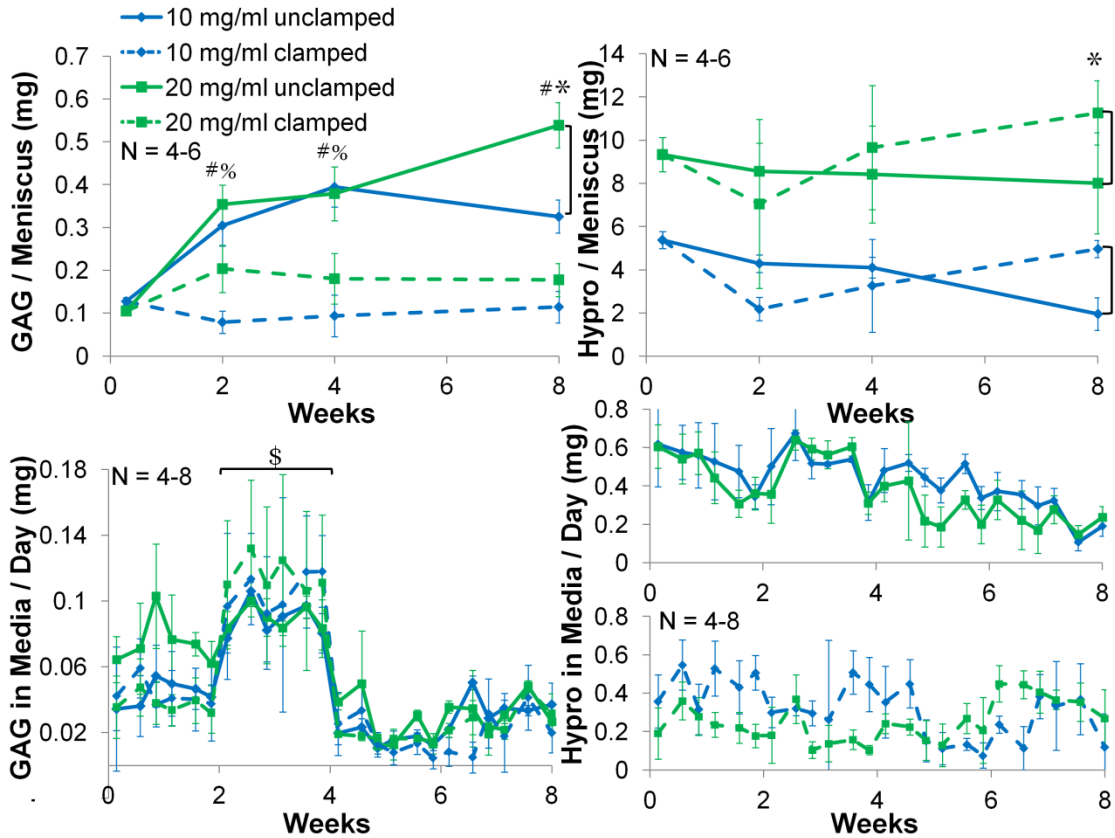


**Figure 6.8:** GAG and collagen content per meniscus (top row) and in media per day (bottom row). Significance between # clamped and unclamped, % 10 vs 20 mg/ml clamped menisci, \* bracket group, and \$ compared to all other data points ( $p < 0.05$ ).

### Mechanical Analysis

Mechanical analysis demonstrated clamped menisci had significant improvements in both the equilibrium and tensile moduli with time in culture. Further, both concentrations of clamped menisci developed anisotropic mechanical properties by 4 weeks (Figure 6.9).

All menisci significantly improved the equilibrium modulus throughout culture ( $p < 0.001$ ), with both concentrations of clamped menisci having significantly higher equilibrium moduli than unclamped menisci by 8 weeks ( $p < 0.001$ ). Further 20 mg/ml clamped menisci had a 17 fold increase in equilibrium modulus over the 8 weeks, resulting in a significantly higher modulus than the 10 mg/ml clamped menisci which

improved 14 fold over 8 weeks ( $p < 0.001$ ). Both concentrations of clamped menisci reached native equilibrium modulus values by 8 weeks <sup>42</sup>.

Tensile analysis demonstrated both concentrations of clamped menisci significantly improved the circumferential tensile modulus over the unclamped controls by 4 weeks ( $p < 0.05$ ), and further improved this difference through 8 weeks (Figure 6.9). By 8 weeks, 10 and 20 mg/ml clamped menisci improved their circumferential tensile properties 5 and 12 fold, respectively. Further, both 10 and 20 mg/ml clamped menisci significantly improved their radial tensile properties ~7 fold by 8 weeks of culture ( $p < 0.001$ )(Data not shown).

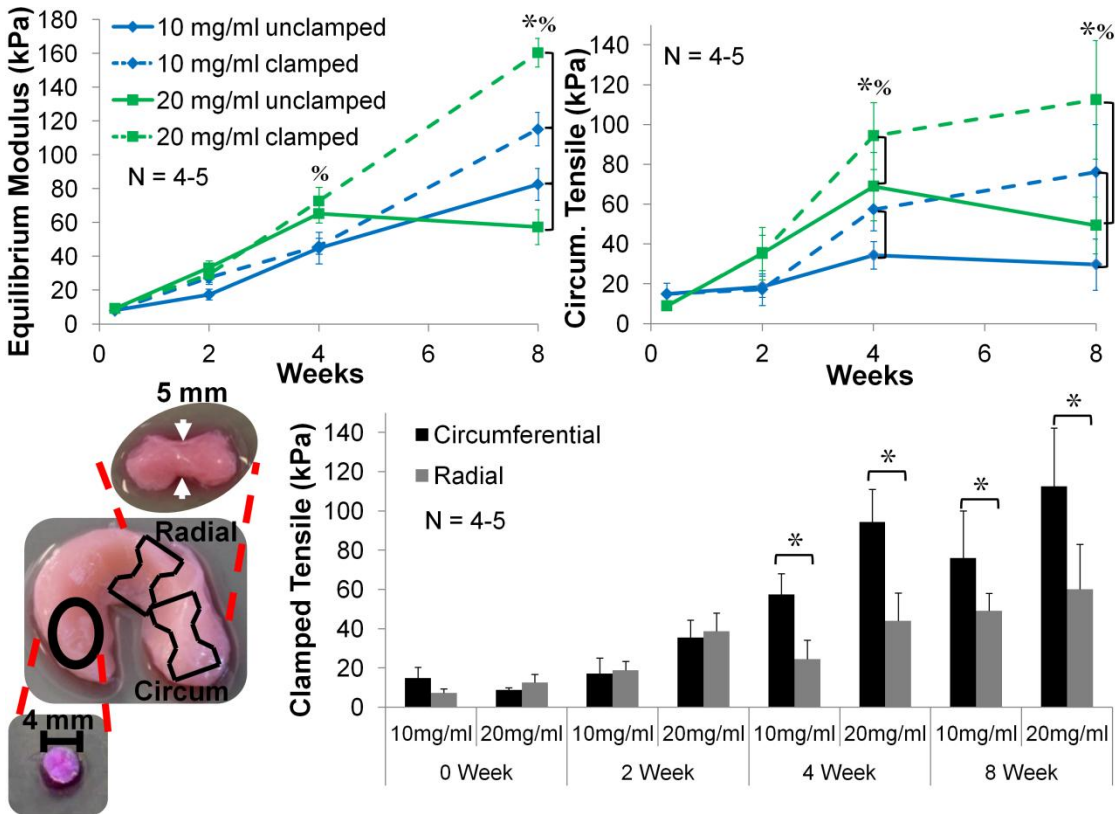


**Figure 6.9:** Equilibrium modulus, tensile modulus, clamped menisci tensile modulus in circumferential and radial direction, and depiction of mechanical samples. Clamped menisci develop superior properties to unclamped menisci by 8 weeks and develop anisotropic tensile properties by 4 weeks. Significance between % 10 vs 20 mg/ml clamped menisci and \* bracket group ( $p < 0.05$ )

Anisotropic tensile properties were analyzed for all menisci by testing both circumferential and radial dog-bone punches (Figure 6.9). Unclamped menisci maintained isotropic properties through 4 weeks of culture; however radial 8 week analysis was unable to be performed due to the significant decreases in unclamped scaffold size with contraction (data not shown). Clamped menisci (both 10 and 20 mg/ml) maintained isotropic properties through 2 weeks of culture, and from 4 weeks on developed anisotropic properties with ~2-3 fold differences between circumferential and radial directions ( $p < 0.001$ ). This ratio of anisotropy matches neonatal meniscus levels of anisotropy at 3 fold (circumferential modulus  $13 \pm 2.5$  MPa, radial modulus  $4.1 \pm 0.43$  MPa, data not shown)

### ***Discussion***

This study demonstrated long-term culture with horn anchored boundary conditions results in development of native-like aligned and sized circumferential fibers, native-like radial organization, increased collagen accumulation, and improved mechanical properties in high density collagen menisci. Clamped menisci (both 10 and 20 mg/ml concentrations) maintained their size and shape while developing circumferential fibers throughout the entire meniscus and radial morphologies that varied from the outer to the inner portion of the meniscus similar to native tissue<sup>4-7, 43</sup>. Further the clamped menisci organization was reflected in the development of anisotropic tensile properties 2-3 fold higher circumferentially compared to radially, similar to the level of anisotropy of neonatal and adult<sup>8,9</sup> menisci.

As discussed in the introduction, it has been well established that mechanical boundary constraints guide the alignment of fibers in cell-seeded low density (1-6mg/ml) collagen gels by harnessing the cellular traction forces along the greatest line of tension<sup>23-27</sup>. In this study horn-anchored boundary constraints were used to

restrict contraction circumferentially, in turn creating a circumferential hoop stress to encourage the alignment of cells and fibers. This study is the first to demonstrate mechanical boundary conditions can be used with meniscal fibrochondrocyte seeded high density collagen gels (10 and 20 mg/ml) to guide the alignment of fibers. Additionally, clamped menisci maintained their size and shape throughout culture, contrary to the contraction typically observed in low density boundary condition culture<sup>23-27</sup>. Contraction is known to decrease with increasing concentrations of collagen<sup>19, 23, 30</sup>, and thus the high concentration of collagen may be responsible for the lack of contraction in clamped menisci.

There appeared to be no adverse affect of collagen concentration on degree of organization. Ten and 20 mg/ml clamped menisci had similar levels of organization, with 20 mg/ml menisci producing larger diameter fibers and significantly better mechanical properties. Recently, doughnut-shaped boundary constraints were used with a scaffold free construct to develop meniscus-like scaffolds; however without collagen fibrils present from the beginning, collagen fiber development was limited<sup>22</sup>. In this study, self-assembled type I collagen fibrils are present within hours of gelling the collagen menisci, providing an infrastructure for cells to align and build on.

Confocal reflectance and picrosirius red staining revealed that horn-anchored boundary conditions guided the formation of circumferentially aligned collagen fibers and native-like radial morphologies by 4 weeks in cell-seeded high density collagen gels. Prolonged culture to 8 weeks resulted in further development of both circumferential and radial organization that mirrored native tissue at various length scales<sup>4-7, 43</sup>. There has been a growing trend in the literature of inclusion of circumferential fibers into meniscal scaffolds<sup>14, 18, 44-47</sup>; however all of these attempts are done by embedding synthetic fibers into the bulk of the scaffold or are single layers instead of entire meniscal scaffolds. These synthetic fibers are often larger

than natural collagen fibril diameters, impeding cellular interactions and penetration into scaffolds, which in turn slows matrix development. Further, often these fibers are mechanically stronger than surrounding bulk material resulting in fracture or extrusion of the fibrous element from the construct<sup>47</sup>. Here we have used mechanical constraints to guide cells to develop collagen fibrils into native sized fibers. Further, this is the first study to our knowledge, to demonstrate native-like radial development<sup>4-7, 43</sup>. By 4 weeks, clamped menisci developed structures resembling radial tie fibers along the peripheral edge of the scaffold and by 8 weeks larger native-like perpendicular fibers developed in the central portion of the scaffold.

Image analysis demonstrated the circumferential fibers developed in clamped menisci had the same alignment and size as native tissue. Collagen gels self-assemble into fibrils with diameters of 20-70 nm within a few hours of gelation<sup>48</sup>. This process is thought to be intrinsic to collagen gels due to the properties of collagen molecules; however the further development of these fibrils to fibers is primarily controlled by cells<sup>48</sup>. It has been reported cell-seeded collagen gels form collagen bundles with diameters of ~2-10  $\mu\text{m}$  and that concentration of the collagen gel has no effect on the fiber diameters<sup>30</sup>. Similarly, in this study, clamped and unclamped menisci developed 2-10  $\mu\text{m}$  fibers by 2 days with no difference between 10 and 20 mg/ml concentrations. Unclamped menisci maintained average fiber diameters of 10  $\mu\text{m}$  throughout culture, while clamped menisci significantly improved fiber diameters to ~30-40  $\mu\text{m}$  by 8 weeks. Interestingly, 20 mg/ml clamped menisci maintained larger diameter fibers throughout culture compared to 10 mg/ml clamped menisci. Clamped menisci fiber diameters at 8 weeks not only matched our native mean diameter calculations, but also match previously reported native meniscal fiber diameters (30-50  $\mu\text{m}$ )<sup>4, 7</sup>. Further, it has been reported native menisci (independent of species, age, or sex) organize fibrils into ~5-10  $\mu\text{m}$  core bundles which group together to form the

larger collagen fibers commonly seen in meniscal sections<sup>5</sup>. In this study, the smallest collagen fiber diameter in clamped menisci (found by using the entire span of the rotated FFT histogram instead of the mean span) was found to increase from 2  $\mu\text{m}$  to 10  $\mu\text{m}$  by 2 weeks of culture, and was maintained at 10  $\mu\text{m}$  through 8 weeks (data not shown). This data provides further support meniscal fibrochondrocytes may have an intrinsic ability to form specific meniscal tissue structures<sup>19, 49</sup>.

Image analysis also demonstrated clamped menisci fiber diameters grew the most between 4 and 8 weeks. It has been reported in both the tendon/ligament<sup>50, 51</sup> and meniscus<sup>52</sup> literature that when cells are grown on aligned matrices they produce not only more collagen, but more organized collagen. This study further supports this theory. Here, clamped menisci started out unorganized. By 4 weeks clamped menisci had circumferentially aligned fibers throughout the entire scaffold but little improvement in size of fibers. The largest growth in collagen fiber diameter was seen from 4 weeks on, once the meniscal fibrochondrocytes had aligned the fibers. Further, a similar trend was seen in collagen concentration. Clamped menisci (both 10 and 20 mg/ml) had a slight decrease in collagen content between 0 and 2 week. From 2 weeks on, when fibers are first observed to begin to align in clamped menisci, collagen content progressively increased to be significantly more than the unclamped counterparts at 8 weeks.

Overall, clamping had little effect on biochemical composition compared to organizational and mechanical improvements. Clamped menisci maintained similar GAG and DNA concentrations from 2 weeks on, and when normalized to DNA, clamped and unclamped menisci produced the same amount of GAG. Additionally, clamped and unclamped menisci had similar release patterns of GAG and collagen content throughout culture. Interestingly, all menisci had a significant increase in GAG release between 2 and 4 weeks, which may correspond to the significant

contraction or reorganization seen in unclamped and clamped menisci during this time period, respectively. Collagen concentration did increase by 8 weeks in clamped menisci, however this increase was minimal compared to the 3-4 fold increase in fiber size, 14-17 fold increase in equilibrium modulus, and 5-12 fold increase in tensile modulus. This suggests boundary conditions play a minimal role in regulating biochemical synthesis and primarily affects organization and mechanical properties. Further, it suggests the alignment, growth and organization of collagen fibers in clamped menisci was primarily responsible for the increased mechanical properties. This provides further support to the theory that organization of ECM rather than amount of ECM dictates the functional maturation of meniscal scaffolds<sup>52</sup> and demonstrates the importance of organization of engineered tissues.

Mechanical properties mirrored organization in clamped menisci not only in overall improvements but also in functional properties. From 4 weeks on, 10 and 20 mg/ml clamped menisci developed anisotropic properties, with the circumferential tensile modulus 2-3 times greater than the radial modulus, similar to the ratio of anisotropy in native menisci<sup>8, 9</sup>. This mirrored the development of distinctly different circumferential and radial organizations in clamped menisci from 4 weeks on. Further, at 8 weeks, when clamped menisci developed native-like organization, clamped menisci developed equilibrium moduli equal to native values (110-490 kPa)<sup>42</sup>. Interestingly, even though clamped menisci developed native sized and aligned fibers by 8 weeks, the tensile moduli remained orders of magnitudes below immature native values (circumferential 13-26 MPa<sup>53</sup>, radial 4 MPa). This suggests further development of collagen fibers is needed which could be facilitated by using mechanical or chemical stimulation to improve collagen fiber density and crosslinking.

We believe the horn-anchored boundary conditions, in addition to influencing circumferential cellular traction forces, might also mimic developmental processes to

result in native-like organization. As discussed earlier, it is well established mechanical boundary constraints guide the alignment of fibers in cell seeded collagen gels, however this would primarily account for the circumferential alignment of fibers in the clamped menisci, and provide little explanation for the native-like radial organization. During development, menisci start out as dense unorganized cellular structures. At 10 weeks the attachments to the tibial plateau are formed<sup>54</sup>. Then at 14 weeks spindle-shaped cells begin to align and form collagen bundles which grow in size with time and perpendicular radial fibers begin to appear<sup>55, 56</sup>. Further, throughout this entire process DNA concentration is continually decreasing<sup>55, 56</sup>. Similarly, in this study, clamped menisci start out as unorganized, homogeneous mixtures of cells and collagen. With time in culture DNA concentrations decrease as collagen fibers align and then grow in both the circumferential and radial direction. It has been demonstrated these early stages of development are intrinsically regulated, but later stages as collagen fibers mature require mechanical stimulation<sup>57</sup>. Thus additional mechanical stimulation may be needed to further develop these clamped collagen menisci.

This study demonstrates the use of biomimetic horn-anchored boundary conditions and long term culture to develop high density type I collagen menisci with organization, levels of tensile anisotropy, and equilibrium moduli that match native tissue. These are some of the most organized meniscal constructs developed to date and demonstrate great promise as either whole or partial meniscal replacements. However, GAG and collagen concentrations remain at ~5% and 15-20% that of native tissue, respectively and the tensile modulus 2 orders of magnitude lower than native tissue. Thus, although clamped collagen menisci are promising meniscal replacements, future work should focus on improving biochemical composition and tensile properties.

## REFERENCES

1. Messner K., Gao J. The menisci of the knee joint. Anatomical and functional characteristics, and a rationale for clinical treatment. *J Anat.***193 ( Pt 2)**:161. 1998.
2. Kale A., Kopuz C., Dikici F., Demir M.T., Corumlu U., Ince Y. Anatomic and arthroscopic study of the medial meniscal horns' insertions. *Knee Surg Sports Traumatol Arthrosc.***18**:754. 2010.
3. Kawamura S., Lotito K., Rodeo S.A. Biomechanics and healing response of the meniscus. *Oper Techn Sport Med.***11**:68. 2003.
4. Petersen W., Tillmann B. Collagenous fibril texture of the human knee joint menisci. *Anat Embryol.***197**:317. 1998.
5. Rattner J.B., Matyas J.R., Barclay L., Holowaychuk S., Sciore P., Lo I.K., et al. New understanding of the complex structure of knee menisci: implications for injury risk and repair potential for athletes. *Scand J Med Sci Sports.***21**:543. 2011.
6. Aspden R.M., Yarker Y.E., Hukins D.W. Collagen orientations in the meniscus of the knee joint. *J Anat.***140 ( Pt 3)**:371. 1985.
7. Kambic H.E., McDevitt C.A. Spatial organization of types I and II collagen in the canine meniscus. *J Orthop Res.***23**:142. 2005.
8. Makris E.A., Hadidi P., Athanasiou K.A. The knee meniscus: structure-function, pathophysiology, current repair techniques, and prospects for regeneration. *Biomaterials.***32**:7411. 2011.
9. Tissakht M., Ahmed A.M. Tensile stress-strain characteristics of the human meniscal material. *J Biomech.***28**:411. 1995.
10. Hasan J., Fisher J., Ingham E. Current strategies in meniscal regeneration. *J Biomed Mater Res B Appl Biomater.* 2013.
11. Khetia E.A., McKeon B.P. Meniscal allografts: biomechanics and techniques. *Sports Med Arthrosc.***15**:114. 2007.

12. Peters G., Wirth C.J. The current state of meniscal allograft transplantation and replacement. *Knee*.**10**:19. 2003.
13. McDermott I. Meniscal tears, repairs and replacement: their relevance to osteoarthritis of the knee. *Br J Sports Med*.**45**:292. 2011.
14. Balint E., Gatt C.J., Jr., Dunn M.G. Design and mechanical evaluation of a novel fiber-reinforced scaffold for meniscus replacement. *J Biomed Mater Res A*.**100**:195. 2012.
15. Ballyns J.J., Gleghorn J.P., Niebrzydowski V., Rawlinson J.J., Potter H.G., Maher S.A., et al. Image-guided tissue engineering of anatomically shaped implants via MRI and micro-CT using injection molding. *Tissue Eng Part A*.**14**:1195. 2008.
16. Huey D.J., Athanasiou K.A. Maturation growth of self-assembled, functional menisci as a result of TGF-beta1 and enzymatic chondroitinase-ABC stimulation. *Biomaterials*.**32**:2052. 2011.
17. Kon E., Chiari C., Marcacci M., Delcogliano M., Salter D.M., Martin I., et al. Tissue engineering for total meniscal substitution: animal study in sheep model. *Tissue Eng Part A*.**14**:1067. 2008.
18. Mandal B.B., Park S.H., Gil E.S., Kaplan D.L. Multilayered silk scaffolds for meniscus tissue engineering. *Biomaterials*.**32**:639. 2011.
19. Puetzer J.L., Bonassar L.J. High density type I collagen gels for tissue engineering of whole menisci. *Acta Biomater*.**9**:7787. 2013.
20. Tienen T.G., Heijkants R.G., de Groot J.H., Schouten A.J., Pennings A.J., Veth R.P., et al. Meniscal replacement in dogs. Tissue regeneration in two different materials with similar properties. *J Biomed Mater Res B Appl Biomater*.**76**:389. 2006.
21. Zur G., Linder-Ganz E., Elsner J.J., Shani J., Brenner O., Agar G., et al. Chondroprotective effects of a polycarbonate-urethane meniscal implant: histopathological results in a sheep model. *Knee Surg Sports Traumatol Arthrosc*.**19**:255. 2011.
22. Higashioka M.M., Chen J.A., Hu J.C., Athanasiou K.A. Building an anisotropic meniscus with zonal variations. *Tissue Eng Part A*.**20**:294. 2014.

23. Bell E., Ivarsson B., Merrill C. Production of a tissue-like structure by contraction of collagen lattices by human fibroblasts of different proliferative potential in vitro. *Proc Natl Acad Sci U S A*.**76**:1274. 1979.
24. Bowles R.D., Williams R.M., Zipfel W.R., Bonassar L.J. Self-assembly of aligned tissue-engineered annulus fibrosus and intervertebral disc composite via collagen gel contraction. *Tissue Eng Part A*.**16**:1339. 2010.
25. Costa K.D., Lee E.J., Holmes J.W. Creating alignment and anisotropy in engineered heart tissue: role of boundary conditions in a model three-dimensional culture system. *Tissue Eng*.**9**:567. 2003.
26. Grinnell F., Lamke C.R. Reorganization of hydrated collagen lattices by human skin fibroblasts. *J Cell Sci*.**66**:51. 1984.
27. Thomopoulos S., Fomovsky G.M., Holmes J.W. The development of structural and mechanical anisotropy in fibroblast populated collagen gels. *J Biomech Eng*.**127**:742. 2005.
28. Lee E.J., Holmes J.W., Costa K.D. Remodeling of engineered tissue anisotropy in response to altered loading conditions. *Ann Biomed Eng*.**36**:1322. 2008.
29. Gould R.A., Chin K., Santisakultarm T.P., Dropkin A., Richards J.M., Schaffer C.B., et al. Cyclic strain anisotropy regulates valvular interstitial cell phenotype and tissue remodeling in three-dimensional culture. *Acta Biomater*.**8**:1710. 2012.
30. Cross V.L., Zheng Y., Won Choi N., Verbridge S.S., Sutermaster B.A., Bonassar L.J., et al. Dense type I collagen matrices that support cellular remodeling and microfabrication for studies of tumor angiogenesis and vasculogenesis in vitro. *Biomaterials*.**31**:8596. 2010.
31. Ballyns J.J., Bonassar L.J. Dynamic compressive loading of image-guided tissue engineered meniscal constructs. *J Biomech*.**44**:509. 2011.
32. Puetzer J.L., Ballyns J.J., Bonassar L.J. The Effect of the Duration of Mechanical Stimulation and Post-Stimulation Culture on the Structure and Properties of Dynamically Compressed Tissue-Engineered Menisci. *Tissue Eng Part A*.**18**:1365. 2012.

33. Carey S.P., Kraning-Rush C.M., Williams R.M., Reinhart-King C.A. Biophysical control of invasive tumor cell behavior by extracellular matrix microarchitecture. *Biomaterials*.**33**:4157. 2012.
34. Mason B.N., Starchenko A., Williams R.M., Bonassar L.J., Reinhart-King C.A. Tuning three-dimensional collagen matrix stiffness independently of collagen concentration modulates endothelial cell behavior. *Acta Biomater*. 2012.
35. Chaudhuri S., Nguyen H., Rangayyan R.M., Walsh S., Frank C.B. A Fourier domain directional filtering method for analysis of collagen alignment in ligaments. *IEEE Trans Biomed Eng*.**34**:509. 1987.
36. Ng C.P., Hinz B., Swartz M.A. Interstitial fluid flow induces myofibroblast differentiation and collagen alignment in vitro. *J Cell Sci*.**118**:4731. 2005.
37. Kim Y.J., Sah R.L., Doong J.Y., Grodzinsky A.J. Fluorometric assay of DNA in cartilage explants using Hoechst 33258. *Anal Biochem*.**174**:168. 1988.
38. Enobakhare B.O., Bader D.L., Lee D.A. Quantification of sulfated glycosaminoglycans in chondrocyte/alginate cultures, by use of 1,9-dimethylmethylene blue. *Anal Biochem*.**243**:189. 1996.
39. Neuman R.E., Logan M.A. The determination of hydroxyproline. *J Biol Chem*.**184**:299. 1950.
40. Ballyns J.J., Wright T.M., Bonassar L.J. Effect of media mixing on ECM assembly and mechanical properties of anatomically-shaped tissue engineered meniscus. *Biomaterials*.**31**:6756. 2010.
41. Gleghorn J.P., Jones A.R., Flannery C.R., Bonassar L.J. Boundary mode frictional properties of engineered cartilaginous tissues. *Eur Cell Mater*.**14**:20. 2007.
42. Sweigart M.A., Zhu C.F., Burt D.M., DeHoll P.D., Agrawal C.M., Clanton T.O., et al. Intraspecies and interspecies comparison of the compressive properties of the medial meniscus. *Ann Biomed Eng*.**32**:1569. 2004.
43. Vanderploeg E.J., Wilson C.G., Imler S.M., Ling C.H., Levenston M.E. Regional variations in the distribution and colocalization of extracellular matrix proteins in the juvenile bovine meniscus. *J Anat*.**221**:174. 2012.

44. Elsner J.J., Portnoy S., Zur G., Guilak F., Shterling A., Linder-Ganz E. Design of a free-floating polycarbonate-urethane meniscal implant using finite element modeling and experimental validation. *J Biomech Eng.***132**:095001. 2010.
45. Fisher M.B., Henning E.A., Soegaard N., Esterhai J.L., Mauck R.L. Organized nanofibrous scaffolds that mimic the macroscopic and microscopic architecture of the knee meniscus. *Acta Biomater.***9**:4496. 2013.
46. Holloway J.L., Lowman A.M., Palmese G.R. Mechanical evaluation of poly(vinyl alcohol)-based fibrous composites as biomaterials for meniscal tissue replacement. *Acta Biomater.***6**:4716. 2010.
47. Kelly B.T., Robertson W., Potter H.G., Deng X.H., Turner A.S., Lyman S., et al. Hydrogel meniscal replacement in the sheep knee: preliminary evaluation of chondroprotective effects. *Am J Sports Med.***35**:43. 2007.
48. Kadler K.E., Holmes D.F., Trotter J.A., Chapman J.A. Collagen fibril formation. *Biochem J.***316 ( Pt 1)**:1. 1996.
49. Ibarra C., Jannetta C., Vacanti C.A., Cao Y., Kim T.H., Upton J., et al. Tissue engineered meniscus: a potential new alternative to allogeneic meniscus transplantation. *Transplant Proc.***29**:986. 1997.
50. Lee C.H., Shin H.J., Cho I.H., Kang Y.M., Kim I.A., Park K.D., et al. Nanofiber alignment and direction of mechanical strain affect the ECM production of human ACL fibroblast. *Biomaterials.***26**:1261. 2005.
51. Wang J.H., Jia F., Gilbert T.W., Woo S.L. Cell orientation determines the alignment of cell-produced collagenous matrix. *J Biomech.***36**:97. 2003.
52. Baker B.M., Mauck R.L. The effect of nanofiber alignment on the maturation of engineered meniscus constructs. *Biomaterials.***28**:1967. 2007.
53. Eleswarapu S.V., Responde D.J., Athanasiou K.A. Tensile properties, collagen content, and crosslinks in connective tissues of the immature knee joint. *PLoS One.***6**:e26178. 2011.
54. Merida-Velasco J.A., Sanchez-Montesinos I., Espin-Ferra J., Rodriguez-Vazquez J.F., Merida-Velasco J.R., Jimenez-Collado J. Development of the human knee joint. *Anat Rec.***248**:269. 1997.

55. Clark C.R., Ogden J.A. Development of the menisci of the human knee joint. Morphological changes and their potential role in childhood meniscal injury. *J Bone Joint Surg Am.***65**:538. 1983.
56. Fukazawa I., Hatta T., Uchio Y., Otani H. Development of the meniscus of the knee joint in human fetuses. *Congenit Anom (Kyoto).***49**:27. 2009.
57. Mikic B., Johnson T.L., Chhabra A.B., Schalet B.J., Wong M., Hunziker E.B. Differential effects of embryonic immobilization on the development of fibrocartilaginous skeletal elements. *J Rehabil Res Dev.***37**:127. 2000.

## CHAPTER 7

### **Effects of Physiologic Loading Patterns on the Development of Tissue Engineered Menisci<sup>\*</sup>**

#### ***Abstract***

This study investigates the use of physiologically distributed load to develop high density type I collagen menisci seeded with bovine fibrochondrocytes. After 4 weeks of loading, menisci matched native organization, tensile anisotropy ratios, and equilibrium moduli. Loaded menisci significantly improved GAG accumulation 200-250%, collagen accumulation 40-55%, equilibrium modulus 1000-1800%, and tensile moduli 500-1200% (radial and circumferential), demonstrating native-like compressive-tensile loading can enhance all fibrocartilage properties. Further, this study demonstrates that local changes in mechanical environment drive heterogeneous tissue synthesis and organization. These are some of the most organized meniscal scaffolds developed to date and demonstrate great promise as meniscal replacements.

#### ***Introduction***

Menisci are dense wedge-shaped fibrocartilaginous crescents in the knee that act primarily to distribute compressive loads over the tibial plateau and help stabilize the knee<sup>1,2</sup>. During each gait cycle, the menisci are exposed to a compressive load from the femoral condyles. Due to the wedge shape of the meniscus, this compressive load pushes the meniscus outward, however firm ligament attachments at the horns hold the meniscus in place and the compressive load is primarily translated into a

---

<sup>\*</sup> This chapter is in preparation for publication: Puetzer JL, Bonassar LJ. Effects of Physiologic Loading Patterns on the Development of Tissue Engineered Menisci. In preparation

circumferential tensile-hoop stress<sup>1, 3</sup>. Thus the compressive vertical force is redirected into a lateral tensile force and spread across the tibial plateau.

The meniscus is able to withstand and distribute the complex loads of the knee primarily due to its organization<sup>4, 5</sup>. Native menisci consist largely of circumferentially aligned collagen bundles in the outer two-thirds of the tissue, anchored by a small number of perpendicular radial tie fibers<sup>6-9</sup>. This organization results in anisotropic tensile properties essential to the function of the tissue which are 3-10 times greater circumferentially compared to the radial direction<sup>6, 7, 10, 11</sup>.

A tear that disrupts this organization decreases the functional capacity of the meniscus and results in pain, mechanical instability and degradation of surrounding cartilage leading to osteoarthritis<sup>2</sup>. In the United States, meniscal repair is one of the most common orthopaedic surgical procedures, resulting in over 1 million surgeries a year<sup>1, 2, 12</sup>. Currently, meniscectomy and replacement with cadaveric allograft is the only treatment option for large irreparable tears that require whole meniscal replacement<sup>1, 2</sup>. A tissue engineered substitute is a promising alternative to allografts and although many attempts have been made to engineer a meniscus<sup>13-21</sup>, none have been successfully implemented in the clinic. These attempts often lack the proper collagen fiber organization, anisotropic mechanical properties, or biochemical properties of native tissue. Recently, we developed injection molded high density collagen menisci with native-like organization and tensile anisotropy by mimicking native horn-anchoring; however further development of biochemical and mechanical properties are needed for these constructs to be successful meniscal replacements(Chapter 6).

Mechanical conditioning has been well established to enhance the *in vitro* development of various types of engineered cartilage(Chapter 2). Specifically, dynamic compression<sup>22-24</sup>, tensile stretching<sup>25, 26</sup>, media mixing<sup>27, 28</sup>, hydrostatic

pressure<sup>29, 30</sup>, and perfusion<sup>23</sup> have all been applied to condition engineered meniscal tissue, often resulting in improved biochemical and mechanical properties. However, this conditioning is unable to mimic the complex compressive-tensile loading environment of the meniscus. Traditionally, compressive loading of engineered cartilage is chondrogenic resulting in increased GAG synthesis and equilibrium modulus, while tensile loading is thought to be fibrogenic, resulting in increased collagen synthesis and tensile properties (Chapter 2)<sup>22, 25, 31</sup>. Each form of loading does not fully enhance all the meniscal fibrocartilage properties. A recent study found that combining tensile and compressive loading improved GAG accumulation, collagen accumulation, compressive properties and tensile properties of scaffold free constructs, however these constructs lack appropriate native collagen organization<sup>32</sup>.

Cell-seeded collagen gels are known to align when exposed to anisotropic mechanical stimulation, increasing the anisotropic mechanical properties of the gel<sup>33-37</sup>. However, the effect of mechanical simulation on fibrochondrocyte seeded gels or high density collagen gels has not been studied.

In this study, we believed that by combining horn-anchored boundary conditions (Chapter 6) with mechanical compression we could create a more physiological bioreactor and further develop the organization, biochemical and mechanical properties of high density collagen menisci. The objectives of this study were to 1) develop a bioreactor to better mimics the complex compressive-tensile loading of native menisci; 2) to investigate the effect of such loading on the organization, composition and mechanical properties of engineered menisci; and 3) determine how local tensile and compressive loads drive differential matrix synthesis. We hypothesize that increased loading of collagen menisci will result in native-like organization, improved composition and anisotropic mechanical properties, and that

local changes in the mechanical environment will drive heterogeneous tissue formation.

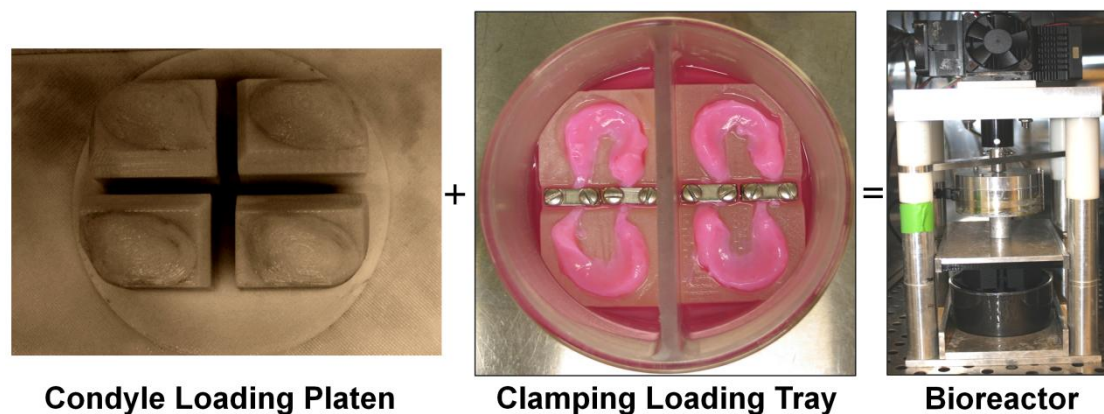


**Figure 7.1:** Custom designed bioreactor with condyle shaped loading platen generated from ovine MRIs and clamping loading tray that mimics native horn attachments. Condyle loading platen compressively loads meniscal scaffolds forcing them outward, as clamping loading tray holds extensions at the horns in place

## ***Materials and Methods***

### **Bioreactor Design and Fabrication**

The loading platen and tray of our custom compressive bioreactor<sup>22, 24</sup> were redesigned to apply a more physiological compressive-tensile loading pattern (Figure 7.1). Condyle-shaped loading platens were designed using the same ovine magnetic resonance image (MRI) used previously to create meniscal molds<sup>14, 22, 38</sup>. Briefly, MRI data sets in DICOM format were visualized, the medial condyle was rendered into a point cloud (SliceOmatic v4.3, Canada), converted to a solid object (Geomagic Studio 4.0, NC), and imported into Solidworks (Concord, MA) to design loading platens that match the surface geometry of the medial condyle. Loading trays were designed to mimic *in vivo* horn attachments as previously described (Chapter 6). Briefly, the tray has a trough at the base of the meniscal scaffolds that the 12mm extensions at the horns of the scaffold lay in. Clamps made of stainless-steel infused with bronze

(Shapeways, NY) screw down over the extensions, clamping them in place throughout culture. Loading platens and trays were printed out of acrylonitrile butadiene styrene (ABS) plastic via a Stratasys 3D printer (Eden Prairie, MN).

### Finite Element Analysis

Finite element (FE) analysis was performed to determine whether the bioreactor would apply physiological loading patterns and to determine a proper loading regime for conditioning constructs. An established linear poroelastic FE model<sup>22, 39</sup> was adapted to create a contact model between the loading platen and meniscus construct using COMSOL MULTIPHYSICS software (COMSOL, Burlington, MA). The meniscus and loading platen were meshed into 70,662 tetrahedral elements (ranging in size from 0.05-30mm and maximal element growth rate of 1.4) resulting in 81,151 degrees of freedom (Figure 7.2A). Convergence analysis was performed to verify there was little change with further decreasing mesh size.

The loading platen was modeled as a rigid plastic with a Young's Modulus of  $2.6 \times 10^6$  kPa, solid density of  $1050 \text{ kg/m}^3$ , and Poisson's ratio of 0.35 based off printed ABS plastic properties. The meniscus was modeled as a linear isotropic poroelastic 20 mg/ml high density collagen gel with Young's Modulus of 10 kPa, solid density of  $1240 \text{ kg/m}^3$ , a Poisson's ratio of 0.2, porosity 96.2%, and permeability of  $1 \times 10^{-14} \text{ m}^2$ . The meniscus was simulated to be fully hydrated with the fluid having an assumed viscosity of 0.001 Pa s and a density of  $1000 \text{ kg/m}^3$ . The scaffold properties were based on values from the literature and previous experiments with high density collagen gels<sup>18, 22, 39, 40</sup>. The meniscal scaffold was modeled as an isotropic gel in order to understand how the load was affecting the collagen gels at the beginning of the experiment when no organization was present.

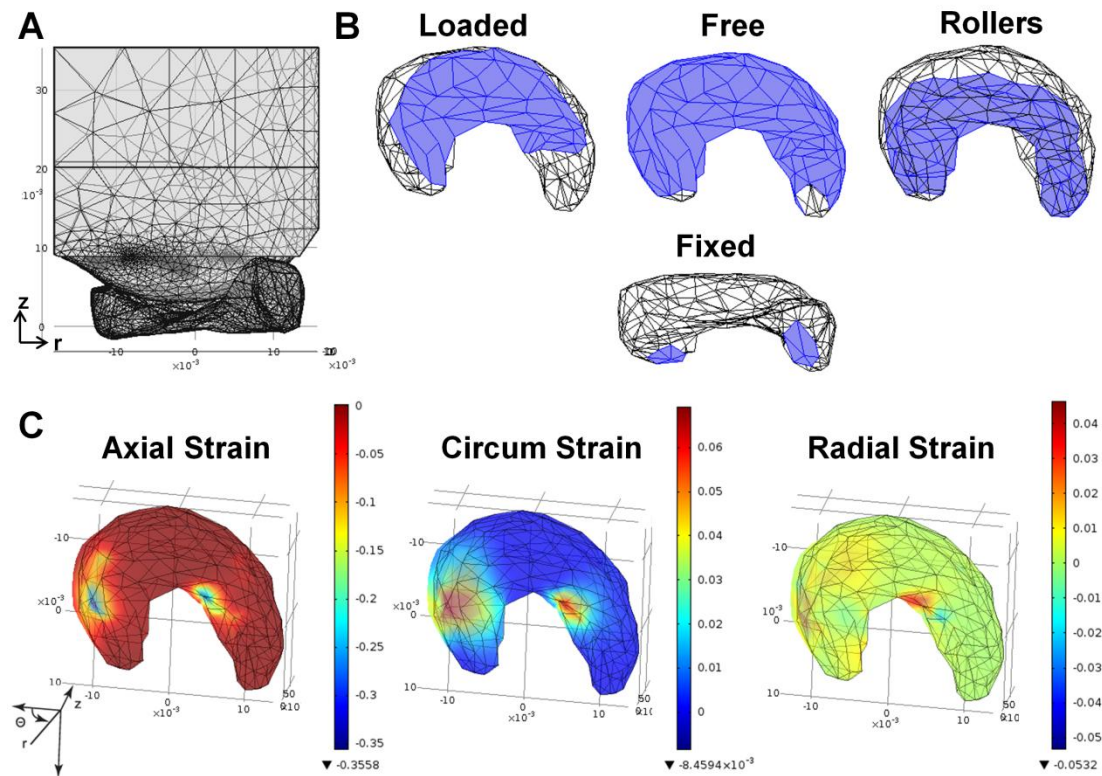


**Figure 7.2:** A) Meshed contact model of loading platen and meniscal construct for linear poroelastic finite element analysis, B) Boundary conditions for FE model. Loaded surface of contact-pair with loading platen, concave surface and faces of meniscus were free for fluid flow and displacement, bottom of the meniscus was fixed axial and allowed to roll in the circumferential and radial directions, and fixed at the horns where extensions would attach. C) Axial, circumferential, and radial volume strain maps for maximal displacement ( $1250\mu\text{m}$ ) of high load regime.

Loading was simulated by moving the loading platen in the axial direction according to the bioreactor sinusoidal loading pattern ( $\text{Amplitude} * (\cos(2\pi t) - 1)$ ) in a time-dependent model. Loading was assumed to be frictionless. The penetration factor used for contact between loading platen and the meniscus was an iterative formula that gradually increases with each time step and is based on the ratio of meniscal stiffness to minimum element size. By decreasing mesh size, degree of penetration was minimized and there was no penetration between surfaces for the final mesh size.

Boundary conditions of the meniscal construct allowed displacement and fluid flow to occur freely on the concave loading surface and along the free faces (Figure 7.2B). The horns of the menisci were fixed where the extensions would attach, and the bottom of the meniscus was fixed axially with rollers in the radial and circumferential direction.

Surface areas of greatest strain across the horns and a similarly sized area from the back of the meniscus (Figure 7.3A) were analyzed with increasing load amplitude simulations to determine the local distribution of directional and principal strains. Percent strain data is report when the loading platen is at maximal displacement ( $t=0.5\text{sec}$ ). Based on this FE analysis a high and low loading regime was chosen that applied ~10% and 5% compressive strain to the horns, respectively. The high load had an amplitude of  $625\mu\text{m}$ , with maximum imposed displacement of  $1250\mu\text{m}$ , and the low load had an amplitude of  $415\mu\text{m}$ , with a maximum displacement of  $830\mu\text{m}$ . These imposed compressive strains are within the range of strains used for other dynamic compressive studies<sup>22, 41-44</sup>. Further 10% compressive strain has been reported to be the most successful loading regime (Chapter 2) and matches the reported 10% compressive strain for native menisci<sup>45-47</sup>.

### Meniscus Fabrication and Dynamic Loading

Meniscal constructs were fabricated as previously described<sup>18</sup>. Briefly, Type I collagen was extracted from Sprague-Dawley rat tails (Pel-Freez Biologicals, Roger, AZ) and reconstituted to 30 mg/ml using previously established techniques<sup>18, 40, 48</sup>. Bovine meniscal fibrochondrocytes were isolated from 1-3 day old calves using collagenase digestion. The collagen solution was then mixed with appropriate volumes of 10x phosphate-buffered saline (PBS), 1x PBS, and 1N NaOH to begin the gelling process<sup>40, 48</sup> and then immediately mixed with the cell solution. The

collagen/cell solution was then injected into ovine meniscal molds(Chapter 6)<sup>14</sup> and incubated for 1 hour at 37°C to create a total of 30 high density 20 mg/ml collagen menisci at 25x10<sup>6</sup> cells/ml. On day 1 all menisci were clamped at the extensions as previously described (Chapter 6), and on day 4 the menisci were sections into static (clamped) culture, high load, or low load groups for up to 4 weeks. Menisci were cultured in media composed of DMEM, 10% FBS, 100 µg/mL penicillin, 100 µg/mL streptomycin, 0.1 mM non-essential amino acids, 50 µg/mL ascorbate, and 0.4 mM L-proline, changed every 2-3 days after loading.

Menisci were loaded twice for an hour with a sinusoidal displacement control 1 Hz waveform, 3 times a week, with an hour of rest between cycles as previously described<sup>22, 24</sup>. The low load group was exposed to an offset and amplitude of 415µm, and the high load group had an offset and amplitude of 625 µm, resulting in ~5 and 10% compressive strain across the horns. To validate FE model predictions, the bioreactor was outfitted with a iLoad TR Digital 10lb Load Cell (loadstar Sensors, Fermont, CA) to measure loads applied to the scaffolds throughout culture. FE predicted loads were compared to load cell data obtained during the first 5 seconds after 5 minutes of loading. In previous studies<sup>22, 24</sup>, as well at this one, very little change in peak to peak load was observed throughout the hour of loading and between the two hours of loading, indicating that the system reaches steady state within the first 5 minutes.

### Post Culture Analysis

At 0, 2 and 4 weeks 4-6 meniscal scaffolds from each group were removed from culture, examined grossly, weighted, photographed and sectioned for analysis of organization, composition and mechanical properties as previously described (Chapter 6)<sup>18</sup>. Briefly, gross construct size and mass was determined by area

calculations of serial photographs taken throughout culture using ImageJ software (NIH, Bethesda, MD) and percent mass calculations determined by comparing total weight of constructs at the completion of culture.

Cross-sections from throughout the meniscal scaffolds in both the circumferential and radial direction were fixed in 10% buffered formalin and stored in 70% ethanol for confocal and histological analysis of collagen and cellular organization. Confocal analysis was performed with a Zeiss 710 confocal microscope at 25x and 40x magnification as previously described (Chapter 6)<sup>18, 48-50</sup>. A 488 nm laser was split between confocal reflectance at 475-510nm to visual collagen and fluorescence at 500-580nm to capture auto-fluorescent cells. 4-8 circumferential confocal images from 4-6 cross-sections throughout multiple menisci (total 16-48 images per treatment group) were analyzed using a previously established (Chapter 6) custom fast Fourier transform (FFT)-based MATLAB code to determine the degree of alignment and mean fiber diameter. Briefly, an initial 2D FFT is performed to determine the maximum angle of alignment and the alignment index (a measure of the degree of alignment where 1 is unaligned and 4.5 is completely aligned)<sup>48, 51, 52</sup>(Chapter 6). The image is then rotated so the maximum angle of alignment is at 90° and the majority of the fibers are vertical. Another FFT is performed. The span of the FFT is averaged and then converted from cycles to microns to determine an average fiber diameter. Cross-sections were further dehydrated, embedded into paraffin blocks, sectioned, stained with picrosirius red, and imaged with polarized light on a Nikon Eclipse TE2000-S microscope to investigate a larger length-scale of collagen organization.

Mechanical properties were determine as previously described using an Enduratec ElectroForc 3200 System (Bose, Eden Prairie, MN)(Chapter 6)<sup>18, 27, 53</sup>. Briefly, two 4 mm diameter plugs from each meniscus were tested via stress relaxation tests in confined compression by imposing 10x50µm steps and the

resulting load was fit to a poroelastic model using a custom MATLAB program<sup>53</sup> to determine the equilibrium modulus. To determine directional tensile moduli, radial and circumferential dogbone punches were tested at a strain rate of 0.75%/s, assuming quasi-static load and ensuring failure occurred between the grips. The reported modulus is the slope of the linear region of the stress-strain curve.

From each meniscus, samples from the horns, back, and extensions were weighed wet (WW), frozen, lyophilized, weighed dry (DW), and digested in papain for biochemical analysis as previously described<sup>14, 24</sup>. DNA, glycosaminoglycan (GAG) and collagen content were determined via the Hoechst DNA assay<sup>54</sup>, a modified 1,9-dimethylmethylene blue (DMMB) assay at pH 1.5<sup>55</sup>, and a hydroxyproline assay<sup>56</sup>, respectively. Media samples collected every 2-3 days were analyzed with the same assays to track biochemical release to the media.

### Statistics

All image analysis, biochemical and mechanical data were analyzed by 2-way ANOVA using Tukey's t-test for post-hoc analysis and all correlation data were analyzed by Pearson's correlation. For both tests  $p < 0.05$  was threshold for statistical significance. All data expressed as mean $\pm$ SD.

## **Results**

### FE Model

FE strain maps demonstrated contact area and axial compressive strains were concentrated across the horns similar to the loading pattern observed in native menisci when the leg is in full extension (Figure 7.2C)<sup>47</sup>. As total displacement of the loading platen increased, the horns were dominated by axial compressive strain, with some strain being translated to tensile circumferential and radial strains. Little to no

contact was applied to the back of the meniscus throughout displacement, and thus tensile strains dominated (Figure 7.3A). Using the FE model, integration of von Mises stress over the surface of the meniscus yielded a maximum load of 0.3N and 0.09N for high and low loads, respectively. This predicted load was significantly correlated with data from the bioreactor load cell ( $p < 0.001$ ), validating the FE model (Figure 7.3B).

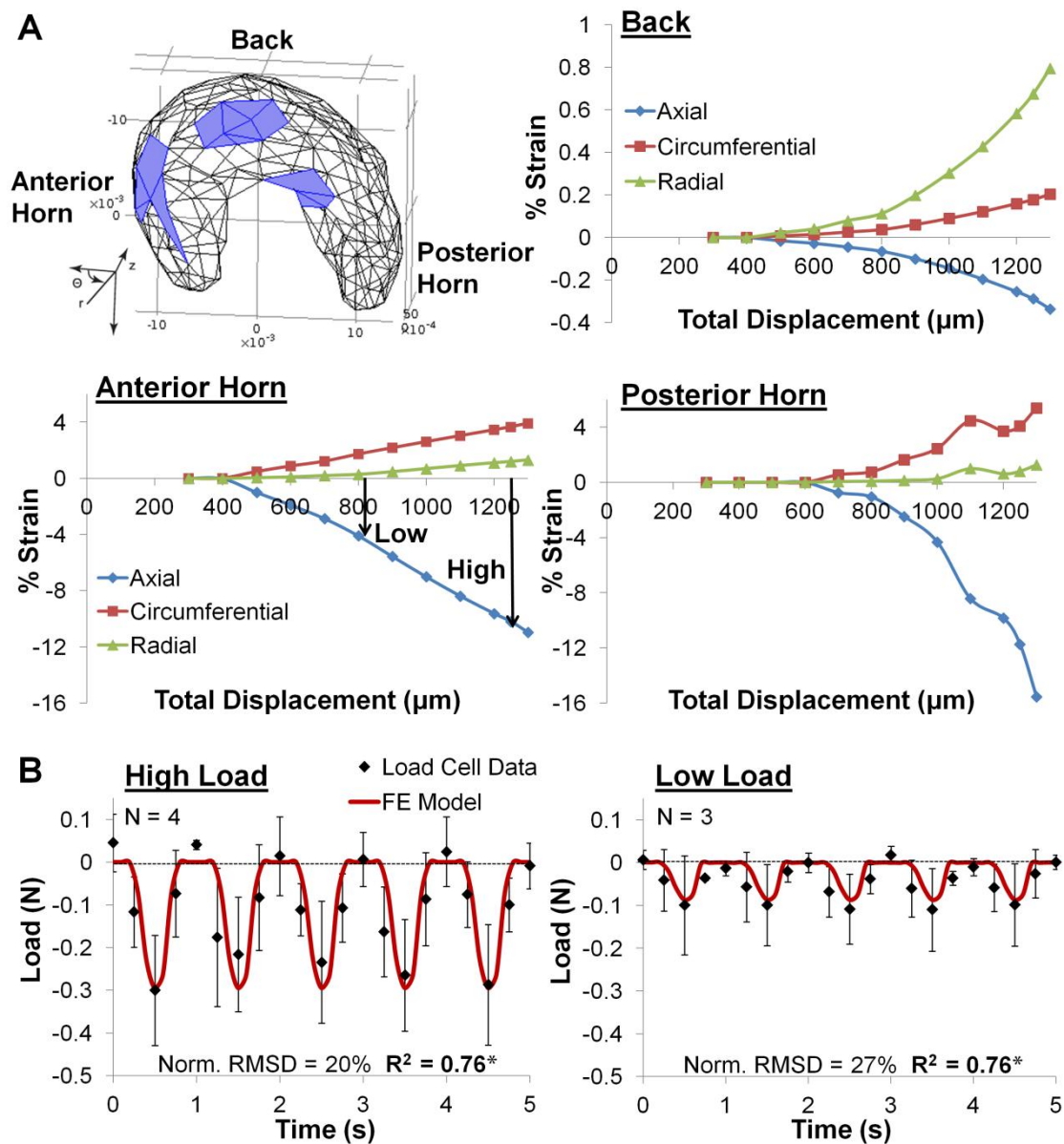


**Figure 7.3:** A) Depiction of areas chosen for back, anterior and posterior horn FE analysis and distribution of axial, circumferential and radial strains for locations as amplitude of sinusoidal loading regime is increased. Strains reported at maximal displacement of loading platen when  $t=0.5$  seconds. From this analysis a high and low loading regime was determine for conditioning constructs that corresponded to  $\sim 10$  and  $5\%$  compressive strain across the horns (depicted on anterior horn graph). B) FE model validation comparing data obtained from the bioreactor load cell during the first 5 sec after 5 mins of loading and the FE model predicted loads across the meniscus. \*Significance determined by Pearson's correlation ( $p < 0.001$ )

Construct Appearance and Shape Fidelity

Gross inspection revealed all menisci maintained size and shape for the duration of culture, with no detrimental effect from loading (Supplemental Figure 7.S1). This was further confirmed by percent area calculations which demonstrated all menisci maintained 100% area throughout culture. Interestingly, mass of low load and static menisci dropped to 90-95% of original mass from two weeks on, while mass of high load menisci increased to 105% (Supplemental Figure 7.S1).

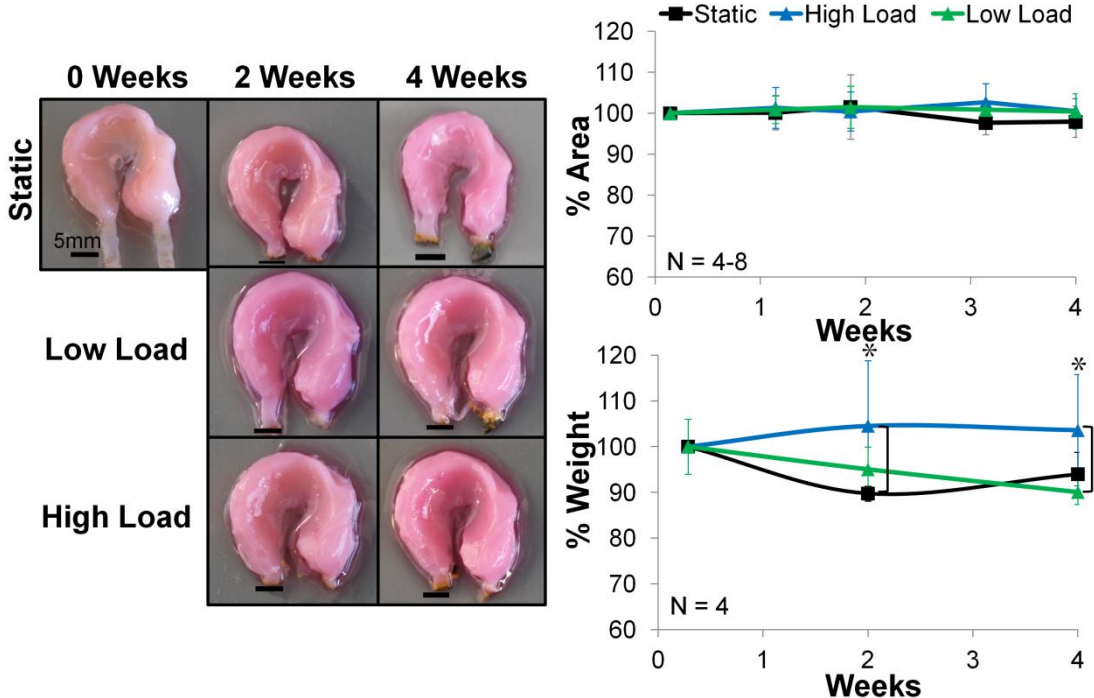


**Figure 7.S1:** A) Photographs of constructs, B) percent area and percent mass of constructs throughout culture. All menisci maintained size and shape throughout culture. Bar=5mm. \*Significance compared to bracketed group (p<0.05)

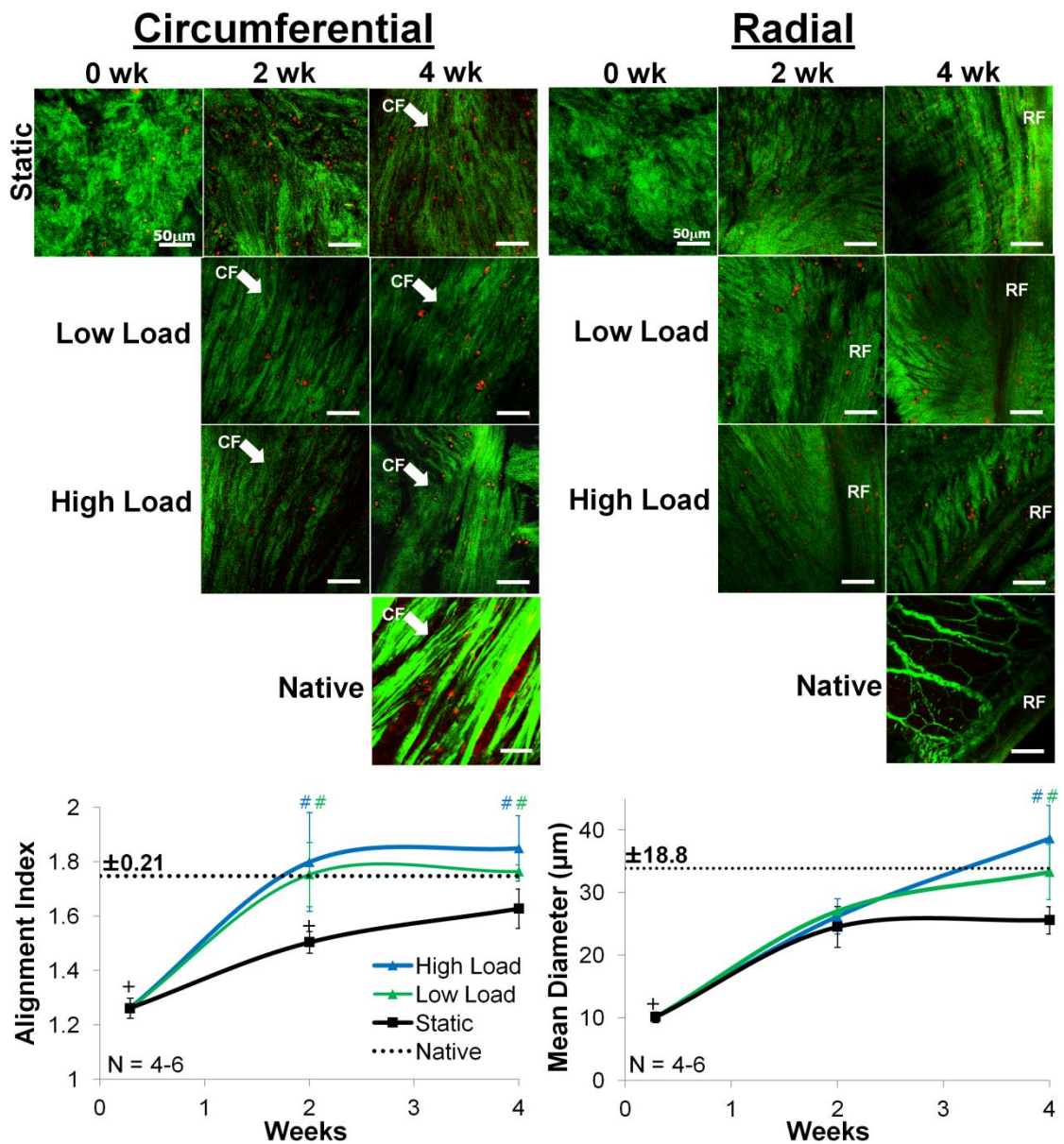


**Figure 7.4:** Circumferential and radial confocal reflectance analysis (green=collagen, red=cells), and circumferential image analysis for alignment index (1 unorganized, 4.5 organized) and mean fiber diameter in engineered and native menisci. Loaded menisci match native alignment and fiber diameter by 2 weeks. CF = circumferential fibers, RF = radial fibers. Significance compared to + native and # static menisci ( $p < 0.05$ )

### Collagen Organization

Confocal reflectance microscopy, image analysis, and picrosirius red staining demonstrated loading accelerated the development of native-like sized and aligned circumferential fibers and radial morphologies over a range of length scales (Figure 7.4-7.7). Confocal reflectance microscopy revealed static menisci develop aligned collagen fibers throughout the entire meniscus and native-like radial morphologies by 4 weeks of culture. Loading (both high and low) accelerated this organization, with circumferential alignment throughout the meniscus and native-like radial fiber development as of 2 weeks. Loading to 4 weeks resulted in further development, with high load menisci appearing the most developed and similar to native menisci (Figure 7.4). Image analysis of circumferential confocal sections from throughout the meniscus confirmed these observations, with both loaded groups having significant improvements in alignment over static menisci ( $p < 0.001$ ) by 2 weeks to match native alignment. Further, both loaded groups improved mean fiber diameter 3-4 fold by 4 weeks, again matching native menisci and having significantly larger fibers than static culture ( $p < 0.02$ , Figure 7.4).

Picrosirius red staining demonstrated that loaded menisci maintained accelerated development over static menisci at double the length scale of confocal analysis (Figure 7.5). By 2 weeks, both loaded groups developed circumferentially aligned fibers and perpendicular radial fibers, similar to native menisci. Static menisci first developed these morphologies by 4 weeks.

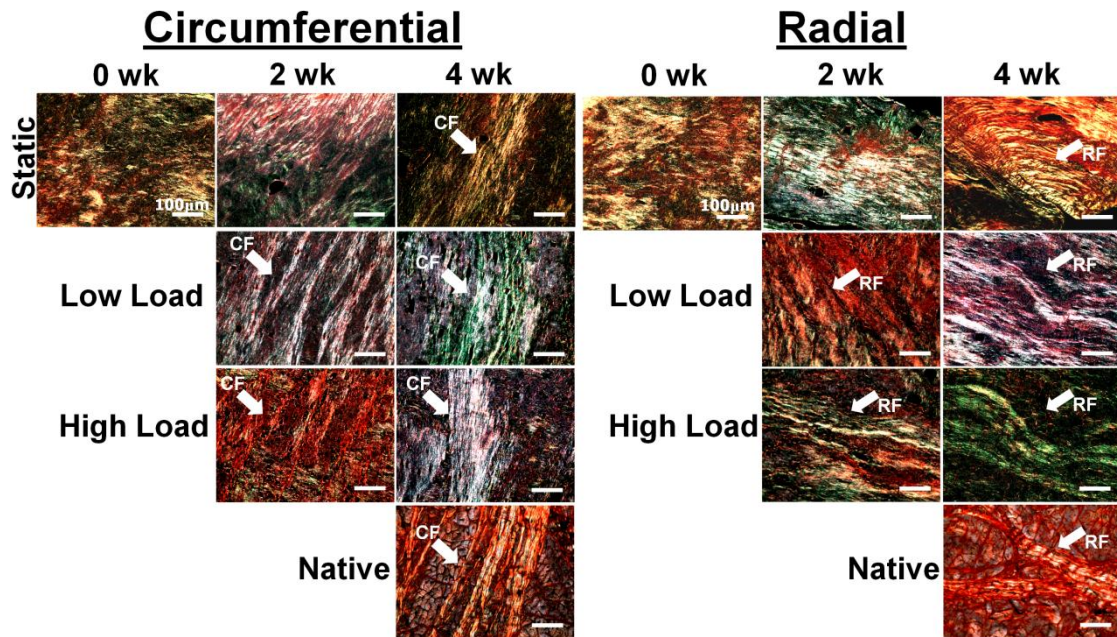


**Figure 7.5:** Circumferential and radial picrosirius red stained samples imaged with polarized light. Loaded menisci have accelerated development of native-like organization. Arrows point to areas of developing circumferential fibers (CF), and radial fibers (RF)

Confocal reflectance was further used to evaluate spatial organization and cellular morphology along fibers in high and low load menisci. Spatial organization in directly loaded cross-sections revealed from 2 weeks on both loaded groups developed circumferentially aligned fibers in the outer 2/3 of the meniscus, similar to native menisci (Figure 7.6). In the inner portion of the meniscus, where compressive loading was higher, a more cartilaginous development was present, with randomly distributed cells within a dense collagen matrix (Figure 7.6). High magnification analysis demonstrated cells maintained a round phenotype along the outside of circumferential collagen fibers, similar to native tissue (Figure 7.7). Interestingly, in radial fibers cells appear elongated and aligned along smaller fibers within large collagen bundles. However, in the surrounding arborized perpendicular fibers the cells returned to a rounded phenotype located along the outside of fibers.

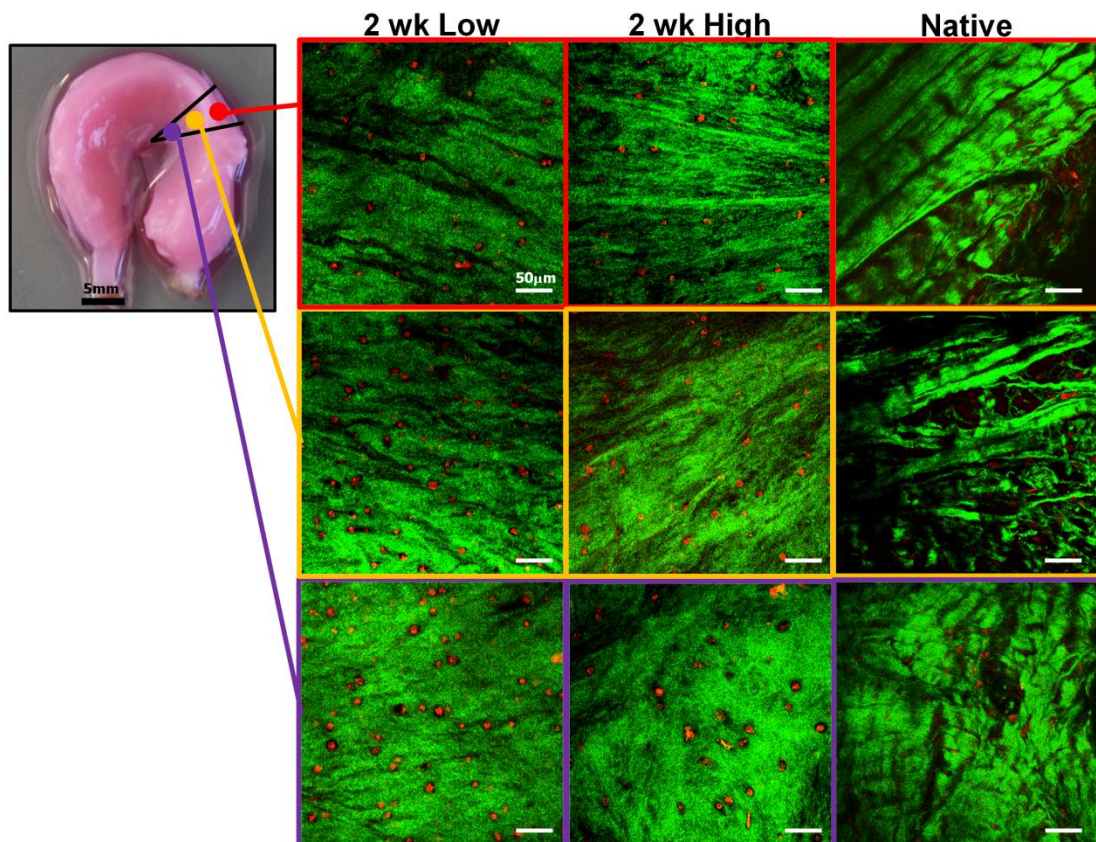


**Figure 7.6:** Confocal reflectance analysis of spatial organization of highly loaded cross-sections (collagen=green, cells=red). The outside and middle portions demonstrate strong circumferential alignment and development of collagen fibers, while the inside has randomly distributed cells within a dense collagen matrix.

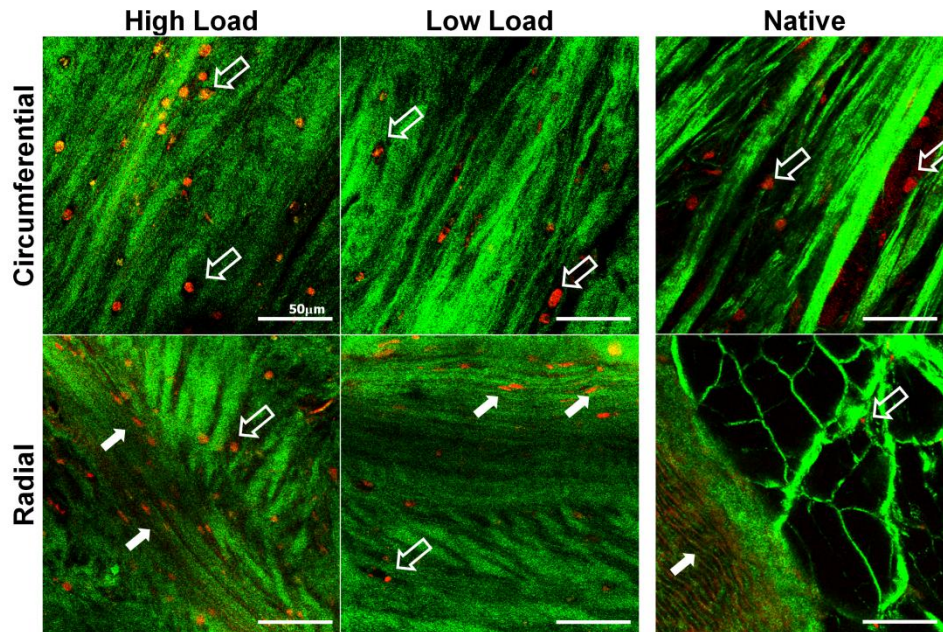


**Figure 7.7:** High magnification confocal reflectance images demonstrate cells of loaded menisci are rounded on the outside of circumferential fibers similar to native menisci (open arrow), while in the radial direction cell appear elongated and spread within large collagen bundles (closed arrow), and rounded along the outside of smaller perpendicular offshoot fibers (open arrow).

### Mechanical Analysis

Starting at 2 weeks, high load menisci had significantly higher equilibrium and tensile moduli than low load and static constructs (Figure 7.8). The equilibrium modulus of high load menisci improved 19 fold by 4 weeks to match native tissue properties (110-490 kPa)<sup>57</sup>. Low load menisci maintained a significantly higher equilibrium modulus than static menisci from 2 weeks on ( $p < 0.02$ ) and improved 11 fold by 4 weeks to be at the lower range of native properties.

The circumferential and radial tensile moduli of high load menisci improved 13 and 6 fold by 4 weeks, respectively (Figure 7.8). Low load and static menisci maintained similar circumferential and radial moduli throughout culture increasing each 10 and 3.5 fold by 4 weeks, respectively. When circumferential and radial tensile properties are compared, both loaded groups start to develop anisotropic

properties at 2 weeks with a 30-40% difference between directions. Static menisci remain isotropic with no difference between circumferential and radial directions at 2 weeks. By 4 weeks, all menisci develop anisotropic tensile properties with ~2 fold greater circumferential modulus compared to radial ( $p < 0.001$ ).

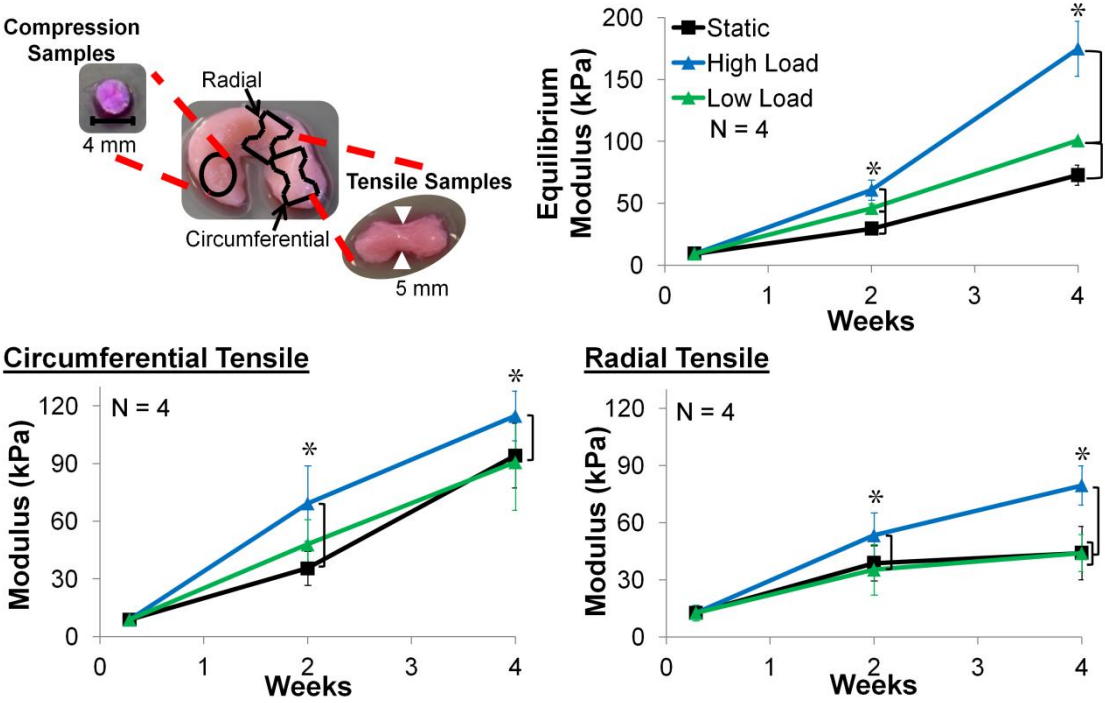


**Figure 7.8:** Depiction of samples used for mechanical testing, equilibrium modulus and tensile moduli in the circumferential and radial direction for engineered menisci. High load menisci developed superior mechanical properties from 2 weeks on and both loaded groups developed anisotropic tensile properties as of 2 weeks. \*Significance compared to bracketed group ( $p < 0.05$ )

### Biochemical Analysis

Loading significantly improved GAG and collagen accumulation over static menisci by 2 weeks (Figure 7.9). All menisci had a similar significant loss in DNA by 2 weeks, but then maintained that level of DNA throughout the remainder of culture (data not shown). Correspondingly, all menisci lost more DNA to the media in the first 2 weeks, with high loaded menisci releasing the most DNA throughout culture ( $p < 0.03$ , data not shown).

Low load menisci improved GAG accumulation 3.5 fold by 2 weeks to be significantly greater than high load and static culture menisci ( $p < 0.01$ ), and maintained this concentration through 4 weeks (Figure 7.9). High load menisci steadily increased GAG concentration throughout culture to match low load's 3.5 fold increase by 4 weeks. At 4 weeks both loaded groups had significantly more GAG than static culture menisci ( $p < 0.001$ ). Both loaded groups had similar release pattern of GAG throughout culture (Figure 7.9). Interestingly, static menisci matched loaded menisci release of GAG for the first two weeks, and then had a dramatic increase in release from two weeks on ( $p < 0.001$ ).

Both high and low load menisci had a significant increase in collagen concentration over static constructs by 2 weeks ( $p < 0.01$ , Figure 7.9). By 4 weeks however, both loaded groups dropped back to initial day 2 and 4 week static menisci collagen concentrations. All menisci had a similar release of collagen to the media throughout culture.

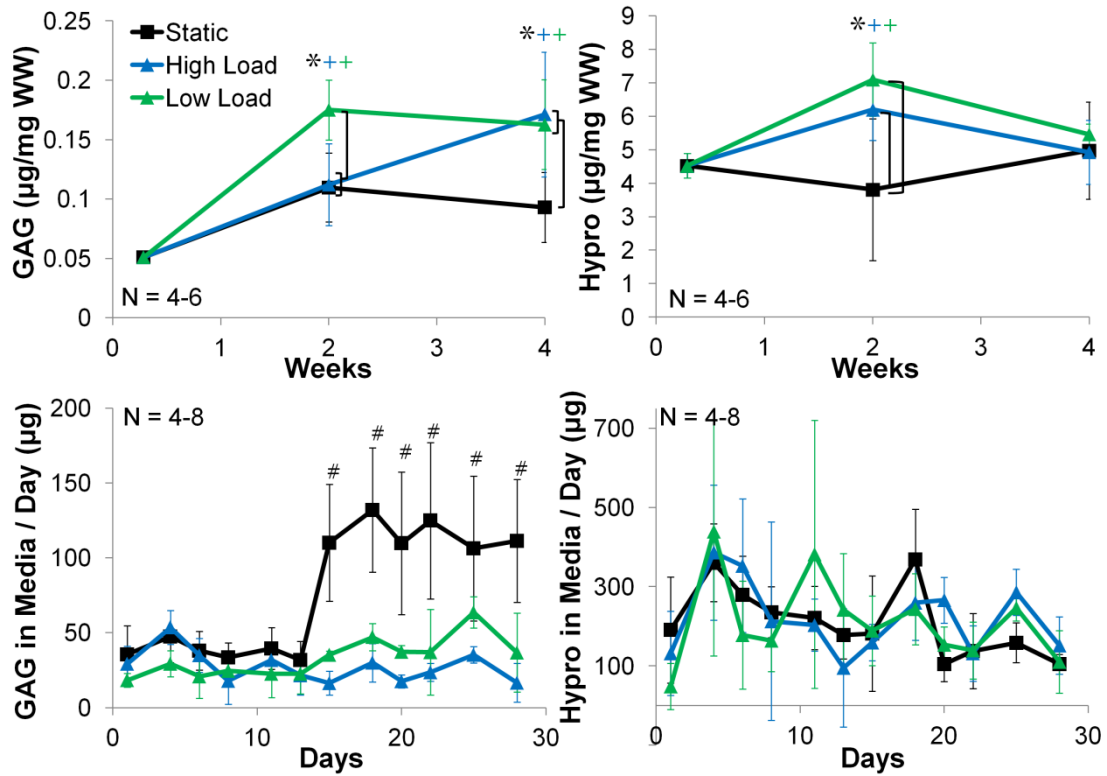


**Figure 7.9:** GAG and collagen content of engineered menisci normalized to wet weight (top row) and in media per day (bottom row). Significance compared to + 0 week, \* bracket group, and # static compared to loaded groups ( $p < 0.05$ )

### Local Mechanical and Biochemical Heterogeneity

In order to investigate the effect of local mechanical environment on biochemical synthesis, FE strain predictions were correlated with spatial biochemical analysis (Figure 7.10). The FE predicted principal strains in the horns and back of the meniscus were used to determine a tensile/compressive strain ratio for the different locations at both high and low load. For both high and low load, the anterior and posterior horns have a ratio below one representing a compressive environment. The back of the meniscus for both high and low loads has a ratio above 1, representing a tensile loading environment.

Spatial biochemical analysis is reported as a ratio of hydroxyproline to GAG concentration at 4 weeks of culture (Figure 7.10). The back of the meniscus at both loading regimes had a significantly higher ratio of collagen/GAG content than the horns at both loading regimes ( $p < 0.03$ ). Generally, there was more GAG production in the horns, and more collagen production in the back of the meniscus. This data significantly correlated with the tensile/compressive strain ratio ( $R^2 = 0.8592$ ,  $p < 0.01$ ). The same correlation was seen when the hydroxyproline data was normalized to account for the initial collagen scaffold ( $R^2 = 0.8302$ , data not shown). As the loading environment became more tensile (tensile/compressive strain ratio increased) the amount of collagen production increased (hydro/GAG ratio increased). This data remained significantly correlated when 2 week data was included ( $R^2 = 0.5716$ ,  $p < 0.004$ ). However, it should be noted that the FE model is predicting the loads at the beginning of culture when no organization is present and thus is not an exact correlation to the strains being applied at 2 and 4 weeks of culture.

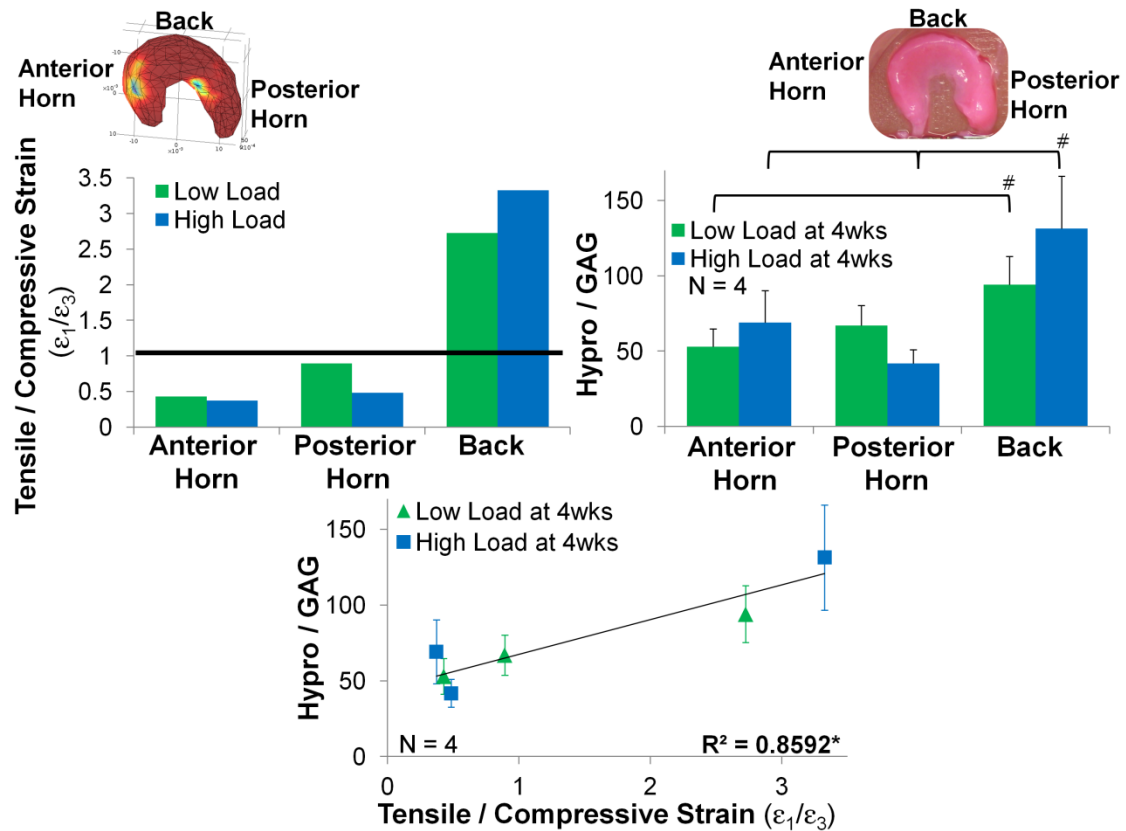


**Figure 7.10:** Local loading environment compared to local biochemical synthesis. Principal strains from FE model are reported as a tensile/compressive strain ratio for different locations within the meniscus. Values below one have more compressive strain, and values above one have more tensile strain. Biochemical analysis from different locations of the meniscus are reported as a hydroxyproline/GAG ratio for loaded menisci at 4 weeks. Loading environment and biochemical synthesis significantly correlate with areas of more tension producing more collagen, and areas of more compression producing more GAG. #Significance between bracketed group ( $p < 0.03$ ) and \*Significant correlation ( $p < 0.01$ )

### Discussion

This study demonstrated the development of a bioreactor that applies physiological loading patterns to condition high density collagen menisci. In a magnitude-dependent manner, mechanical conditioning improved organization, composition and mechanical properties. All menisci developed organization and tensile anisotropy similar to native menisci by 4 weeks; however loading accelerated and improved this development, with the high load group demonstrating the most

development. Further, local changes in the mechanical environment drove heterogeneous tissue organization and composition.

FE analysis demonstrated the bioreactor applies loads with more compression in the horns and tensile loads in the back, similar to physiologic contact areas and strain distributions in native menisci when the leg is in full extension<sup>47</sup>. Strain magnitudes depended on the location within the meniscus<sup>45</sup>. Strain magnitudes in the horns at high load matched previously predicted and measured radial (~1%), circumferential (~3-4%) and axial strains (~9-13%) for porcine and human menisci<sup>45-47</sup>.

Loading accelerated and improved native-like organization in high density collagen menisci. Loaded menisci matched native circumferential alignment and fiber diameters in half the time as static clamped menisci (2 and 4 weeks compared to 4 and 8 weeks, Chapter 6). Similarly, loaded menisci developed native-like radial morphologies by 2 weeks, while static menisci first develop these morphologies by 4 weeks. At 4 weeks, the high load menisci were the most developed menisci produced to date. This study supports that cell-seeded collagen gels align when exposed to anisotropic mechanical stimulation<sup>33-37</sup>, and for the first time demonstrates this to be true in high density collagen and large sized constructs. However, the improved organization may not just be from anisotropic mechanical stimulation.

The native-like organization in loaded menisci may be partially due to mimicking *in vivo* strain distributions and developmental processes. The improved circumferential organization in loaded menisci is easily explained by mechanical conditioning; however the improved radial organization is more unexpected. Meniscal fibrochondrocytes are thought to have an intrinsic ability to form specific structures<sup>18, 58, 59</sup>. Further, it has been demonstrated that the early stages of development, when the meniscus begins to align cells and form aligned collagen bundles, are intrinsically regulated<sup>60</sup>. However, mechanical stimulation is needed in

order for collagen fibers to continue to grow and develop, and if it is removed the meniscus fails to mature and ultimately degenerates<sup>60, 61</sup>. The circumferential and radial fibers continue to align and develop through adolescents with increased joint motion and weight-bearing, further demonstrating the importance of mechanical stimulation in development<sup>61</sup>. In this study, meniscal fibrochondrocytes appear to have an intrinsic ability to form radial morphologies, as evident by development of static clamped menisci by 4 weeks. However mechanical stimulation greatly accelerated and improved this development, mirroring *in vivo* developmental processes and demonstrating the importance of recapitulating native loading environments when developing engineered tissues. This bioreactor could provide a platform to further understanding and examine the different phases of meniscal development *in vitro*.

In addition to collagen fiber organization, cellular organization in loaded menisci mirrored native tissue. It is believed the varying characteristics of cells throughout the meniscus are essential to the ability of the meniscus to respond to different mechanical environments<sup>59</sup>. In this study, cells appeared rounded and aligned along the outside of circumferential fibers in the periphery of loaded menisci. While towards the inside edge of the menisci, the cells were rounded and randomly distributed within a dense collagen matrix, similar to native tissue<sup>59, 62</sup>. Interestingly, in the radial direction cells appeared elongated and encapsulated within large fibers that run from the outer edge of the meniscus inward. Previously, it has been reported that cells are within radial tie fibers in native tissue and appear fusiform/elongate within type VI collagen<sup>9, 62, 63</sup>. Type VI collagen has been shown to have a fibrous organization in the radial direction of menisci, particularly around blood vessels<sup>62, 63</sup>. Cells have also been shown to appear fusiform and aligned within collagen fibers early in development at 25 weeks gestation<sup>65</sup>, suggesting the radial fibers observed in this

study may be earlier in development than the circumferential fibers. Further development of scaffolds and investigations of types of collagen are needed.

Mirroring developments in organization, loading accelerated and improved the mechanical properties of collagen menisci in a magnitude-dependent manner. By 4 weeks, the equilibrium modulus of high load menisci improved 19-fold to match native properties (110-490 kPa)<sup>57</sup>. Similar to accelerated organization, both loaded groups developed anisotropic tensile properties by 2 weeks, which matched native levels of anisotropy by 4 weeks (Chapter 6)<sup>10, 11</sup>. Although high load menisci improved the circumferential and radial tensile moduli 6-13 fold, by 4 weeks of culture, the moduli are still 2 orders of magnitude below immature native values (circumferential 13-26 MPa<sup>66</sup>, radial 4 MPa, Chapter 6) despite collagen fibers matching native alignment and size. This suggests a need for further development of collagen fibers with either prolonged mechanical stimulation or chemical stimulation to improve density and crosslinking.

As stated in the introduction, compressive loading of engineered cartilage is traditionally chondrogenic resulting in increased GAG synthesis and equilibrium modulus, while tensile loading is thought to be fibrogenic, resulting in increased collagen synthesis and tensile properties (Chapter 2)<sup>22, 25, 31</sup>. Neither type of loading alone fully enhances all the fibrocartilage characteristics of menisci. In this study, we applied a compressive-tensile load and compared to static menisci, loaded menisci significantly increased GAG accumulation (200-250%), collagen accumulation (40-55%), equilibrium modulus (50-150%) and tensile moduli (25-80%). This is similar to that observed in a previous study that applied compressive-tensile loading to scaffold free constructs<sup>32</sup>. This loading regime appears to be ideal for fibrochondrogenic development.

Although, GAG and collagen concentrations significantly improved by 2 weeks of loading, collagen concentration dropped back to static values by 4 weeks. This may indicate that the cells have adapted their matrix to withstand the loading environment and a higher level of loading is needed after 2 weeks, or the primary response of long term loading may be matrix remodeling rather than synthesis. The FE model in this study is for an unorganized collagen meniscus to determine the effect of loading at the beginning of culture. It would be interesting in future studies to adapt the FE model to a more anisotropic model to mirror meniscus development to better understand the load being applied at 2 and 4 weeks.

Interestingly, in this study we observed a significant increase in release of GAG to the media for static samples at 2 weeks, while loaded menisci maintained a consistent release of GAG throughout culture. This is contrary to that previously seen with mechanical conditioning of chondrocyte and fibrochondrocytes seeded scaffolds, in which loading significantly increases release of GAG at 2 weeks<sup>22, 42</sup>. It is believed that proteoglycan turnover induced by mechanical loading is necessary for development of biomechanically functional tissue; however prolong catabolic responses often results in degradation of the tissue<sup>24, 42, 43, 67, 68</sup>. It has been suggested this dramatic increase in GAG release at 2 weeks could be an injurious-like response of the cells due to a lack of organization and physical cues to help transmit the load<sup>42</sup>. In this study, the static menisci are exposed to continuous mechanical loads from the horn-anchored clamps that restrict contraction, and possibly at 2 weeks the organization is not far enough along to stop the dramatic catabolic release of GAG to the media. However, the loaded menisci have accelerated organization, and avoid this injurious response, while maintaining a steady beneficial catabolic response. To further investigate this, future studies should concentrate on MMP and aggrecanase expression during culture.

Finally, in this study we investigated whether local mechanical environments can drive heterogeneous tissue organization and synthesis in a single scaffold. As previously mentioned, it has been demonstrated that compressive loading often results in chondrogenic development, and tensile loading in fibrogenic development (Chapter 2)<sup>22, 25, 31</sup>, however all of this work has been done with a single form of loading. Using our FE model we were able to correlate areas of more compression (horns) or tension (back) with organization and biochemical synthesis. Organizationally, the more compressive loading environment, toward the inside edge of the meniscus, had cartilage-like development with rounded cells within a dense collagen matrix. In the outer 2/3 of the meniscus where there was more tensile load, we observed circumferential fiber development. This spatial organization with more homogeneous chondrogenic organization on the inside leading into circumferential fiber development in the middle to deep zone is similar to that previously reported for native tissue<sup>2, 7, 62</sup>. Biochemically, a significant correlation between loading environment and biochemical synthesis was found. In areas of more compression, there was more GAG accumulation, and in areas of more tensile load there was more collagen accumulation. However, it should be noted the FE model does not account for organizational improvements with time, and may not be an exact representation of the loading environments at 4 weeks. Further studies updating the FE model to account for the improved organization and examining the distribution of type I and II collagen and aggrecan within the tissue would help to further examine and compare these regional differences to native tissue.

This study demonstrates the use of physiologically distributed load to develop high density type I collagen menisci with organization, levels of tensile anisotropy, and equilibrium moduli that match native tissue, highlighting the importance of recapitulating native loading environments when engineering tissues. Further, it

demonstrates that local changes in mechanical environment will drive heterogeneous tissue formation. These are some of the most organized engineered menisci developed to date and demonstrate great promise as either whole or partial meniscal replacements. However, GAG and collagen concentrations remain at ~5% and 20% that of native tissue when normalized to wet weight, respectively and the tensile modulus is 2 orders of magnitude lower than native tissue. Thus, although loaded fibrochondrocyte-seeded collagen menisci are promising meniscal replacements, future work should focus on using a more clinically appropriate cell source, improving GAG composition and tensile properties.

## REFERENCES

1. Kawamura S., Lotito K., Rodeo S.A. Biomechanics and healing response of the meniscus. *Oper Techn Sport Med.***11**:68. 2003.
2. Hasan J., Fisher J., Ingham E. Current strategies in meniscal regeneration. *J Biomed Mater Res B Appl Biomater.* 2013.
3. AufderHeide A.C., Athanasiou K.A. Mechanical stimulation toward tissue engineering of the knee meniscus. *Ann Biomed Eng.***32**:1161. 2004.
4. Fithian D.C., Kelly M.A., Mow V.C. Material properties and structure-function relationships in the menisci. *Clin Orthop Relat Res.***19**. 1990.
5. Haut Donahue T.L., Hull M.L., Rashid M.M., Jacobs C.R. How the stiffness of meniscal attachments and meniscal material properties affect tibio-femoral contact pressure computed using a validated finite element model of the human knee joint. *J Biomech.***36**:19. 2003.
6. Petersen W., Tillmann B. Collagenous fibril texture of the human knee joint menisci. *Anat Embryol.***197**:317. 1998.
7. Rattner J.B., Matyas J.R., Barclay L., Holowaychuk S., Sciore P., Lo I.K., et al. New understanding of the complex structure of knee menisci: implications for injury risk and repair potential for athletes. *Scand J Med Sci Sports.***21**:543. 2011.
8. Aspden R.M., Yarker Y.E., Hukins D.W. Collagen orientations in the meniscus of the knee joint. *J Anat.***140 ( Pt 3)**:371. 1985.
9. Kambic H.E., McDevitt C.A. Spatial organization of types I and II collagen in the canine meniscus. *J Orthop Res.***23**:142. 2005.
10. Makris E.A., Hadidi P., Athanasiou K.A. The knee meniscus: structure-function, pathophysiology, current repair techniques, and prospects for regeneration. *Biomaterials.***32**:7411. 2011.
11. Tissakht M., Ahmed A.M. Tensile stress-strain characteristics of the human meniscal material. *J Biomech.***28**:411. 1995.

12. Khetia E.A., McKeon B.P. Meniscal allografts: biomechanics and techniques. *Sports Med Arthrosc.***15**:114. 2007.
13. Balint E., Gatt C.J., Jr., Dunn M.G. Design and mechanical evaluation of a novel fiber-reinforced scaffold for meniscus replacement. *J Biomed Mater Res A.***100**:195. 2012.
14. Ballyns J.J., Gleghorn J.P., Niebrzydowski V., Rawlinson J.J., Potter H.G., Maher S.A., et al. Image-guided tissue engineering of anatomically shaped implants via MRI and micro-CT using injection molding. *Tissue Eng Part A.***14**:1195. 2008.
15. Huey D.J., Athanasiou K.A. Maturation growth of self-assembled, functional menisci as a result of TGF-beta1 and enzymatic chondroitinase-ABC stimulation. *Biomaterials.***32**:2052. 2011.
16. Kon E., Chiari C., Marcacci M., Delcogliano M., Salter D.M., Martin I., et al. Tissue engineering for total meniscal substitution: animal study in sheep model. *Tissue Eng Part A.***14**:1067. 2008.
17. Mandal B.B., Park S.H., Gil E.S., Kaplan D.L. Multilayered silk scaffolds for meniscus tissue engineering. *Biomaterials.***32**:639. 2011.
18. Puetzer J.L., Bonassar L.J. High density type I collagen gels for tissue engineering of whole menisci. *Acta Biomater.***9**:7787. 2013.
19. Tienen T.G., Heijkants R.G., de Groot J.H., Schouten A.J., Pennings A.J., Veth R.P., et al. Meniscal replacement in dogs. Tissue regeneration in two different materials with similar properties. *J Biomed Mater Res B Appl Biomater.***76**:389. 2006.
20. Zur G., Linder-Ganz E., Elsner J.J., Shani J., Brenner O., Agar G., et al. Chondroprotective effects of a polycarbonate-urethane meniscal implant: histopathological results in a sheep model. *Knee Surg Sports Traumatol Arthrosc.***19**:255. 2011.
21. Higashioka M.M., Chen J.A., Hu J.C., Athanasiou K.A. Building an anisotropic meniscus with zonal variations. *Tissue Eng Part A.***20**:294. 2014.
22. Ballyns J.J., Bonassar L.J. Dynamic compressive loading of image-guided tissue engineered meniscal constructs. *J Biomech.***44**:509. 2011.

23. Petri M., Ufer K., Toma I., Becher C., Liidakis E., Brand S., et al. Effects of perfusion and cyclic compression on in vitro tissue engineered meniscus implants. *Knee Surg Sports Traumatol Arthrosc.***20**:223. 2012.
24. Puetzer J.L., Ballyns J.J., Bonassar L.J. The Effect of the Duration of Mechanical Stimulation and Post-Stimulation Culture on the Structure and Properties of Dynamically Compressed Tissue-Engineered Menisci. *Tissue Eng Part A.***18**:1365. 2012.
25. Baker B.M., Shah R.P., Huang A.H., Mauck R.L. Dynamic tensile loading improves the functional properties of mesenchymal stem cell-laden nanofiber-based fibrocartilage. *Tissue Eng Part A.***17**:1445. 2011.
26. Vanderploeg E.J., Imler S.M., Brodtkin K.R., Garcia A.J., Levenston M.E. Oscillatory tension differentially modulates matrix metabolism and cytoskeletal organization in chondrocytes and fibrochondrocytes. *J Biomech.***37**:1941. 2004.
27. Ballyns J.J., Wright T.M., Bonassar L.J. Effect of media mixing on ECM assembly and mechanical properties of anatomically-shaped tissue engineered meniscus. *Biomaterials.***31**:6756. 2010.
28. Neves A.A., Medcalf N., Brindle K.M. Influence of stirring-induced mixing on cell proliferation and extracellular matrix deposition in meniscal cartilage constructs based on polyethylene terephthalate scaffolds. *Biomaterials.***26**:4828. 2005.
29. Gunja N.J., Athanasiou K.A. Effects of hydrostatic pressure on leporine meniscus cell-seeded PLLA scaffolds. *J Biomed Mater Res A.***92**:896. 2010.
30. Gunja N.J., Uthamanthil R.K., Athanasiou K.A. Effects of TGF-beta1 and hydrostatic pressure on meniscus cell-seeded scaffolds. *Biomaterials.***30**:565. 2009.
31. Grad S., Eglin D., Alini M., Stoddart M.J. Physical Stimulation of Chondrogenic Cells In Vitro: A Review. *Clin Orthop Relat Res.* 2011.
32. Huey D.J., Athanasiou K.A. Tension-compression loading with chemical stimulation results in additive increases to functional properties of anatomic meniscal constructs. *PLoS One.***6**:e27857. 2011.

33. Ferdous Z., Lazaro L.D., Iozzo R.V., Hook M., Grande-Allen K.J. Influence of cyclic strain and decorin deficiency on 3D cellularized collagen matrices. *Biomaterials*.**29**:2740. 2008.
34. Girton T.S., Barocas V.H., Tranquillo R.T. Confined compression of a tissue-equivalent: collagen fibril and cell alignment in response to anisotropic strain. *J Biomech Eng*.**124**:568. 2002.
35. Gould R.A., Chin K., Santisakultarm T.P., Dropkin A., Richards J.M., Schaffer C.B., et al. Cyclic strain anisotropy regulates valvular interstitial cell phenotype and tissue remodeling in three-dimensional culture. *Acta Biomater*.**8**:1710. 2012.
36. Tower T.T., Neidert M.R., Tranquillo R.T. Fiber alignment imaging during mechanical testing of soft tissues. *Ann Biomed Eng*.**30**:1221. 2002.
37. Vader D., Kabla A., Weitz D., Mahadevan L. Strain-induced alignment in collagen gels. *PLoS One*.**4**:e5902. 2009.
38. Ballyns J.J., Cohen D.L., Malone E., Maher S.A., Potter H.G., Wright T., et al. An optical method for evaluation of geometric fidelity for anatomically shaped tissue-engineered constructs. *Tissue Eng Part C Methods*.**16**:693. 2010.
39. Babalola O.M., Bonassar L.J. Parametric finite element analysis of physical stimuli resulting from mechanical stimulation of tissue engineered cartilage. *J Biomech Eng*.**131**:061014. 2009.
40. Cross V.L., Zheng Y., Won Choi N., Verbridge S.S., Sutermeister B.A., Bonassar L.J., et al. Dense type I collagen matrices that support cellular remodeling and microfabrication for studies of tumor angiogenesis and vasculogenesis in vitro. *Biomaterials*.**31**:8596. 2010.
41. Aufderheide A.C., Athanasiou K.A. A direct compression stimulator for articular cartilage and meniscal explants. *Ann Biomed Eng*.**34**:1463. 2006.
42. Kisiday J.D., Lee J.H., Siparsky P.N., Frisbie D.D., Flannery C.R., Sandy J.D., et al. Catabolic responses of chondrocyte-seeded peptide hydrogel to dynamic compression. *Ann Biomed Eng*.**37**:1368. 2009.
43. Nicodemus G.D., Bryant S.J. Mechanical loading regimes affect the anabolic and catabolic activities by chondrocytes encapsulated in PEG hydrogels. *Osteoarthritis Cartilage*.**18**:126. 2010.

44. Zielinska B., Killian M., Kadmiel M., Nelsen M., Haut Donahue T.L. Meniscal tissue explants response depends on level of dynamic compressive strain. *Osteoarthritis Cartilage*.**17**:754. 2009.
45. Freutel M., Seitz A.M., Galbusera F., Bornstedt A., Rasche V., Knothe Tate M.L., et al. Medial meniscal displacement and strain in three dimensions under compressive loads: MR assessment. *J Magn Reson Imaging*. 2013.
46. Seitz A.M., Lubomierski A., Friemert B., Ignatius A., Durselen L. Effect of partial meniscectomy at the medial posterior horn on tibiofemoral contact mechanics and meniscal hoop strains in human knees. *J Orthop Res*.**30**:934. 2012.
47. Zielinska B., Donahue T.L. 3D finite element model of meniscectomy: changes in joint contact behavior. *J Biomech Eng*.**128**:115. 2006.
48. Bowles R.D., Williams R.M., Zipfel W.R., Bonassar L.J. Self-assembly of aligned tissue-engineered annulus fibrosus and intervertebral disc composite via collagen gel contraction. *Tissue Eng Part A*.**16**:1339. 2010.
49. Carey S.P., Kraning-Rush C.M., Williams R.M., Reinhart-King C.A. Biophysical control of invasive tumor cell behavior by extracellular matrix microarchitecture. *Biomaterials*.**33**:4157. 2012.
50. Mason B.N., Starchenko A., Williams R.M., Bonassar L.J., Reinhart-King C.A. Tuning three-dimensional collagen matrix stiffness independently of collagen concentration modulates endothelial cell behavior. *Acta Biomater*. 2012.
51. Chaudhuri S., Nguyen H., Rangayyan R.M., Walsh S., Frank C.B. A Fourier domain directional filtering method for analysis of collagen alignment in ligaments. *IEEE Trans Biomed Eng*.**34**:509. 1987.
52. Ng C.P., Hinz B., Swartz M.A. Interstitial fluid flow induces myofibroblast differentiation and collagen alignment in vitro. *J Cell Sci*.**118**:4731. 2005.
53. Gleghorn J.P., Jones A.R., Flannery C.R., Bonassar L.J. Boundary mode frictional properties of engineered cartilaginous tissues. *Eur Cell Mater*.**14**:20. 2007.
54. Kim Y.J., Sah R.L., Doong J.Y., Grodzinsky A.J. Fluorometric assay of DNA in cartilage explants using Hoechst 33258. *Anal Biochem*.**174**:168. 1988.

55. Enobakhare B.O., Bader D.L., Lee D.A. Quantification of sulfated glycosaminoglycans in chondrocyte/alginate cultures, by use of 1,9-dimethylmethylene blue. *Anal Biochem.***243**:189. 1996.
  
56. Neuman R.E., Logan M.A. The determination of hydroxyproline. *J Biol Chem.***184**:299. 1950.
  
57. Sweigart M.A., Zhu C.F., Burt D.M., DeHoll P.D., Agrawal C.M., Clanton T.O., et al. Intraspecies and interspecies comparison of the compressive properties of the medial meniscus. *Ann Biomed Eng.***32**:1569. 2004.
  
58. Ibarra C., Jannetta C., Vacanti C.A., Cao Y., Kim T.H., Upton J., et al. Tissue engineered meniscus: a potential new alternative to allogeneic meniscus transplantation. *Transplant Proc.***29**:986. 1997.
  
59. Hellio Le Graverand M.P., Ou Y., Schield-Yee T., Barclay L., Hart D., Natsume T., et al. The cells of the rabbit meniscus: their arrangement, interrelationship, morphological variations and cytoarchitecture. *J Anat.***198**:525. 2001.
  
60. Mikic B., Johnson T.L., Chhabra A.B., Schalet B.J., Wong M., Hunziker E.B. Differential effects of embryonic immobilization on the development of fibrocartilaginous skeletal elements. *J Rehabil Res Dev.***37**:127. 2000.
  
61. Clark C.R., Ogden J.A. Development of the menisci of the human knee joint. Morphological changes and their potential role in childhood meniscal injury. *J Bone Joint Surg Am.***65**:538. 1983.
  
62. Vanderploeg E.J., Wilson C.G., Imler S.M., Ling C.H., Levenston M.E. Regional variations in the distribution and colocalization of extracellular matrix proteins in the juvenile bovine meniscus. *J Anat.***221**:174. 2012.
  
63. Chevrier A., Nelea M., Hurtig M.B., Hoemann C.D., Buschmann M.D. Meniscus structure in human, sheep, and rabbit for animal models of meniscus repair. *J Orthop Res.***27**:1197. 2009.
  
64. Andrews S.H., Rattner J.B., Abusara Z., Adesida A., Shrive N.G., Ronsky J.L. Tie-fibre structure and organization in the knee menisci. *J Anat.* 2014.
  
65. Fukazawa I., Hatta T., Uchio Y., Otani H. Development of the meniscus of the knee joint in human fetuses. *Congenit Anom (Kyoto).***49**:27. 2009.

66. Eleswarapu S.V., Responde D.J., Athanasiou K.A. Tensile properties, collagen content, and crosslinks in connective tissues of the immature knee joint. *PLoS One*.**6**:e26178. 2011.
67. Blain E.J. Mechanical regulation of matrix metalloproteinases. *Front Biosci*.**12**:507. 2007.
68. De Croos J.N., Dhaliwal S.S., Grynblas M.D., Pilliar R.M., Kandel R.A. Cyclic compressive mechanical stimulation induces sequential catabolic and anabolic gene changes in chondrocytes resulting in increased extracellular matrix accumulation. *Matrix Biol*.**25**:323. 2006.

## CHAPTER 8

### **Conclusions**

The focus of this dissertation was to investigate the effect of mechanical stimulation, growth factor stimulation, and material choice on the structure, composition, and mechanical properties of tissue engineered menisci. The ultimate long-term goal of this project was to move toward a viable engineered whole meniscal replacement with properties similar to native tissue. The completion of this body of work resulted in the development of anatomically-correct meniscal constructs with native-like organization, native equilibrium modulus, and anisotropic tensile properties. First, mechanical and chemical stimulation was found to significantly improve biochemical and mechanical properties of alginate menisci (Chapters 3 and 4). Next, high density type I collagen gels were investigated as a potential new scaffold choice and were found to be superior to alginate (Chapter 5). Finally, mechanical stimulation was used to guide native-like organization and development in high density collagen menisci. The effects of biomimetic horn-anchored boundary conditions were investigated (Chapter 6). Then these horn-anchored conditions were combined with compressive loading to develop and investigate the effect of a bioreactor capable of applying physiologic loading patterns (Chapter 7). This chapter discusses the main findings of this dissertation and possible future directions.

In chapters 3 and 4 we investigated the effect of mechanical and chemical stimulation to further improve the properties of alginate menisci. In chapter 3 we demonstrated the importance of timing and duration of loading. We reported that 2 weeks of loading was a critical threshold for improvements in properties, but extended loading past two weeks provided no further development, and thus was not necessary. Further, we found static culture after two weeks of loading could not only

maintain properties of alginate menisci, but also improve them with significant improvements in collagen bundle formation, GAG content, collagen content, and the equilibrium modulus. A common belief in tissue engineering is often the more time spent in a bioreactor, the better the properties of the constructs, however this study clearly demonstrates this is not always true. This study supports the growing trend seen in the literature that prolonged stimulation is not optimal for engineered tissues<sup>1-3</sup>, and provides a new *in vitro* mechanism for conditioning engineered menisci.

In chapter 4 IGF-I treatment for 4 weeks was found to significantly improve biochemical and mechanical properties of alginate menisci, improving GAG content to 60% native tissue and matching native equilibrium modulus. Interestingly, IGF-I treatment also resulted in the development of a distinct surface layer with similar composition and organization to the superficial layer of native tissue. Further, this surface layer stained positive for lubricin, a glycoprotein often localized to the surface of native menisci and known to aid in lubrication. This was the first study to demonstrate the accumulation of endogenous lubricin in engineered meniscal scaffolds. In a follow-up study we investigated the functional properties of this surface layer with a more robust high density collagen scaffold<sup>4</sup>. IGF-I treatment again resulted in the development of a well definite superficial layer, much like native tissue, and this surface layer was shown to aid in lubrication by decreasing the boundary friction coefficient to be similar to native tissue<sup>4</sup>. An engineered meniscal replacement will most likely need a well organized superficial zone and the ability to localize lubricin at the surface in order to be functional when implanted. These studies combined suggest IGF-I treatment may be a means of producing a functional surface zone.

In chapters 3 and 4 we used mechanical and chemical stimulation to generate matrix, improve mechanical properties, and maintain shape fidelity of alginate

menisci. However, these alginate menisci still had collagen and GAG concentrations inferior to native menisci and poor tensile properties. Further, due to the lack of ligands in alginate<sup>5</sup>, a large amount of produced matrix and cells were being lost to the media during culture. For these reasons we were interested in investigating a new scaffold choice and type I collagen was an attractive alternative to alginate. As mentioned previously, type I collagen is the major component of the meniscus and its fiber organization plays a large role in ability of the meniscus to transmit the loads of the knee<sup>6, 7</sup>. Further, collagen is composed of fibrils that allow for increased tensile properties, better retention of cells and matrix, and a place for cells to attach and remodel the matrix<sup>8, 9</sup>. Low density collagen gels (1-5 mg/ml) have been studied for decades, but have been avoided in orthopaedic and injection molding applications due to weak mechanical strength, low shape fidelity and high contraction<sup>8</sup>. However, high density gels (10-20 mg/ml) were recently shown to be able to overcome many of these shortcomings<sup>8</sup>, creating a possibility that collagen gels could be successful in meniscal tissue engineering. To date, very few studies have characterized cell-seed high density collagen gels in simple or complicated geometries such as the meniscus.

In chapter 5 we developed a method of injection molding high density collagen gels to produce cell-seeded collagen menisci. Since very little work had been performed at the time, we investigated both 10 and 20 mg/ml collagen menisci to observe the effect of concentration on high density collagen gels. By 4 weeks of culture, collagen menisci preserved their DNA content, while significantly improving GAG and collagen concentrations above alginate controls. Interestingly, we found that meniscal fibrochondrocytes produced the same amount of matrix in both alginate and collagen constructs. Collagen gels only retained the matrix better, rather than influencing the rate of total matrix production by cells. This data was in contrast with a previous study that suggested fibrochondrocytes produced more matrix when

seeded on fibers rather than encapsulated in gels<sup>10</sup>. However, this study did not investigate amount of extracellular matrix released to the media and thus did not calculate total production<sup>10</sup>. Mechanically, collagen menisci matched alginate equilibrium modulus while developing a 3-6 fold higher tensile modulus by 4 weeks. Overall 10 and 20 mg/ml collagen menisci performed similarly, however 20 mg/ml menisci had higher mechanical properties and contracted less. Both concentrations of collagen menisci contracted with time in culture, but the contraction was uniform and demonstrated fibrochondrocytes were able to reorganize the collagen gels into a more fibrous appearance. This ability of the fibrochondrocytes to contract the collagen gels provided a promising mechanism for driving toward native organization.

In chapter 6 we attempted to harness the contraction power of fibrochondrocytes to force circumferential alignment in high density collagen menisci. It has been well established that cellular traction forces can be used to align collagen fibers under a variety of mechanical boundary conditions<sup>11-15</sup>; however, none of this work had been done in high density collagen gels or in as complex geometries as the meniscus. Extensions were added to the horns of meniscal scaffolds and culture trays were created which allowed the extensions to be clamped down and secured throughout culture. This culture condition not only mimics the native horn attachment sites but also restricts contraction circumferentially, in turn creating hoop stress to encourage circumferential alignment. Again 10 and 20 mg/ml collagen menisci were investigated to determine whether concentration of collagen would have an effect on organization. After 8 weeks of culture, clamped menisci preserved their size and shape while developing native-like aligned and sized circumferential fibers, native-like radial organizations, increased collagen accumulation, and improved mechanical properties compared to unclamped menisci. The clamped menisci organization was further reflected in the development of anisotropic tensile properties that matched anisotropic

ratios of native menisci with 2-3 fold higher circumferential moduli compared to radial moduli. Both concentrations of collagen menisci performed similarly and there appeared to be no adverse affect of collagen concentration on development, with 20 mg/ml collagen menisci having larger diameter collagen fibers and significantly better mechanical properties.

Recently, there has been a growing trend of inclusion of circumferential fibers into meniscal scaffolds<sup>16-21</sup>, however all of these attempts involve synthetic fibers embedded into the bulk of the scaffold and/or are single layers. These synthetic fibers are often larger than natural collagen fibril diameters impeding cellular interactions and penetration into scaffolds, which in turn slows matrix development. In this study we used mechanical constraints to guide cells to develop collagen fibrils into native sized fibers. Further, this is the first study to our knowledge to demonstrate native-like radial developments which varied with location in the meniscus.

Horn-anchored boundary conditions had little effect on biochemical synthesis, and although collagen fiber alignment and size matched native tissue, tensile properties were still 1-2 orders of magnitude below native tissue. Thus mechanical stimulation was an attractive means of improving biochemical and mechanical properties further.

In chapter 7 we combined the horn-anchored boundary conditions with compressive loading to develop a more biomimetic bioreactor and investigated its effect on the development of 20 mg/ml fibrochondrocyte-seeded collagen menisci. Compressive loading was applied with a loading platen the shape of the femoral condyles and finite element (FE) analysis was performed to determine proper loading regimes for conditioning engineered menisci. FE analysis demonstrated the bioreactor applied physiological loading patterns with more compression in the horns and more tensile strain in the back of the meniscus. Loading was found to accelerate the development of 20 mg/ml collagen menisci over static clamped menisci and by 4

weeks these constructs matched native circumferential and radial organization, tensile anisotropy ratios, and equilibrium modulus.

Compressive loading of engineered cartilage is thought to be chondrogenic, resulting in increased GAG synthesis and equilibrium modulus, while tensile loading is thought to be fibrogenic, resulting in increased collagen synthesis and tensile properties<sup>22-24</sup>(see chapter 2). Neither type of loading alone has been shown to fully enhance all the fibrocartilage characteristics of menisci. In this study, 4 weeks of compressive-tensile loading resulted in 3.5 fold increase in GAG accumulation, 1.5 fold increase in collagen accumulation, 19 fold increase in equilibrium modulus, and 6-13 fold increase in tensile moduli. This demonstrates that a combined compressive-tensile loading regime can increase all the fibrocartilage characteristics of menisci and may suggest this loading regime is ideal for fibrocartilage development.

Finally, this study demonstrated local changes in mechanical environment can drive heterogeneous tissue synthesis and organization. Combining FE analysis with local organization and biochemical analysis we found more compressive loading environments drive GAG accumulation and articular cartilage-like development, while more tensile loading environments drive collagen accumulation and fibrous tissue development. These are the first meniscal scaffolds to demonstrate native-like circumferential organization that vary with radial position (i.e. cartilage-like development on the inner edge, and circumferentially aligned fibers in the outer 2/3 of the meniscus).

The culture techniques of chapters 6 and 7 may be mimicking developmental processes. The improved circumferential organization in clamped and loaded menisci are easily explained by the mechanical stimulations applied, however the improved radial organization is more unexpected. During development, menisci start out as

unorganized cellular structures. By 10 weeks the attachments to the tibial plateau are visible<sup>25</sup>. By 14 weeks spindle-shaped cells begin to align and form collagen bundles and with time perpendicular radial fibers begin to appear<sup>26, 27</sup>. Meniscal fibrochondrocytes are thought to have an intrinsic ability to form specific structures<sup>28-30</sup> and it has been demonstrated that these early stages of development are intrinsically regulated<sup>31</sup>. However, mechanical stimulation is needed in order for collagen fibers to continue to grow and develop and if removed, the meniscus ultimately fails to mature and degenerates<sup>26, 31</sup>. The importance of mechanical stimulation in development is further evident as the meniscus continues to develop with increased joint motion and weight-bearing throughout adolescence<sup>26</sup>. In chapters 6 and 7, meniscal fibrochondrocytes appear to have an intrinsic ability to form radial morphologies due to the development observed in clamped menisci. However, similar to *in vivo* development, mechanical stimulation greatly accelerated and improved this organization. These chapters demonstrate the importance of recapitulating native loading environments when developing engineered tissues and additionally demonstrate tissue engineering may be a promising method of deciphering developmental mechanisms.

Overall, this body of work has made significant advancements in the field of engineered menisci. This work has been at the forefront of a paradigm shift in the field from unorganized scaffold to driving toward capturing native organization in engineered menisci. Meniscal organization is believed to be fundamental to successful meniscal load distribution *in vivo*. These are some of the most organized meniscal tissues produced to date and demonstrate great promise as meniscal replacements. Further developments are needed in order for these scaffolds to serve as standalone whole meniscal replacements.

### ***Future Directions***

The work presented in this dissertation lays the foundation for a number of future directions. These directions include *in vitro* steps to further improve the meniscal construct so that it may serve as standalone whole meniscal replacements, use of the developed culture techniques to evaluate developmental processes and collagen cross-linking *in vitro*, and use of the developed meniscal constructs in a partial meniscal replacement model.

### ***In Vitro* Development toward Whole Meniscal Replacements**

The completion of this dissertation produced an engineered meniscal constructs with native organization, equilibrium modulus, and anisotropy. However GAG and collagen concentrations remain at ~5% and 20% weight wet of native tissue, respectively and the tensile properties are 1-2 orders of magnitude below native tissue. This opens the door to many avenues of further improvement.

### ***Growth Factors***

Several studies have reported growth factor treatment to improve proliferation, biochemical synthesis, and mechanical properties in engineered meniscal constructs<sup>32-35</sup>. Further, we have seen these improvements first hand with IGF-I treatment of alginate menisci (Chapter 4)<sup>36</sup>. Transforming growth factor (TGF)- $\beta$ , IGF-I, basic fibroblast growth factor (bFGF), and platelet-derived growth factor (PDGF) have all been studied in meniscus tissue engineering and have shown to improve properties. Future work could investigate the treatment of clamped high density collagen menisci with these growth factors to improve overall GAG and collagen concentrations while influencing organization with horn-anchored boundary conditions. Further, it would be interesting to investigate whether these clamped

collagen menisci have a surface zone capable of lubricating already due to their increased organization or whether IGF-I treatment is needed to further develop the surface zone.

### *Increased Loading*

In chapter 7, loading significantly increased collagen concentrations by 2 weeks, however prolonged loading past two weeks resulted in a decrease in collagen content. This may indicate that the cells have adapted their matrix to withstand the loading environment and a higher level of loading is needed after 2 weeks. Currently, the finite element (FE) model used in this study is for an unorganized collagen meniscus so to determine the effect of loading at the beginning of culture. It would be interesting in future studies to adapt the FE model to a more anisotropic model to mirror the meniscus development. This way it would be possible to know what loads are being applied at 2 and 4 weeks and adjust accordingly. Often in bioreactor studies of engineered tissues, delayed loading results in limited or no stimulation of the cells due to the cells having time to build up their surrounding pericellular matrix (Chapter 2). The cells are believed to not feel the load and thus are not stimulated to produce matrix. In chapter 7, it is possible the cells have organized the matrix enough to withstand the load being applied, and a higher level of load is needed to observe further improvements in biochemical synthesis. It is also possible that the decrease in collagen is due to inducing a prolonged catabolic response as discussed in Chapter 2, and if loading is removed further improvements would be observed. However, this is unlikely since there is no significant increase in release of GAG and collagen to the media and GAG accumulations continue to increase through 4 weeks. The significant improvements in organization with loading most likely reduced the risk of introducing this injurious-like response.

### *Combining Growth Factor Treatment and Loading*

Combination of growth factor treatment and the physiological loading applied in chapter 7 could help to further improve biochemical components. It has been suggested that meniscal fibrochondrocytes respond to biochemical and mechanical stimuli via separate cellular pathways<sup>37, 38</sup>. This suggests that the combination of growth factor treatment with mechanical loading could lead to a synergic improvement in mechanical and biochemical properties.

### *Clinically Relevant Cell Source*

All of the work completed in this dissertation was performed with bovine meniscal fibrochondrocytes, which are not an ideal cell source for translating to clinical applications. A human cell source will most likely have to be incorporated for this to be clinically relevant. Currently, many groups are investigating a variety of cell sources for meniscal repair including, autologous meniscal fibrochondrocytes (MFC), the use of allogeneic MFCs, and the differentiation of human embryonic stem cells or adult mesenchymal stem cells (MSCs)<sup>39</sup>. Previously, it has been demonstrated that meniscal fibrochondrocytes obtained from surgical debris are a potent cell source for engineered meniscal constructs<sup>40</sup> however the number of cells that could be obtained from a patient using this method is limited. Co-culture of MFCs with MSCs has been shown to improve differentiation of stem cells<sup>41, 42</sup>, and could provide a means of obtaining enough cells for engineering a whole meniscal replacement. Current investigations in the lab have found that a co-culture of 50% bovine MFCs and 50% MSCs in high density collagen sheet gels results in increased matrix synthesis and differentiation<sup>43</sup>. This is a promising avenue for further translation into large anatomically correct meniscal scaffolds, and ultimately the clinic.

### *Engineering of Meniscal Roots*

Currently one of the major pitfalls of whole meniscal replacements is attachment methods for anchoring the replacement *in vivo*. Several groups have produced meniscal replacements that are strong enough to withstand loading *in vivo*, however the attachments to the tibial plateau are too weak and inevitably fail<sup>44</sup>. The clamping culture dish and meniscal scaffolds with extensions developed in chapter 6 could provide a means of developing improved attachments. The culture environment of the extensions of the menisci in this dish could be changed to be more osteogenic with media or bone clamps used instead of steel clamps. These options could encourage the development of bone, as well as a bone to cartilage interface similar to the ligament attachments of native menisci, which could serve as a means to securely anchor replacements *in vivo*.

### *Improve Crosslinking and Density of Collagen Fibers*

It is believed the specific organization of collagen, including fiber density, diameter, orientation and degree of crosslinking are fundamental to the mechanical integrity of engineered tissues<sup>45</sup>. In chapters 6 and 7, meniscal constructs develop circumferential fibers that were aligned to the same degree as native tissue and were the same size as native tissue, however tensile properties were still 1-2 orders of magnitude below native properties. This suggests a need for further development of crosslinks and density of collagen.

There are two major types of crosslinks within collagen: those initiated by nonenzymatic glycation and those initiated by the enzyme lysyl oxidase<sup>46</sup>. Both types play important roles in stabilization and development of collagen fibers. Lysyl oxidase bonds are believed to stabilize newly formed collagen fibrils, while nonenzymatic

bonds are thought to form later between collagen helices<sup>47</sup>. Copper sulfate and hydroxylysine treatment have been shown to enhance lysyl oxidase crosslinking<sup>45</sup>, while non-enzymatic ribose treatment can improve glycation<sup>48</sup> in engineered scaffolds. These would be interesting, non-toxic, chemical treatment paths for improving the crosslinking of fibers in collagen menisci. Further, temporal application of both non-enzymatic and enzymatic chemical treatments could result in a synergetic improvement due to the believed time frame of these crosslinks in fiber development<sup>47</sup>. Additionally it has been suggested hypoxia can induce lysyl oxidase crosslinking<sup>49</sup> providing another means of improving collagen crosslinking.

Collagen concentration of the menisci could be improved by subcutaneous implantation after clamping and loading. The cells have arranged the matrix of the meniscal constructs to resemble native organization and implanting *in vivo*, without detrimental mechanical load, could stimulate the cells to dramatically increase collagen synthesis. This method could be used to improve collagen accumulation and tensile properties to native levels before implanting the scaffold as a whole meniscal replacement.

#### Use of Culture Techniques for Alternative Applications

The clamping culture dish and biomimetic bioreactor open the door to investigating further scientific questions outside of use purely for the development of a whole meniscal replacement.

#### *Developmental Research*

Very few studies have investigated the development of menisci<sup>25-27, 31</sup>, however from these studies it appears we may be mimicking developmental processes by clamping and loading the meniscal constructs. This culture system could provide a

means to further investigate developmental processes of the meniscus. It would be interesting to clamp the menisci for a few weeks and then introduce loading to further mimic the developmental process and see how this affects organizational development of the scaffolds. It would also be interesting to use this culture system to develop meniscal scaffolds and then remove loading, or break an extension to see if the meniscal fibrochondrocytes will revert and ultimately degenerate. This would provide further support for the importance of the meniscal attachments *in vivo*, mechanical stimulation during development, and the intrinsic nature of meniscal fibrochondrocytes.

#### *Analysis of Collagen Fiber Development In Vitro*

Collagen is a major structural protein of the body. Collagen fibers provide the tensile strength in multiple tissues, particularly orthopaedic tissues such as tendons, menisci, cartilage, and bone. Tissue engineers are currently striving to create mechanically similar replacements of these tissues, however these attempts often fail to create organized collagen fibers that are essential to long term mechanical success. It is poorly understood how these collagen fibers develop *in vitro*, and knowing more about this process could help to further develop orthopaedic tissue engineering as a whole.

Collagen crosslinking is the final step in the synthesis of collagen fibers, and is known to occur during or after self assembly of fibrils<sup>50</sup>. Although collagen gels have been studied for over 60 years, and the broad principles of collagen assembly are generally accepted, the molecular mechanisms of fiber assembly are still poorly understood. There is a need to understand the role of the cell and the chemical crosslinking events during the development of a fibril to a fiber<sup>51</sup>. Using a simplified rectangular clamping device, high density cell-seeded collagen gels, and Raman

spectroscopy it could be possible to investigate the chemical crosslinking events of a developing collagen fiber. Raman micro-spectroscopy provides a unique, rapid, label-free, non-destructive method of analyzing the molecular and biochemical composition and structure of cells and tissues. It has been used to identify collagen and specific molecular changes within native tissue<sup>52</sup> and collagen gels<sup>53</sup>, however, it has not been applied to developing collagen fibers. Recent advances have made it possible to perform Raman analysis on living cells within scaffolds. Combining Raman analysis with the non-toxic chemical crosslinking treatments discussed previously could provide new insight into how collagen fibers develop chemically and the effect of crosslinkers at various stages of fiber development. This would provide a means to further develop and analyze collagen fibers of multiple engineered tissues.

#### *In Vivo* Partial Meniscal Replacement

While means of attachment, biochemical, and mechanical properties remain a challenge for whole meniscal replacements, many studies have turned to partial meniscal replacement as an option of treating large meniscal tears<sup>44</sup>. If tears do not disrupt the outer rim of the meniscus, it is possible to successfully replace a large portion of the inside of the meniscus. In this method, the native horn ligaments are still attached to the outer rim of the meniscus and tibial plateau. This provides a means of anchoring the meniscus, while the rim provides the mechanical strength needed to withstand *in vivo* loading. Using this method, meniscal replacements do not need to have as well developed mechanical and biochemical properties as native tissue<sup>44</sup>. We believe, using this method, our high density collagen menisci could be applied as large partial meniscal replacements in sheep models. Preliminary work has demonstrated collagen menisci can hold sutures and be attached to the outer rim of sheep menisci *in situ*.

The ultimate goal of this research is to move toward a total meniscal replacement, and while all of the work presented here has been performed *in vitro*, it has made substantial progress and opened up many new research questions and directions. This work establishes the potential of collagen constructs as meniscal replacements and provides the platform necessary to move to *in vivo* partial replacement studies. These steps lay the ground work for providing a new clinical treatment option for whole meniscus replacement.

## REFERENCES

1. Kisiday J.D., Lee J.H., Siparsky P.N., Frisbie D.D., Flannery C.R., Sandy J.D., et al. Catabolic responses of chondrocyte-seeded peptide hydrogel to dynamic compression. *Ann Biomed Eng.***37**:1368. 2009.
2. Kock L.M., Schulz R.M., van Donkelaar C.C., Thummler C.B., Bader A., Ito K. RGD-dependent integrins are mechanotransducers in dynamically compressed tissue-engineered cartilage constructs. *J Biomech.***42**:2177. 2009.
3. Villanueva I., Hauschulz D.S., Mejjic D., Bryant S.J. Static and dynamic compressive strains influence nitric oxide production and chondrocyte bioactivity when encapsulated in PEG hydrogels of different crosslinking densities. *Osteoarthritis Cartilage.***16**:909. 2008.
4. Bonnevie E.D., Puetzer J.L., Bonassar L.J. Enhanced boundary lubrication properties of engineered menisci by lubricin localization with insulin-like growth factor I treatment. *J Biomech.* 2013.
5. Awad H.A., Wickham M.Q., Leddy H.A., Gimble J.M., Guilak F. Chondrogenic differentiation of adipose-derived adult stem cells in agarose, alginate, and gelatin scaffolds. *Biomaterials.***25**:3211. 2004.
6. Kawamura S., Lotito K., Rodeo S.A. Biomechanics and healing response of the meniscus. *Oper Techn Sport Med.***11**:68. 2003.
7. Sweigart M.A., Athanasiou K.A. Toward tissue engineering of the knee meniscus. *Tissue Eng.***7**:111. 2001.
8. Cross V.L., Zheng Y., Won Choi N., Verbridge S.S., Sutermaster B.A., Bonassar L.J., et al. Dense type I collagen matrices that support cellular remodeling and microfabrication for studies of tumor angiogenesis and vasculogenesis in vitro. *Biomaterials.***31**:8596. 2010.
9. Mueller S.M., Shortkroff S., Schneider T.O., Breinan H.A., Yannas I.V., Spector M. Meniscus cells seeded in type I and type II collagen-GAG matrices in vitro. *Biomaterials.***20**:701. 1999.

10. Aufderheide A.C., Athanasiou K.A. Comparison of scaffolds and culture conditions for tissue engineering of the knee meniscus. *Tissue Eng.***11**:1095. 2005.
11. Bell E., Ivarsson B., Merrill C. Production of a tissue-like structure by contraction of collagen lattices by human fibroblasts of different proliferative potential in vitro. *Proc Natl Acad Sci U S A.***76**:1274. 1979.
12. Bowles R.D., Williams R.M., Zipfel W.R., Bonassar L.J. Self-assembly of aligned tissue-engineered annulus fibrosus and intervertebral disc composite via collagen gel contraction. *Tissue Eng Part A.***16**:1339. 2010.
13. Costa K.D., Lee E.J., Holmes J.W. Creating alignment and anisotropy in engineered heart tissue: role of boundary conditions in a model three-dimensional culture system. *Tissue Eng.***9**:567. 2003.
14. Grinnell F., Lamke C.R. Reorganization of hydrated collagen lattices by human skin fibroblasts. *J Cell Sci.***66**:51. 1984.
15. Thomopoulos S., Fomovsky G.M., Holmes J.W. The development of structural and mechanical anisotropy in fibroblast populated collagen gels. *J Biomech Eng.***127**:742. 2005.
16. Balint E., Gatt C.J., Jr., Dunn M.G. Design and mechanical evaluation of a novel fiber-reinforced scaffold for meniscus replacement. *J Biomed Mater Res A.***100**:195. 2012.
17. Elsner J.J., Portnoy S., Zur G., Guilak F., Shterling A., Linder-Ganz E. Design of a free-floating polycarbonate-urethane meniscal implant using finite element modeling and experimental validation. *J Biomech Eng.***132**:095001. 2010.
18. Fisher M.B., Henning E.A., Soegaard N., Esterhai J.L., Mauck R.L. Organized nanofibrous scaffolds that mimic the macroscopic and microscopic architecture of the knee meniscus. *Acta Biomater.***9**:4496. 2013.
19. Holloway J.L., Lowman A.M., Palmese G.R. Mechanical evaluation of poly(vinyl alcohol)-based fibrous composites as biomaterials for meniscal tissue replacement. *Acta Biomater.***6**:4716. 2010.
20. Mandal B.B., Park S.H., Gil E.S., Kaplan D.L. Multilayered silk scaffolds for meniscus tissue engineering. *Biomaterials.***32**:639. 2011.

21. Kelly B.T., Robertson W., Potter H.G., Deng X.H., Turner A.S., Lyman S., et al. Hydrogel meniscal replacement in the sheep knee: preliminary evaluation of chondroprotective effects. *Am J Sports Med.***35**:43. 2007.
22. Baker B.M., Shah R.P., Huang A.H., Mauck R.L. Dynamic tensile loading improves the functional properties of mesenchymal stem cell-laden nanofiber-based fibrocartilage. *Tissue Eng Part A.***17**:1445. 2011.
23. Ballyns J.J., Bonassar L.J. Dynamic compressive loading of image-guided tissue engineered meniscal constructs. *J Biomech.***44**:509. 2011.
24. Grad S., Eglin D., Alini M., Stoddart M.J. Physical Stimulation of Chondrogenic Cells In Vitro: A Review. *Clin Orthop Relat Res.* 2011.
25. Merida-Velasco J.A., Sanchez-Montesinos I., Espin-Ferra J., Rodriguez-Vazquez J.F., Merida-Velasco J.R., Jimenez-Collado J. Development of the human knee joint. *Anat Rec.***248**:269. 1997.
26. Clark C.R., Ogden J.A. Development of the menisci of the human knee joint. Morphological changes and their potential role in childhood meniscal injury. *J Bone Joint Surg Am.***65**:538. 1983.
27. Fukazawa I., Hatta T., Uchio Y., Otani H. Development of the meniscus of the knee joint in human fetuses. *Congenit Anom (Kyoto).***49**:27. 2009.
28. Ibarra C., Jannetta C., Vacanti C.A., Cao Y., Kim T.H., Upton J., et al. Tissue engineered meniscus: a potential new alternative to allogeneic meniscus transplantation. *Transplant Proc.***29**:986. 1997.
29. Puetzer J.L., Bonassar L.J. High density type I collagen gels for tissue engineering of whole menisci. *Acta Biomater.***9**:7787. 2013.
30. Hellio Le Graverand M.P., Ou Y., Schield-Yee T., Barclay L., Hart D., Natsume T., et al. The cells of the rabbit meniscus: their arrangement, interrelationship, morphological variations and cytoarchitecture. *J Anat.***198**:525. 2001.
31. Mikic B., Johnson T.L., Chhabra A.B., Schalet B.J., Wong M., Hunziker E.B. Differential effects of embryonic immobilization on the development of fibrocartilaginous skeletal elements. *J Rehabil Res Dev.***37**:127. 2000.

32. Ionescu L.C., Lee G.C., Huang K.L., Mauck R.L. Growth factor supplementation improves native and engineered meniscus repair in vitro. *Acta Biomater.* 2012.
33. Pangborn C.A., Athanasiou K.A. Growth factors and fibrochondrocytes in scaffolds. *Journal of Orthopaedic Research.***23**:1184. 2005.
34. Stewart K., Pabbruwe M., Dickinson S., Hollander A.P., Chaudhuri J.B. The effect of growth factor treatment on meniscal chondrocyte proliferation and differentiation on polyglycolic acid scaffolds. *Tissue Engineering.***13**:271. 2007.
35. Zaleskas J.M., Kinner B., Freyman T.M., Yannas I.V., Gibson L.J., Spector M. Growth factor regulation of smooth muscle actin expression and contraction of human articular chondrocytes and meniscal cells in a collagen-GAG matrix. *Experimental Cell Research.***270**:21. 2001.
36. Puetzer J.L., Brown B.N., Ballyns J.J., Bonassar L.J. The effect of IGF-I on anatomically shaped tissue-engineered menisci. *Tissue Eng Part A.***19**:1443. 2013.
37. Huey D.J., Athanasiou K.A. Tension-compression loading with chemical stimulation results in additive increases to functional properties of anatomic meniscal constructs. *PLoS One.***6**:e27857. 2011.
38. Imler S.M., Doshi A.N., Levenston M.E. Combined effects of growth factors and static mechanical compression on meniscus explant biosynthesis. *Osteoarthritis Cartilage.***12**:736. 2004.
39. Makris E.A., Hadidi P., Athanasiou K.A. The knee meniscus: structure-function, pathophysiology, current repair techniques, and prospects for regeneration. *Biomaterials.***32**:7411. 2011.
40. Baker B.M., Nathan A.S., Huffman G.R., Mauck R.L. Tissue engineering with meniscus cells derived from surgical debris. *Osteoarthritis Cartilage.***17**:336. 2009.
41. Cui X., Hasegawa A., Lotz M., D'Lima D. Structured three-dimensional co-culture of mesenchymal stem cells with meniscus cells promotes meniscal phenotype without hypertrophy. *Biotechnol Bioeng.***109**:2369. 2012.
42. Saliken D.J., Mulet-Sierra A., Jomha N.M., Adesida A.B. Decreased hypertrophic differentiation accompanies enhanced matrix formation in co-cultures of outer

meniscus cells with bone marrow mesenchymal stromal cells. *Arthritis Res Ther.***14**:R153. 2012.

43. McCorry M.C., Puetzer J.L., Bonassar L.J. Mesenchymal Stem Cell Co-Culture with Meniscus Fibrochondrocytes Facilitates an Increase in Matrix Production. Proceedings of the Orthopaedic Research Society, New Orleans, LA. **Poster #1338**. 2014.
44. Vrancken A.C., Buma P., van Tienen T.G. Synthetic meniscus replacement: a review. *Int Orthop.***37**:291. 2013.
45. Makris E.A., MacBarb R.F., Responde D.J., Hu J.C., Athanasiou K.A. A copper sulfate and hydroxylysine treatment regimen for enhancing collagen cross-linking and biomechanical properties in engineered neocartilage. *FASEB J.***27**:2421. 2013.
46. Reiser K., McCormick R.J., Rucker R.B. Enzymatic and nonenzymatic cross-linking of collagen and elastin. *FASEB J.***6**:2439. 1992.
47. Robins S.P. Biochemistry and functional significance of collagen cross-linking. *Biochem Soc Trans.***35**:849. 2007.
48. Roy R., Boskey A.L., Bonassar L.J. Non-enzymatic glycation of chondrocyte-seeded collagen gels for cartilage tissue engineering. *J Orthop Res.***26**:1434. 2008.
49. Makris E.A., Hu J.C., Athanasiou K.A. Hypoxia-induced collagen crosslinking as a mechanism for enhancing mechanical properties of engineered articular cartilage. *Osteoarthritis Cartilage.***21**:634. 2013.
50. Kadler K.E., Holmes D.F., Trotter J.A., Chapman J.A. Collagen fibril formation. *Biochem J.***316 ( Pt 1)**:1. 1996.
51. Harris J.R., Soliakov A., Lewis R.J. In vitro fibrillogenesis of collagen type I in varying ionic and pH conditions. *Micron.***49**:60. 2013.
52. Su L., Cloyd K.L., Arya S., Hedegaard M.A., Steele J.A., Elson D.S., et al. Raman spectroscopic evidence of tissue restructuring in heat-induced tissue fusion. *J Biophotonics*. 2013.

53. Hwang Y.J., Lyubovitsky J.G. The structural analysis of three-dimensional fibrous collagen hydrogels by raman microspectroscopy. *Biopolymers*.**99**:349. 2013.

## CHAPTER 9

### **Tissue Engineering and Collagen Gels: A Total STEM Experience<sup>\*</sup>**

#### ***Preface***

During the course of my graduate studies, I had the privilege to participate in Cornell's Learning Initiative in Medicine and Bioengineering (CLIMB) GK-12 program funded by National Science Foundation (NSF). The program pairs graduate students with local area middle and high school teachers. The student and teacher work together to enhance the science curriculum by developing new inquiry based lessons and providing hands on science demonstrations. The program starts in the summer with a 6 week immersion term for the teacher. The teacher works in the lab alongside the graduate student gaining skills and an appreciation for research. During this time the student and teacher also begin to prepare an inquiry based curriculum and attend workshops weekly on inquiry based teaching. Then during the school year, the graduate student frequently visits the classroom to act as a science mentor and implement the developed curriculum.

I was paired with Lorraine Buckley, an AP biology teacher at Susquehanna Valley High School in Conkling, NY. During the summer of 2012, Lorraine spent 6 weeks in our lab learning how to create cell-seeded collagen gels and investigating the effect of riboflavin crosslinking on cell-seeded high density collagen gels. She gained a great appreciation for research and science that she then related back to her students at multiple times throughout the school year.

Lorraine and I worked together to develop an inquiry based curriculum. Since the students were in AP biology and about to graduate and head off to college, Lorraine

---

<sup>\*</sup> This chapter is in preparation for publication: Puetzer JL, Buckley, L, Archer, SD, Bonassar LJ. Tissue Engineering and Collagen Gels: A Total STEM Experience. In preparation

wanted a lesson that would help prepare them for college. She also wanted the lesson to cover a wide range of science, technology, engineering and mathematics (STEM) skills. We decided to create a lesson based around tissue engineering. Using tissue engineering, we were able to really capture the student's attention with the prospect of creating living tissues. We were also able to cover a wide range of STEM fields and demonstrate to the student that by using lessons they had already learned in biology, physics, chemistry, and mathematics they could achieve a lot. This was a very powerful lesson for showing the students how all of their core classes can work together and be applied in the real world.

Overall the students really enjoyed the inquiry based lesson. Students who typically were not interested in science became the most inquisitive and interested. At first the students were uncomfortable not being told exactly what to do. They would often ask if they had the right answer. This was a great way to demonstrate to them the scientific method and how in science we never know the correct answer from the beginning.

In addition to the inquiry based lesson, I represented a scientist in their classroom, providing examples of how the lessons they learned could be applied in the real world. As a mentor, I was able to go on a field trip with the class and have the class visit Cornell to see different labs. This was a great opportunity to really connect with the students of the class, talk with them about their future plans, and answer any questions they had about college. Additionally, of the nine students in the class, eight were females. It was especially rewarding to be able to be a mentor to each of them, and demonstrate to them how females can be involved in science.

The GK-12 program was an extremely rewarding experience. It allowed me to really hone my presentation and teaching skills. It taught me a lot about how to communicate science effectively and the value of inquiry based lessons to allow

students to truly grasp difficult science concepts. This experience has cemented my desire to teach and provided lessons I will carry with me the rest of my career. Further, it is my hope that the curriculum Lorraine and I developed can be a useful resource for others. In May I will adapt the lesson to give a crash course in tissue engineering to undergraduate and graduate students at the University of Puerto Rico in Mayaguez and then I hope to publish this lesson so it can be a useful resource for both high schools and undergraduate education. The remainder of this chapter will present the curriculum we developed, the worksheet for students, and an assessment quiz.

### **Introduction**

The objective of the following lesson is to provide the student with a total STEM experience by learning about tissue engineering, current research practices, and the principals of scientific inquiry. The student will investigate how collagen gels through ionic and thermogenic processes and the effect of these processes on the strength of collagen gels. In turn the students will learn what tissue engineers must keep in mind when developing new biomaterials and how the choices they make will affect the viability of the cells. This lesson will cover the NY State Math, Science and Technology Standards 1, 3, 4, 6 and 7 and should take 2-3 days over 80 minute class periods.

The lesson is composed of three experiments. In the first experiment the students will explore the effect of NaOH on collagen gelling. They will attempt to gel collagen using different concentrations of NaOH. They will see firsthand that although lower concentrations of NaOH may make a stronger gel, this will ultimately kills the cells by exposing them to too acidic of an environment. This lesson will

reinforce lessons of chemistry and pH, while demonstrating how chemistry plays a large role in cellular viability.

In the second experiment the students will explore how temperature affects the gelation of collagen. Contrary to what many of the students will assume, the collagen will gel best with heat due to the added energy the heat provides to the system. This lesson will reinforce lessons in physics and chemistry. Further by removing the collagen from heat and placing it on ice, it provides a clear example of how crosslinks work.

In the final experiment the students are challenged to use what they have learned about collagen to create the strongest gel possible while still keeping the cells alive. Encourage them to change anything they want to as long as the cells remain alive. They could attempt to mix it back and forth more or leave it on heat for a given amount of time. They can also attempt to use more collagen, but if they increase the amount of collagen used they will have to think about how to change the NaOH concentration to match. The students will have to work through the scientific method coming up with ideas, testing them, and repeating the process to continually improve their gels. This lesson will reinforce lessons in physics, mathematics, biology and chemistry.

At the completion of this curriculum the students will be able to carry on a conversation about tissue engineering and current research areas. Further, they will be able to define collagen and explain how collagen gels chemically and thermogenically. The students will gain hands-on experience with hydrogels and calculating their strength. In the end the students will have a complete STEM experience with concepts from physics, chemistry, mathematics, and biology reinforced. Further, they will have a better understanding of what must be considered when engineering tissues.

## ***Science Content for the Teacher***

### Tissue Engineering Content

Tissue engineering is a field that applies the principals of biology and engineering towards the development of biological substitutes that improve, repair or replace tissue function. It can be used for both therapeutic and diagnostic reasons. Traditional transplant surgeries are often plagued by limited supply of organs, long waiting lists, and possible immune rejection or disease transmission. Tissue engineering provides a solution to these problems by providing a means to create and grow new tissues, increasing the overall supply. Further engineered tissues are often made from the patient's own cells and biocompatible materials thus reducing the risk of infection. Finally, engineered tissues are living, growing materials and thus can grow with the patient or self repair. This provides a benefit over the traditional metal and polymer implants that often have shorter lifetimes.

There are three main components of tissue engineering; cells, scaffolds and signaling by chemical or mechanical stimulus. Tissue engineering consists of the combination of these components to create living tissues. The central idea is that cells are placed on a biodegradable scaffold. These scaffolds are usually in the shape of the tissue to be created and can be made from synthetic or natural materials. The cells then grow on the scaffold and with time produce their extracellular matrix (ECM: the material surrounding cells composed of proteins, carbohydrates and lipids). With time the scaffold degrades and is replaced by the cell-made ECM, thus resulting in a cell produced tissue. Chemical or mechanical stimulation can then be used to further simulate the cells to create their ECM and speed up the process. The signaling is especially important to encourage cells to produce the proteins necessary for the specific tissue being created, ie glycosaminoglycans for cartilage or insulin for the

pancreas. Once the engineered tissue is complete it can then be transplanted into the patient.

Students often are very interested in the different tissues that have been attempted to be engineered. On the Cornell BME Climb website a tissue engineering presentation is available which includes examples of some of these tissues including tissue engineered ears, heart valves, skin, bladders, wind pipes, blood vessels, heart patches, cartilage, bone, muscles, and menisci. Many of these, such as the skin, bladder and wind pipe have actually been implemented into the clinic and are successfully used to treat patients already. There are notes in the presentation on these tissues and a link to a very informative video on the process of tissue engineering an ear.

### Scaffold Content

The majority of this lesson will concentrate on the scaffold component of tissue engineering and the important things to keep in mind when selecting a scaffold for your engineered tissue. Scaffolds provide the structural support and shape to the construct. They provide a place for cell attachment and growth and are usually biodegradable and biocompatible. Scaffolds are characterized as either natural or synthetic. Natural scaffolds are often derived from the ECM components, are biocompatible, usually mechanically weak, and are somewhat preprogrammed to encourage cells to produce certain proteins. Examples of natural scaffolds include alginate derived from seaweed, decellularized organs, and collagen. Synthetic scaffolds are polymers, made by controlled repeatable processes. They range in degradation and mechanical properties, and have a range of biological responses. Examples include polyurethane, Teflon, polyethylene.

Properties that tissue engineers look for in scaffolds are biocompatibility, biodegradability, correct chemical and mechanical properties to mimic the desired tissue, proper geometry, and ability to be sterilized. It is important to use a scaffold which will degrade at a rate comparable to the amount of time it takes the cells to produce an ECM to replace it. Understanding this balance between degradation and new ECM is not well understood and is something the field is still trying to perfect. Additionally, scientist must keep in mind the optimal porosity and pore size of the scaffolds so that cells can infiltrate the scaffolds and still obtain nutrients from the media.

Finally, scaffolds can either be premade to the desired shape and seeded with cells on top, allowing the cells to infiltrate into the scaffold on their own, or the cells can be mixed into the scaffolds before they are gelled thus ensuring cells are well mixed throughout the scaffold in the beginning. Both these techniques have their positives and negatives. Scaffolds premade and seeded with cells later can often be stronger mechanically but take more time to culture as you wait for cells to infiltrate. Scaffolds with encapsulated cells allow for cells to be well spread throughout the scaffold to start with, however scaffold choices are limited to what can gel or harden without killing the cells. Often these scaffolds consist of hydrogels, such as alginate, agarose, or collagen where the gelation is caused by chemical or temperature changes that are not dangerous to the cell.

### Collagen Content

Collagen is a structural protein found in skin and connective tissues. It is the most abundant protein in the body, making up 25-35% of all proteins in the body. It can be found throughout the body in skin, fibrous tissues such as tendons and ligaments, cornea, cartilage, bone, blood vessels, the stomach, intervertebral discs, and the

meniscus. Collagen is a major component of the ECM and provides the structure and support for the cells.

Collagen's structure consists of 3 polypeptide chains wrapped together to form a tropocollagen structure similar to the double helix structure of DNA but with 3 strands instead of 2. The tropocollagen bundles together to form collagen fibrils, which further bundle together to form collagen fibers. This trend continues to form larger and larger fibers. A schematic of the collagen making up of tendons is provided in the tissue engineering presentation.

Collagen gels have been used in tissue engineering for decades. Collagen gels are a great choice of scaffold since it is the major component of a cells ECM and it is extremely biocompatible. Further, it can be formed into a gel, thus allowing the cells to be encapsulated within the scaffold before creation of the gel. There are a lot of factors that play into how collagen gels and this lesson will allow the students to investigate on their own how this process occurs.

Collagen gels are often derived in the laboratory from rat tail tendons. The tendons are pulled and dried. They are then placed in acetic acid for 48 hours. The collagen bundles are held together by numerous hydrogen bonds. When put in acid, the hydrogen bonds are broken as the strands protonate, or bind hydrogen atoms. When scientists are ready to create a collagen gel, they mix the acidic collagen solution with a base, raising the pH. As the pH rises the collagen strands deprotonate and reform the hydrogen bonds between the strands. Further, scientist put collagen gels in a heated environment to increase the gelation. The temperature adds energy to the system to allow the reactions to proceed. Thus collagen gels both chemically and thermogenically.

Using collagen in this lesson is beneficial since it gels in a complex way allowing for the students to use many fields, such as chemistry, physics and biology to

determine how it gels. Further students are interested in learning about collagen since they have heard a lot about its use in cosmetics.

### ***Preparation***

This curriculum is divided into a presentation and 3 experiments. For all the experiments you will need a source of collagen. If you have access to a centrifuge and lyophilizer the easiest way to gain this collagen is by pulling it from rat tails. If not, then collagen can be purchased online from sigma, however it can be expensive and you will most likely need to use smaller concentrations. A possible source is bovine achilles tendon sold in a 1 or 5 g bottle for \$50-100 (VWR catalog number AAJ60218-06). This will be more than enough collagen for the experiment but will not work as well as the rat tail collagen. Other sources of collagen can be found on Sigma's website by searching collagen.

If you do have access to a cooling centrifuge and lyophilizer, you can purchase frozen rat tails from Rockland antibodies and assays (catalog #RB-T297). Then about a month or more before you plan to do the curriculum you can have the students pull their own collagen. This can be a great way to start introducing them to collagen and they can see how strong it makes tendons. Further it's a great way to practice dissection skills. On the Cornell BME Climb website there is an additional presentation on collagen and rat tails.

#### How to pull collagen from the rat tails

- Cut a line down the length of the tail through the skin portion only.
- Starting at the base of the tail, peel the skin off.
- Using a rat-tooth forceps and starting at the tip of the tail, grab hold of the white tendons surrounding the tail and pull straight up out of the tail. Continue to pull the

tendons by working around the tail and then down toward the base. It is important to pull from the tip down to the base; if you pull from the base (ie where the tail would attach to the rat) it will be much harder to pull the tendons off the tail.

- If each student pulls 2 or more tails you should have plenty of collagen.
- Dry the tendons and weigh them.
- Then place the tendons in 0.1% acetic acid at 150 ml/gram for at least 48 hours and store in a refrigerator.
- After 48 hours centrifuge the collagen at 4500 rpm at 4°C for 90 mins to remove insolubilized collagen, blood, muscle tissue, ect.
- Collect the clear supernatant and discard the pellet.
- Freeze the clear supernatant overnight, and then place on lyophilizer until collagen is dry (takes around 5-7 days)

Whether you purchased collagen or pulled it from rat tails, you will now weigh the dried collagen and reconstitute it in 0.1% acetic acid at 20 mg/ml. This will take a week or two to reconstitute and you should shake it occasionally to ensure it reconstitutes correctly. Store in the refrigerator and it will be good for years.



**Figure 9.1:** Supplies needed for each group

Supplies for each group (Figure 9.1)

- 20 ml of 20 mg/ml collagen (keep on ice throughout the experiments)
- 25 ml each of working solution with 0.1%, 2.5%, and 5% NaOH
- 20 ml 1x PBS mixed with Phenol Red dye (labeled media on worksheet)
  - o 15 mg/L of Phenol Red dye
  - o Powder PBS can be purchased from VWR (#45000-442 )
- 3- 3ml syringes
- 1 three-way stopcock
- 1 precision syringe tips – wide bore
- Beaker with water to clean out syringes between trials
- Glass plate or petri dish

The working solution consists of 10x PBS, 1xPBS, and 1N NaOH. The following concentrations are based on a 20 mg/ml collagen solution. If you use a different collagen solution numbers will need to change.

**Table 9.1 Collagen Working Solutions**

<b>1% NaOH Working Solution</b>	<b>2.5% NaOH Working Solution</b>	<b>5% NaOH Working Solution</b>
10ml 10x PBS	10ml 10x PBS	10ml 10x PBS
14.25ml 1x PBS	13.3ml 1x PBS	11.25ml 1x PBS
0.75ml 1N NaOH	1.7ml 1N NaOH	3.75 1N NaOH

For experiment 2 you will additionally need ice and a hot plate set to ~37°C and for experiment 3 you will need a ruler, scale and small weights.

***Classroom Procedure***

DAY 1: 80 min class period

*Engage (Time: 20 mins )*

The lesson can begin by engaging the students by providing background on what tissue engineering is and the importance of scaffolds. Presentation with notes is posted on the Cornell BME Climb website. Finish the lesson with an introduction to collagen. Further explain that in order to use collagen gels in tissue engineering we must first obtain it from tendons. Explain how researchers pull tendons from rat tails and place it in acetic acid to lower the pH. This breaks the hydrogen bonds and solubilizes the collagen. Ask them to think about how we might be able to make this collagen gel to form engineered tissues.

## Experiment 1: The Effect of NaOH

*Engage (Time: 5 mins )*

You can introduce the first experiment by telling the students they are all now researchers in a lab and you need them to determine how collagen gels so that we may create an engineered tissue. You want them to be able when all three experiments are over to provide you with a protocol for developing the strongest collagen gel they can make while still keeping the cells alive. Make sure to stress they must keep the cells in mind throughout the entire experiment.

For all the experiments the students will fill one syringe each with 0.3 ml working solution, 0.8 ml collagen, and 0.3 ml media (in this case the media is water with phenol red dye indicator, however if it were a real experiment the media would be where the cells are located). Demonstrate filling each syringe and remove as many air bubbles as possible. A syringe tip may be needed to suck collagen up into the syringe. Then hook the working solution and collagen syringe to the three way stopcock and clear out as much air as possible. Shut off the valve of the three way stopcock that does not have a syringe and mix the collagen and working solution back and forth about 10-20 times. Then quickly remove the empty syringe, and replace it with the media. Mix the media and collagen/working solution back and forth about 10-20 times. Finally, quickly flip the 3-way stop cock to the empty syringe and inject the collagen mixture onto the glass plate.

Demonstrate using the 2.5% working solution so you can show them how gelled collagen should appear. It should be a solid gel and still pink in color. After each gel, have the students rinse the syringes and stopcock out in a beaker of distilled or deionizer water.

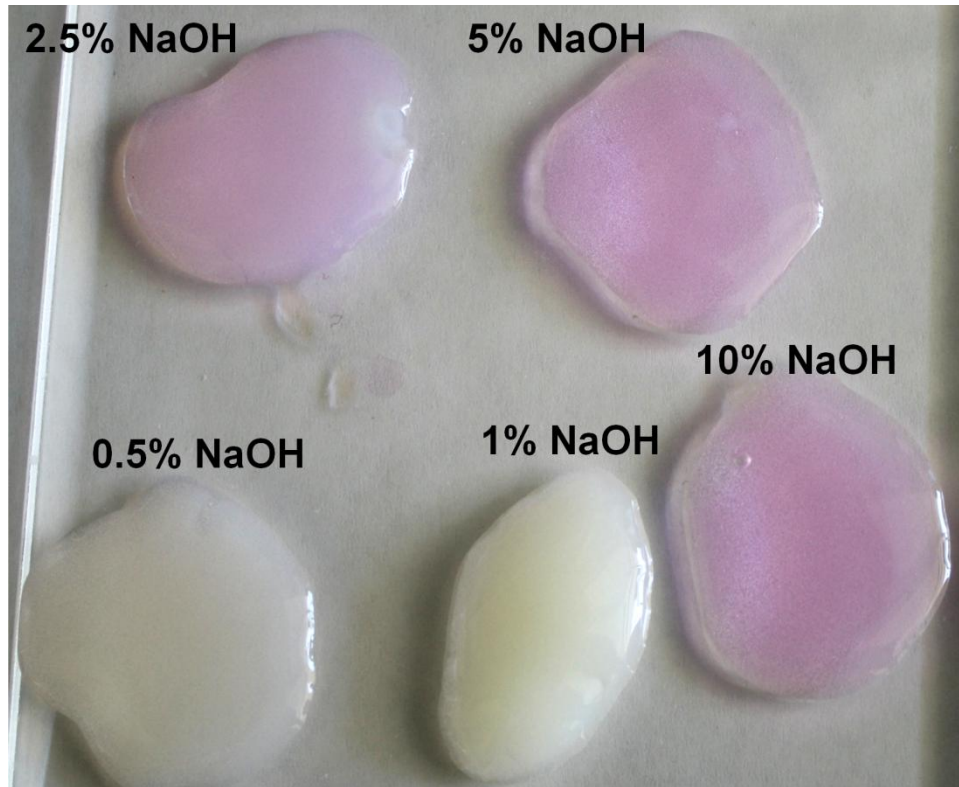


**Figure 9.2:** Examples of collagen gels made with different NaOH concentrations

*Explore (Time: 20 mins)*

Allow the students to work through Experiment 1 worksheet. It will require them to form a hypothesis, write down their observation, results, and determine if their hypothesis was correct. Remind them to pay attention to how long it took to gel, the color of the gel, and how well it gelled. This will be repeated in all experiments and is an excellent example of the scientific method and how it is a repetitive process. Figure 9.2 has representative examples of what the collagen gels will look like at different concentrations of NaOH.

*Explain and Expand (Time: 10 mins)*

Once the students are done, ask them which concentration of NaOH they would suggest to use. 5% should not gel, 1% will gel very quickly and strongly but the phenol red should change the gel to a yellow color indicating it is very acidic, while the 2.5% will be pink and strong. The students should suggest 2.5%, however if they do suggest the 1% remind them about the cells. You can discuss how Phenol red is a pH indicator, and when it is pink or red the cells are happy, however when it changes to yellow it is very acidic and the cells will die.

You can then ask them why 2.5% worked. Guide them by reminding them that you made the tendons liquid to start with by putting it in an acidic solution and breaking the hydrogen bonds. You can go further and ask them what pH an acidic solution is and what pH is a measure of. They can start to figure out that a low pH means there are a lot of hydrogen ions in the solution and they attach to the collagen strands causing them to disconnect from each other.

Then ask them what NaOH is, ie is it a base? You can guide them to the answer by talking about their observation with phenol red. You can explain phenol red is a dye indicator that is red or pink around pH of 7, but turns yellow at lower pH and purple at high pH. If you go back to thinking about the colors of the gels, they can determine NaOH is a base and must be raising the pH of the collagen solution.

Finally you can explain how as the pH rises, there are more OH<sup>-</sup> ions in the solution. The OH<sup>-</sup> ions pull the hydrogen ions off the collagen strands and open up places for the collagen strands to interact and form bonds again, thus the collagen gels.

Experiment 2: The Effect of Temperature

*Explore (Time: 15 mins)*

Have the students continue working on the worksheet on experiment 2. This time they can use the NaOH solution they found worked best to make all their collagen gels. They should inject the collagen solution onto a glass plate cooled on top of ice or onto a glass plate on a heat plate set to  $\sim 37^{\circ}\text{C}$  (Figure 9.3). This will work best if the glass plates on the ice and hot plate have had plenty of time to cool off or heat up before the collagen is injected onto the plates. Also, make sure the hot plate is not too hot, if it is over  $\sim 39^{\circ}\text{C}$  it will begin to cook the collagen make it so it does not gel at all.

You can encourage them to record results such as time it takes to gel. They could even repeat it a few times and create a graph with their findings. Also, as before they should pay attention to how well it gels and its color.

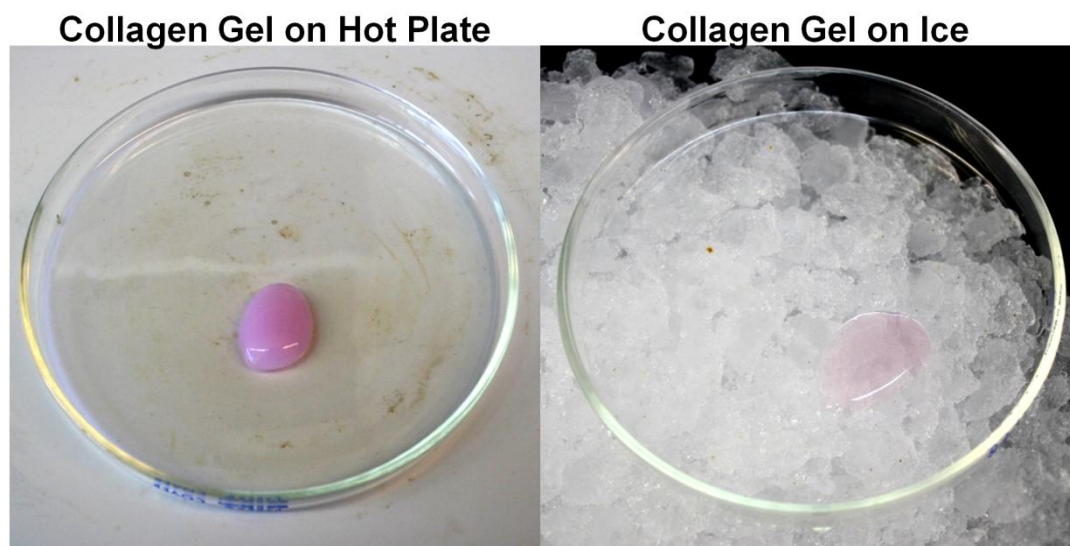


**Figure 9.3:** Examples of collagen gels on hot plate and ice

*Explain (Time: 5 mins)*

Ask the students what the effect of temperature was. The collagen on heat should gel immediately while the collagen on the cold will not gel at all. You can ask them why they think the one on heat gelled, while the cold did not. Most of the

students will assume the collagen would have gelled on the cold and melted on the heat. You can guide them to why the heat gelled by explaining heat is a form of energy and thus it is providing energy for the bonds (crosslinks) to occur between the collagen strands.

*Expand (Time: 5 mins)*

You can demonstrate that in fact the heat has allowed for the crosslinking to occur by telling the students to put their hot gelled collagen onto the ice. If the crosslinks have not formed the collagen should return to a liquid on the ice, however it will remain a solid thanks to the crosslinks.

***Day 2: 80 min class period***

Experiment #3: Recommend a Formula to make a Collagen Gel

*Engage (Time: 5 mins )*

Challenge the students to develop the strongest collagen gel possible while still keeping the cells alive. You can even provide a prize for the team that makes the strongest gel! Tell them they are the researchers and they make the decisions. Make sure they work through the worksheet and develop hypothesis for each experiment. This demonstrates that research is a repetitive process where you constantly make changes and repeat.

*Explore (Time: 60 mins)*

They should have all the supplies from the previous two experiments. Encourage them to change anything they want to as long as the cells remain alive. They could attempt to mix it back and forth more or leave it on heat for a given amount of time. They can also attempt to use more collagen, but if they increase the amount of

collagen used they will have to think about how to change the NaOH concentration to match. Also, encourage them to be very specific in how they are making their gels, so they can accurately report how they made each gel (ie, how long left on heat, amounts mixed, amount of times mixed back and forth).

The students will test the strength of their gel by using the set up shown in Figure 9.4 and the formulas  $\text{stress} = \text{Force}/\text{Area}$  and  $\text{Force} = \text{mass} \times \text{acceleration}$ . They will make their collagen gels on the glass plates, slide it into the rack and then put an empty conical tube on top. They can then fill the conical tube with water slowly until the gel breaks. Once the tube is full of water they can begin putting circle weights on top of the tub slowly until the collagen breaks. After it breaks they can use a scale to determine how much the conical tube, water and weights all weigh together. This will provide the mass the gel can take, and the area can be obtained by calculating the area of the bottom of the conical tube.

Allow the students to try many variations. You can report the strongest gel stress throughout class also to drive the competition. If you have extra collagen it can be fun to provide a little 30 mg/ml collagen for the students to attempt to make gels with also. The higher concentration of collagen will make a stronger gel.

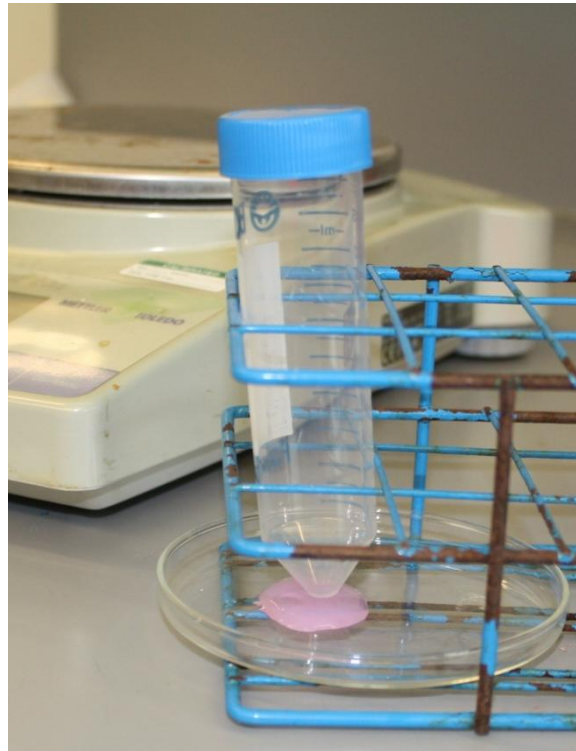


**Figure 9.3:** Strength test setup

*Explain (Time: 5 mins)*

You can explain a little about why as scientist we would choose to use stress instead of force to examine the strength of the gels. Explain how the same force applied over different areas causes very different stress, such as if a pencil and a thumb are pushed into a surface at the same force, the pencil will have a much bigger stress than the thumb.

The students may often ask for the right answer. This is a great opportunity to explain in research there is no right answer, and it is all about making educated guess and then testing those ideas.

*Expand (Time: 10 mins)*

Students can present their finds to the class and discuss what they found works and what didn't work. They can also be required to write up the protocol, or present a graph of their different stress calculations.

### **Assessment**

Assessment was performed using the attached assessment quiz. Students took the quiz before and several days after the activity to gauge their new understanding of tissue engineering and collagen. To reinforce how science needs to be communicated, students can be required to present their protocols for the strongest gel to the class as a presentation or protocol write up.

### **Safety**

Safety concerns are minimal; however, students should be required to wear gloves to promote proper lab safety and should be cautious around hot plates and syringe tips.

## **Student Worksheet**

### **Tissue Engineering using Collagen Gels**

You are now undergraduate researchers and I need you to determine how collagen gels and provide me with a protocol for developing the strongest collagen gel you can make while still keeping our cells alive.

For all of the following experiments you will do the following for mixing.

- 0.3 ml working solution
- 0.8 ml collagen
- 0.3 ml media

#### **Experiment 1: The Effect of NaOH**

Investigate the effects of NaOH in the gelling of collagen. *Remember the cells must stay alive during the mixing and the media contains phenol red which is a dye indicator for pH.*

#### **Supplies**

- 20 ml of Collagen (keep this on ice throughout the experiment)
- 25 mls each of working solution with 1%, 2.5%, and 5% NaOH
- 20 mls of media
- 3 syringes
- 1 three-way stopcock
- 3 precision syringe tips
- Beaker with water to clean out syringes between trials

#### **Experimental procedure**

1. What do you know already? Think about the current state of the collagen, NaOH, and media.
2. What is your hypothesis? Be specific!!
3. Observations and Results...(i.e. color, time to gelling, ect)
4. Was your hypothesis correct? Do you need more testing?

## **Experiment 2: Effect of Temperature**

### **Supplies**

- 20 mls of Collagen (keep this on ice throughout the experiment)
- 20 mls each of working solution with 0.5%, 2.5%, and 10% NaOH
- 20 mls of media
- 3 syringes
- 1 three-way stopcock
- 3 precision syringe tips
- Beaker with water to clean out syringes between trials
- Bucket of ice
- Hot plate set to  $\sim 37^{\circ}\text{C}$

### **Experimental procedure**

1. What do you know already? What observations can you make?

2. What is your hypothesis? Be specific!!

3. Observations and Results

4. Was your hypothesis correct? Do you need more testing?



## Assessment Quiz (answers in red)

### Tissue Engineering Assessment

- 1. What is Tissue Engineering? (Explain in 1-2 sentences) What are the 3 components of Tissue Engineering?**

Tissue Engineering is a field that applies the principals of biology and engineering toward the development of biological substitutes that improve, repair or replace tissue function.

The 3 components are cells, scaffolds and signaling (chemical or mechanical stimulus).

- 2. What is collagen?**

Collagen is a structural protein found in skin and connective tissues. It is the most abundant protein in the body, providing structure and support.

- a. Where is it found?**

Skin, fibrous tissue, tendons, ligaments, cornea, cartilage, bone, blood vessels, stomach, ect.

- b. What does it do?**

Provides structure and support

- c. How can we use it in Tissue Engineering?**

It can be used as a scaffold or gel to grow cells on and create engineered tissues

- 3. How does collagen gel ( e.i. ionically, thermogenically, chemically, mechanically)? Provide details on how this gelling process occurs.**

Collagen gels chemically and thermogenically. First NaOH is added to raise the pH of the acidic collagen solution, causing hydrogen ions to release from

the collagen strands. Then heat is used to add energy to the system allowing for bonds to form between the collagen strands resulting in a hydrogel.

- 4. What are some considerations when Tissue Engineering and working with cells? Specifically, what are some considerations for the scaffold you use and the process you use for creating your scaffold?**

Biocompatibility, biodegradability, properties, geometry, pore size, ability to sterilize.

Must consider how scaffolds are made and whether cells will be seeded after they are formed or before they are formed.

- 5. What is the mathematical formula for calculating stress?**

Stress = Force/Area

## APPENDIX A

### Matlab Code for Collagen Bundle Analysis

The following code was written in MATLAB to analyze collagen bundle formation in picrosirius red images of alginate menisci (Chapter 3). The code isolates collagen bundles based on color, size, and shape. It provides a collagen bundle count and area for each image. In chapter 3, data from the code was collected and analyzed to determine the percentage of fibers per samples, the average number of collagen bundles per mm<sup>2</sup>, and the average size of collagen bundles. The code was written for use with brightfield picrosirius red images and would need color modification to be used with different stains. Code developed by Derin Sevenler and Jenny Puetzer.

```
clear
I = imread('im3.jpg');
red = I(:,:,1);
green = I(:,:,2);
blue = I(:,:,3);
close all

k = red - green;
se = strel('disk',3);

figure; imshow(I);
title('click on a fiber (preferably the darkest one)');
[c r] = ginput(1);
c = floor(c);
r = floor(r);
fiber_val = mean(mean(green((r-5):(r+5),(c-5):(c+5))));
k(green<(fiber_val-25)) = 0;
```

```

% Convert to black-white
k = imdilate(k,strel('disk',2));
thresh = graythresh(k)+.05; %was .07
bw = im2bw(k,thresh);

% Dilate, fill and remove artifacts by filtering
n = bwareaopen(bw,500); %was 100
n = imdilate(n,se);
n = imfill(n,'holes');
n = bwareaopen(n,500);
n = imdilate(n,strel('disk',5));
n = imfill(n,'holes');
figure; imshow(n);

% Detect boundaries in bw image
[B,L] = bwboundaries(n,'noholes');
stats = regionprops(L,'Area','Centroid', 'Perimeter');
num_fibers = length(B);
% Display the label matrix, and determine fiber properties and store them in an array

areas = zeros(size(B));
perimeters = areas;
imshow(label2rgb(L, @jet, [.5 .5 .5]));
hold on;
for k = 1:num_fibers
    boundary = B{k};
    plot(boundary(:,2), boundary(:,1), 'w', 'LineWidth', 2)
    areas(k) = stats(k).Area;
    perimeters(k) = stats(k).Perimeter;
end
areas
total_area = sum(areas)
fprintf('number of fibers is %1.0f \n',num_fibers);

```

## APPENDIX B

### Investigation of Riboflavin Treatment of High Density Collagen Gels

#### Introduction

In chapter 5, high density collagen menisci exhibited significant contraction. By 4 weeks of static culture both 10 and 20 mg/ml collagen menisci had a 40% reduction in area and mass. It has been reported a deviation of more than 10% in meniscal size can result in detrimental loading across the joint<sup>1</sup>, thus it is important to control contraction. Photochemical crosslinking with riboflavin has been used both by our lab<sup>2</sup> and others<sup>3</sup> to slow contraction in low density cell-seeded collagen gels with minimal affect on viability. However, the effect of riboflavin crosslinking on high density collagen gels and large constructs such as the meniscus was unknown. We hypothesized photochemically crosslinked high density type I collagen gels would produce constructs with less contraction, while maintaining biochemical properties similar to non-crosslinked menisci.

#### Materials and Methods

Meniscal constructs were fabricated as described in chapter 5<sup>4</sup>. Briefly, type I collagen was extracted from rat tails and reconstituted at 20 and 30 mg/ml using previously established techniques<sup>5, 6</sup>. The collagen was then returned to neutral pH and osmolarity with NaOH and PBS to begin the gelation process<sup>5, 6</sup>. This collagen solution was immediately mixed with bovine meniscal fibrochondrocytes and injected into meniscal molds<sup>4</sup>. The molds were allowed to gel at 37°C for 50 minutes to obtain 10 and 20 mg/ml collagen menisci at  $25 \times 10^6$  cells/ml. The following day riboflavin treated menisci were incubated in 0.25mM riboflavin in PBS at 37°C for 2 hours and then exposed to 458nm light for 40 seconds to induce crosslinking<sup>3</sup>. Following

crosslinking, riboflavin-PBS solution was replaced with fresh meniscal media<sup>4</sup>. After 24 hours, cell culture media was changed again to wash out excess riboflavin. Both riboflavin treated and untreated menisci at 10 and 20 mg/ml collagen concentration were cultured for up to 4 weeks.

Upon completion of culture, menisci were processed as described in chapter 5<sup>4</sup>. Briefly, photographs taken throughout culture were analyzed with ImageJ to track contraction. Tissue samples, from the face, center and bottom were analyzed biochemically. The samples were weighed wet (WW), frozen, lyophilized, and weighed again to obtain dry weight (DW) and analyzed for DNA, GAG and collagen content via the Hoechst DNA assay<sup>7</sup>, a modified DMMB assay<sup>8</sup>, and a hydroxyproline assay<sup>9</sup>, respectively. All data were analyzed using 2 or 3 way ANOVA with Tukey's t-test for post-hoc analysis ( $p < 0.05$  for significance), and expressed as mean $\pm$ SD.

## **Results**

Riboflavin treated menisci maintained their size for 1-1½ weeks and then significantly contracted to match untreated meniscal size by 4 weeks of culture (Figure B.1). 20 mg/ml treated menisci maintained their size longer than 10mg/ml treatment menisci.

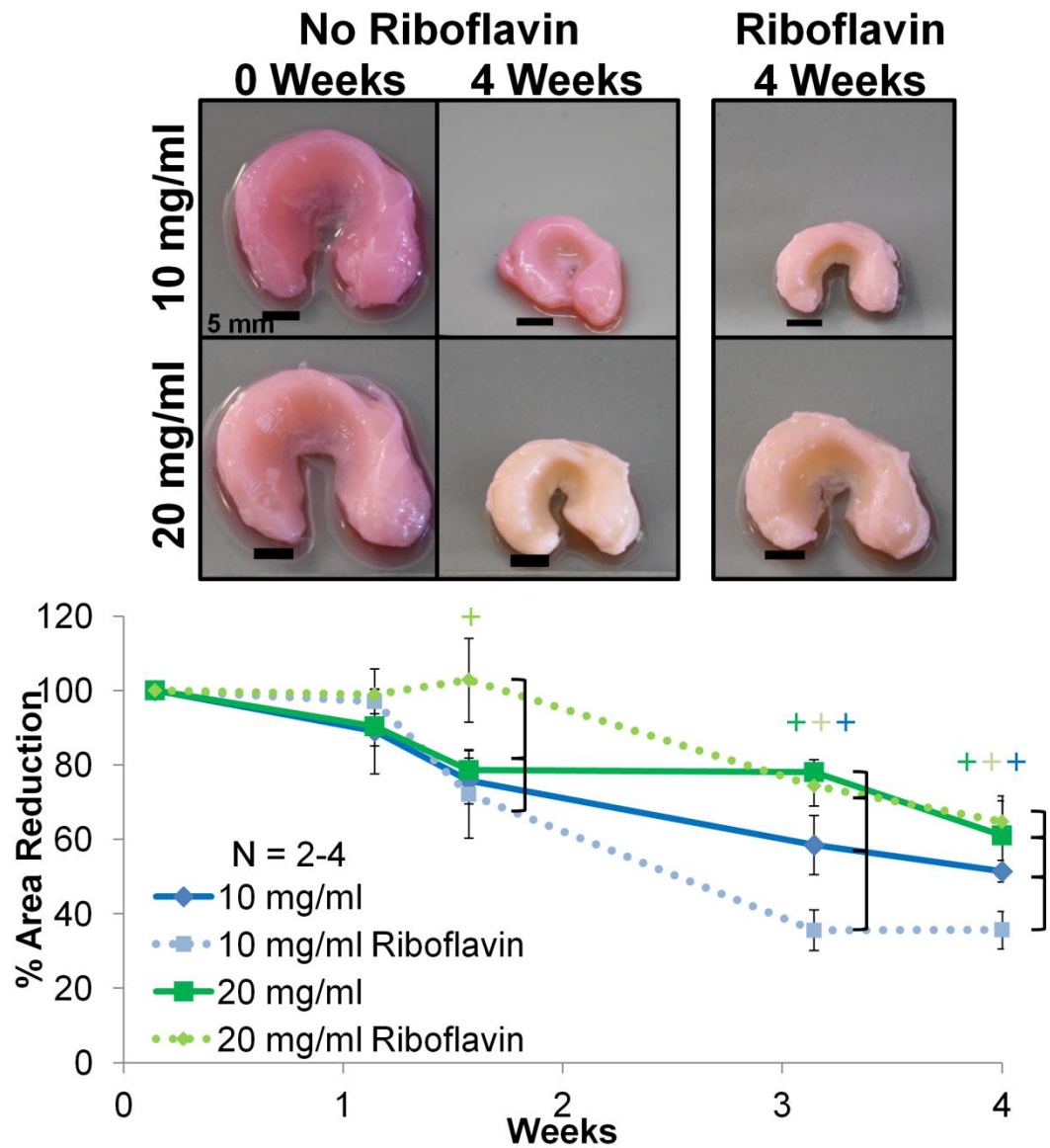


**Figure B.1:** Photographs of constructs and percent area retention of collagen menisci with time. + significance between bracket groups ( $p < 0.05$ )

Riboflavin treatment did result in a significant drop in DNA content by 4 weeks of culture compared to untreated menisci at 0 and 4 weeks (Figure B.2). Both treated and untreated menisci had significant increases in GAG and collagen content by 4 weeks. When GAG content was normalized to DNA content to account for the decrease in DNA in riboflavin treated menisci, both treated and untreated menisci

accumulated the same amount of GAG by 4 weeks. All menisci had similar levels of collagen concentration by 4 weeks as well, reflecting the uniform 40-50% contraction of the scaffolds by 4 weeks.

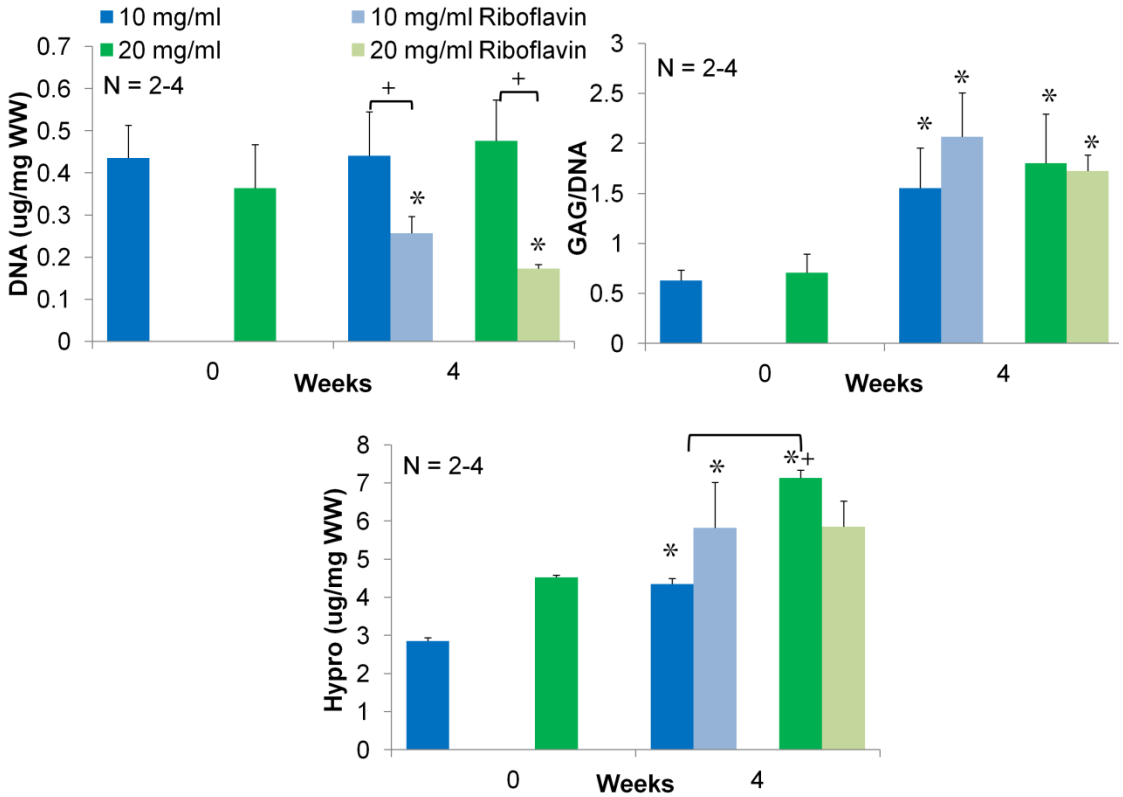


**Figure B.2:** Biochemical content in scaffolds. DNA and hypro normalized to wet weight and GAG normalized to DNA. Significance compared to \*0 week and + bracket groups ( $p < 0.05$ )

### Discussion

Riboflavin treatment slowed contraction for 1-1½ weeks in high density collagen menisci; however it had no affect on long term culture. Additional treatments of riboflavin may be needed to slow contraction for longer periods of time. Riboflavin treatment resulted in a decrease in viability as indicated by a decrease in DNA at 4 weeks; however biochemical production of the cells was not affected. All menisci had

significant increase in GAG accumulation and collagen concentration by 4 weeks, most likely due to the overall contraction of the scaffolds.

As discussed in chapter 5<sup>4</sup>, contraction is an inherent properties of cell-seed collagen gels, which decreases with increasing concentrations of collagen<sup>6, 10, 11</sup>. This contraction is beneficial since it results in increased collagen density, biochemical properties, mechanical properties, and improved collagen organization. Thus limiting contraction long-term with multiple treatments of riboflavin may not be the optimal choice for ensuring the constructs are appropriately sized. The contraction can be accommodated for since it is uniform and consistent. Molds could be oversized and constructs could be allowed to contract to a given size to increase biochemical and mechanical properties. Riboflavin could then be used to stop or slow contraction at the desired size and properties. Riboflavin treatment is a promising final treatment option before removing menisci from culture. Future studies should investigate multiple treatments of riboflavin and the depth penetration of the light during riboflavin treatment.

## REFERENCES

1. Dienst M., Greis P.E., Ellis B.J., Bachus K.N., Burks R.T. Effect of lateral meniscal allograft sizing on contact mechanics of the lateral tibial plateau: an experimental study in human cadaveric knee joints. *Am J Sports Med.***35**:34. 2007.
2. Mozia R.I., Bowels R., Saroka J., Gebhard H., Hartl R., Bonassar L.J. Riboflavin crosslinking of composite tissue engineered intervertebral discs. presented at the" 2011 Annual Meeting of the Orthopaedic Research Society, Long Beach, California, Year.
3. Ibusuki S., Halbesma G.J., Randolph M.A., Redmond R.W., Kochevar I.E., Gill T.J. Photochemically cross-linked collagen gels as three-dimensional scaffolds for tissue engineering. *Tissue Eng.***13**:1995. 2007.
4. Puetzer J.L., Bonassar L.J. High density type I collagen gels for tissue engineering of whole menisci. *Acta Biomater.***9**:7787. 2013.
5. Bowles R.D., Williams R.M., Zipfel W.R., Bonassar L.J. Self-assembly of aligned tissue-engineered annulus fibrosus and intervertebral disc composite via collagen gel contraction. *Tissue Eng Part A.***16**:1339. 2010.
6. Cross V.L., Zheng Y., Won Choi N., Verbridge S.S., Sutermaster B.A., Bonassar L.J., et al. Dense type I collagen matrices that support cellular remodeling and microfabrication for studies of tumor angiogenesis and vasculogenesis in vitro. *Biomaterials.***31**:8596. 2010.
7. Kim Y.J., Sah R.L., Doong J.Y., Grodzinsky A.J. Fluorometric assay of DNA in cartilage explants using Hoechst 33258. *Anal Biochem.***174**:168. 1988.
8. Enobakhare B.O., Bader D.L., Lee D.A. Quantification of sulfated glycosaminoglycans in chondrocyte/alginate cultures, by use of 1,9-dimethylmethylene blue. *Anal Biochem.***243**:189. 1996.
9. Neuman R.E., Logan M.A. The determination of hydroxyproline. *J Biol Chem.***184**:299. 1950.
10. Bell E., Ivarsson B., Merrill C. Production of a tissue-like structure by contraction of collagen lattices by human fibroblasts of different proliferative potential in vitro. *Proc Natl Acad Sci U S A.***76**:1274. 1979.

11. Vernon R.B., Sage E.H. Contraction of fibrillar type I collagen by endothelial cells: A study in vitro. *Journal of Cellular Biochemistry*.**60**:185. 1996.

## APPENDIX C

### MATLAB Code for Fiber Alignment and Diameter

The following code was written in MATLAB using fast Fourier transforms to analyze collagen fiber alignment and diameter in confocal images (Chapter 6 and 7). The code is not limited to confocal images, and could be used to analyze any image, include images from brightfield, fluorescence, or second-harmonic generation (SHG). This version of the code builds on a previously reported MATLAB code used to analyze the alignment of collagen fibers in SHG images<sup>1</sup>. This code will determine the major angle of alignment, the alignment index, the smallest fiber diameter, and mean fiber diameter. The code has been validated with ImageJ diameter calculations and analysis of phantom images with set alignment and diameter sizes. Further, major angle of alignment measurements are calculated using fast Fourier transforms and radon transforms for comparison and validation.

The code contains the programs, diameter.m, fourierTransform.m, radonTransform.m, sumangle.m, allindex.m, and CalculateDiameter.m . Diameter.m is the main program and will call the rest of the files. The theory for this technique is discussed in the methods of Chapter 6. This code is written by Robby Bowles, Esther Koo, and Jenny Puetzer.

#### ***Diameter.m***

%Diameter code using a 2D Fast Fourier Transform and Radon Transform.

%Will calculate the diameter of confocal meniscus fibers and indicate

%the alignment of those fibers. Data is saved into an EXCEL file.

%-----%

clear all

close all

```

prompt = 'Name of the image? \n';
result = input(prompt);

%Call up image and show it
Im1 =(result);
A = imread(Im1);
s1 = figure;
subplot(3, 3, 1);
squareImage = imresize (A, [512 512]);
imshow(A);

%Resize and convert to grayscale if necessary
n = ndims(A);
grayImage = squareImage;

if n == 3           %If original image is color
    grayImage = rgb2gray(A);
end

imshow(grayImage)
title('Original Image')

%Obtain fft2 of image
transformedImage1 = fourierTransform(grayImage);

%Radon Transform of the fourier transformed image
[rotateAngle, valueAtAngle, radonMatrix, vectorLoc, rawAngle] =
radonTransform(transformedImage1);

%Uncomment the following three lines to see a graphical representation of how
%the Radon transform works

```

```

%figure
%plot (vectorLoc, radonMatrix(:,rotateAngle))
%title('Radon Tranform 1')

%figure
figure(s1)
subplot (3,3,2)
image(transformedImage1)
axis square
title('FFT2 Transform')
%pause

%Determine alignment index
[highestFreqAngle, freqNumber, SInfo] = sumangle (transformedImage1) ;
highestFreqAngle
[Index, AlignmentIndex] = allindex (SInfo);
fprintf('Alignment Index is %c\n', AlignmentIndex)

%Plot histogram of data
subplot (3,3,3)
plot(radonMatrix);
title('Angle Histogram Data')

%Rotate orginal image by rotateAngle clockwise and display
B = imrotate (grayImage, -rotateAngle);
%B = imrotate (grayImage, -105);
subplot(3,3,4);
%squareImage = imresize (B, [512 512]);
%image(squareImage);
figure
image(B);
axis square
title('Rotated Image')

```

```
pause
```

```
%Crop image to a desired size and resize to original image dimensions
```

```
%C = imcrop (squareImage,[150 200 200 200]);
```

```
C = imcrop(B, [150 150 350 350]);
```

```
E = imresize (C, [512 512]);
```

```
figure
```

```
image(E)
```

```
pause
```

```
%Take a fft2 of the rotated image
```

```
transformedImage2 = fourierTransform(E);
```

```
subplot(3,3,5)
```

```
image(transformedImage2)
```

```
axis square
```

```
title('FFT2 Transform2')
```

```
%Second Radon Transform
```

```
[rotateAngle2, valueAtAngle2, radonMatrix2, vectorloc2, rawAngle2] =
```

```
radonTransform(transformedImage2);
```

```
%Uncomment the following three lines to see how the Radon Transform works
```

```
% figure
```

```
% plot (vectorLoc, radonMatrix(:,rotateAngle))
```

```
% title('Radon Tranform 2')
```

```
figure(s1)
```

```
subplot (3,3,6)
```

```
plot(radonMatrix2);
```

```
title('Angle Histogram Data')
```

```
%Determine what portion of the fft image to generate a histogram from
```

```
x3Min = 1;
```

```

x3Max = 512;
y3Min = 1;
y3Max = 512;
smallerMatrix = zeros(1,size(transformedImage2,2));
for x3 = x3Min:x3Max
    for y3 = y3Min:y3Max
        smallerMatrix (x3, y3) = transformedImage2(x3,y3);
    end
end

%Calculate the span of the histogram (where values of matrix are not zero)
smallerMatrixSum = sum(smallerMatrix);
span = 0;
for vl = 1:size(smallerMatrixSum, 2)    %vl = vector index
    if smallerMatrixSum(vl)>0
        span = span+1;
    end
end

%Calculate the span by first appearance of nonzero
ind = find(smallerMatrixSum, 1, 'first')
ind2=find(smallerMatrixSum,1, 'last')
smallspan=ind2-ind;
new_diameter=CalculateDiameter(smallspan, A)

%Calculate the corresponding diameter in micrometers
micrometerDiameter = CalculateDiameter(span, A);
fprintf('The span is %d pixels, and the diameter is %6.4f micrometers \n', span,
micrometerDiameter)

subplot(3,3,8)
hold on

```

```

plot (smallerMatrixSum)
xlabel('location')
ylabel('number of dots')
hold off

%calculate span of average size
m = mean(nonzeros(smallerMatrixSum(1:257)));
%m = mean(nonzeros(smallerMatrixSum));
spanmean = 0;
for vl = 1:size(smallerMatrixSum, 2)      %vl = vector index
    if smallerMatrixSum(vl)>m
        spanmean = spanmean+1;
    end
end
halfSpanm = spanmean/2;
diameter = 512/halfSpanm
mean_micrometerDiameter = diameter /2.78

ind3 = find(smallerMatrixSum >= m, 1, 'first')
ind4 = find(smallerMatrixSum >= m, 1, 'last')
mean_span = ind4-ind3
mean_diameter = CalculateDiameter(mean_span, A)

%Identify the peak in the angle histogram
%C is the max number of dots, I is the location of the max number
[C,I] = max(smallerMatrixSum);

%Export data to Excel file
d = {'Image Name', 'Alignment Index', '1st Angle', '2nd Angle', 'Span (pixel)', 'Diameter (um)', 'Mean Diameter (um)', 'New Diameter (um)', 'Mean_diameter (um)';...
    result AlignmentIndex rotateAngle rotateAngle2 span micrometerDiameter
    mean_micrometerDiameter new_diameter mean_diameter};
[fileName, pathName] = uiputfile('*.xls', 'Save File');

```

```
disp(fileName)
xlswrite(fileName, d, 'FirstImage', 'E1');
```

```
%Open up recently created file
winopen(fileName)
```

### ***fourierTransform.m***

```
function [outputImage] = fourierTransform(inputImage)
```

```
F=fftshift(fft2(inputImage));
[x,y] = size(inputImage);
```

```
%Create Magnitude image(matrix) of FFT
```

```
for i=1:x
    for j=1:y
        M(i,j)=sqrt(real(F(i,j))^2 + imag(F(i,j))^2); %magnitude of FFT
    end
end
```

```
%Scale image matrix and set threshold to 350
```

```
outputImage =M*.01;
contrastThreshold = 350;
```

```
%Contrast Image
```

```
for i = 1:x
    for j =1:y
        if outputImage(i,j)< contrastThreshold
            outputImage(i,j) = 0;
        else
            outputImage(i,j) = 1000;
        end
    end
end
```

end

### ***radonTransform.m***

```
function [angle, maxval,R, xp, maxloc_col] = radonTransform(fftlImage)

theta = 0:1:190;
[R, xp] = radon(fftlImage, theta);
%xp is a vector containing the locations of the projections

%Find the value of the maximum projection, and note the indices of where it is in the
%matrix
[maxval, maxloc] = max(R(:));

%Convert the index to a real number
[maxloc_row maxloc_col] = ind2sub(size(R), maxloc);

%Adjust the value of the angle to be measured from the horizontal axis
Adjustedmaxloc_col = abs(maxloc_col+90);
fprintf('Location of max value is at (%d, %d) at %d degrees \n', maxloc_row, maxval,
Adjustedmaxloc_col)
angle = Adjustedmaxloc_col;
%There is an error of about +/- 2 degrees, and so need to account for that

end
```

### ***Sumangle.m***

```
function [maxAngle, maxNumberDots, S] = sumangle(image) %Value of is needed for
allindex func
clear H
```

```

clear S

%0 degrees
clear Q
clear a %angle from 0 degrees
clear ps1
clear n
clear i
clear j
a = 1;
try
  for n = 1:256
    j = 256;
    for i = 256:1:512
      Q(i,j)=image(i,j);
    end
  end
end
ps1 = sum(Q);
H(a) = sum(ps1);

%5 degrees
clear Q
clear a
clear ps1
clear n
clear i
clear j
a = 5;
try
  for n = 1:256
    j = (256 + (1-n));
    for i = (256-((16-a)*(1-n))):1:(266+((16-a)*(n-1)))

```

```

        Q(i,j)=image(i,j);
    end
end
end
ps1 = sum(Q);
H(a) = sum(ps1);

%10 degrees
clear Q
clear a
clear ps1
clear n
clear i
clear j
a = 10;
try
    for n = 1:256
        j = (256 + (1-n));
        for i = (256-((16-a)*(1-n))):1:(261+((16-a)*(n-1)))
            Q(i,j)=image(i,j);
        end
    end
end
ps1 = sum(Q);
H(a) = sum(ps1);

%15 degrees
clear Q
clear a
clear ps1
clear n
clear i
clear j

```

```

a = 15;
try
  for n = 1:256
    j = (256 + (1-n));
    for i = (256-((19-a)*(1-n))):1:(259+((19-a)*(n-1)))
      Q(i,j)=image(i,j);
    end
  end
end
ps1 = sum(Q);
H(a) = sum(ps1);

```

%20 degrees

```

clear Q
clear a
clear ps1
clear n
clear i
clear j
a = 20;
try
  for n = 1:256
    j = (256 + (1-n));
    for i = (256-((23-a)*(1-n))):1:(258+((23-a)*(n-1)))
      Q(i,j)=image(i,j);
    end
  end
end
ps1 = sum(Q);
H(a) = sum(ps1);

```

%25 degrees

```
clear Q
```

```

clear a
clear ps1
clear n
clear i
clear j
a = 25;
try
  for n = 1:256
    j = (256 + (1-n));
    for i = (256-((27-a)*(1-n))):1:(257+((27-a)*(n-1)))
      Q(i,j)=image(i,j);
    end
  end
end
ps1 = sum(Q);
H(a) = sum(ps1);

%30 degrees
clear Q
clear a
clear ps1
clear n
clear i
clear j
a = 30;
try
  for n = 1:2:256
    j = (256 + (1-n));
    for i = (256+((34-a)*(((n+1)/2)-1))):1:(259+((34-a)*(((n+1)/2)-1)))
      Q(i,j)=image(i,j);
    end
  end
end
end

```

```
ps1 = sum(Q);  
H(a) = sum(ps1);
```

```
%35 degrees
```

```
clear Q  
clear a  
clear ps1  
clear n  
clear i  
clear j  
a = 35;  
try  
  for n = 1:2:256  
    j = (256 + (1-n));  
    for i = (256+((38-a)*(((n+1)/2)-1))):1:(258+((38-a)*(((n+1)/2)-1)))  
      Q(i,j)=image(i,j);  
    end  
  end  
end  
ps1 = sum(Q);  
H(a) = sum(ps1);
```

```
%40 degrees
```

```
clear Q  
clear a  
clear ps1  
clear n  
clear i  
clear j  
a = 40;  
try  
  for n = 1:3:256  
    j = (256 + (1-n));
```

```

        for i = (256+((44-a)*(((n+2)/3)-1)):1:(259+((44-a)*(((n+2)/3)-1)))
            Q(i,j)=image(i,j);
        end
    end
end
ps1 = sum(Q);
H(a) = sum(ps1);

%45 degrees
clear Q
clear a
clear ps1
clear n
clear i
clear j
a = 45;
try
    for n = 1:256
        i = (256 - (1-n));
        j = (256 + (1-n));
        Q(i,j)=image(i,j);
    end
end
ps1 = sum(Q);
H(a) = sum(ps1);

%50 degrees
clear Q
clear a
clear ps1
clear n
clear i

```

```

clear j

a = 50;
try
  for n = 1:3:256
    i = (256 - (1-n));
    for j = (256-((54-a)*(((n+2)/3)-1))):-1:(253-((54-a)*(((n+2)/3)-1)))
      Q(i,j)=image(i,j);
    end
  end
end
ps1 = sum(Q);
H(a) = sum(ps1);

%55 degrees
clear Q
clear a
clear ps1
clear n
clear i
clear j
a = 55;
try
  for n = 1:2:256
    i = (256 - (1-n));
    for j = (256-((58-a)*(((n+1)/2)-1))):-1:(254-((58-a)*(((n+1)/2)-1)))
      Q(i,j)=image(i,j);
    end
  end
end
ps1 = sum(Q);
H(a) = sum(ps1);

```

```

%60 degrees
clear Q
clear a
clear ps1
clear n
clear i
clear j
a = 60;
try
  for n = 1:2:256
    i = (256 - (1-n));
    for j = (256-((64-a)*((n+1)/2)-1)):-1:(253-((64-a)*((n+1)/2)-1))
      Q(i,j)=image(i,j);
    end
  end
end
ps1 = sum(Q);
H(a) = sum(ps1);

```

```

%65 degrees
clear Q
clear a
clear ps1
clear n
clear i
clear j
a = 65;
try
  for n = 1:256
    i = (256 - (1-n));
    for j = (256+((67-a)*(1-n))):-1:(255-((67-a)*(n-1)))
      Q(i,j)=image(i,j);
    end
  end
end

```

```

    end
end
ps1 = sum(Q);
H(a) = sum(ps1);

%70 degrees
clear Q
clear a
clear ps1
clear n
clear i
clear j
a = 70;
try
    for n = 1:256
        i = (256 - (1-n));
        for j = (256+((73-a)*(1-n))):-1:(254-((73-a)*(n-1)))
            Q(i,j)=image(i,j);
        end
    end
end
ps1 = sum(Q);
H(a) = sum(ps1);

%75 degrees
clear Q
clear a
clear ps1
clear n
clear i
clear j
a = 75;
try

```

```

for n = 1:256
    i = (256 - (1-n));
    for j = (256+((79-a)*(1-n))):-1:(253-((79-a)*(n-1)))
        Q(i,j)=image(i,j);
    end
end
end
ps1 = sum(Q);
H(a) = sum(ps1);

```

%80 degrees

```

clear Q
clear a
clear ps1
clear n
clear i
clear j
a = 80;
try
    for n = 1:256
        i = (256 - (1-n));
        for j = (256+((86-a)*(1-n))):-1:(251-((86-a)*(n-1)))
            Q(i,j)=image(i,j);
        end
    end
end
ps1 = sum(Q);
H(a) = sum(ps1);

```

%85 degrees

```

clear Q
clear a
clear ps1

```

```

clear n
clear i
clear j
a = 85;
try
  for n = 1:256
    i = (256 - (1-n));
    for j = (256+((96-a)*(1-n))):-1:(246-((96-a)*(n-1)))
      Q(i,j)=image(i,j);
    end
  end
end
ps1 = sum(Q);
H(a) = sum(ps1);

```

%90 degrees

```

clear Q
clear a
clear ps1
clear n
clear i
clear j
a = 90;
try
  for n = 1:256
    i = 256;
    for j = 256:-1:1
      Q(i,j)=image(i,j);
    end
  end
end
ps1 = sum(Q);
H(a) = sum(ps1);

```

```

%95 degrees
clear Q
clear a
clear ps1
clear n
clear i
clear j
a = 95;
try
  for n = 1:256
    i = (256 + (1-n));
    for j = (256+((106-a)*(1-n)))-1:(246-((106-a)*(n-1)))
      Q(i,j)=image(i,j);
    end
  end
end
ps1 = sum(Q);
H(a) = sum(ps1);

```

```

%100 degrees
clear Q
clear a
clear ps1
clear n
clear i
clear j
a = 100;
try
  for n = 1:256
    i = (256 + (1-n));
    for j = (256+((106-a)*(1-n)))-1:(251-((106-a)*(n-1)))
      Q(i,j)=image(i,j);
    end
  end
end

```

```

        end
    end
end
ps1 = sum(Q);
H(a) = sum(ps1);

%105 degrees
clear Q
clear a
clear ps1
clear n
clear i
clear j
a = 105;
try
    for n = 1:256
        i = (256 + (1-n));
        for j = (256+((109-a)*(1-n))):-1:(253-((109-a)*(n-1)))
            Q(i,j)=image(i,j);
        end
    end
end
ps1 = sum(Q);
H(a) = sum(ps1);

%110 degrees
clear Q
clear a
clear ps1
clear n
clear i
clear j
a = 110;

```

```

try
  for n = 1:256
    i = (256 + (1-n));
    for j = (256+((113-a)*(1-n))):-1:(254-((113-a)*(n-1)))
      Q(i,j)=image(i,j);
    end
  end
end
ps1 = sum(Q);
H(a) = sum(ps1);

```

%115 degrees

```

clear Q
clear a
clear ps1
clear n
clear i
clear j
a = 115;

```

```

try
  for n = 1:256
    i = (256 + (1-n));
    for j = (256+((117-a)*(1-n))):-1:(255-((117-a)*(n-1)))
      Q(i,j)=image(i,j);
    end
  end
end
ps1 = sum(Q);
H(a) = sum(ps1);

```

%120 degrees

```

clear Q
clear a

```

```

clear ps1
clear n
clear i
clear j
a = 120;
try
  for n = 1:2:256
    i = (256 + (1-n));
    for j = (256-((124-a)*(((n+1)/2)-1))):-1:(253-((124-a)*(((n+1)/2)-1)))
      Q(i,j)=image(i,j);
    end
  end
end
ps1 = sum(Q);
H(a) = sum(ps1);

```

%125 degrees

```

clear Q
clear a
clear ps1
clear n
clear i
clear j
a = 125;
try
  for n = 1:2:256
    i = (256 + (1-n));
    for j = (256-((128-a)*(((n+1)/2)-1))):-1:(254-((128-a)*(((n+1)/2)-1)))
      Q(i,j)=image(i,j);
    end
  end
end
ps1 = sum(Q);

```

```
H(a) = sum(ps1);
```

```
%130 degrees
```

```
clear Q
```

```
clear a
```

```
clear ps1
```

```
clear n
```

```
clear i
```

```
clear j
```

```
a = 130;
```

```
try
```

```
for n = 1:3:256
```

```
    i = (256 + (1-n));
```

```
        for j = (256-((134-a)*(((n+2)/3)-1)):-1:(253-((134-a)*(((n+2)/3)-1)))
```

```
            Q(i,j)=image(i,j);
```

```
        end
```

```
    end
```

```
end
```

```
ps1 = sum(Q);
```

```
H(a) = sum(ps1);
```

```
%135 degrees
```

```
clear Q
```

```
clear a
```

```
clear ps1
```

```
clear n
```

```
clear i
```

```
clear j
```

```
a = 135;
```

```
try
```

```
for n = 1:256
```

```
    i = (256 + (1-n));
```

```
    j = (256 + (1-n));
```

```

        Q(i,j)=image(i,j);
    end
end
ps1 = sum(Q);
H(a) = sum(ps1);

%140 degrees
clear Q
clear a
clear ps1
clear n
clear i
clear j
a = 140;
try
    for n = 1:3:256
        j = (256 + (1-n));
        for i = (256-((144-a)*((n+2)/3)-1)):-1:(253-((144-a)*((n+2)/3)-1))
            Q(i,j)=image(i,j);
        end
    end
end
ps1 = sum(Q);
H(a) = sum(ps1);

%145 degrees
clear Q
clear a
clear ps1
clear n
clear i
clear j
a = 145;

```

```

try
  for n = 1:2:256
    j = (256 + (1-n));
    for i = (256-((148-a)*(((n+1)/2)-1)):-1:(254-((148-a)*(((n+1)/2)-1)))
      Q(i,j)=image(i,j);
    end
  end
end

```

```

ps1 = sum(Q);
H(a) = sum(ps1);

```

%150 degrees

```
clear Q
```

```
clear a
```

```
clear ps1
```

```
clear n
```

```
clear i
```

```
clear j
```

```
a = 150;
```

```
try
```

```
  for n = 1:2:256
```

```
    j = (256 + (1-n));
```

```
    for i = (256-((154-a)*(((n+1)/2)-1)):-1:(253-((154-a)*(((n+1)/2)-1)))
```

```
      Q(i,j)=image(i,j);
```

```
    end
```

```
  end
```

```
end
```

```
ps1 = sum(Q);
```

```
H(a) = sum(ps1);
```

%155 degrees

```
clear Q
```

```

clear a
clear ps1
clear n
clear i
clear j
a = 155;
try
  for n = 1:256
    j = (256 + (1-n));
    for i = (256+((157-a)*(1-n))):-1:(255-((157-a)*(n-1)))
      Q(i,j)=image(i,j);
    end
  end
end
ps1 = sum(Q);
H(a) = sum(ps1);

```

%160 degrees

```

clear Q
clear a
clear ps1
clear n
clear i
clear j
a = 160;
try
  for n = 1:256
    j = (256 + (1-n));
    for i = (256+((163-a)*(1-n))):-1:(254-((163-a)*(n-1)))
      Q(i,j)=image(i,j);
    end
  end
end
end

```

```
ps1 = sum(Q);  
H(a) = sum(ps1);
```

```
%165 degrees
```

```
clear Q  
clear a  
clear ps1  
clear n  
clear i  
clear j  
a = 165;  
try  
  for n = 1:256  
    j = (256 + (1-n));  
    for i = (256+((169-a)*(1-n))):-1:(253-((169-a)*(n-1)))  
      Q(i,j)=image(i,j);  
    end  
  end  
end  
ps1 = sum(Q);  
H(a) = sum(ps1);
```

```
%170 degrees
```

```
clear Q  
clear a  
clear ps1  
clear n  
clear i  
clear j  
a = 170;  
try  
  for n = 1:256  
    j = (256 + (1-n));
```

```

        for i = (256+((176-a)*(1-n)):-1:(251-((176-a)*(n-1)))
            Q(i,j)=image(i,j);
        end
    end
end
ps1 = sum(Q);
H(a) = sum(ps1);

%175 degrees
clear Q
clear a
clear ps1
clear n
clear i
clear j
a = 175;
try
    for n = 1:256
        j = (256 + (1-n));
        for i = (256+((186-a)*(1-n)):-1:(246-((186-a)*(n-1)))
            Q(i,j)=image(i,j);
        end
    end
end
ps1 = sum(Q);
H(a) = sum(ps1);

[Z,L] =
min([H(1),H(5),H(10),H(15),H(20),H(25),H(30),H(35),H(40),H(45),H(50),H(55),H(60),H
(70),H(75),H(80),H(85),H(90),H(95),H(100),H(105),H(110),H(115),H(120),H(125),H(1
30),H(135),H(140),H(145),H(150),H(155),H(160),H(165),H(170),H(175)]);

%Determine what angle has the highest frequency of dots and how many dots

```

```

%it would be
maxNumberDots = H(1); %initialization
maxAngle = 0;
for g2 = 5:5:175
    if H(g2)> maxNumberDots
        maxNumberDots = H(g2);
        maxAngle = g2;
    end
end

```

```

for a = 1:1:175
S(a) = H(a) - 0;
end

```

```

% for a = 1:1:1
%   S(a) = H(a) - Z;
% end

```

### ***allindex.m***

```

function [I,AI] = allindex(allInfo)

```

```

[C,I] = max(allInfo);

```

```

%allInfo is a vector

```

```

%summing within 20 degrees in both directions of maximum aligned fiber

```

```

if ((I>20) && (I<160))

```

```

    sr = sum([allInfo(I),allInfo(I+5),allInfo(I+10),allInfo(I+15),allInfo(I+20),allInfo(I-
5),allInfo(I-10),allInfo(I-15),allInfo(I-20)]);

```

```

elseif (I == 20)

```

```

    sr =
sum([allInfo(10),allInfo(15),allInfo(20),allInfo(25),allInfo(30),allInfo(5),allInfo(1),allInfo(
35),allInfo(40)]);
elseif (l == 15)
    sr =
sum([allInfo(10),allInfo(15),allInfo(20),allInfo(25),allInfo(30),allInfo(35),allInfo(5),allInfo
(1),allInfo(175),]);
elseif (l == 10)
    sr =
sum([allInfo(10),allInfo(15),allInfo(20),allInfo(25),allInfo(30),allInfo(5),allInfo(1),allInfo(
175),allInfo(170)]);
elseif (l==5)
    sr =
sum([allInfo(5),allInfo(10),allInfo(15),allInfo(20),allInfo(25),allInfo(1),allInfo(175),allInfo
(170),allInfo(165)]);
elseif (l==1)
    sr =
sum([allInfo(1),allInfo(5),allInfo(10),allInfo(15),allInfo(20),allInfo(175),allInfo(170),allInf
o(165),allInfo(160)]);
elseif (l==175)
    sr =
sum([allInfo(175),allInfo(1),allInfo(5),allInfo(10),allInfo(15),allInfo(170),allInfo(165),allIn
fo(160),allInfo(155)]);
elseif (l==170)
    sr =
sum([allInfo(170),allInfo(175),allInfo(1),allInfo(5),allInfo(10),allInfo(165),allInfo(160),all
nfo(155),allInfo(150)]);
elseif (l==165)
    sr =
sum([allInfo(170),allInfo(175),allInfo(1),allInfo(5),allInfo(145),allInfo(165),allInfo(160),a
llInfo(155),allInfo(150)]);
elseif (l==160)

```

```
sr =  
sum([allInfo(170),allInfo(175),allInfo(1),allInfo(145),allInfo(140),allInfo(165),allInfo(160  
) ,allInfo(155),allInfo(150)]);  
end
```

```
sall = sum(allInfo);  
%sAll2 = sum(sall);
```

```
fracall = (sr/sall);
```

```
AI = (fracall/.22);
```

### ***CalculateDiameter.m***

```
function [micrometerDiameter] = CalculateDiameter(pixelSpan, originalImage)
```

```
[x y] = size(originalImage);  
halfSpan = pixelSpan/2;  
diameter = x/halfSpan;  
%halfSpan = x/pixelSpan;  
%diameter = halfSpan/2;
```

```
%Convert the diameter in pixels to a value in micrometers, conversion is based on a  
scale bar placed over the confocal image in ImageJ
```

```
micrometerDiameter = diameter /2.78;
```

```
end
```

```
%350 by 350 is 2.78 pixels/um  
%300 by 300 is 3.3 pixels/um  
%250 by 250 is 3.920 pixels/um
```

## REFERENCE

1. Bowles R.D., Williams R.M., Zipfel W.R., Bonassar L.J. Self-assembly of aligned tissue-engineered annulus fibrosus and intervertebral disc composite via collagen gel contraction. *Tissue Eng Part A*.**16**:1339. 2010.

## APPENDIX D

### MATLAB Code for Load Cell Data Analysis

The following code was written in MATLAB to analysis load cell data from the bioreactor in chapters 3 and 7. The code filters, smoothes, and analyzes the load cell data to report average peak-to-peak load calculations at 5, 15, 30 and 45 minutes of each loading cycle to determine loads experienced by meniscal constructs during loading and to validate FE models. This code was written by Jeff Ballyns, and Jenny Puetzer and calls a MATLAB peakfinder.m file written by Nathanael C. Yoder.

#### ***Pkpk.m***

```
% loading imported data from .lvm file
```

```
%load loaddata.mat
```

```
% assigning variables to columns
```

```
time = data(:,1);
```

```
lode = data(:,2);
```

```
motion = data(:,3);
```

```
figure(1)
```

```
plot(time,lode)
```

```
hold on
```

```
% red plot
```

```
[a,b] = butter(1,.1); %designs a order 1 lowpass butterworth filter with normalized  
cutoff frequency of .1
```

```
smoothed = filtfilt(a,b,lode);
```

```
plot(time,smoothed,'r')
```

```
% green plot
```

```

[c,d] = butter(1,.4);
filtered = filtfilt(c,d,lode);
plot(time,filtered,'g')

% motion plot
plot(time,(motion-86446.5)./10000,'k')

%slope = diff(smoothed)./diff(time);

%set threshold value
n = .05;

%determins data at 5 mins
time_5= time>=300 & time<=360;
location_5 = find(time_5);
filtered_5 = filtered(location_5);
ftime_5 = time(location_5);

[peakLoc_5, peakMax_5] = peakfinder(filtered_5, n, 1);
plot(ftime_5(peakLoc_5), peakMax_5, 'k+')
[peakLoc2_5, peakMin_5] = peakfinder(filtered_5, n, -1);
plot(ftime_5(peakLoc2_5), peakMin_5, 'kd')

if (length(peakMax_5) ~= length(peakMin_5));
    if (length (peakMax_5)>length(peakMin_5));
        peakMax_5 = peakMax_5(1:length(peakMin_5));
    else
        peakMin_5 = peakMin_5(1:length(peakMax_5));
    end
end
end

%Length_max = length(peakMax_5)
%Lenght_min = length(peakMin_5)

```

```

Peak_Peak_5 = abs(peakMax_5 - peakMin_5)
Average_5 = mean(Peak_Peak_5)
Mode_5 = mode(Peak_Peak_5)

t_5 = ftime_5(peakLoc_5);
t_5 = t_5(1: length(Peak_Peak_5));

mean_max_5=mean(peakMax_5);
mean_min_5=mean(peakMin_5);
mode_max_5=mode(peakMax_5);
mode_min_5=mode(peakMin_5);
peak_peak_average_5=abs(mean_max_5-mean_min_5)
peak_peak_mode_5 =abs(mode_max_5-mode_min_5)

%determins data at 15 mins
time_15= time>=900 & time<=960;
location_15 = find(time_15);
filtered_15 = filtered(location_15);
ftime_15 = time(location_15);

[peakLoc_15, peakMax_15] = peakfinder(filtered_15, n, 1);
plot(ftime_15(peakLoc_15), peakMax_15, 'k+')
[peakLoc2_15, peakMin_15] = peakfinder(filtered_15, n, -1);
plot(ftime_15(peakLoc2_15), peakMin_15, 'kd')

if (length(peakMax_15) ~= length(peakMin_15));
    if (length (peakMax_15)>length(peakMin_15));
        peakMax_15 = peakMax_15(1:length(peakMin_15));
    else
        peakMin_15 = peakMin_15(1:length(peakMax_15));
    end
end

```

```
end
```

```
%Length_max = length(peakMax_15)
```

```
%Lenght_min = length(peakMin_15)
```

```
Peak_Peak_15 = abs(peakMax_15 - peakMin_15)
```

```
Average_15 = mean(Peak_Peak_15)
```

```
Mode_15 = mode(Peak_Peak_15)
```

```
t_15 = ftime_15(peakLoc_15);
```

```
t_15 = t_15(1: length(Peak_Peak_15));
```

```
mean_max_15=mean(peakMax_15);
```

```
mean_min_15=mean(peakMin_15);
```

```
mode_max_15=mode(peakMax_15);
```

```
mode_min_15=mode(peakMin_15);
```

```
peak_peak_average_15=abs(mean_max_15-mean_min_15)
```

```
peak_peak_mode_15 =abs(mode_max_15-mode_min_15)
```

```
%determins data at 30 mins
```

```
time_30= time>=1800 & time<=1860;
```

```
location_30 = find(time_30);
```

```
filtered_30 = filtered(location_30);
```

```
ftime_30 = time(location_30);
```

```
[peakLoc_30, peakMax_30] = peakfinder(filtered_30, n, 1);
```

```
plot(ftime_30(peakLoc_30), peakMax_30, 'k+')
```

```
[peakLoc2_30, peakMin_30] = peakfinder(filtered_30, n, -1);
```

```
plot(ftime_30(peakLoc2_30), peakMin_30, 'kd')
```

```
if (length(peakMax_30) ~= length(peakMin_30));
```

```
    if (length (peakMax_30)>length(peakMin_30));
```

```
        peakMax_30 = peakMax_30(1:length(peakMin_30));
```

```

else
    peakMin_30 = peakMin_30(1:length(peakMax_30));
end
end

%Length_max = length(peakMax_30)
%Lenght_min = length(peakMin_30)

Peak_Peak_30 = abs(peakMax_30 - peakMin_30)
Average_30 = mean(Peak_Peak_30)
Mode_30 = mode(Peak_Peak_30)

t_30 = ftime_30(peakLoc_30);
t_30 = t_30(1: length(Peak_Peak_30));

mean_max_30=mean(peakMax_30);
mean_min_30=mean(peakMin_30);
mode_max_30=mode(peakMax_30);
mode_min_30=mode(peakMin_30);
peak_peak_average_30=abs(mean_max_30-mean_min_30)
peak_peak_mode_30 =abs(mode_max_30-mode_min_30)

%determins data at 45 mins
time_45= time>=2700 & time<=2760;
location_45 = find(time_45);
filtered_45 = filtered(location_45);
ftime_45 = time(location_45);

[peakLoc_45, peakMax_45] = peakfinder(filtered_45, n, 1);
plot(ftime_45(peakLoc_45), peakMax_45, 'k+')
[peakLoc2_45, peakMin_45] = peakfinder(filtered_45, n, -1);
plot(ftime_45(peakLoc2_45), peakMin_45, 'kd')

```

```

if (length(peakMax_45) ~= length(peakMin_45));
    if (length (peakMax_45)>length(peakMin_45));
        peakMax_45 = peakMax_45(1:length(peakMin_45));
    else
        peakMin_45 = peakMin_45(1:length(peakMax_45));
    end
end
end

%Length_max = length(peakMax_45)
%Lenght_min = length(peakMin_45)

Peak_Peak_45 = abs(peakMax_45 - peakMin_45)
Average_45 = mean(Peak_Peak_45)
Mode_45 = mode(Peak_Peak_45)

t_45 = ftime_45(peakLoc_45);
t_45 = t_45(1: length(Peak_Peak_45));

mean_max_45=mean(peakMax_45);
mean_min_45=mean(peakMin_45);
mode_max_45=mode(peakMax_45);
mode_min_45=mode(peakMin_45);
peak_peak_average_45=abs(mean_max_45-mean_min_45)
peak_peak_mode_45 =abs(mode_max_45-mode_min_45)

%Analysis of all data at once
%[peakLoc, peakMax] = peakfinder(filtered, 1/4, 1);
%plot(time(peakLoc), peakMax, 'k+')
%[peakLoc2, peakMin] = peakfinder(filtered, 1/4, -1);
%plot(time(peakLoc2), peakMin, 'kd')
%mean_max=mean(peakMax)
%mean_min=mean(peakMin)

```

```
%mode_max=mode(peakMax)
%mode_min=mode(peakMin)
%length_max = length(peakMax);
%length_min = length(peakMin);
%sum_max = sum(peakMax);
%sum_min = sum(peakMin);
%average_max = sum_max / length_max;
%average_min = sum_min / length_min;
%peak_peak=abs(average_max-average_min)
%peak_peak_mode =abs(mode_max-mode_min)
```

```
hold off
```

```
figure(2)
subplot(2, 2, 1);
plot( t_5, Peak_Peak_5)
xlabel('Time(s)')
ylabel('Peak to Peak difference')
legend('5 mins')
```

```
subplot(2, 2, 2);
plot(t_15 , Peak_Peak_15)
xlabel('Time(s)')
ylabel('Peak to Peak difference')
legend('15 mins')
```

```
subplot(2,2, 3)
plot(t_30 , Peak_Peak_30)
xlabel('Time(s)')
ylabel('Peak to Peak difference')
legend('30 mins')
```

```
subplot(2, 2, 4)
```

```
plot(t_45 , Peak_Peak_45)
xlabel('Time(s)')
ylabel('Peak to Peak difference')
legend('45 mins')
```

```
% throwing out data
```

```
%set point for throwing out below
```

```
x = 0.2
```

```
%throw out data for 5 mins
```

```
ePk_Pk_5= Peak_Peak_5>=x;
elocation_5 = find(ePk_Pk_5);
ePeak_Peak_5 = Peak_Peak_5(elocation_5);
etime_5 = t_5(elocation_5);
```

```
%throw out data for 15 mins
```

```
ePk_Pk_15= Peak_Peak_15>=x;
elocation_15 = find(ePk_Pk_15);
ePeak_Peak_15 = Peak_Peak_15(elocation_15);
etime_15 = t_15(elocation_15);
```

```
%throw out data for 30 mins
```

```
ePk_Pk_30= Peak_Peak_30>=x;
elocation_30 = find(ePk_Pk_30);
ePeak_Peak_30 = Peak_Peak_30(elocation_30);
etime_30 = t_30(elocation_30);
```

```
%throw out data for 45 mins
```

```
ePk_Pk_45= Peak_Peak_45>=x;
elocation_45 = find(ePk_Pk_45);
ePeak_Peak_45 = Peak_Peak_45(elocation_45);
```

```
eftime_45 = t_45(elocation_45);
```

```
%Graph new data
```

```
figure(3)
```

```
subplot(2, 2, 1);
```

```
plot( eftime_5, ePeak_Peak_5)
```

```
xlabel('Time(s)')
```

```
ylabel('Peak to Peak difference')
```

```
legend('5 mins')
```

```
subplot(2, 2, 2);
```

```
plot(eftime_15 , ePeak_Peak_15)
```

```
xlabel('Time(s)')
```

```
ylabel('Peak to Peak difference')
```

```
legend('15 mins')
```

```
subplot(2,2, 3)
```

```
plot(eftime_30 , ePeak_Peak_30)
```

```
xlabel('Time(s)')
```

```
ylabel('Peak to Peak difference')
```

```
legend('30 mins')
```

```
subplot(2, 2, 4)
```

```
plot(eftime_45 , ePeak_Peak_45)
```

```
xlabel('Time(s)')
```

```
ylabel('Peak to Peak difference')
```

```
legend('45 mins')
```

```
time_5= time>=300 & time<=305;
```

```
location_5 = find(time_5);
```

```
filtered_5 = filtered(location_5)
```

```
ftime_5 = time(location_5)
```

```
motion_5 = (motion(location_5)-86446.5)/10000
```

```

time_6= time>=305 & time<=310;
location_6 = find(time_6);
filtered_6 = filtered(location_6)
ftime_6 = time(location_6)
motion_6 = (motion(location_6)-86446.5)./10000

```

### ***peakfinder.m***

```

function varargout = peakfinder(x0, thresh, extrema)
%PEAKFINDER Noise tolerant fast peak finding algorithm
% INPUTS:
%   x0 - A real vector from the maxima will be found (required)
%   thresh - The amount above surrounding data for a peak to be
%   identified (default = (max(x0)-min(x0))/4). Larger values mean
%   the algorithm is more selective in finding peaks.
%   extrema - 1 if maxima are desired, -1 if minima are desired
%   (default = maxima, 1)
% OUTPUTS:
%   peakLoc - The indicies of the identified peaks in x0
%   peakMag - The magnitude of the identified peaks
%
% [peakLoc] = peakfinder(x0) returns the indicies of local maxima that
%   are at least 1/4 the range of the data above surrounding data
%
% [peakLoc] = peakfinder(x0,thresh) returns the indicies of local max
%   that are at least thresh above surrounding data.
%
% [peakLoc] = peakfinder(x0,thresh,extrema) returns the maxima of the
%   data if extrema > 0 and the minima of the data if extrema < 0
%
% [peakLoc, peakMag] = peakfinder(x0,...) returns the indicies of the
%   local maxima as well as the magnitudes of those maxima
%

```

```

% If called with no output the identified maxima will be plotted along
%   with the input data.
%
%Note: If repeated values are found the first is identified as the peak
%
% Ex: % Runs on 1.5 million point vector in under a second on my machine
%t = 0:.00002:30;y =10*cos(2*pi*5*t)+randn(size(t))+5*cos(2*pi*2*t);peakfinder(y)
% Copyright Nathanael C. Yoder 2009 (ncyoder@purdue.edu)

```

```

error(nargchk(1,4,nargin,'struct'));

```

```

error(nargoutchk(0,2,nargout,'struct'));

```

```

len0 = numel(x0);

```

```

if len0 ~= length(x0)

```

```

    error('PEAKFINDER:Input','The input data must be a vector')

```

```

end

```

```

if ~isreal(x0)

```

```

    warning('PEAKFINDER:NotReal','Absolute value of data will be used')

```

```

    x0 = abs(x0);

```

```

end

```

```

if nargin < 2

```

```

    thresh = (max(x0)-min(x0))/4;

```

```

    extrema = 1;

```

```

elseif nargin < 3

```

```

    extrema = 1;

```

```

else

```

```

    extrema = sign(extrema(1)); % Should only be 1 or -1 but make sure

```

```

    if extrema == 0

```

```

        error('PEAKFINDER:ZeroMaxima','Either 1 (for maxima) or -1 (for minima)
must be input for extrema');

```

```

    end

```

```

end

```

```

x0 = extrema*x0(:); % Make this so we are finding maxima
dx0 = diff(x0);
dx0(dx0 == 0) = -eps; % This is so we find the first of repeated values
signTerm = dx0(1:end-1).*dx0(2:end);
ind = find(signTerm < 0)+1;

x = [x0(1);x0(ind);x0(end)];
signDx = sign(diff(x(1:3)));
ind = [1;ind;len0];

len      = numel(x);
minMag   = min(x);
tempMag  = minMag;
foundPeak = 0;
leftMin  = -inf;

% Deal with first point a little differently since tacked it on
if signDx(1) < 0
    ii = 0;
    if signDx(1) == signDx(2)
        x(2) = [];
        ind(2) = [];
        len = len-1;
    end
else
    ii = 1;
    if signDx(1) == signDx(2)
        x(1) = [];
        ind(1) = [];
        len = len-1;
    end
end

```

```

end

% Preallocate max number of extrema
maxPeaks = ceil(len/2);
peakLoc = zeros(maxPeaks,1);
peakMag = zeros(maxPeaks,1);
cInd = 1;
% Loop through extrema
while ii < len-1
    ii = ii+1; % Peaks
    % Reset peak finding
    if foundPeak == 1
        if (x(ii) < peakMag(end)-thresh || x(ii) > peakMag(end))
            tempMag = minMag;
            foundPeak = 0;
        end
    end
    % Found new peak
    if x(ii) > leftMin + thresh && x(ii) > tempMag
        tempLoc = ii;
        tempMag = x(ii);
    end
    ii = ii+1; % Valleys
    % Come down at least thresh from peak
    if foundPeak == 0 && tempMag > thresh + x(ii)
        foundPeak = 1;
        leftMin = x(ii);
        peakLoc(cInd) = tempLoc;
        peakMag(cInd) = tempMag;
        cInd = cInd+1;
    elseif x(ii) < leftMin % New left minima

```

```

        leftMin = x(ii);
    end
end

% Check end point
if x(end) > tempMag
    tempMag = x(end);
    tempLoc = len;
end
if tempMag > leftMin + thresh
    peakLoc(cInd) = tempLoc;
    peakMag(cInd) = tempMag;
    cInd = cInd + 1;
end

% Create output
peakInds = ind(peakLoc(1:cInd-1));
peakMags = peakMag(1:cInd-1);
if extrema < 0
    peakMags = -peakMags;
    x0 = -x0;
end
if nargout == 0
    figure;
    plot(1:len0,x0,peakInds,peakMags,'ro','linewidth',2)
else
    varargout = {peakInds,peakMags};
end
end

```